Table of contents:

1. General experimental procedures

If not stated otherwise, all reactions and manipulations were carried out under an atmosphere of dry nitrogen using Schlenk techniques or in an inert-atmosphere glovebox. Toluene and THF were distilled from Na/benzophenone and degassed by three freeze-pump-thaw cycles prior to use. CH_2Cl_2 was distilled from CaH_2. C_6D_6 and $CDCl_3$ were stored over molecular sieves (3 Å). Heptamethyldisilazane ($(Me_3Si)_2NMe$) was freshly distilled and stored over molecular sieves (3 Å). Reaction mixtures in flasks were heated by using an oil bath and reaction mixtures in sealed NMR tubes or ampoules were heated in an oven. The starting materials, mesityldimethoxyborane ($MesB(OMe)_2$),[S1] 6,7-dibromo-1,4-dihydro-1,4-epoxynaphthalene,[S2] 2,3-dibromonaphthalene,[S3] 2-bromo-3-iodonaphthalene (**18**),[S3] 1,4-dibromo-2,5-diiodobenzene (**20**),[S4] and 1,5-dibromo-9,10-dihydroxy-9,10-diydro-9,10-diboraanhracene (**25**)[S5] were prepared according to literature procedures. 4-*tert*-Butylphenylacetylene (*Acros Organics*), tri-*n*-butylstannylacetylene (*Alfa Aesar*), $Pd(PPh_3)_2Cl_2$ (*Heraeus*), $Pd(PtBu_3)_2$ (*Sigma Aldrich*), and $[Au(PPh_3)NTf_2]$ (*abcr*; NTf_2 = bis(trifluoromethane)sulfonimide) were used as received.

NMR spectra were recorded at 298 K using the following spectrometers: Bruker Avance-300 or Avance-500. Chemical shift values are referenced to (residual) solvent signals ($^1H/^{13}C\{^1H\}$; C_6D_6: δ = 7.16/128.06 ppm, $CDCl_3$: δ = 7.26/77.16 ppm) or external $BF_3{\cdot}Et_2O$ (^{11}B: 0.00 ppm). Abbreviations: s = singlet, d = doublet, dd = doublet of doublets, ddd = doublet of doublets of doublets, vt = virtual triplet, q = quartet, m = multiplet, br. = broad, n.o. = not observed. Resonances of carbon atoms attached to boron atoms were typically broadened and sometimes not observed due to the quadrupolar relaxation of boron. Boron resonances of triarylborane compounds are typically very broad ($h_{1/2}$ > 1100 Hz) and were observed only in highly concentrated samples. Resonance assignments were aided by ^{H,H}COSY, ^{H,C}HSQC, and ^{H,C}HMBC spectra. **Note:** The numbering scheme employed for the assignment of NMR resonances deviates from the IUPAC nomenclature. For simplicity, only chemically inequivalent positions are numbered; for better comparability, identical fragments have always been given the same numbers.

UV/Vis absorption spectra were recorded at room temperature using a *Varian* Cary 50 Scan or a *Varian* Cary 60 Scan UV/Vis spectrophotometer. Photoluminescence (PL) spectra were recorded at room temperature using a *Jasco* FP-8300 spectrofluorometer equipped with a calibrated *Jasco* ILF-835 100 mm diameter integrating sphere and analyzed using the *Jasco* FWQE-880 software. For PL quantum yield (Φ_{PL}) measurements, each sample was carefully degassed with argon using an injection needle and a septum-capped cuvette. Under these conditions the Φ_{PL} of the fluorescence standard 9,10-diphenylanthracene was determined as 97% (lit.: 97%).[S6,S7] For all Φ_{PL} measurements, at least three samples of different concentrations were used (range between 10^{-5} and 10^{-7} mol L^{-1}). Due to self-absorption, slightly lower Φ_{PL} values were observed at higher concentrations. This effect was corrected by applying a method reported by *Bardeen et al.*, which slightly improved the Φ_{PL} values (4% at most).[S8] Cyclic voltammetry (CV) measurements were performed in a glovebox at room temperature in a one-chamber, three-electrode cell using an *EG&G* Princeton Applied Research 263A potentiostat. A platinum disk electrode (2.00 mm diameter) was used as the working electrode with a platinum wire counter electrode and a silver wire reference electrode, which was coated with AgCl by immersion into HCl/HNO_3 (3:1). Prior to measurements, the solvents CH_2Cl_2 and THF were dried with CaH_2 and NaK, respectively, and degassed by three freeze-pump-thaw cycles. $[nBu_4N][PF_6]$ (*Sigma Aldrich*; used as received) was employed as the supporting electrolyte (0.1 mol L^{-1}). All potential values were referenced against the FcH/FcH^+ redox couple (FcH = ferrocene; $E_{1/2}$ = 0 V). Scan rates were varied between 100 and 400 mV s^{-1}. High-resolution mass spectra were measured in positive mode using a *Thermo Fisher Scientific* MALDI LTQ Orbitrap XL spectrometer and 2,5-dihydroxybenzoic acid or α-cyano-4-hydroxycinnamic acid as the matrix.
Flash chromatography was performed with a *Biotage* Isolera One system using *Interchim* puriFlash cartridges (25 μm spherical silica).

2. Syntheses, purification methods, and analytical data

2.1. Preparation of the alkyne precursors

2.1.1 General procedure for Negishi coupling reactions with 15

*n*BuLi (in *n*-hexane) was added dropwise with stirring at 0 °C to a solution of **15** in THF (30 mL). After complete addition, the solution was treated with neat anhydrous $ZnCl_2$ and allowed to warm to room temperature. The respective aryl iodide and $Pd(PPh_3)_2Cl_2$ were added. The reaction mixture was heated to 50 °C for 5 h, allowed to cool to room temperature, and treated with *i*PrOH (1 mL) and *n*-hexane (20 mL). The solution was filtered through a short pad of Celite® and silica gel (eluent = EtOAc). All volatiles were removed from the filtrate under reduced pressure and the residue was purified by column chromatography on silica gel (*c*-hexane).

2.1.1.1 Synthesis of 17:

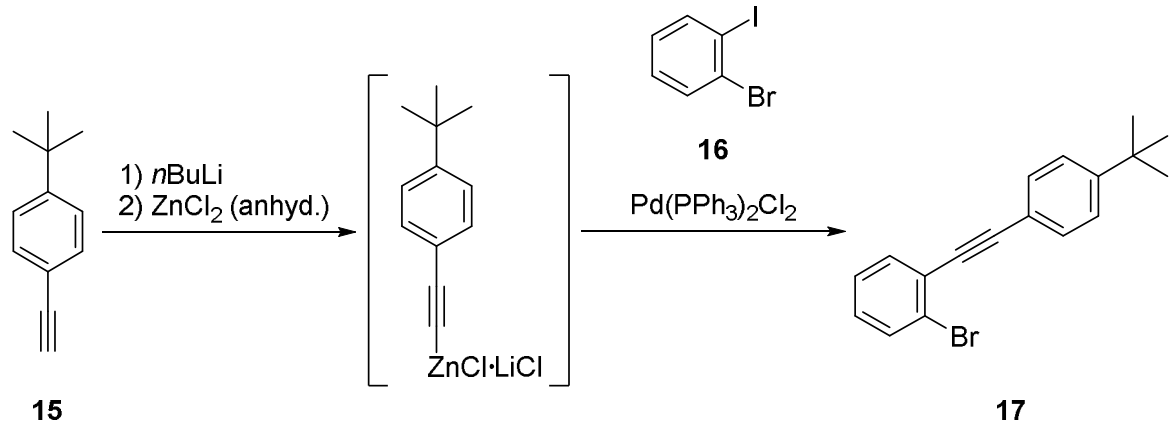

The synthesis was performed according to the general procedure described above using **15** (1.4 mL, 7.8 mmol), *n*BuLi (1.43 M in *n*-hexane, 5.00 mL, 7.15 mmol), $ZnCl_2$ (1.16 g, 8.48 mmol), **16** (0.91 mL, 7.1 mmol), and $Pd(PPh_3)_2Cl_2$ (0.050 g, 0.071 mmol). Recrystallization from MeOH afforded **17** as a yellow solid. Yield: 2.05 g (6.54 mmol, 93%).
The ^{1}H-NMR chemical shifts correspond to the reference values.[S9]

^{1}H NMR (400.1 MHz, $CDCl_3$): δ = 7.61 (ddd, ^3J(H,H) = 8.0 Hz, ^4J(H,H) = 1.3 Hz, ^5J(H,H) = 0.4 Hz, 1H), 7.57–7.50 (m, 3H), 7.41–7.36 (m, 2H), 7.28 (vtd, ^4J(H,H) = 1.3 Hz, 1H), 7.16 (ddd, ^3J(H,H) = 8.0 Hz, ^4J(H,H) = 7.4 Hz, ^5J(H,H) = 1.8 Hz, 1H), 1.33 (s, 9H).
R_f (*c*-hexane) = 0.45.

2.1.1.2 Synthesis of 19:

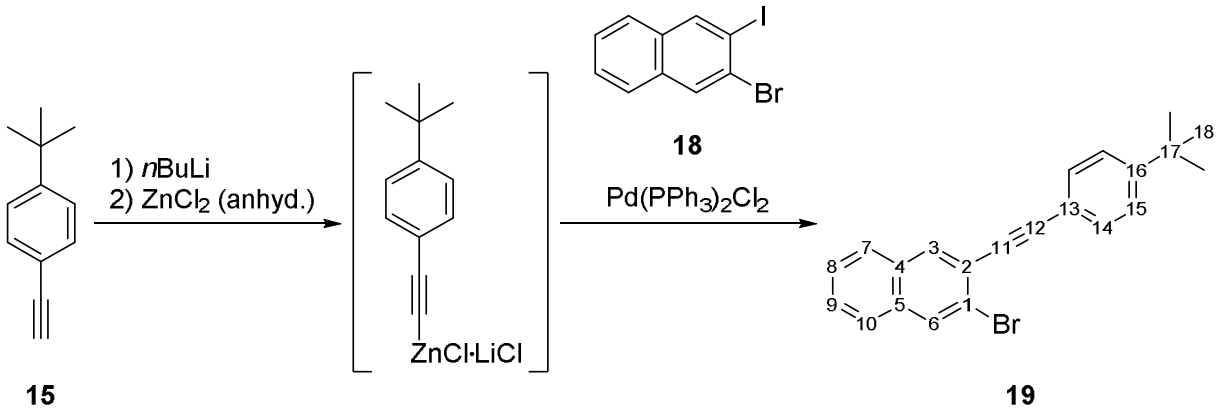

The synthesis was performed according to the general procedure described above using **15** (1.8 mL, 9.9 mmol), *n*BuLi (1.53 M in *n*-hexane, 6.20 mL, 9.50 mmol), $ZnCl_2$ (1.47 g, 10.8 mmol), **18** (3.00 g, 9.00 mmol), and $Pd(PPh_3)_2Cl_2$ (0.064 g, 0.090 mmol). **19** was obtained as a yellowish solid. Yield: 2.27 g (6.25 mmol, 69%). Single crystals were obtained by recrystallization of **19** from *n*-hexane.
Note: **19** can also be synthesized by using 2,3-dibromonaphthalene and $Pd(dppf)Cl_2$ under the same conditions (Yield: 61%).

^{1}H NMR (500.2 MHz, $CDCl_3$): δ = 8.12 (s, 1H; H-6), 8.08 (s, 1H; H-3), 7.80–7.77 (m, 1H; H-7), 7.75–7.72 (m, 1H; H-10), 7.58–7.55 (m, 2H; H-14), 7.52–7.48 (m, 2H; H-8,9), 7.42–7.40 (m, 2H; H-15), 1.35 (s, 9H; H-18).
^{13}C{^{1}H} NMR (125.8 MHz, $CDCl_3$): δ = 152.2 (C-16), 133.7 (C-5), 133.0 (C-3), 132.0 (C-4), 131.6 (C-14), 131.1 (C-6), 127.7 (C-7), 127.6 (C-9), 127.0 (C-10), 127.0 (C-8), 125.6 (C-15), 123.1 (C-2), 122.3 (C-1), 120.1 (C-13), 94.0 (C-12), 87.9 (C-11), 35.0 (C-17), 31.3 (C-18).
HRMS: Calculated *m/z* for $[C_{22}H_{19}Br]^+$: 362.06646, found: 362.06609.
R_f (*c*-hexane) = 0.20.

2.1.1.3 Synthesis of 21:

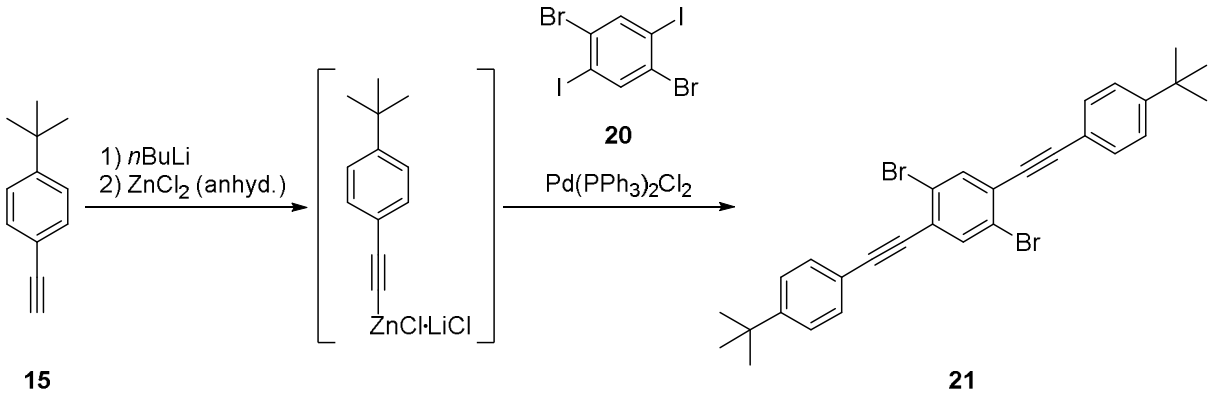

The synthesis was performed according to the general procedure described above using **15** (2.3 mL, 13 mmol), *n*BuLi (1.44 M in *n*-hexane, 8.80 mL, 12.7 mmol), $ZnCl_2$ (1.84 g, 13.5 mmol), **20** (3.00 g, 6.15 mmol), and $Pd(PPh_3)_2Cl_2$ (0.043 g, 0.062 mmol). **21** was obtained as a colorless solid. Yield: 3.23 g (5.89 mmol, 96%).
The ^{1}H-NMR chemical shifts correspond to the reference values.[S10]

^{1}H NMR (250.1 MHz, $CDCl_3$): δ = 7.77 (s, 2H), 7.54–7.49 (m, 4H), 7.42–7.37 (m, 4H), 1.34 (s, 18H).
R_f (*c*-hexane) = 0.41.

2.1.1.4 Synthesis of 24:

Synthesis of the iodinated precursor 23:

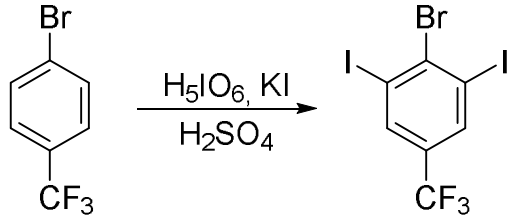

22 **23**

The synthesis was adapted from the procedure published by *Tilley et al.*;[S9] H_5IO_6 was used instead of KIO_4: H_5IO_6 (3.13 g, 13.8 mmol) and KI (6.85 g, 41.3 mmol) were slowly dissolved in conc. H_2SO_4 (125 mL) and the resulting brown solution was stirred for 30 min at room temperature. **22** (3.5 mL, 25 mmol) was added dropwise and the mixture was stirred at room temperature for 15 h, whereupon the viscosity increased and a solid precipitated. The reaction mixture was carefully poured onto ice (400 g) and the resulting suspension was filtered. The filter cake was treated with H_2O (approx. 250 mL) until the filtrate was tested neutral (pH ≈ 7). Recrystallisation from MeOH afforded **23** as a colorless crystalline solid. Yield: 10.77 g (22.59 mmol, 90%).
The ^{1}H-NMR chemical shift corresponds to the reference value.[S9]

^{1}H NMR (250.1 MHz, $CDCl_3$): δ = 8.06 (q, ^4J(H,F) ≈ 1 Hz).

Synthesis of 24:

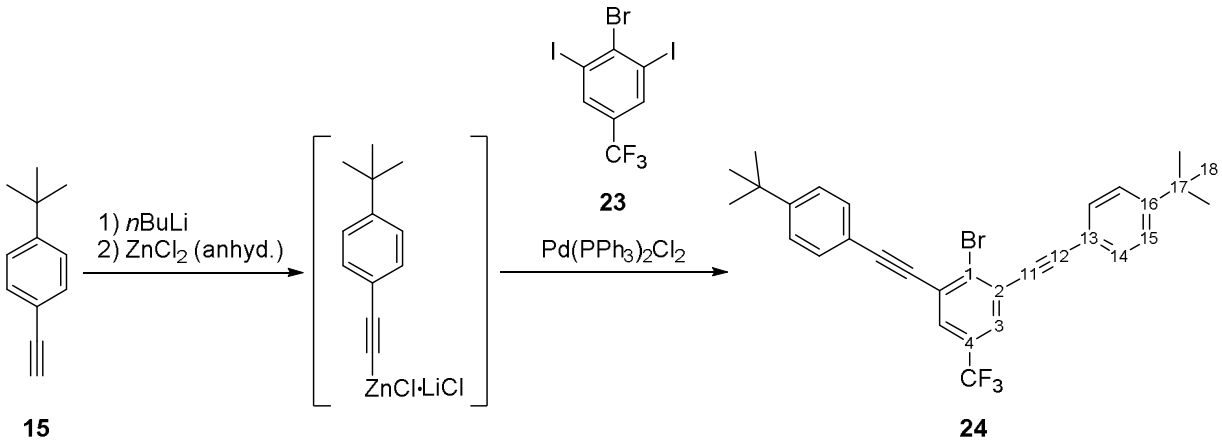

15 **24**

The synthesis was performed according to the general procedure described above using **15** (2.4 mL, 13 mmol), *n*-BuLi (1.44 M in *n*-hexane, 9.00 mL, 12.9 mmol), $ZnCl_2$ (1.89 g, 13.8 mmol), **23** (3.00 g, 6.29 mmol), and $Pd(PPh_3)_2Cl_2$ (0.044 g, 0.063 mmol). **24** was obtained as a yellowish solid. Yield: 3.31 g (6.16 mmol, 98%). Single crystals were obtained by slow evaporation of a solution of **24** in *n*-hexane.

^{1}H NMR (500.2 MHz, $CDCl_3$): δ = 7.70 (q, ^4J(H,F) ≈ 1 Hz, 2H; H-3), 7.56–7.53 (m, 4H; C-14), 7.43–7.40 (m, 4H; C-15), 1.34 (s, 18H; H-18).
^{13}C{^{1}H} NMR (125.8 MHz, $CDCl_3$): δ = 152.8 (C-16), 132.2 (q, ^4J(C,F) = 1.1 Hz; C-2), 131.8 (C-14), 129.9 (q, ^2J(C,F) = 33.5 Hz; C-4), 128.6 (q, ^3J(C,F) = 3.7 Hz; C-3), 127.7 (C-1), 125.7 (C-15), 123.4 (q, ^1J(C,F) = 272.0 Hz; CF_3), 119.3 (C-13), 96.2 (C-12), 86.6 (C-11), 35.1 (C-17), 31.3 (C-18).
^{19}F{^{1}H} NMR (470.4 MHz, $CDCl_3$): δ = −63.08 (s, CF_3).
HRMS: Calculated *m/z* for $[C_{31}H_{28}BrF_3+H]^+$: 537.13992 found: 537.13844.
R_f (*c*-hexane) = 0.37.

2.2. Preparation of the borinic and boronic acids

2.2.1 General procedure for the Br/B-exchange reactions

A Schlenk flask was charged with the respective *ortho*-alkynyl-substituted aryl bromide and kept under a dynamic vacuum for 0.5 h. The solid was dissolved in THF (30 mL) and the clear solution cooled to −78 °C. *t*BuLi (in *n*-pentane) was added dropwise to the solution and stirring at −78 °C was continued for 1 h. Either $MesB(OMe)_2$ or $B(OMe)_3$ was added and the reaction mixture allowed to warm to room temperature overnight. The mixture was treated with 2 N aqueous HCl (20 mL) and stirred for 1 h. The two liquid phases were separated, and the aqueous phase was extracted with CH_2Cl_2 (3 × 30 mL). The combined organic phases were washed with H_2O (1 × 50 mL) and brine (1 × 50 mL) and dried over Na_2SO_4. After filtration, the solvent was removed from the filtrate under reduced pressure.

2.2.1.1 Synthesis of 1a:

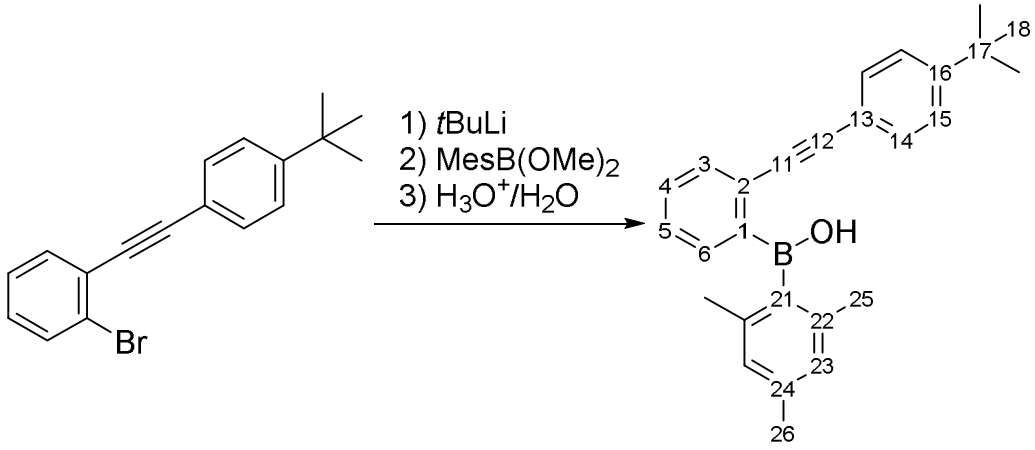

17 **1a**

The synthesis was conducted according to the general procedure described above using **17** (1.00 g, 3.19 mmol), *t*BuLi (1.60 M in *n*-pentane, 2.20 mL, 3.51 mmol), and $MesB(OMe)_2$ (0.75 mL, 3.5 mmol). The crude product was purified by column chromatography on silica gel (*c*-hexane → *c*-hexane:CH_2Cl_2 (3:1)). **1a** was obtained as a yellowish solid. Yield: 0.936 g (2.46 mmol, 77%). Single crystals were obtained by slow evaporation of a solution of **1a** in *n*-hexane.

^{1}H NMR (500.2 MHz, $CDCl_3$): δ = 8.52 (br, 1H; OH), 7.63 (ddd, ^3J(H,H) = 7.6 Hz, ^4J(H,H) = 1.2 Hz, ^5J(H,H) = 0.7 Hz, 1H; H-3), 7.53–7.51 (m, 2H; H-14), 7.47–7.43 (m, 2H; H-4,6), 7.42–7.40 (m, 2H; H-15), 7.28 (vtd, ^4J(H,H) = 1.2 Hz, 1H; H-5), 6.85 (m, 2H; H-23), 2.32 (s, 3H; H-26), 2.23 (s, 6H; H-25), 1.34 (s, 9H; H-18).
^{13}C{^{1}H} NMR (125.8 MHz, $CDCl_3$): δ = 152.7 (C-16), 139.3 (C-22), 138.9 (C-6), 137.7 (C-24), 136.8 (br; C-1,21), 133.1 (C-3), 131.6 (C-14), 131.3 (C-4), 128.5 (C-5), 127.3 (C-23), 126.4 (C-2), 125.7 (C-15), 119.1 (C-13), 94.4 (C-12), 89.2 (C-11), 35.0 (C-17), 31.3 (C-18), 22.2 (C-25), 21.4 (C-26).
^{11}B NMR (96.3 MHz, $CDCl_3$): δ = 49 ($h_{1/2}$ ≈ 800 Hz).
HRMS: Calculated *m*/*z* for $[C_{27}H_{29}BO]^+$: 380.23060 found: 380.23036.
R_f (3:1 *c*-hexane/DCM) = 0.40.

2.2.1.2 Synthesis of 2a:

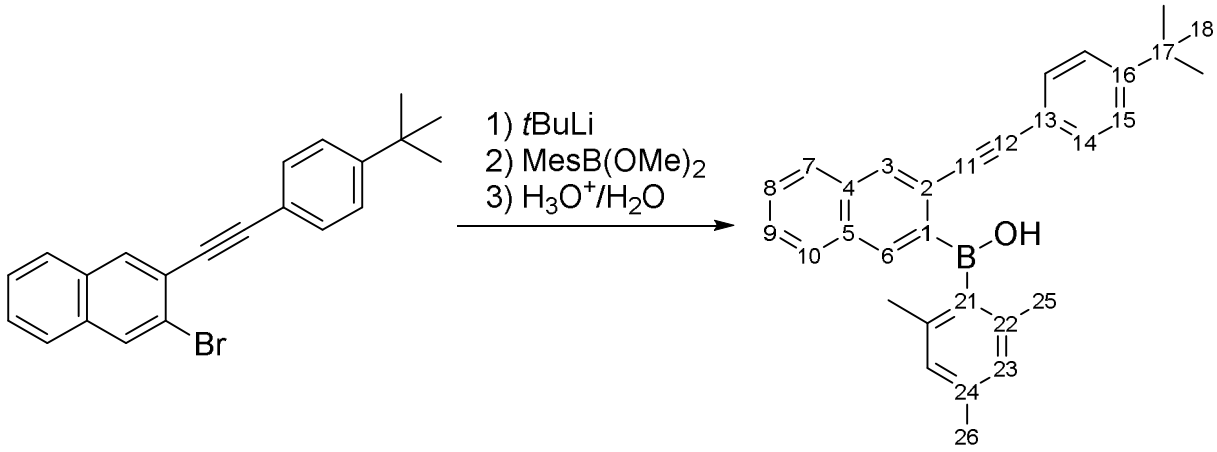

19 **2a**

The synthesis was conducted according to the general procedure described above using **19** (1.00 g, 2.75 mmol), *t*BuLi (1.60 M in *n*-pentane, 1.90 mL, 3.03 mmol), and $MesB(OMe)_2$ (0.65 mL, 3.0 mmol). The crude product was purified by column chromatography on silica gel (*c*-hexane:CH_2Cl_2 (3:1)). **2a** was obtained as a colorless solid. Yield: 0.693 g (1.61 mmol, 59%). Single crystals were obtained by slow evaporation of a solution of **2a** in *n*-hexane.

^{1}H NMR (500.2 MHz, $CDCl_3$): δ = 8.65 (br, 1H; OH), 8.14 (s, 1H; H-3), 8.00 (s, 1H; H-6), 7.83 (d, ^3J(H,H) = 8.1 Hz, 1H; H-7), 7.75 (d, ^3J(H,H) = 8.0 Hz, 1H; H-10), 7.57–7.54 (m, 3H; H-8,14), 7.47 (ddd, ^3J(H,H) = 8.0, ^3J(H,H) = 7.8, ^4J(H,H) = 0.8 Hz, 1H; H-9), 7.44–7.41 (m, 2H; H-15), 6.89 (s, 2H; H-23), 2.35 (s, 3H; H-26), 2.27 (s, 6H; H-25), 1.35 (s, 9H; H-18).
^{13}C{^{1}H} NMR (125.8 MHz, $CDCl_3$): δ = 152.6 (C-16), 141.3 (C-6), 139.6 (C-22), 137.8 (C-24), 136.9(*) (br; C-21), 134.4 (C-4), 133.2 (C-3), 132.7 (C-5), 131.6 (C-14), 129.1 (C-10), 128.4 (C-8), 127.5 (C-7), 127.3 (C-23), 127.1 (C-9), 125.8 (C-15), 122.2 (C-2), 119.2 (C-13), 93.9 (C-12), 89.6 (C-11), 35.1 (C-17), 31.3 (C-18), 22.4 (C-25), 21.4 (C-26); n.o. (C-1); (*) unequivocally detected only in the ^{H,C}HMBC spectrum.
^{11}B NMR (96.3 MHz, $CDCl_3$): δ = 49 ($h_{1/2} \approx 800$ Hz).
HRMS: Calculated *m*/*z* for $[C_{31}H_{31}BO]^+$: 430.24625 found: 430.24591.
R_f (3:1 *c*-hexane/DCM) = 0.21.

2.2.1.3 Synthesis of 3a:

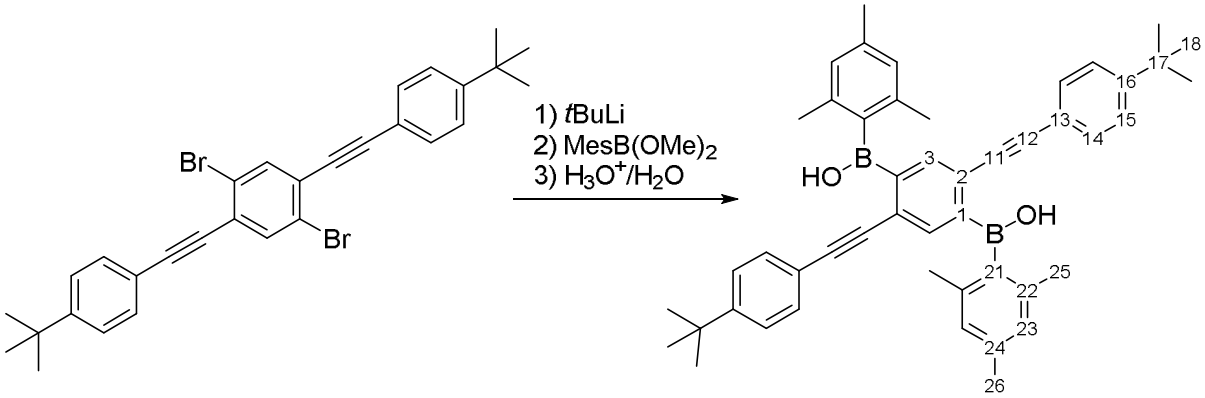

21 **3a**

The synthesis was conducted according to the general procedure described above using **21** (1.00 g, 1.82 mmol), *t*BuLi (1.60 M in *n*-pentane, 2.40 mL, 3.83 mmol), and $MesB(OMe)_2$ (0.80 mL, 3.7 mmol). The crude product was washed with acetone (4 × 5 mL), *n*-hexane (4 × 3 mL), and MeCN (4 × 2 mL) and dried under a dynamic vacuum. In order to remove traces of residual acetone, the solid was dissolved in toluene (100 mL) and the solution again evaporated to dryness. **3a** was obtained as a colorless solid. Yield: 0.552 g (0.809 mmol, 44%). Single crystals were obtained by recrystallization of **3a** from acetone.

^{1}H NMR (500.2 MHz, $CDCl_3$): δ = 8.42 (s, 2H; OH), 7.71 (s, 2H; H-3), 7.47–7.45 (m, 4H; H-14), 7.39–7.37 (m, 4H; H-15), 6.88 (s, 4H; H-23), 2.34 (s, 6H; H-26), 2.27 (s, 12H; H-25), 1.32 (s, 18H; H-18).
^{13}C{^{1}H} NMR (125.8 MHz, $CDCl_3$): δ = 152.8 (C-16), 142.4 (C-3), 139.6 (br; C-1), 139.5 (C-22), 138.1 (C-24), 136.1 (br; C-21), 131.6 (C-14), 127.5 (C-23), 126.1 (C-2), 125.7 (C-15), 118.8 (C-13), 96.1 (C-12), 89.1 (C-11), 35.0 (C-17), 31.3 (C-18), 22.4 (C-25), 21.4 (C-26).
^{11}B NMR (96.3 MHz, $CDCl_3$): δ = 47 ($h_{1/2} \approx 1350$ Hz).
HRMS: Calculated *m*/*z* for $[C_{48}H_{52}B_2O_2]^+$: 682.41479 found: 602.41205.

2.2.1.4 Synthesis of 7a:

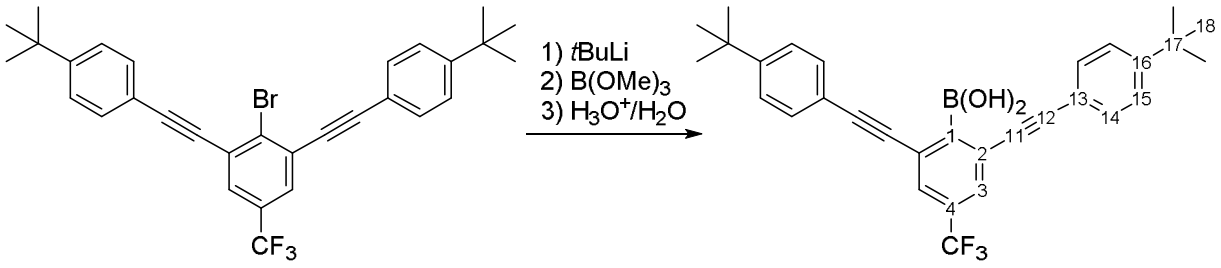

24 **7a**

The synthesis was conducted according to the general procedure described above using **24** (1.00 g, 1.86 mmol), *t*BuLi (1.60 M in *n*-pentane, 1.30 mL, 2.05 mmol), and $B(OMe)_3$ (0.25 mL, 2.2 mmol). The crude product was taken up in *n*-hexane (100 mL) and extracted into MeCN (3 × 50 mL). The solvent was removed from the extract under reduced pressure to afford a mixture of **7a** and its respective boroxine. This mixture was dissolved in MeOH (100 mL) and H_2O (1 mL), and treated with F_3CCOOH (0.5 mL) at a temperature of 60 °C for 5 min. All volatiles were removed under reduced pressure. The free boronic acid **7a** was obtained as an off-white solid. Yield: 0.864 g (1.72 mmol, 92%). Single crystals of the diisopropyl ester of **7a** (**7a^{iPr}**) were obtained by recrystallization of **7a** from *i*PrOH.

^{1}H NMR (500.2 MHz, $CDCl_3$): δ = 7.78 (q, ^4J(H,F) ≈ 1 Hz, 2H; H-3), 7.52–7.50 (m, 4H; H-14), 7.43–7.40 (m, 4H; H-15), 6.28 (s, 2H; OH), 1.34 (s, 18H; H-18).
^{13}C{^{1}H} NMR (125.8 MHz, $CDCl_3$): δ = 153.2 (C-16), 139.6(*) (C-1), 132.4 (q, ^2J(C,F) = 33.3 Hz; C-4), 131.7 (C-14), 128.9 (q, ^3J(C,F) = 3.8 Hz; C-3), 128.7 (C-2), 125.8 (C-15), 123.3 (q, ^1J(C,F) = 273.0 Hz; CF_3), 118.5 (C-13), 95.7 (C-12), 87.6 (C-11), 35.1 (C-17), 31.3 (C-18); (*) unequivocally detected only in the ^{H,C}HMBC spectrum.
^{11}B NMR (96.3 MHz, $CDCl_3$): δ = 29 ($h_{1/2}$ ≈ 450 Hz).
^{19}F{^{1}H} NMR (470.4 MHz, $CDCl_3$): δ = −63.52 (s, CF_3).
HRMS: Calculated *m*/*z* for $[C_{31}H_{30}BO_2+H]^+$: 503.23637 found: 503.23464.

2.3. Preparation of the B,O-PAHs

2.3.1 General procedure for the cycloaddition reaction

A Schlenk tube was charged with the respective borinic or boronic acid and evacuated for 0.5 h. The solid was dissolved in $CHCl_3$ and the catalyst [$Au(PPh_3)NTf_2$] was added at room temperature. In most cases, the cyclization reaction occurred instantaneously (the synthesis of **8a** required a reaction time of several hours). The reaction mixture was filtered over a short plug of silica gel with $CHCl_3$ as eluent. All volatiles were removed from the filtrate under reduced pressure.

2.3.1.1 Synthesis of 4a:

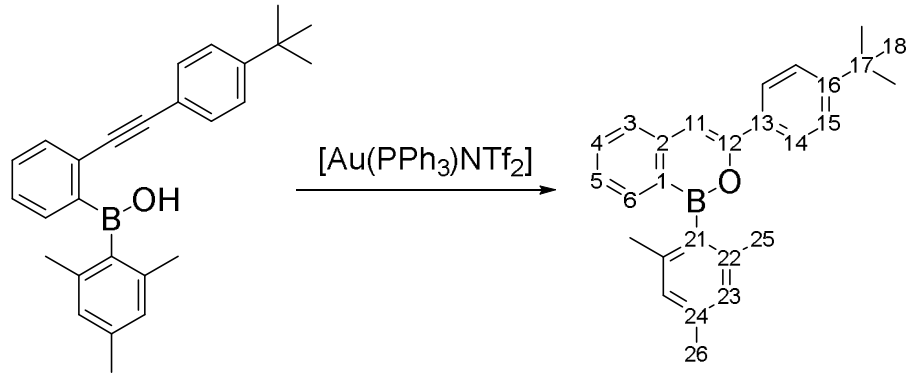

1a **4a**

The synthesis was conducted according to the general procedure described above using **1a** (0.050 g, 0.13 mmol), $CHCl_3$ (1 mL), and [$Au(PPh_3)NTf_2$] (0.001 g, 0.001 mmol). **4a** was obtained as a colorless solid. Yield: 0.050 g (0.13 mmol, quant.). Single crystals were obtained by slow evaporation of a solution of **4a** in *n*-hexane.

^{1}H NMR (500.2 MHz, $CDCl_3$): δ = 7.95–7.93 (m, 2H; H-14), 7.77 (dd, ^3J(H,H) = 7.5 Hz, ^4J(H,H) = 1.4 Hz, 1H; H-6), 7.68 (ddd, ^3J(H,H) = 8.3 Hz, ^3J(H,H) = 7.1 Hz, ^4J(H,H) = 1.4 Hz, 1H; H-4), 7.62–7.60 (m, 1H; H-3), 7.48–7.46 (m, 2H; H-15), 7.35 (vtd, ^4J(H,H) = 1.2 Hz, 1H; H-5), 7.23 (s, 1H; H-11), 6.95 (s, 2H; H-23), 2.39 (s, 3H; H-26), 2.21 (s, 6H; H-25), 1.37 (s, 9H; H-18).
^{13}C{^{1}H} NMR (125.8 MHz, $CDCl_3$): δ = 152.4 (C-12), 152.3 (C-16), 141.7 (C-2), 140.6 (C-22), 138.2 (C-24), 136.5 (C-6), 134.9(*) (C-21), 133.2 (C-4), 132.6 (C-13), 129.5(*) (C-1), 127.4 (C-23), 126.4 (C-3), 126.2 (C-5), 125.7 (C-15), 125.2 (C-14), 106.2 (C-11), 34.9 (C-17), 31.4 (C-18), 22.8 (C-25), 21.5 (C-26); (*) unequivocally detected only in the ^{H,C}HMBC spectrum.
^{11}B NMR (96.3 MHz, $CDCl_3$): δ = 46 ($h_{1/2} \approx$ 1000 Hz).
HRMS: Calculated *m/z* for $[C_{27}H_{29}BO]^+$: 380.23060, found: 380.23111.
UV/Vis ($CHCl_3$): λ_{max} (ε) = 301 (21861), 312 (20685), 332 (12098 $mol^{-1}dm^3cm^{-1}$), 348 nm (sh).
Fluorescence ($CHCl_3$, λ_{ex} = 301 nm): λ_{max} = 390 nm; Φ_{PL} = 8%.
Cyclic voltammetry (THF, [*n*Bu_4N][PF_6] 0.1 M, 200 mV s^{-1}, vs. FcH/FcH^+): Cathodic scan: E_{pc} = −3.60 V, E_{pa} = −2.69 V; anodic scan: E_{pa} = −0.06 V.
Melting point: 95 °C.

2.3.1.2 Synthesis of 5a:

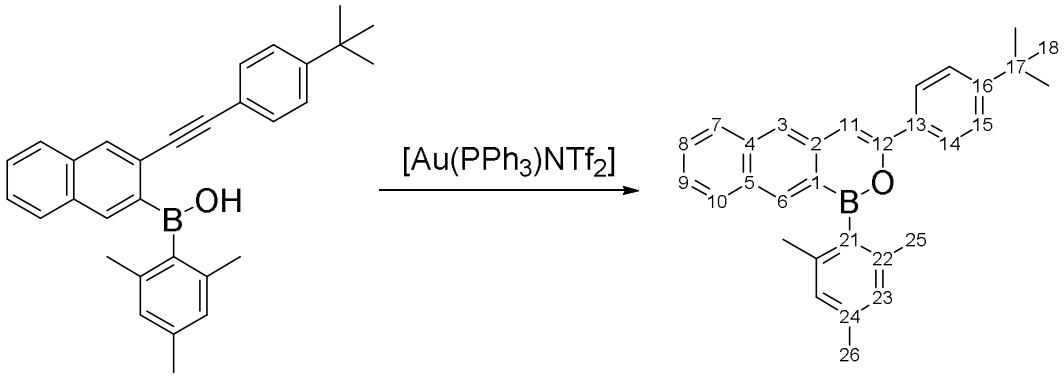

2a **5a**

The synthesis was conducted according to the general procedure described above using **2a** (0.050 g, 0.12 mmol), $CHCl_3$ (1 mL), and $[Au(PPh_3)NTf_2]$ (0.001 g, 0.001 mmol). The crude product was taken up in *n*-pentane (10 mL) and filtered again. All volatiles were removed from the filtrate under reduced pressure and the solid residue was washed with MeCN (1 × 0.5 mL). **5a** was obtained as a yellowish solid. Yield: 0.045 g (0.10 mmol, 90%).

^{1}H NMR (500.2 MHz, $CDCl_3$): δ = 8.36 (s, 1H; H-6), 8.05 (s, 1H; H-3), 7.98–7.94 (m, 3H; H-7,14), 7.89 (d, ^3J(H,H) = 8.1 Hz, 1H; H-10), 7.57 (ddd, ^3J(H,H) = 8.1, ^3J(H,H) = 6.8, ^4J(H,H) = 1.2 Hz, 1H; H-8), 7.49–7.47 (m, 2H; H-15), 7.45 (ddd, ^3J(H,H) = 8.1, ^3J(H,H) = 6.8, ^4J(H,H) = 1.1 Hz, 1H; H-9), 7.34 (s, 1H; H-11), 7.00 (s, 2H; H-23), 2.42 (s, 3H; H-26), 2.25 (s, 6H; H-25), 1.37 (s, 9H; H-18).
^{13}C{^{1}H} NMR (125.8 MHz, $CDCl_3$): δ = 152.2 (C-16), 151.3 (C-12), 140.7 (C-22), 138.9 (C-6), 138.4 (C-24), 137.0 (C-2), 136.5 (C-4), 135.0(*) (C-21), 132.7 (C-13), 132.1 (C-5), 130.3 (C-1), 129.4 (C-10), 128.1 (C-8), 127.9 (C-7), 127.4 (C-23), 125.7 (C-15), 125.4 (C-9), 125.2 (C-14), 124.0 (C-3), 106.1 (C-11), 34.9 (C-17), 31.4 (C-18), 22.8 (C-25), 21.5 (C-26); (*) unequivocally detected only in the ^{H,C}HMBC spectrum.
^{11}B NMR (96.3 MHz, $CDCl_3$): δ = 46 ($h_{1/2}$ ≈ 1100 Hz).
HRMS: Calculated *m*/*z* for $[C_{31}H_{31}BO]^+$: 430.24625, found: 430.24624.
UV/Vis ($CHCl_3$): λ_{max} (ε) = 290(45925), 297 (45316), 328 (sh), 339 (34508), 351 (20644 $mol^{-1}dm^3cm^{-1}$), 379 (sh), 395 nm (sh).
Fluorescence ($CHCl_3$, λ_{ex} = 339 nm): λ_{max} = 426 (sh), 445 nm; Φ_{PL} = 20%.
Cyclic voltammetry (THF, [*n*Bu$_4$N][PF$_6$] 0.1 M, 200 mV s^{-1}, vs. FcH/FcH$^+$): $E_{1/2}$ = −2.58 V.
Melting point: 140 °C.

2.3.1.3 Synthesis of 6a:

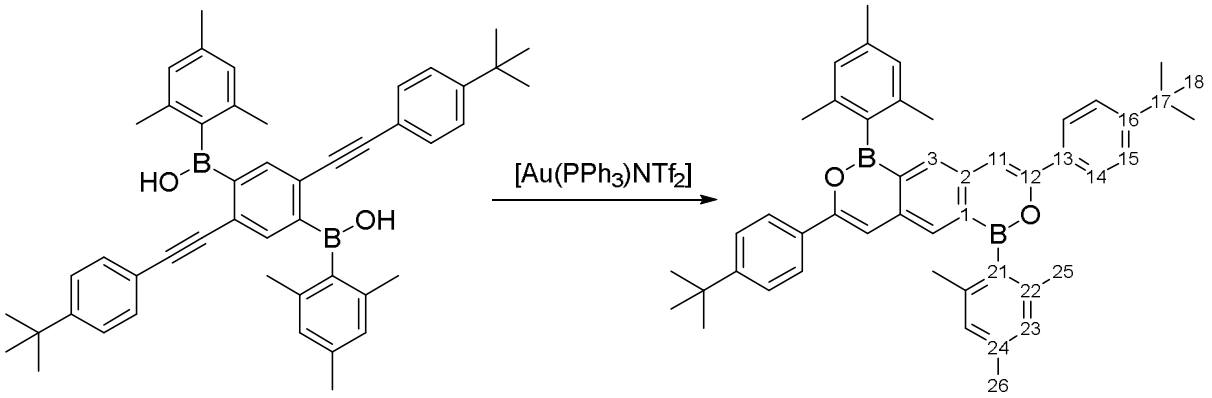

3a **6a**

The synthesis was conducted according to the general procedure described above using **3a** (0.050 g, 0.073 mmol), $CHCl_3$ (1 mL), and $[Au(PPh_3)NTf_2]$ (0.001 g, 0.001 mmol). The crude product was washed with *n*-hexane (3 × 0.5 mL). **6a** was obtained as a yellowish solid. Yield: 0.041 g (0.060 mmol, 82%). Single crystals were obtained by slow evaporation of a saturated solution of **6a** in EtOAc:*n*-pentane (1:1) at 0 °C.

^{1}H NMR (500.2 MHz, $CDCl_3$): δ = 8.03 (s, 2H; H-3), 7.93–7.90 (m, 4H; H-14), 7.47–7.46 (m, 4H, H-15), 7.27 (s, 2H; H-11), 7.03 (s, 4H, H-23), 2.45 (s, 6H; H-26), 2.28 (s, 12H; H-25), 1.37 (s, 18H, H-18).
^{13}C{^{1}H} NMR (125.8 MHz, $CDCl_3$): δ = 152.2 (C-16), 151.6 (C-12), 140.7 (C-24), 138.6 (C-2), 138.5 (C-22), 134.7 (C-21), 134.7 (C-3), 133.4 (C-1), 132.5 (C-13), 127.5 (C-23), 125.8 (C-15), 125.1 (C-14), 106.4 (C-11), 34.9 (C-17), 31.4 (C-18), 22.9 (C-25), 21.5 (C-26).
^{11}B NMR (96.3 MHz, $CDCl_3$): δ = 43 ($h_{1/2}$ ≈ 2000 Hz).
HRMS: Calculated *m/z* for $[C_{48}H_{52}B_2O_2]^+$: 682.41479, found: 682.41546
UV/Vis ($CHCl_3$): λ_{max} (ε) = 312 (sh), 326 (sh), 343 (sh), 360 (75215), 373 (56253), 404 (13108), 425 nm (8628 $mol^{-1}dm^3cm^{-1}$).
Fluorescence ($CHCl_3$, λ_{ex} = 360 nm): λ_{max} = 452, 475, 507 (sh) nm; Φ_{PL} = 41%.
Cyclic voltammetry (THF, [*n*Bu_4N][PF_6] 0.1 M, 200 mV s^{-1}, vs. FcH/FcH^+): E_{pc} = −2.88 V.
Melting point: >300 °C (decomposition)

2.3.1.4 Synthesis of 8a:

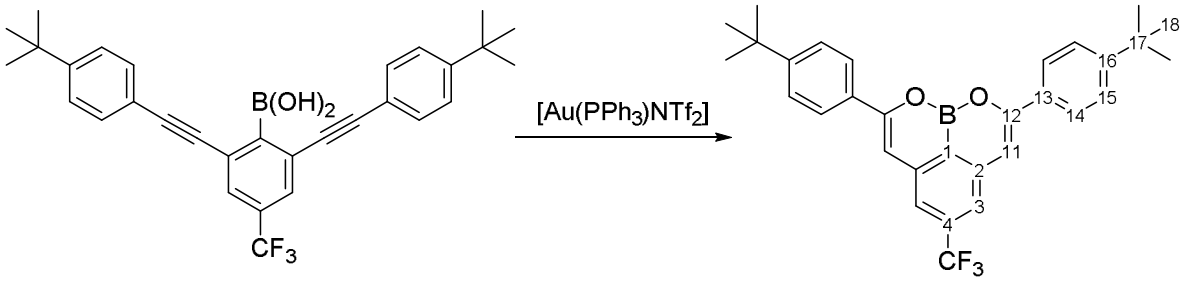

7a **8a**

The synthesis was conducted according to the general procedure described above using **7a** (0.050 g, 0.10 mmol), $CHCl_3$ (1 mL), and $[Au(PPh_3)NTf_2]$ (0.001 g, 0.001 mmol). The crude product was taken up in *n*-pentane (10 mL) and filtered. All volatiles were removed from the filtrate under reduced pressure. **8a** was obtained as a yellowish solid. Yield: 0.043 g (0.086 mmol, 86%). Single crystals were obtained by slow evaporation of a solution of **8a** in *n*-hexane.

^{1}H NMR (500.2 MHz, $CDCl_3$): δ = 7.91–7.88 (m, 4H; H-14), 7.52–7.49 (m, 4H; H-15), 7.48 (s, 2H; H-3), 6.97 (s, 2H; H-11), 1.38 (s, 18H; H-18).
^{13}C{^{1}H} NMR (125.8 MHz, $CDCl_3$): δ = 154.2 (C-12), 152.9 (C-16), 141.9 (C-2), 136.0 (q, ^2J(C,F) = 31.6 Hz; C-4), 132.4 (br; C-1), 132.4 (C-13), 125.8 (C-15), 125.5 (C-14), 124.3 (q, ^1J(C,F) = 273.5 Hz; CF_3), 117.1 (q, ^3J(C,F) = 3.8 Hz; C-3), 104.2 (C-11), 34.9 (C-17), 31.4 (C-18).
^{11}B NMR (96.3 MHz, $CDCl_3$): δ = 29 ($h_{1/2}$ ≈ 750 Hz).
^{19}F{^{1}H} NMR (470.4 MHz, $CDCl_3$): δ = −62.81 (s, CF_3).
HRMS: Calculated *m*/*z* for $[C_{31}H_{30}B_2O_2]^+$: 502.22855, found: 502.22908.
UV/Vis ($CHCl_3$): λ_{max} (ε) = 270 (13015), 314 (25351), 329 (sh), 366 (5963), 386 nm (4312 $mol^{-1}dm^3cm^{-1}$).
Fluorescence ($CHCl_3$, λ_{ex} = 314 nm): λ_{max} = 397, 419, 443, 468, 510 nm (sh); Φ_{PL} = 43%.
Cyclic voltammetry (THF, [*n*Bu_4N][PF_6] 0.1 M, 200 mV s^{-1}, vs. FcH/FcH^+): E_{pa} = 0.20 V.
Melting point: 79 °C.

2.4. Preparation of the B,N-PAHs

2.4.1 General procedure for the cycloaddition reaction

An NMR tube was charged with the respective borinic or boronic acid and evacuated for 0.5 h. In the glovebox, neat $(Me_3Si)_2NMe$ and C_6D_6 (1 mL) were added. The tube was flame-sealed under vacuum and heated to 120 °C for 2 d in the cases of **4b** and **5b** and for 2–3 d in the cases of **6b**, **8ab**, and **8c** (at this point, the quantitative conversion was confirmed by in situ NMR spectroscopy at room temperature). The resulting pale yellow solution was transferred to a new NMR tube, evaporated to dryness, and kept under a dynamic vacuum overnight. The solid residue was dissolved in $CDCl_3$ (1 mL) and $[Au(PPh_3)NTf_2]$ was added. The NMR tube was flame-sealed under vacuum and heated to 60 °C for several hours (the reaction progress was monitored by NMR spectroscopy). The solution was cooled to room temperature and filtered over a short plug of silica gel with $CHCl_3$ as eluent. All volatiles were removed from the filtrate under reduced pressure.

2.4.1.1 Synthesis of 4b:

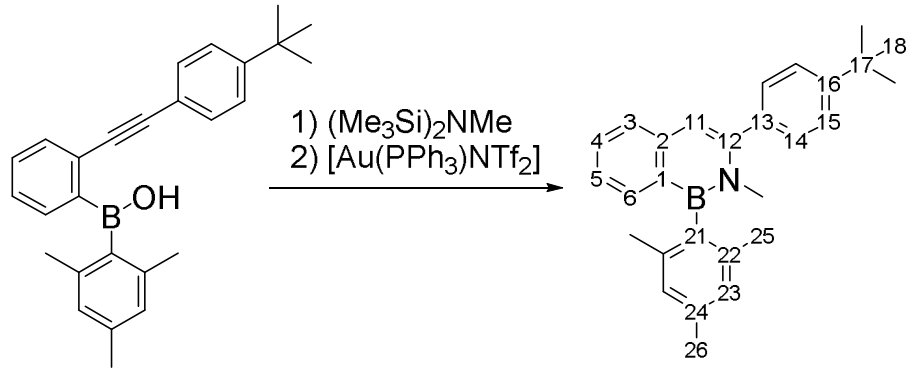

1a **4b**

The synthesis was conducted according to the general procedure described above using **1a** (0.050 g, 0.13 mmol), $(Me_3Si)_2NMe$ (0.024 mg, 0.14 mmol), and $[Au(PPh_3)NTf_2]$ (0.005 g, 0.007 mmol). The solution was heated to 60 °C for 4 h. The crude product was washed with MeCN (4 × 0.25 mL) and *n*-pentane (0.20 mL). **4b** was obtained as a colorless solid. Yield: 0.034 g (0.086 mmol, 66%). Single crystals of **4b** were grown from hot MeCN.

^{1}H NMR (500.2 MHz, $CDCl_3$): δ = 7.60–7.55 (m, 3H; H-3,4,6), 7.49–7.46 (m, 2H; H-15), 7.40–7.38 (m, 2H; H-14), 7.25–7.22 (m, 1H; H-5), 6.95 (s, 2H; H-23), 6.69 (s, 1H; H-11), 3.18 (s, 3H; NMe), 2.38 (s, 3H; H-26), 2.10 (s, 6H; H-25), 1.40 (s, 9H; H-18).
^{13}C{^{1}H} NMR (125.8 MHz, $CDCl_3$): δ = 151.0 (C-16), 146.4 (C-12), 140.9 (C-2), 139.8 (C-22), 138.0 (br; C-21), 137.0 (C-24), 136.2 (C-13), 135.5 (C-6), 132.8 (br; C-1), 130.7 (C-4), 129.1 (C-14), 127.2 (C-23), 126.1 (C-3), 125.2 (C-15), 124.3 (C-5), 113.1 (C-11), 38.8 (NMe), 34.8 (C-17), 31.5 (C-18), 22.7 (C-25), 21.4 (C-26).
^{11}B NMR (96.3 MHz, $CDCl_3$): δ = 39 ($h_{1/2}$ ≈ 850 Hz).
HRMS: Calculated *m/z* for $[C_{27}H_{29}BO]^+$: 380.23060, found: 380.23111.
UV/Vis ($CHCl_3$): λ_{max} (ε) = 293 (14001 $mol^{-1}dm^3cm^{-1}$), 323 (sh), 332 nm (sh).
Fluorescence ($CHCl_3$, λ_{ex} = 293 nm): λ_{max} = 383 nm; Φ_{PL} = 4%.
Cyclic voltammetry (THF, [*n*Bu_4N][PF_6] 0.1 M, 200 mV s^{-1}, vs. FcH/FcH^+): no redox potential observed.
Melting point: 175 °C.

2.4.1.2 Synthesis of 5b:

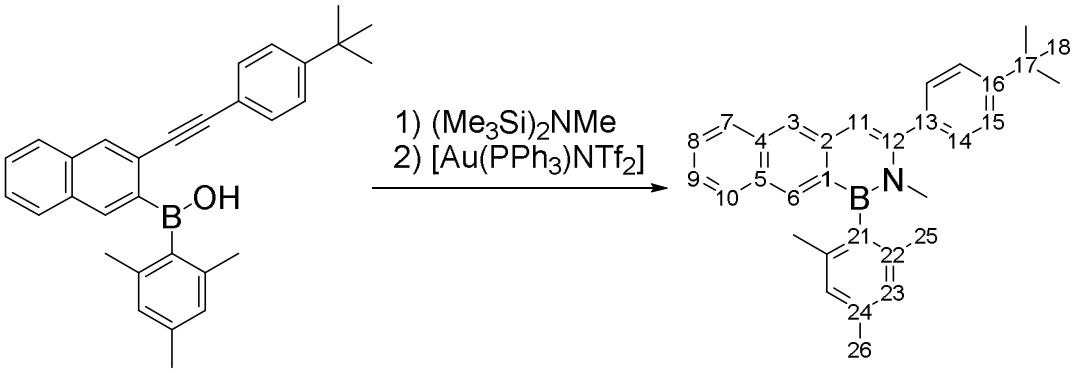

The synthesis was conducted according to the general procedure described above using **2a** (0.050 g, 0.12 mmol), $(Me_3Si)_2NMe$ (0.021 mg, 0.12 mmol), and $[Au(PPh_3)NTf_2]$ (0.004 g, 0.006 mmol). The reaction solution was heated to 60 °C for 4 h. The crude product was washed with MeCN (4 × 0.25 mL) and *n*-pentane (0.20 mL). **5b** was obtained as a yellowish solid. Yield: 0.037 g (0.083 mmol, 72%). Single crystals were obtained by recrystallization of **5b** from MeCN.

^{1}H NMR (500.2 MHz, $CDCl_3$): δ = 8.16 (s, 1H; H-6), 8.05 (s, 1H; H-3), 7.93 (dd, ^3J(H,H) = 8.5, ^4J(H,H) = 1.2 Hz, 1H; H-7), 7.86 (dd, ^3J(H,H) = 8.5, ^4J(H,H) = 1.2 Hz, 1H; H-10), 7.51–7.48 (m, 3H; H-8,15), 7.45–7.43 (m, 2H; H-14), 7.38 (ddd, ^3J(H,H) = 8.5, ^3J(H,H) = 8.3, ^4J(H,H) = 1.2 Hz, 1H; H-9), 7.00 (s, 2H; H-23), 6.80 (s, 1H; H-11), 3.16 (s, 3H; NMe), 2.43 (s, 3H; H-26), 2.15 (s, 6H; H-25), 1.41 (s, 9H; H-18).
^{13}C{^{1}H} NMR (125.8 MHz, $CDCl_3$): δ = 151.0 (C-16), 145.9 (C-12), 139.8 (C-22), 138.0 (br; C-21), 137.5 (C-2), 137.2 (C-24), 136.8 (C-6), 136.3 (C-13), 135.1 (C-4), 131.5 (br; C-1), 131.1 (C-5), 129.1 (C-10), 129.1 (C-14), 127.7 (C-7), 127.3 (C-23), 126.7 (C-8), 125.2 (C-15), 124.4 (C-9), 123.4 (C-3), 113.1 (C-11), 38.6 (NMe), 34.8 (C-17), 31.5 (C-18), 22.6 (C-25), 21.5 (C-26).
^{11}B NMR (96.3 MHz, $CDCl_3$): δ = 41 ($h_{1/2} \approx$ 850 Hz).
HRMS: Calculated *m*/*z* for $[C_{32}H_{34}BN]^+$: 443.27788, found: 443.27859.
UV/Vis ($CHCl_3$): λ_{max} (ε) = 268 (44824), 326 (9621), 341 (12571 $mol^{-1}dm^3cm^{-1}$), 379 (sh), 405 nm (sh).
Fluorescence ($CHCl_3$, λ_{ex} = 341 nm): λ_{max} = 428 (sh), 448, 470 nm (sh); Φ_{PL} = 32%.
Cyclic voltammetry (THF, [*n*Bu_4N][PF_6] 0.1 M, 200 mV s^{-1}, vs. FcH/FcH^+): $E_{1/2}$ = -2.80 V.
Melting point: 207 °C.

2.4.1.3 Synthesis of 6b:

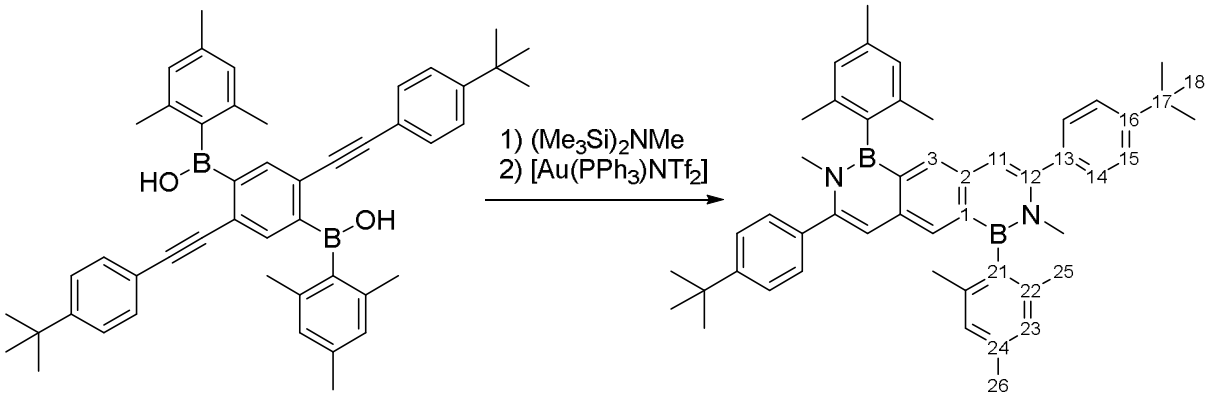

3a **6b**

The synthesis was conducted according to the general procedure described above using **3a** (0.050 g, 0.073 mmol), $(Me_3Si)_2NMe$ (0.032 mg, 0.18 mmol), and $[Au(PPh_3)NTf_2]$ (0.003 g, 0.004 mmol). The reaction solution was heated to 60 °C for 2 d. The crude product was taken up in cold CH_2Cl_2 (5 mL) and filtered through a syringe filter (45 µm). The filter cake was dissolved in warm $CHCl_3$ (15 mL), the solution was pressed through the filter, and all volatiles were removed from the filtrate under reduced pressure. The solid residue was washed with *n*-pentane (0.2 mL). **6b** was obtained as a yellow solid. Yield: 0.033 g (0.047 mmol, 64%).

^{1}H NMR (500.2 MHz, $CDCl_3$): δ = 7.77 (s, 2H; H-3), 7.41–7.40 (m, 4H; H-15), 7.35–7.34 (m, 4H; H-14), 6.92 (s, 4H; H-23), 6.64 (s, 2H; H-11), 3.17 (s, 6H; NMe), 2.36 (s, 6H; H-26), 2.10 (s, 12H; H-25), 1.36 (s, 18H; H-18).
^{13}C{^{1}H} NMR (125.8 MHz, $CDCl_3$): δ = 150.7 (C-16), 144.8 (C-12), 139.8 (C-22), 138.1(*) (C-21), 136.9 (C-24), 136.7 (C-2), 136.3 (C-13), 135.0(*) (C-1), 133.2 (C-3), 129.0 (C-14), 127.2 (C-23), 125.0 (C-15), 114.1 (C-11), 38.8 (NMe), 34.8 (C-17), 31.5 (C-18), 22.7 (C-25), 21.4 (C-26); (*) unequivocally detected only in the ^{H,C}HMBC spectrum.
^{11}B NMR (96.3 MHz, $CDCl_3$): δ = 39 ($h_{1/2}$ ≈ 1800 Hz).
HRMS: Calculated *m*/*z* for $[C_{50}H_{58}B_2N_2]^+$: 708.47806, found: 708.47997.
UV/Vis ($CHCl_3$): λ_{max} (ε) = 347 (27027 $mol^{-1}dm^3cm^{-1}$), 388 nm (sh).
Fluorescence ($CHCl_3$, λ_{ex} = 347 nm): λ_{max} = 426, 446 nm; Φ_{PL} = 16%.
Cyclic voltammetry (THF, [*n*Bu$_4$N][PF$_6$] 0.1 M, 200 mV s^{-1}, vs. FcH/FcH$^+$): $E_{1/2}$ = −3.00 V.
Melting point: >300 °C (decomposition).

2.4.1.4 Synthesis of 8c:

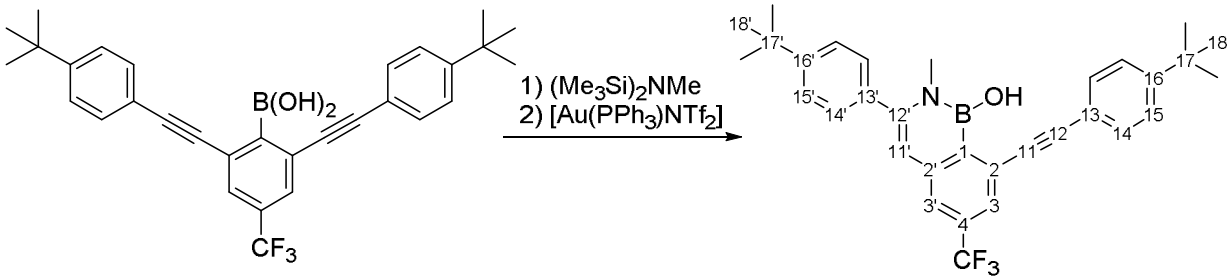

7a **8c**

The synthesis was conducted according to the general procedure described above using **7a** (0.050 g, 0.10 mmol), $(Me_3Si)_2NMe$ (0.026 mg, 0.15 mmol), and $[Au(PPh_3)NTf_2]$ (0.002 g, 0.002 mmol). The solution was heated to 60 °C for 4 h. The crude product was taken up in *n*-pentane (10 mL) and filtered. All volatiles were removed from the filtrate under reduced pressure. **8c** was obtained as an amber-colored solid. Yield: 0.048 g (0.093 mmol, 94%).

^{1}H NMR (500.2 MHz, $CDCl_3$): δ = 7.66 (s, 1H; H-3), 7.63 (s, 1H; H-3'), 7.58–7.55 (m, 2H; H-14), 7.47–7.43 (m, 4H; H-15,15'), 7.34–7.31 (m, 2H; H-14'), 7.14 (s, 1H; OH), 6.24 (s, 1H; H-11'), 3.22 (s, 3H; NMe), 1.39 (s, 9H; H-18'), 1.36 (s, 9H; H-18).
^{13}C{^{1}H} NMR (125.8 MHz, $CDCl_3$): δ = 153.0 (C-16), 151.5 (C-16'), 149.3 (C-12'), 143.2 (C-2'), 135.1 (C-13'), 131.9 (q, ^{2}J(C,F) = 32.3 Hz; C-4), 131.6 (C-14), 128.7 (C-14'), 127.8(*) (C-1), 126.7 (C-2), 125.9 (C-15), 125.3 (C-15'), 124.4 (q, ^{3}J(C,F) = 3.4 Hz; C-3), 124.0 (q, ^{1}J(C,F) = 272.8 Hz; CF_3), 123.3 (q, ^{3}J(C,F) = 3.9 Hz; C-3'), 118.7 (C-13), 107.0 (C-11'), 94.6 (C-12), 89.1 (C-11), 35.1 (C-17), 34.9 (C-17'), 33.6 (NMe), 31.5 (C-18'), 31.3 (C-18);); (*) unequivocally detected only in the ^{H,C}HMBC spectrum.
^{11}B NMR (96.3 MHz, $CDCl_3$): δ = 29 ($h_{1/2}$ ≈ 550 Hz).
^{19}F{^{1}H} NMR (470.4 MHz, $CDCl_3$): δ = −63.05 (s, CF_3).
HRMS: Calculated *m/z* for $[C_{32}H_{33}BNO]^+$: 515.26018, found: 515.26207.
UV/Vis ($CHCl_3$): λ_{max} (ε) = 294 (30871), 310 (29122 $mol^{-1}dm^3cm^{-1}$), 350 nm (sh).
Melting point: ca. 70 °C (with decomposition).

2.4.1.5 Synthesis of 8ab:

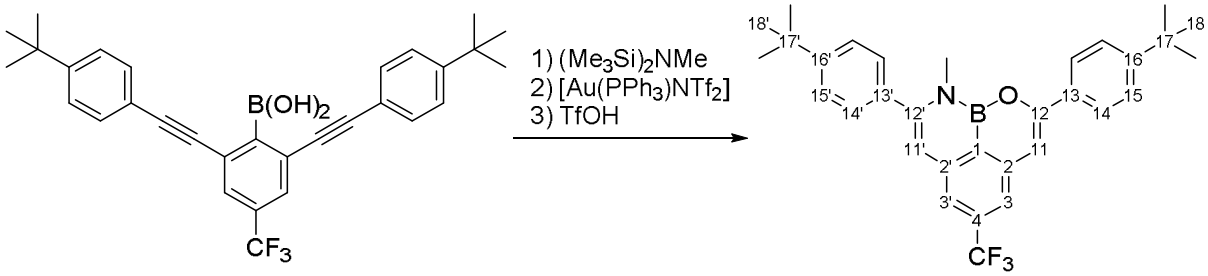

7a **8ab**

The synthesis was conducted according to the general procedure described above using **7a** (0.050 g, 0.10 mmol), $(Me_3Si)_2NMe$ (0.026 mg, 0.15 mmol), and $[Au(PPh_3)NTf_2]$ (0.002 g, 0.002 mmol). The solution was heated to 60 °C for 4 h. The solid residue was taken up in *n*-pentane (10 mL) and filtered. All volatiles were removed from the filtrate under reduced pressure. The solid residue was dissolved in CH_2Cl_2 (20 mL) and 5 drops of neat F_3CSO_3H (TfOH; approx. 0.015 g, 0.10 mmol) were added. The reaction mixture was stirred at room temperature for 5 min and evaporated to dryness. The crude product was washed with H_2O (3 × 2 mL) and MeCN (0.5 mL), taken up in in *n*-pentane (10 mL), and filtered. All volatiles were removed from the filtrate under reduced pressure. **8ab** was obtained as a yellowish solid. Overall yield: 0.032 g (0.062 mmol, 62%).

^{1}H NMR (500.2 MHz, $CDCl_3$): δ = 7.88–7.86 (m, 2H; H-14), 7.51–7.47 (m, 4H; H-15,15'), 7.42 (s, 1H; H-3') 7.37–7.34 (m, 2H; H-14'), 7.31 (s, 1H; H-3), 6.89 (s, 1H; H-11), 6.34 (s, 1H; H-11'), 3.31 (s, 3H; NMe), 1.40 (s, 9H; H-18'), 1.38 (s, 9H; H-18).
^{13}C{^{1}H} NMR (125.8 MHz, $CDCl_3$): δ = 153.6 (C-12), 152.4 (C-16), 151.5 (C-16'), 149.2 (C-12'), 141.8 (C-2), 140.8 (C-2'), 135.0 (C-13'), 134.1 (q, ^2J(C,F) = 31.1 Hz; C-4), 133.2 (C-13), 128.9 (C-14'), 126.2(*) (C-1), 125.7 (C-15'), 125.3 (C-14), 125.2 (C-15), 124.7 (q, ^1J(C,F) = 272.9 Hz; CF_3), 116.9 (q, ^3J(C,F) = 3.8 Hz; C-3'), 113.9 (q, ^3J(C,F) = 3.5 Hz; C-3), 108.1 (C-11'), 104.2 (C-11), 34.9 (C-17), 34.9 (C-17'), 33.0 (NMe), 31.5 (C-18'), 31.4 (C-18); (*) unequivocally detected only in the ^{H,C}HMBC spectrum.
^{11}B NMR (96.3 MHz, $CDCl_3$): δ = 29 ($h_{1/2}$ ≈ 750 Hz).
^{19}F{^{1}H} NMR (470.4 MHz, $CDCl_3$): δ = −62.56 (s, CF_3).
HRMS: Calculated *m/z* for $[C_{32}H_{33}BNO]^+$: 515.26018, found: 515.26016.
UV/Vis ($CHCl_3$): λ_{max} (ε) = 307 (30228), 315 (sh), 329 (27393), 374 (10481 $mol^{-1}dm^3cm^{-1}$), 393 nm (sh).
Fluorescence ($CHCl_3$, λ_{ex} = 294 nm): λ_{max} = 398 (sh), 415, 434, 461 (sh), 491 nm (sh); Φ_{PL} = 34%.
Cyclic voltammetry (THF, [*n*Bu$_4$N][PF$_6$] 0.1 M, 200 mV s^{-1}, vs. FcH/FcH$^+$): E_{pc} = −2.76 V.
Melting point: 82 °C.

Note: The ^{1}H and ^{13}C{^{1}H} chemical shifts in positions 11–18 agree well with the shifts of **8a** in the same positions. Also, the shifts in positions 11'–18' agree with the shifts of **8c** in these positions.

2.5. Late-stage functionalization of 9

2.5.1 Synthesis of 9:

Synthesis of the precursor 26:

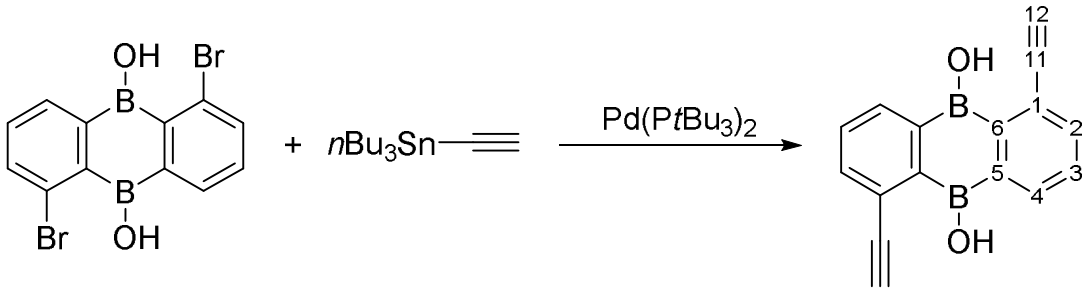

25 **26**

A Schlenk tube was charged with **25** (0.10 g, 0.27 mmol) and kept under a dynamic vacuum for 0.5 h. The solid was dissolved in toluene (20 mL). $Pd(P\textit{t}Bu_3)_2$ (0.014 g, 0.027 mmol) and $\textit{n}Bu_3SnC{\equiv}CH$ (0.19 g, 0.60 mmol) were added. The reaction mixture was stirred at room temperature overnight and evaporated to dryness. The solid residue was dissolved in $CHCl_3$ and filtered over a short plug of silica gel with $CHCl_3$ as eluent. All volatiles were removed from the filtrate under reduced pressure and the crude product was washed with *n*-hexane (3 × 2 mL) to afford **26** as a light brown solid. Yield: 0.036 g (0.14 mmol, 52%).

^{1}H NMR (500.2 MHz, $CDCl_3$): δ = 8.62 (s, 2H; OH), 8.28 (dd, ^3J(H,H) = 7.4 Hz, ^4J(H,H) = 1.3 Hz, 2H; H-4), 7.70 (dd, ^3J(H,H) = 7.5 Hz, ^4J(H,H) = 1.3 Hz, 2H; H-2), 7.57 (vt, 2H; H-3), 3.62 (s, 2H, H-12).
^{13}C{^{1}H} NMR (125.8 MHz, $CDCl_3$): δ = 144.7(*) (br.; C-5), 141.9(*) (br.; C-6), 136.7 (C-2), 134.1 (C-4), 130.9 (C-3), 124.3 (C-1), 85.3 (C-11), 82.2 (C-12); (*) unequivocally detected only in the ^{H,C}HMBC spectrum.
^{11}B NMR (96.3 MHz, $CDCl_3$): δ = 41 ($h_{1/2}$ ≈ 500 Hz).
HRMS: Calculated *m/z* for $[C_{16}H_{10}B_2O_2+H]^+$: 257.09397, found: 257.09412.

Synthesis of 9:

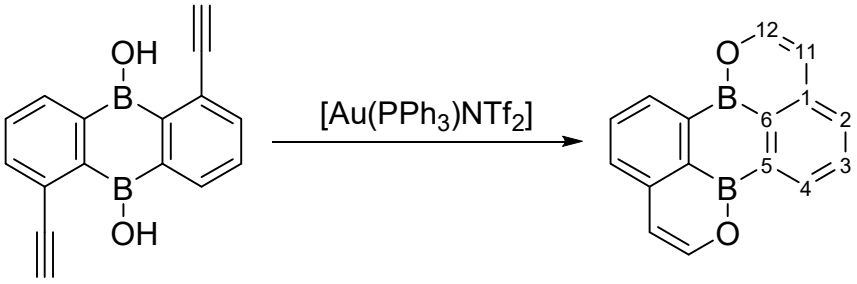

26 **9**

A Schlenk tube was charged with **26** (0.040 g, 0.16 mmol) and evacuated for 0.5 h. The solid was dissolved in CH_2Cl_2 (10 mL) and [Au(PPh3)NTf2] (0.012 g, 0.016 mmol) was added at room temperatur. The solution was heated to 60 °C for 4 h. The reaction mixture was filtered over a short plug of silica gel with $CHCl_3$ as eluent. All volatiles were removed from the filtrate under reduced pressure. The crude product was washed with *n*-hexane (2 × 1 mL) and MeCN (2 × 1 mL). **9** was obtained as a yellow solid. Yield: 0.037 g (0.14 mmol, 88%). Single crystals of **9** were grown from hot CH_2Cl_2.

^{1}H NMR (500.2 MHz, $CDCl_3$): δ = 8.17 (dd, ^3J(H,H) = 7.1 Hz, ^4J(H,H) = 0.7 Hz, 2H; H-4), 7.73 (dd, ^3J(H,H) = 7.7 Hz, ^3J(H,H) = 7.1 Hz, 2H; H-3), 7.58 (dd, ^3J(H,H) = 7.7 Hz, ^4J(H,H) = 0.7 Hz, 2H; H-2), 7.56 (d, ^3J(H,H) = 5.4 Hz, 2H; H-12), 6.65 (d, ^3J(H,H) = 5.4 Hz, 2H; H-11).
^{13}C{^{1}H} NMR (125.8 MHz, $CDCl_3$): δ = 144.4 (C-12), 140.5 (br.; C-5), 139.5 (C-1), 136.7 (br.; C-6), 132.7 (C-3), 130.9 (C-4), 128.9 (C-2), 111.8 (C-11).
^{11}B NMR (96.3 MHz, $CDCl_3$): δ = 40 ($h_{1/2}$ ≈ 457 Hz).
HRMS: Calculated *m*/*z* for $[C_{16}H_{10}B_2O_2]^+$: 256.08614, found: 256.08692.
UV/Vis ($CHCl_3$): λ_{max} (ε) = 355 (6631), 371 (11202), 389 nm (10413 $mol^{-1}dm^3cm^{-1}$).
Fluorescence ($CHCl_3$, λ_{ex} = 370 nm): λ_{max} = 400, 418, 437 nm; Φ_{PL} = 30%.
Cyclic voltammetry (THF, [*n*Bu$_4$N][PF$_6$] 0.1 M, 200 mV s^{-1}, vs. FcH/FcH$^+$): $E_{1/2}$ = −2.29 V.
Melting point: 231 °C.

2.5.2 Synthesis of 10:

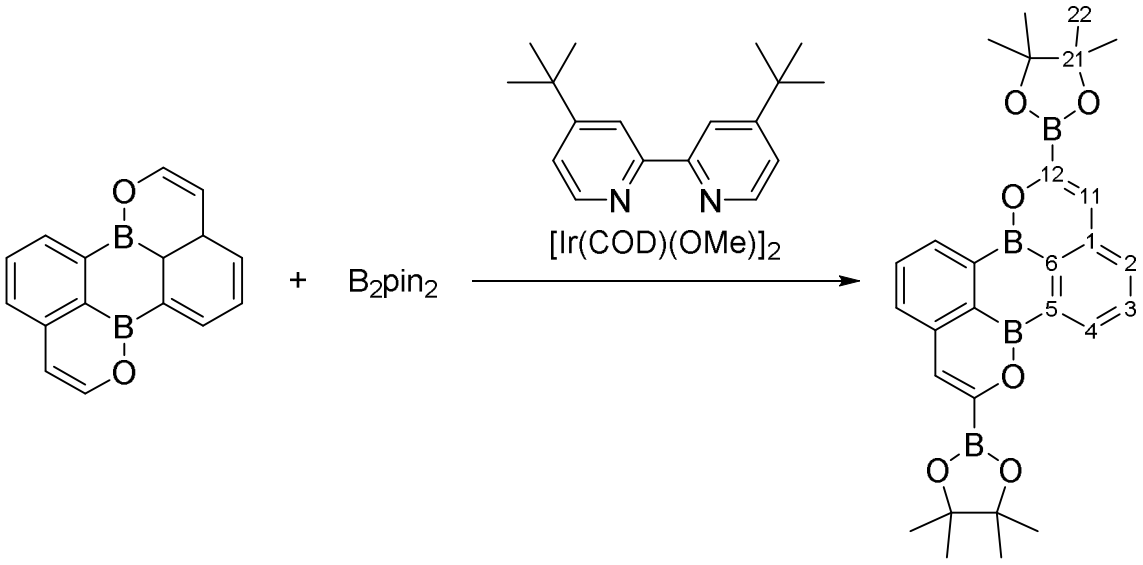

9 **10**

A Schlenk flask was charged with **9** (0.050 g, 0.19 mmol), B_2pin_2 (0.15 g, 0.59 mmol), 4,4'-di-*tert*-butyl-2,2'-bipyridine (0.003 g, 0.011 mmol), and $[Ir(COD)(\mu\text{-}OMe)]_2$ (0.004 g, 0.006 mmol) and evacuated for 0.5 h. The solids were dissolved in THF (30 mL). The reaction mixture was heated to 80 °C for 42 h, allowed to cool to room temperature, and evaporated to dryness. The crude product was washed with *c*-hexane (3 × 4 mL) and MeCN (2 × 4 mL). **10** was obtained as a grey solid. Yield: 0.060 g (0.12 mmol, 63%). Single crystals were grown by slow evaporation of a solution of **10** in C_6H_6 at 5 °C.

^{1}H NMR (500.2 MHz, $CDCl_3$): δ = 8.40 (dd, ^3J(H,H) = 7.1 Hz, ^4J(H,H) = 1.0 Hz, 2H; H-4), 7.75 (dd, ^3J(H,H) = 7.8 Hz, ^3J(H,H) = 7.1 Hz, 2H; H-3), 7.62 (dd, ^3J(H,H) = 7.8 Hz, ^4J(H,H) = 1.0 Hz, 2H; H-2), 7.39 (s, 2H; H-11), 1.42 (s, 24H; H-22).
^{13}C{^{1}H} NMR (125.8 MHz, $CDCl_3$): δ = 149.7(*) (br.; C-12), 140.7(*) (br.; C-5), 138.1 (C-1), 138.0(*) (br.; C-6), 132.7 (C-4), 132.4 (C-3), 129.5 (C-2), 124.1 (C-11), 84.6 (C-21), 25.0 (C-22); (*) unequivocally detected only in the ^{H,C}HMBC spectrum.
^{11}B NMR (96.3 MHz, $CDCl_3$): δ = 42 ($h_{1/2}$ ≈ 600 Hz; BO), 29 ($h_{1/2}$ ≈ 450 Hz; BO_2).
HRMS: Calculated *m/z* for $[C_{28}H_{32}B_4O_6]^+$: 507.26019, found: 507.25929.
UV/Vis ($CHCl_3$): λ_{max} (ε) = 350 (6217), 366 (11242), 383 nm (10850 $mol^{-1}dm^3cm^{-1}$).
Fluorescence ($CHCl_3$, λ_{ex} = 350 nm): λ_{max} = 393, 411, 430 nm; Φ_{PL} = 34%.
Cyclic voltammetry (THF, [nBu$_4$N][PF$_6$] 0.1 M, 200 mV s^{-1}, vs. FcH/FcH$^+$): $E_{1/2}$ = –2.27 V.
Melting point: 259 °C.

3. Plots of ^{1}H, $^{13}C\{^{1}H\}$, ^{11}B, and $^{19}F\{^{1}H\}$ NMR spectra

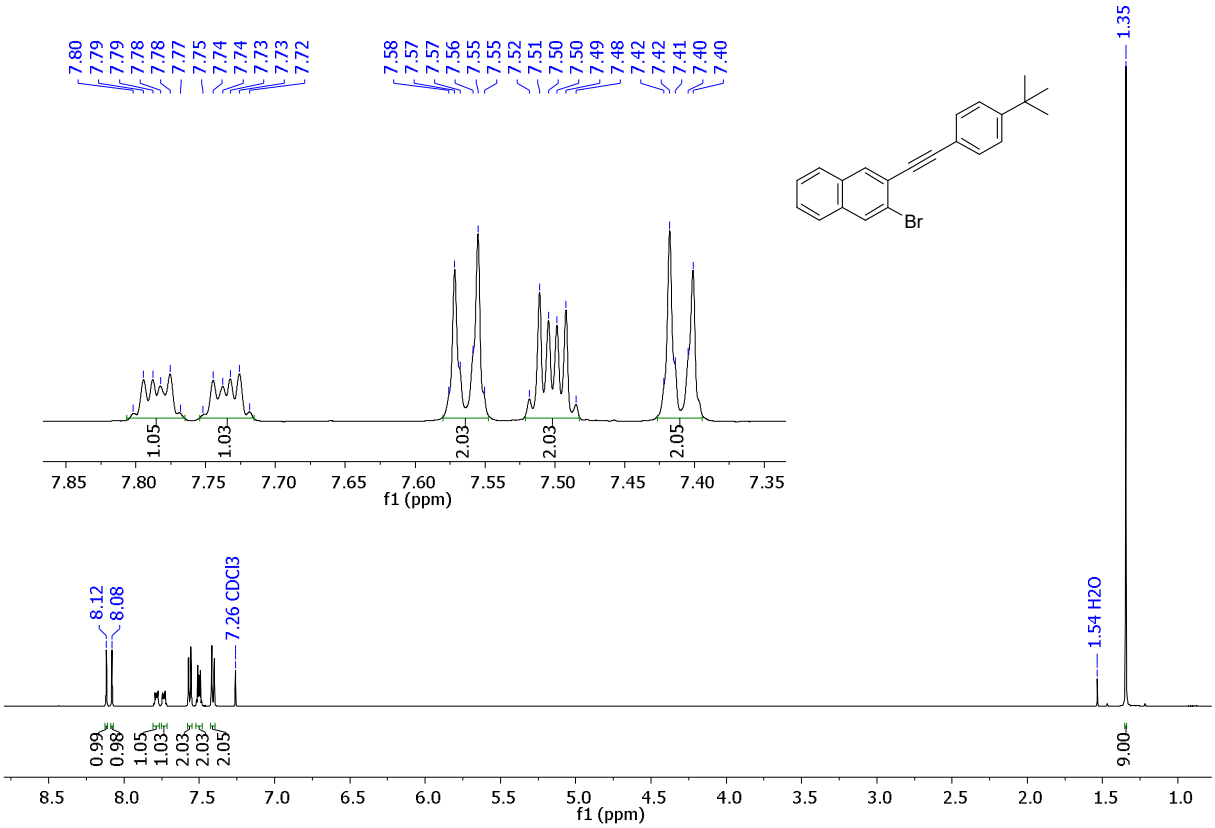

Figure S1: ^{1}H NMR spectrum of **19** ($CDCl_3$, 500.2 MHz).

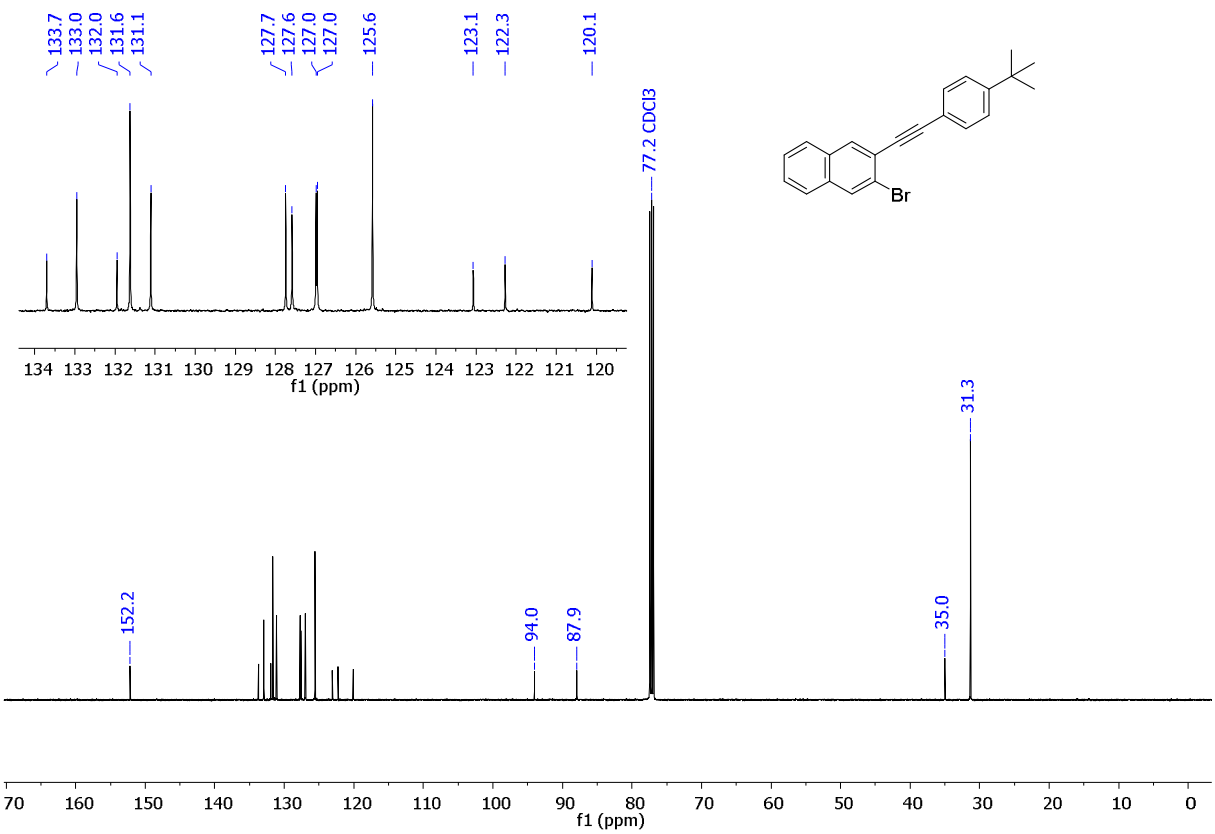

Figure S2: $^{13}C\{^{1}H\}$ NMR spectrum of **19** ($CDCl_3$, 125.8 MHz).

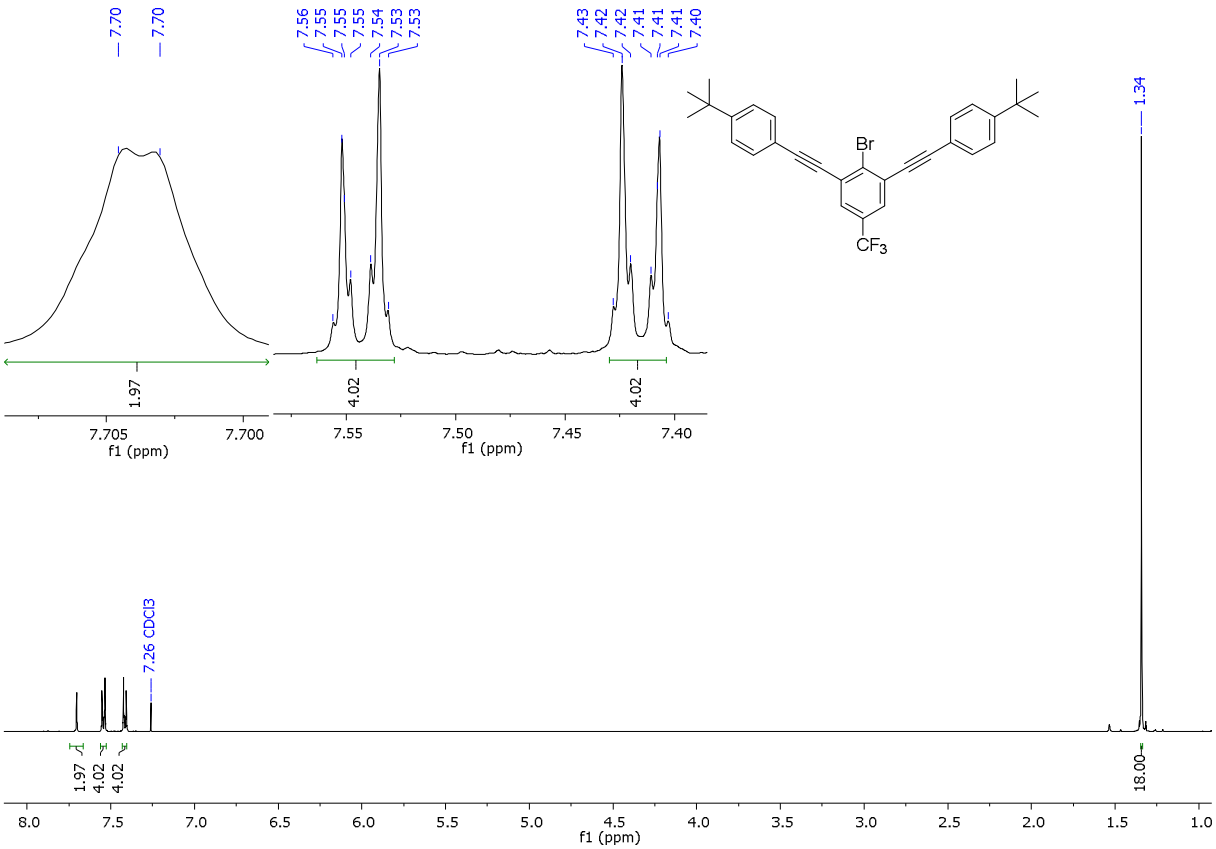

Figure S3: ^{1}H NMR spectrum of **24** ($CDCl_3$, 500.2 MHz).

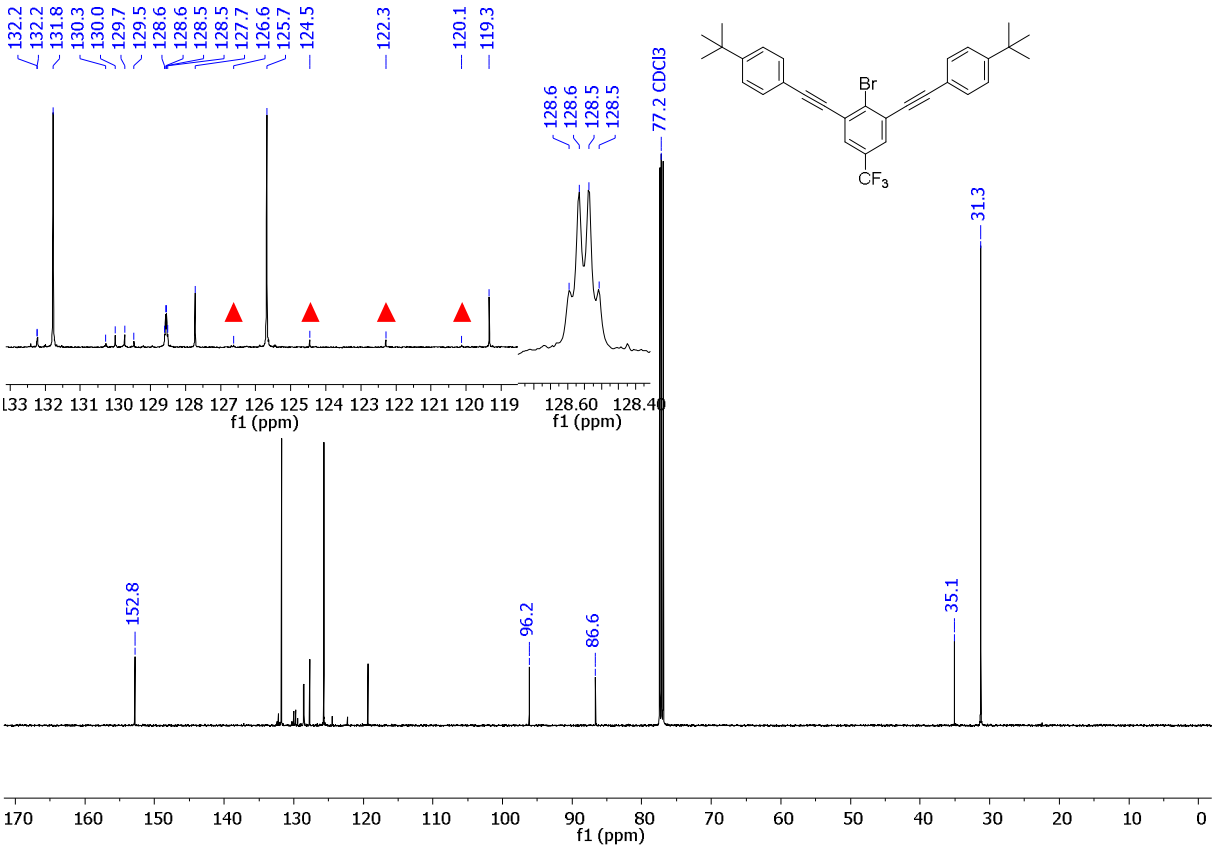

Figure S4: ^{13}C{^{1}H} NMR spectrum of **24** ($CDCl_3$, 125.8 MHz; ▲: CF_3 resonance).

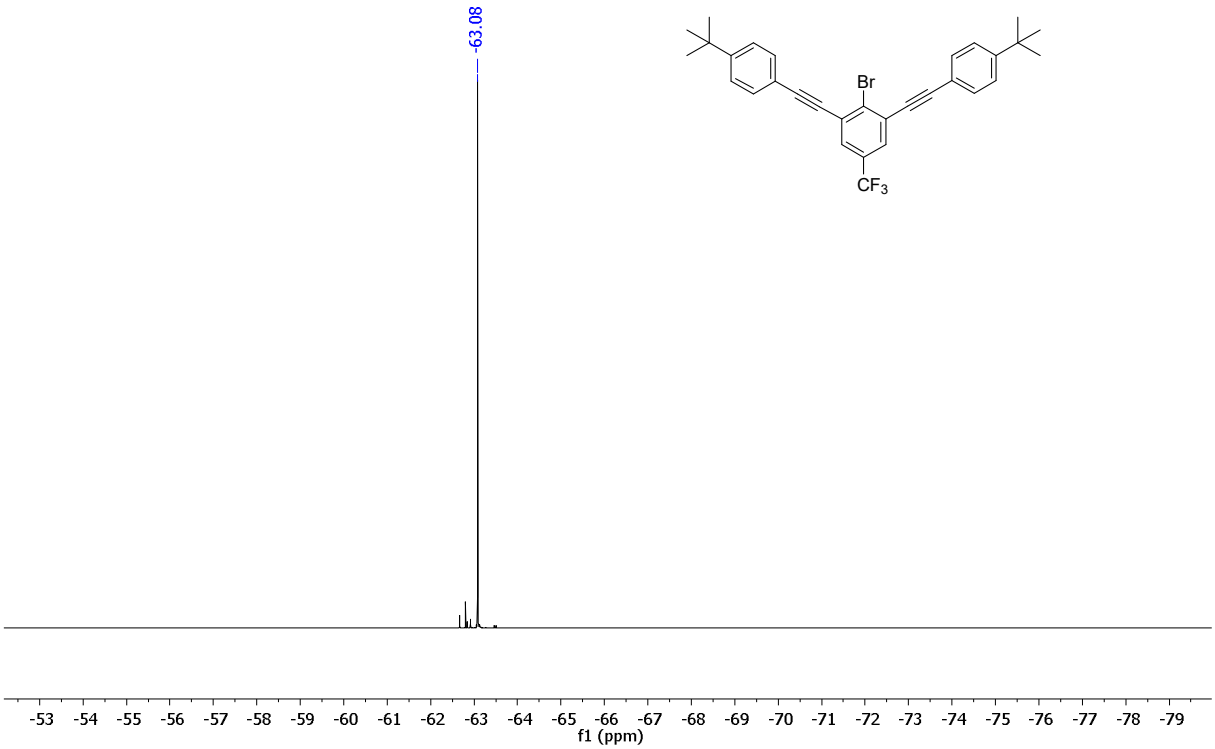

Figure S5: $^{19}F\{^{1}H\}$ NMR spectrum of **24** ($CDCl_3$, 470.4 MHz).

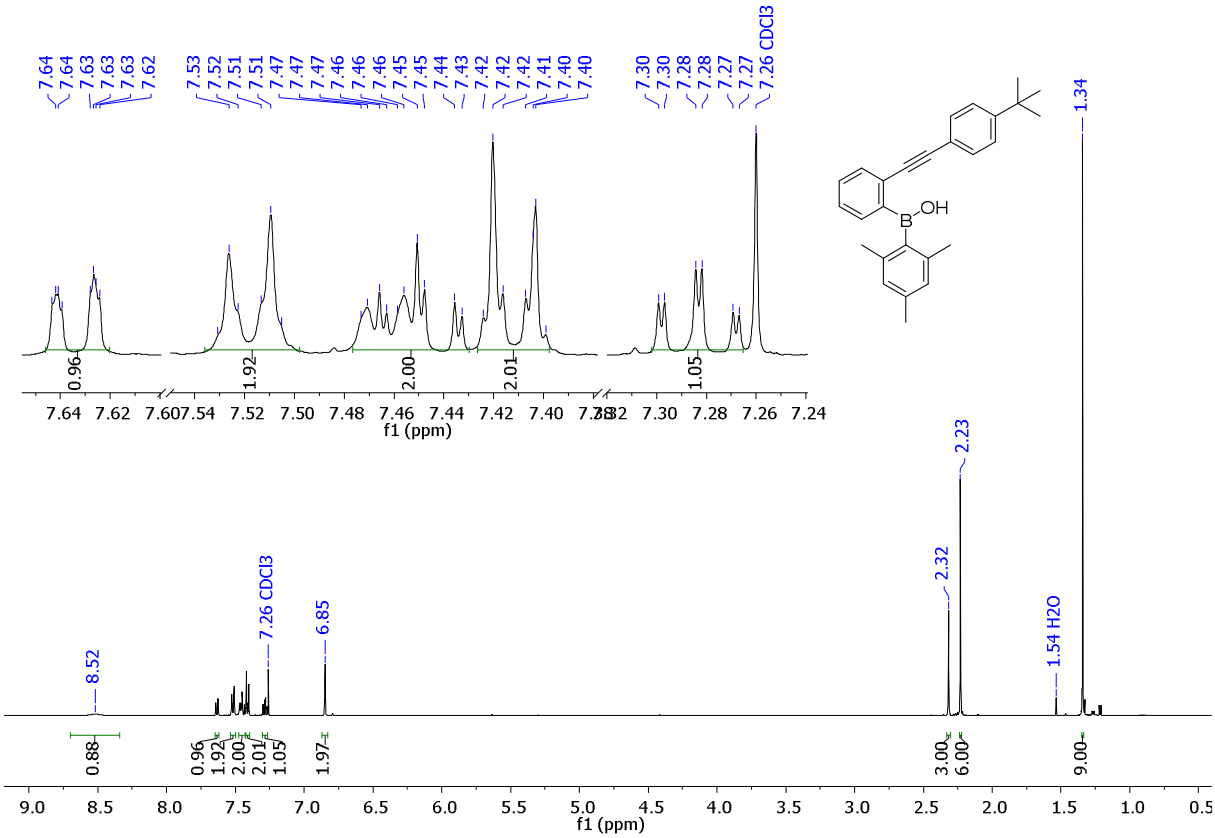

Figure S6: ^{1}H NMR spectrum of **1a** ($CDCl_3$, 500.2 MHz).

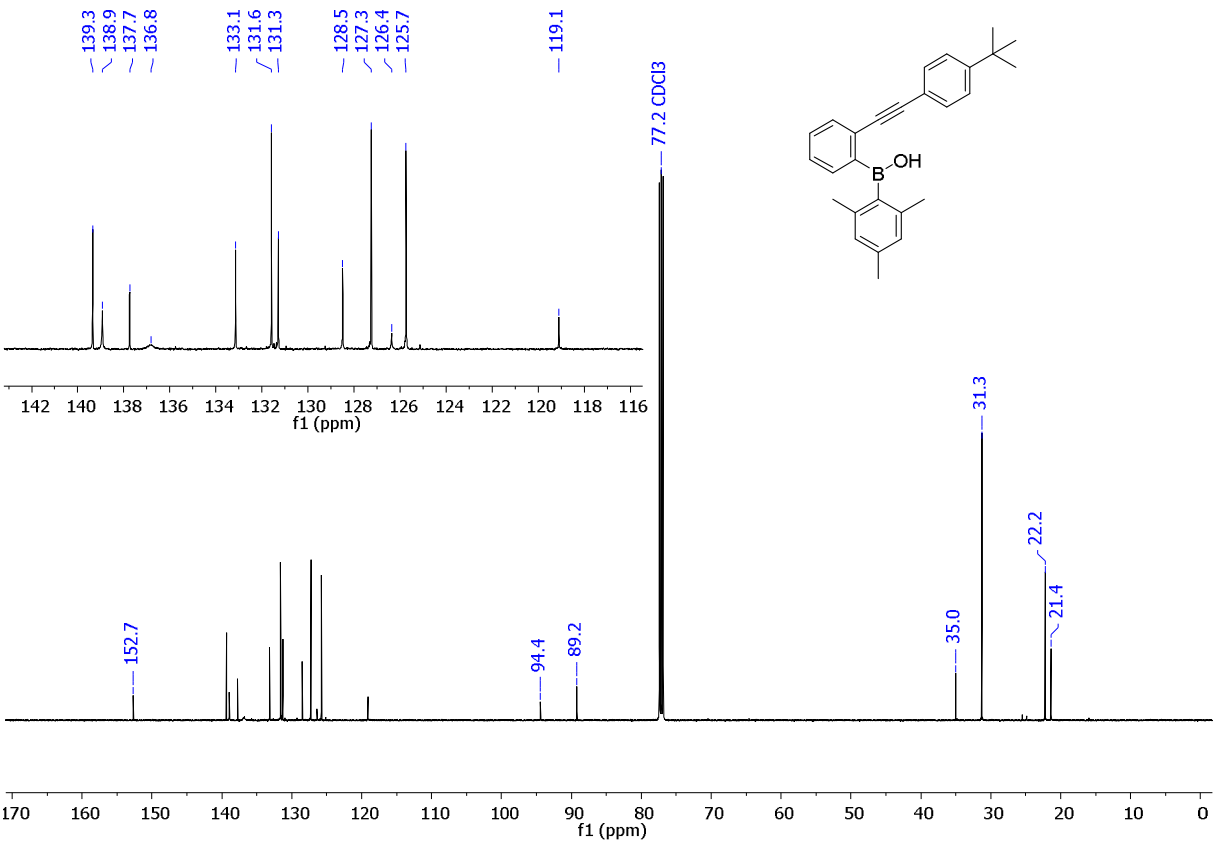

Figure S7: $^{13}C\{^{1}H\}$ NMR spectrum of **1a** ($CDCl_3$, 125.8 MHz).

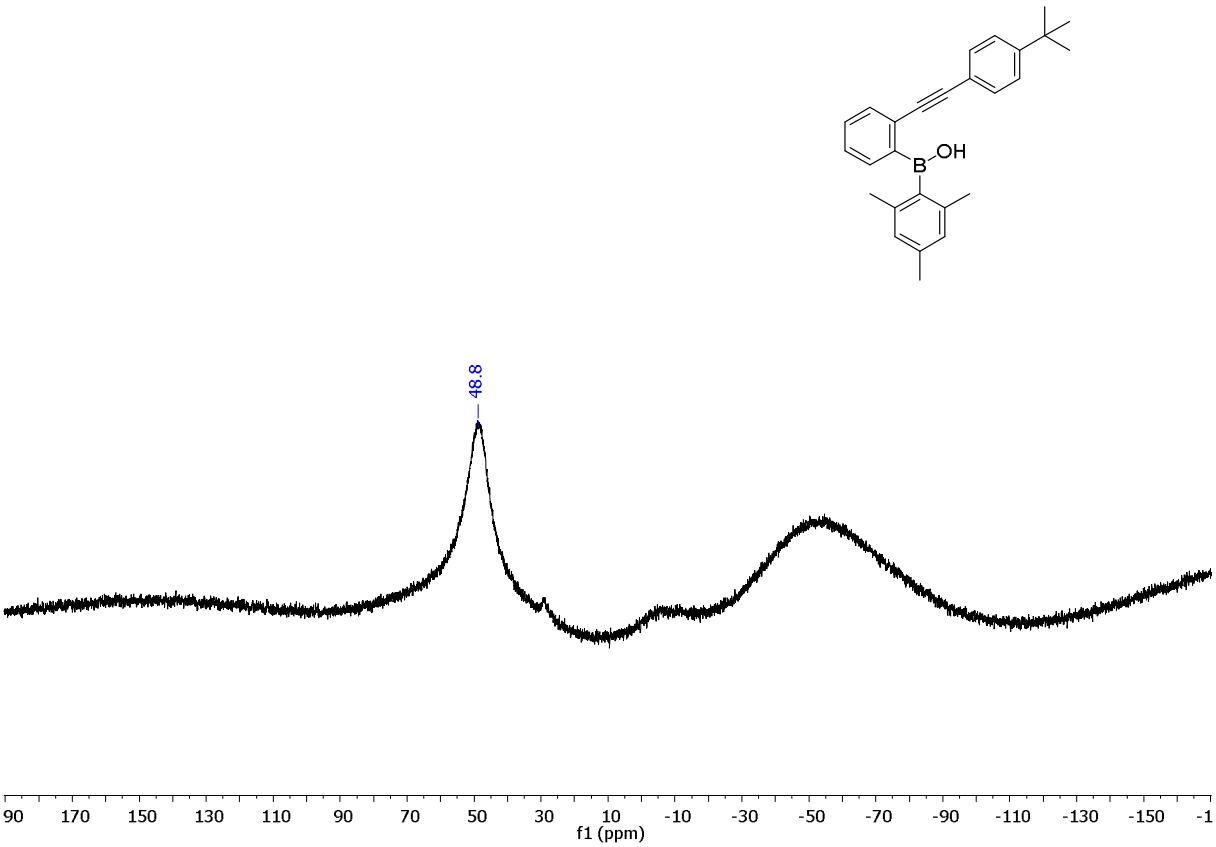

Figure S8: ^{11}B NMR spectrum of **1a** ($CDCl_3$, 96.3 MHz).

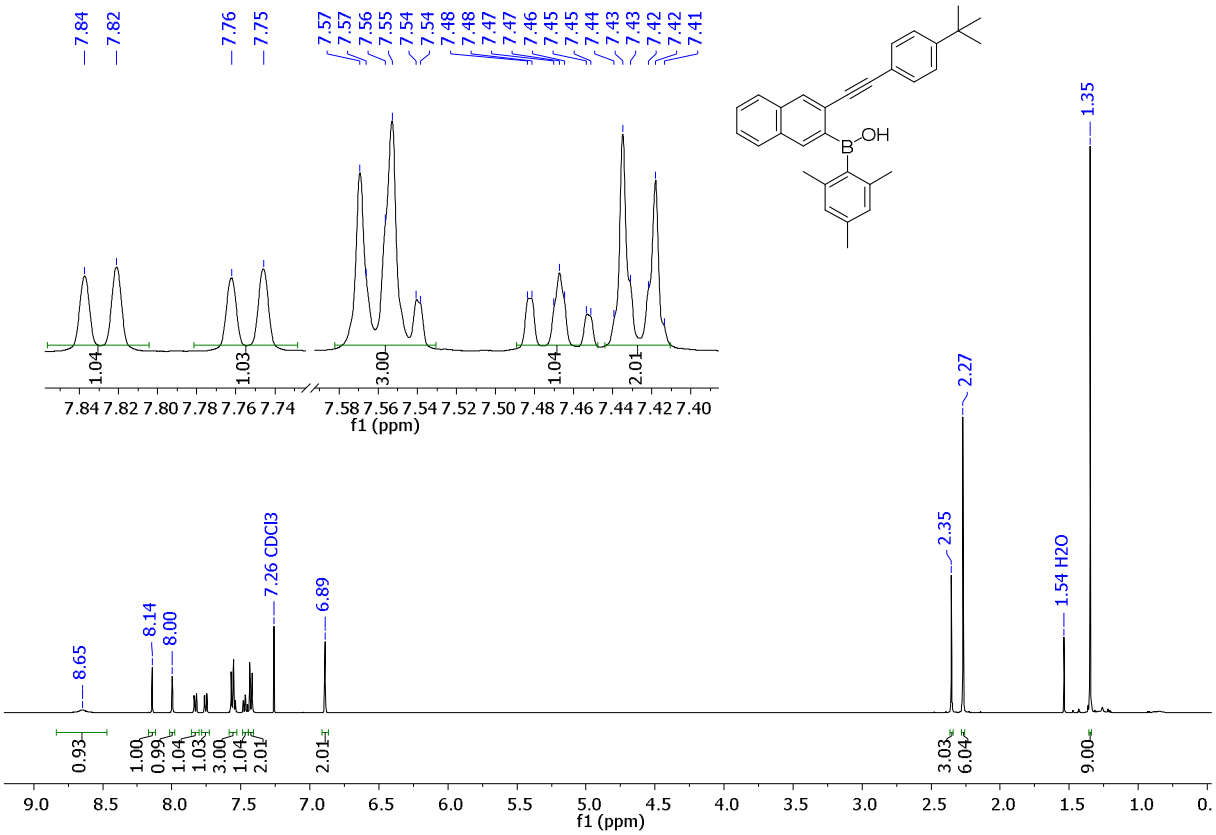

Figure S9: ^{1}H NMR spectrum of **2a** ($CDCl_3$, 500.2 MHz).

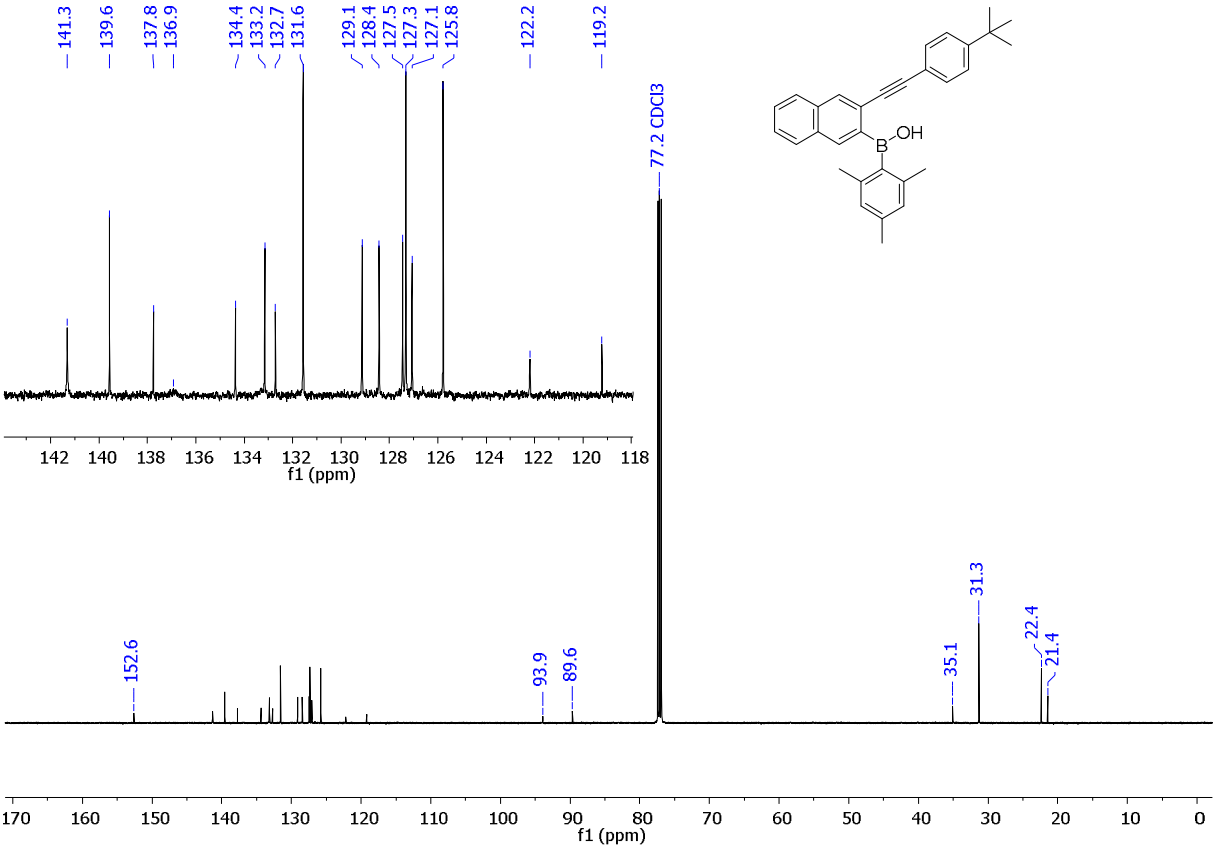

Figure S10: $^{13}C\{^{1}H\}$ NMR spectrum of **2a** ($CDCl_3$, 125.8 MHz).

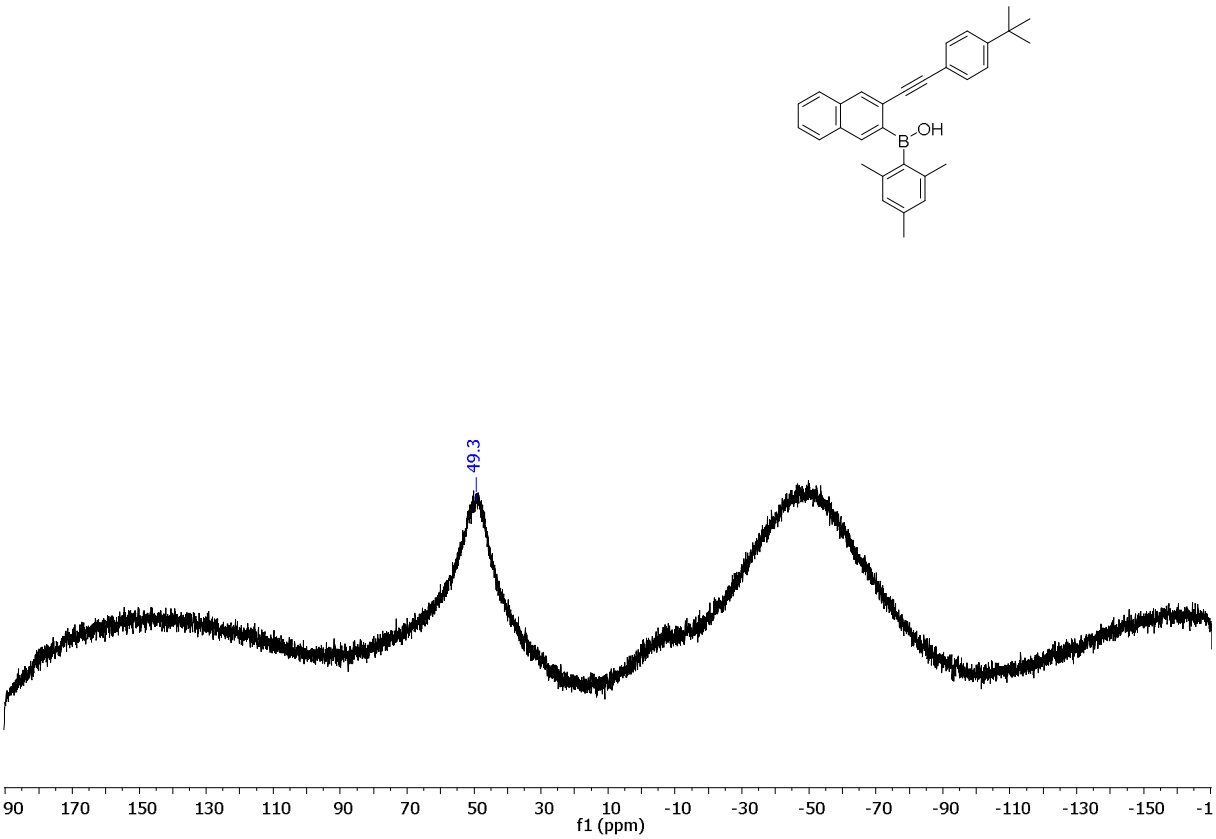

Figure S11: ^{11}B NMR spectrum of **2a** ($CDCl_3$, 96.3 MHz).

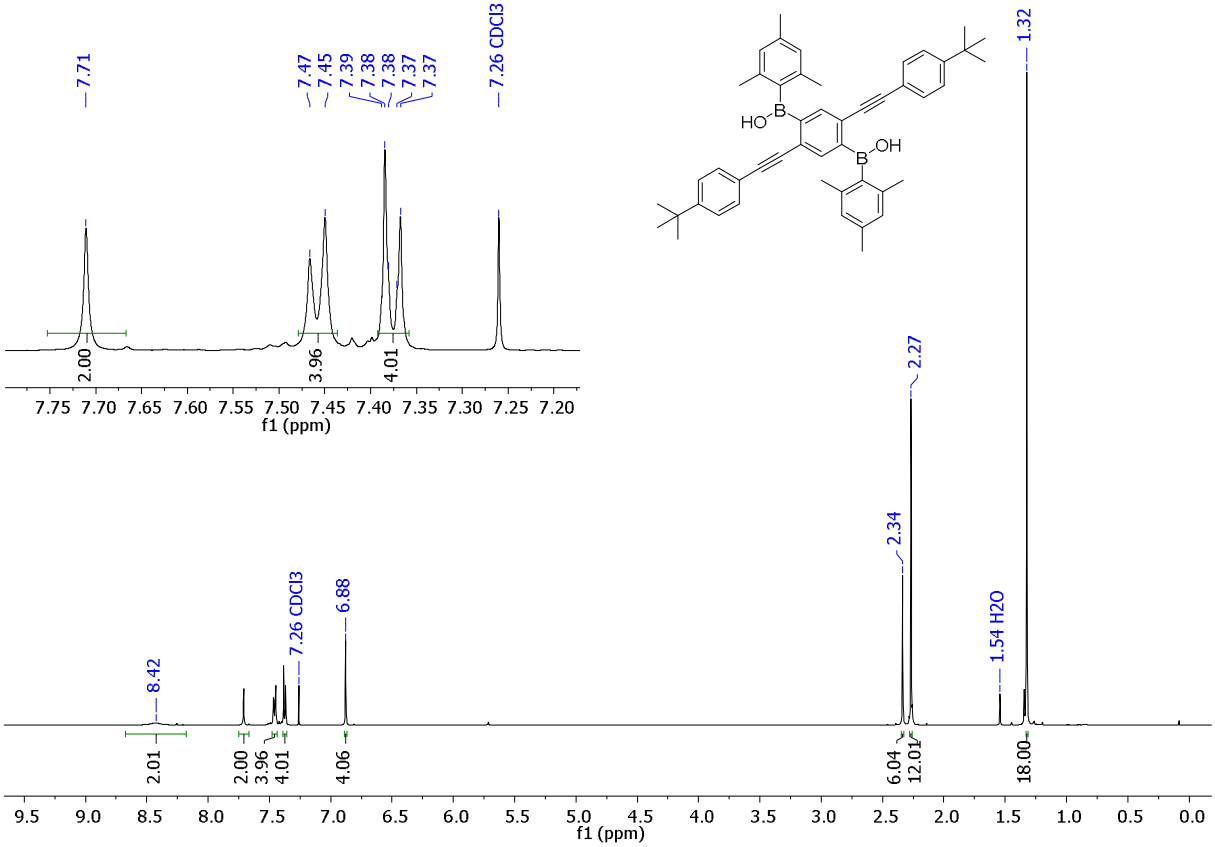

Figure S12: ^{1}H NMR spectrum of **3a** ($CDCl_3$, 500.2 MHz).

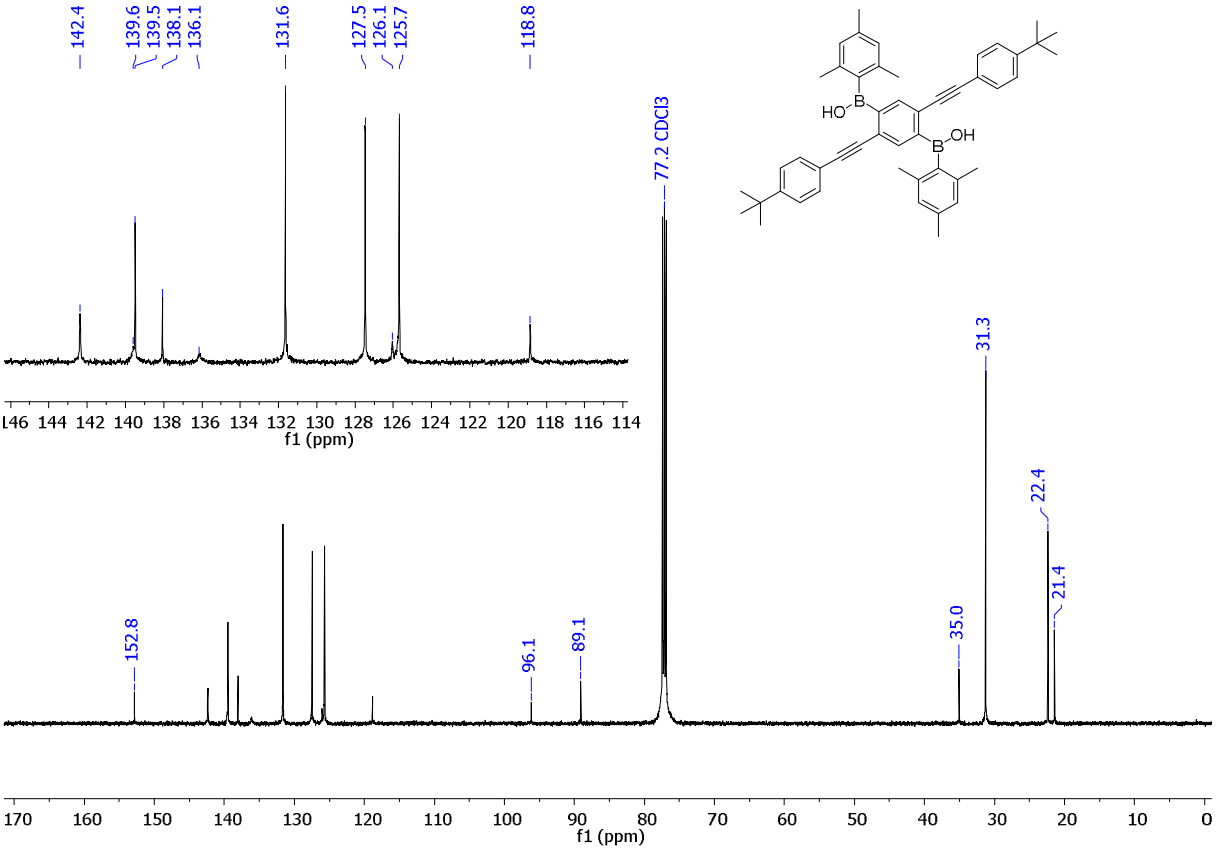

Figure S13: $^{13}C\{^{1}H\}$ NMR spectrum of **3a** ($CDCl_3$, 125.8 MHz).

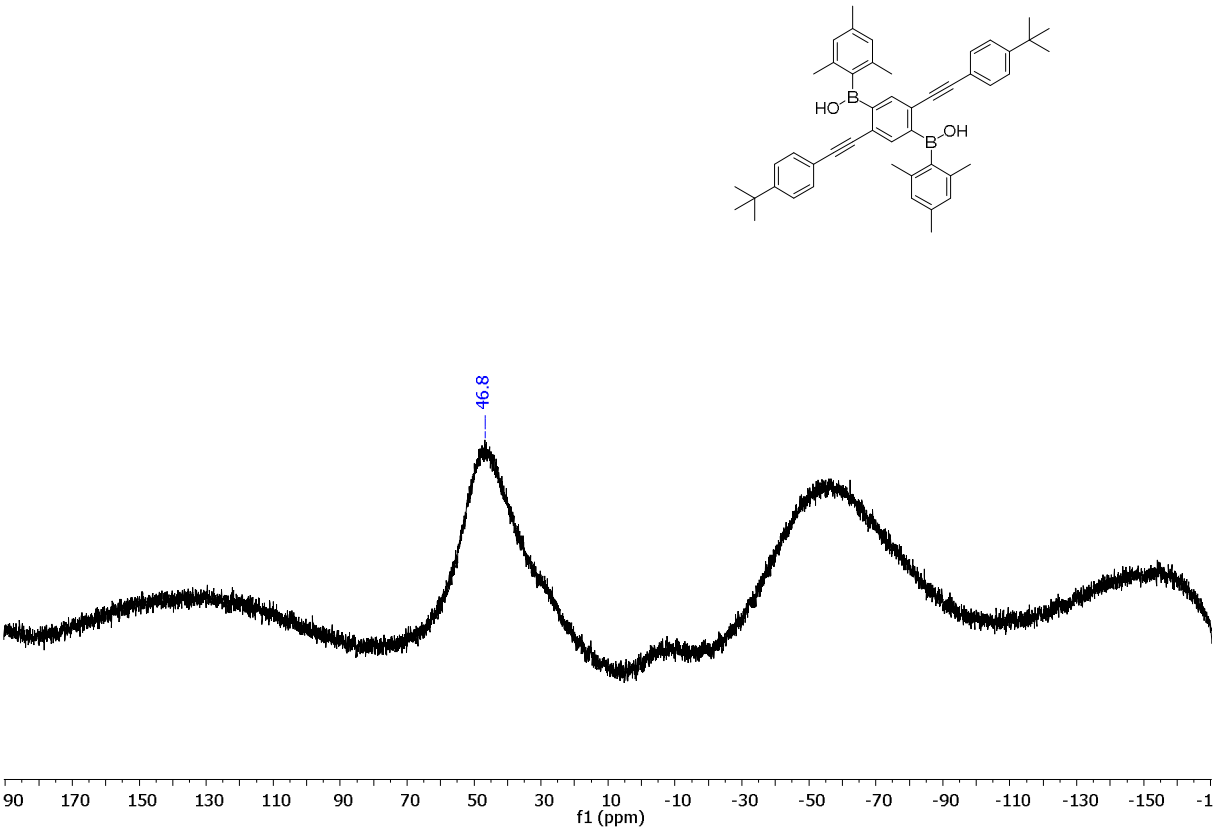

Figure S14: ^{11}B NMR spectrum of **3a** ($CDCl_3$, 96.3 MHz).

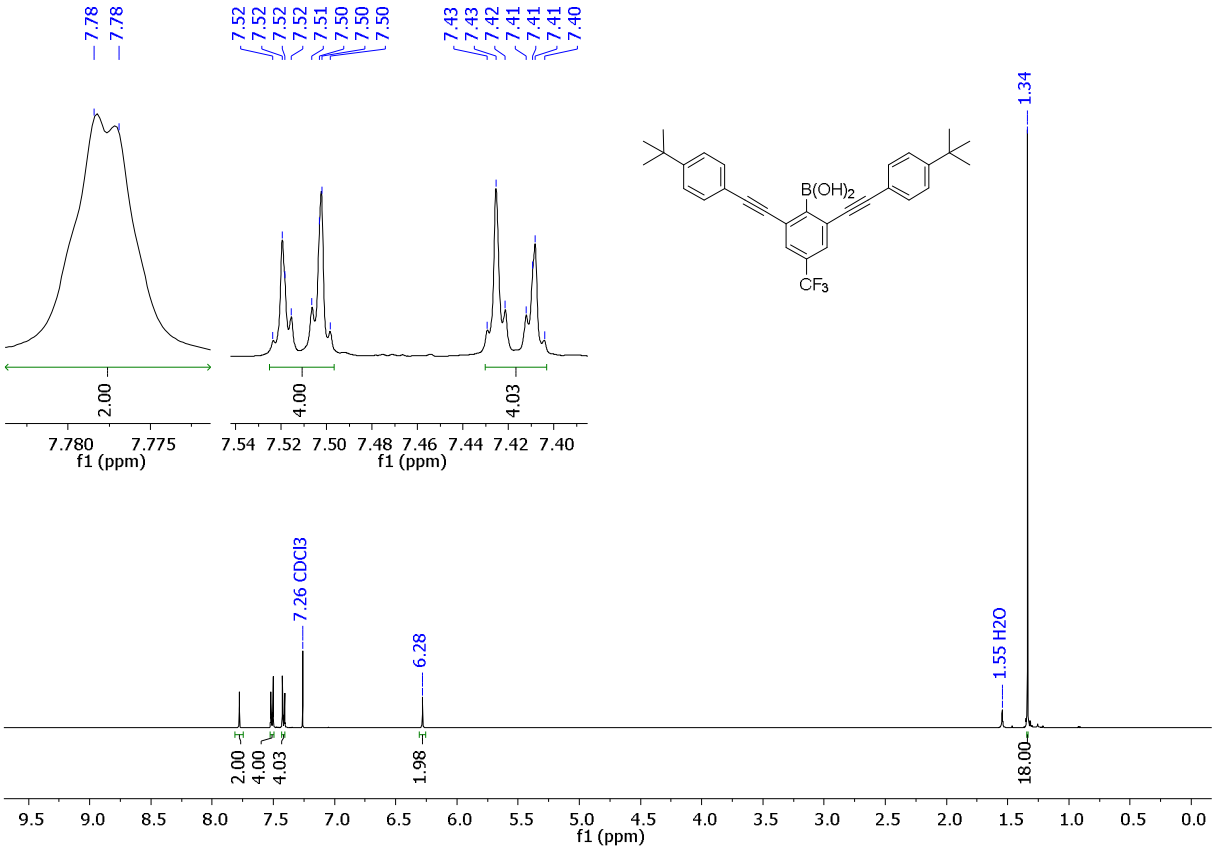

Figure S15: ^{1}H NMR spectrum of **7a** ($CDCl_3$, 500.2 MHz).

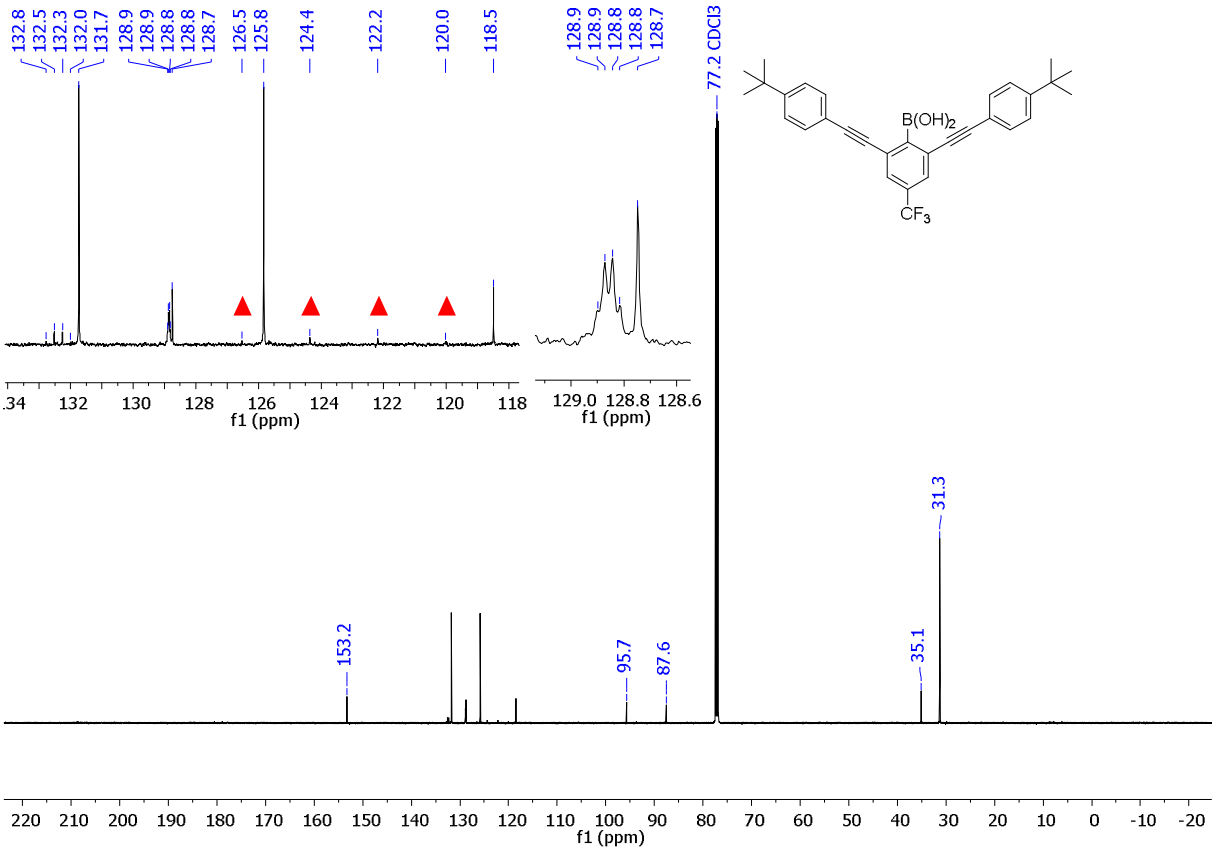

Figure S16: $^{13}C\{^{1}H\}$ NMR spectrum of **7a** ($CDCl_3$, 125.8 MHz; ▲: CF_3 resonance).

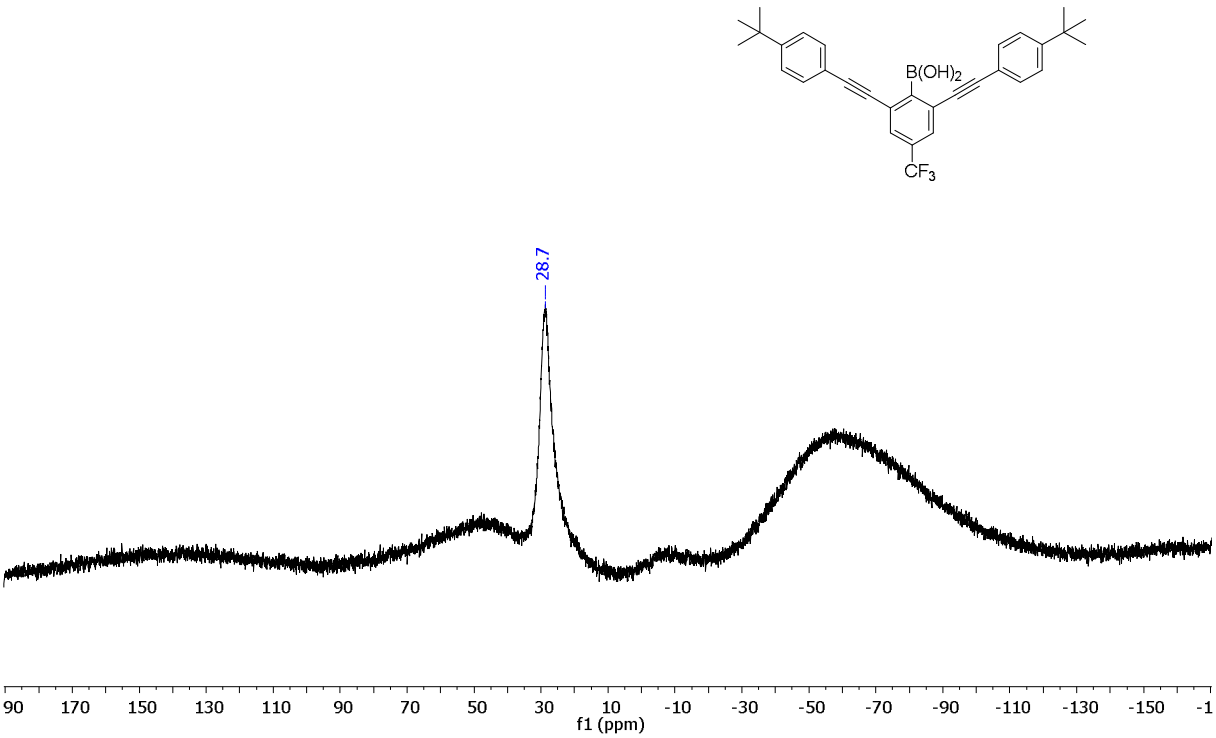

Figure S17: ^{11}B NMR spectrum of **7a** ($CDCl_3$, 96.3 MHz).

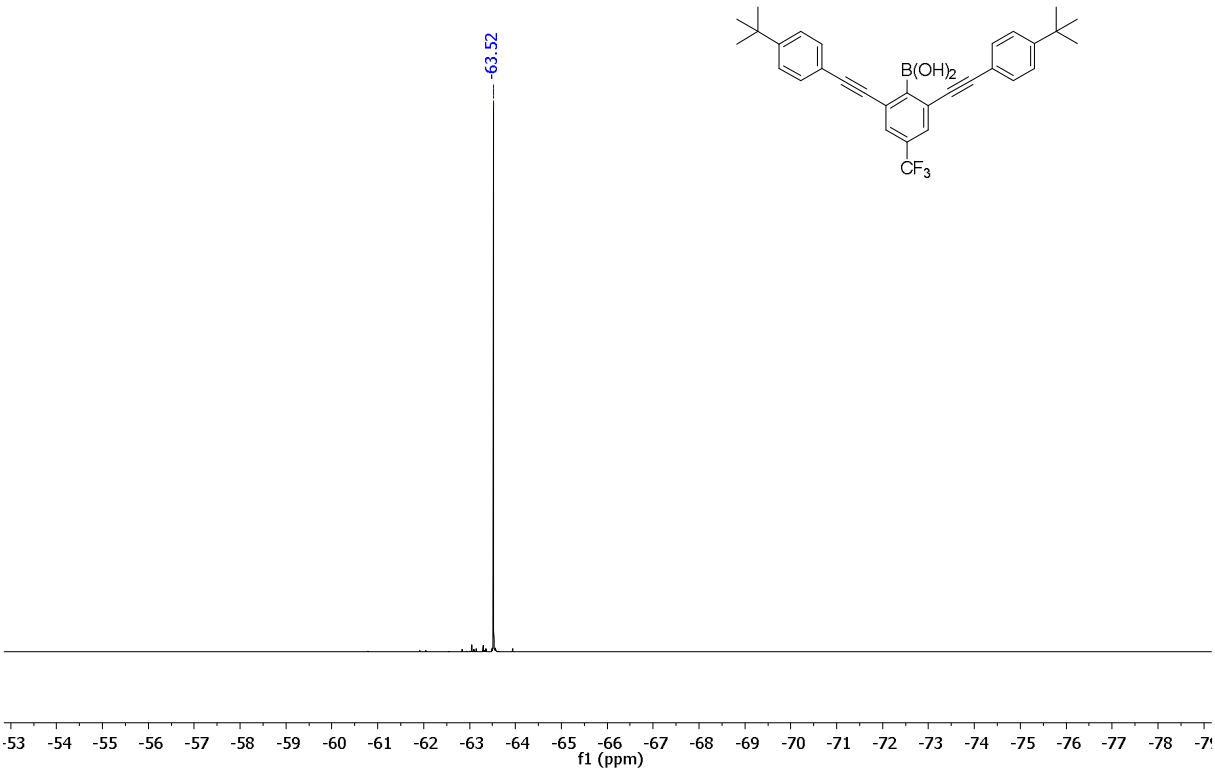

Figure S18: $^{19}F\{^1H\}$ NMR spectrum of **7a** ($CDCl_3$, 470.4 MHz).

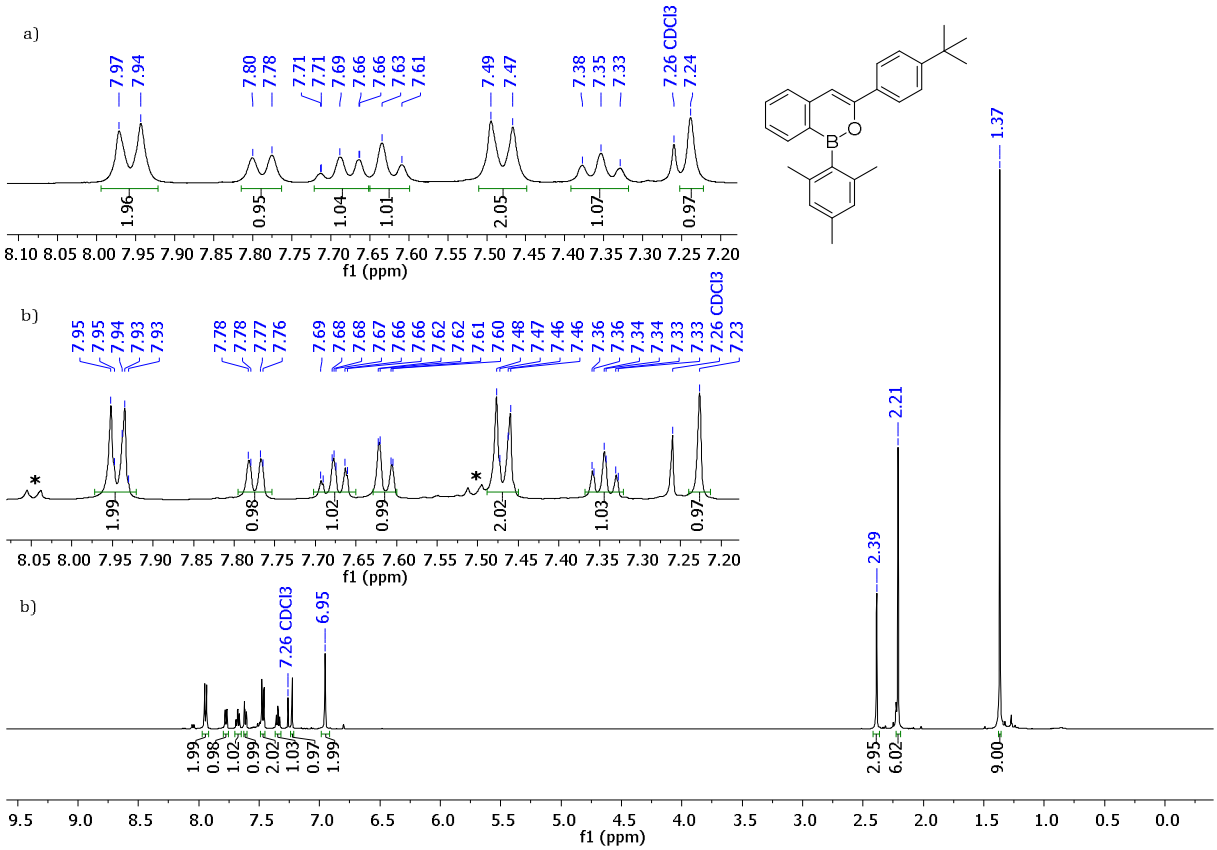

Figure S19: ^{1}H NMR spectrum of **4a** ($CDCl_3$): a) 300.1 MHz (immediate measurement of the pure sample), b) 500.2 MHz (same sample, recorded after 1 week in solution under non-inert conditions). **Note**: The comparison of the spectra a) and b) shows that **4a** is not fully stable toward air and moisture in solution (see the small resonances marked with asterisks).

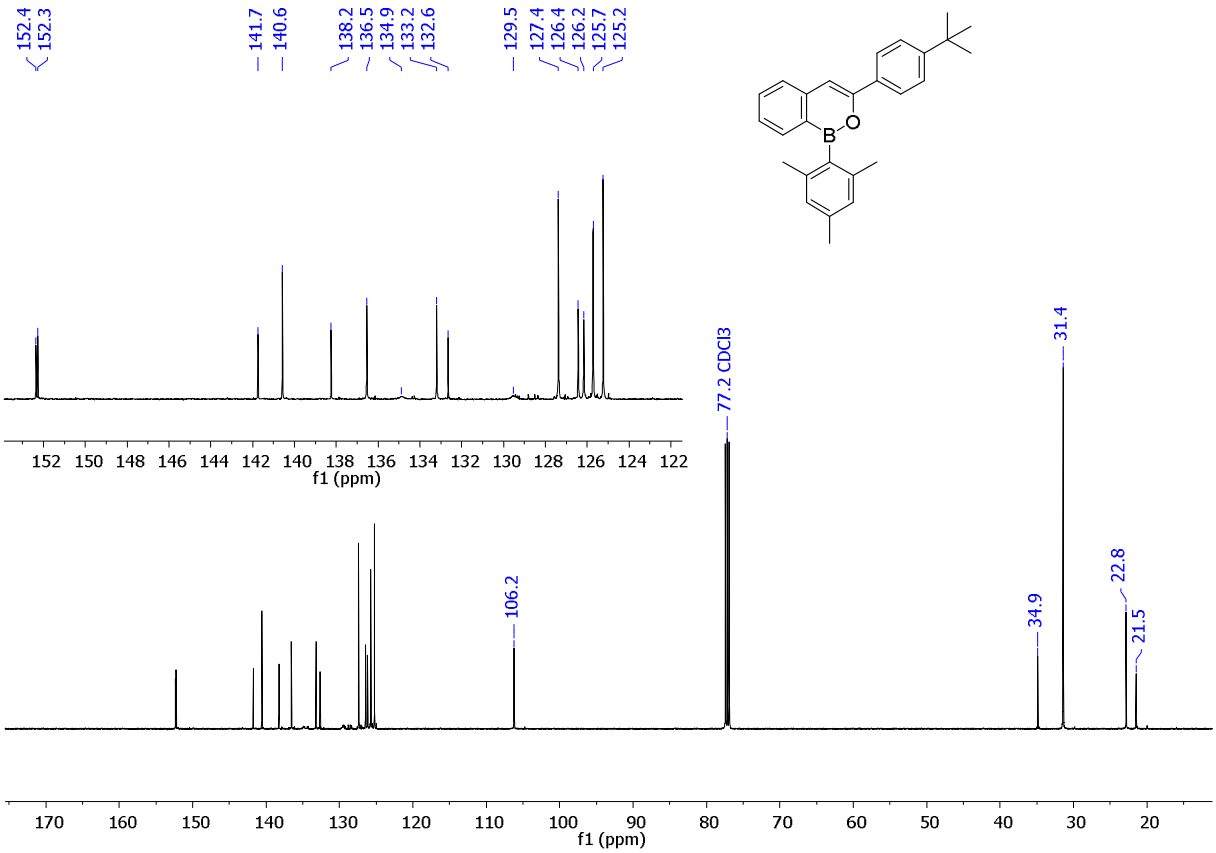

Figure S20: $^{13}C\{^{1}H\}$ NMR spectrum of **4a** ($CDCl_3$, 125.8 MHz; recorded after 1 week in solution under non-inert conditions).

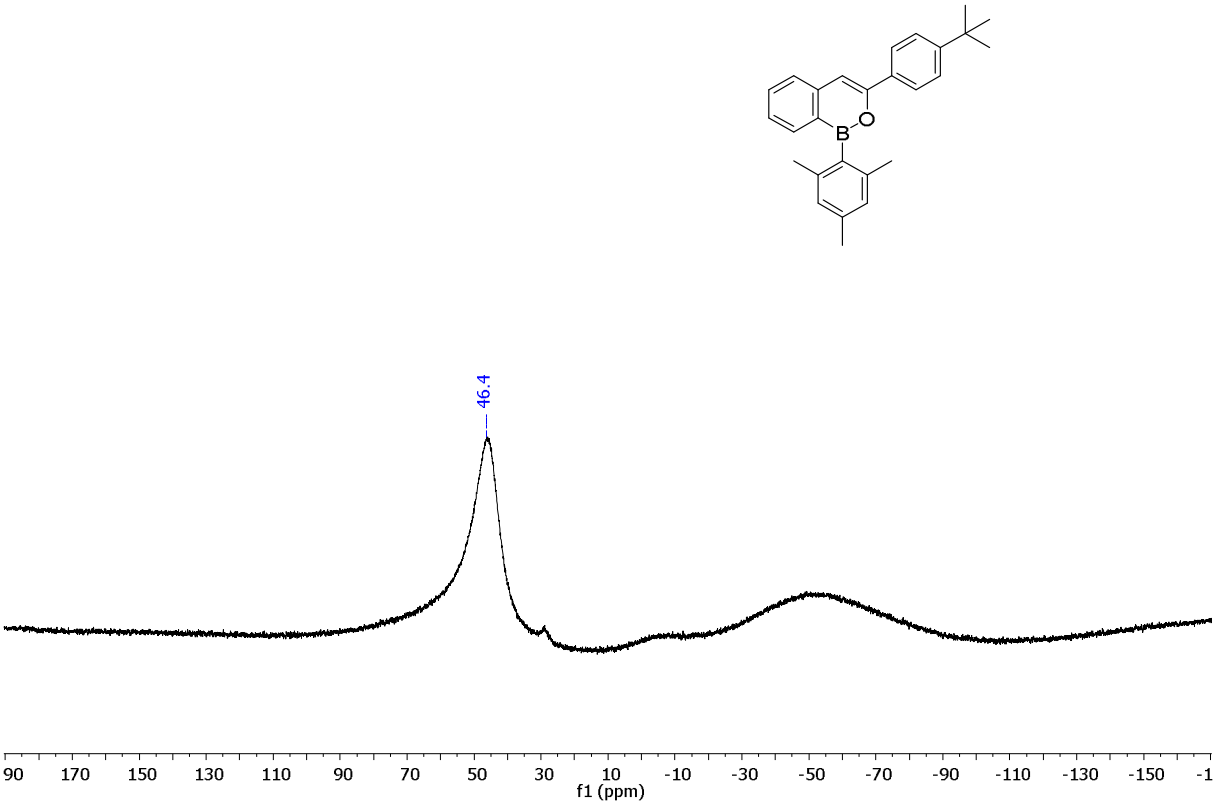

Figure S21: ^{11}B NMR spectrum of **4a** ($CDCl_3$, 96.3 MHz).

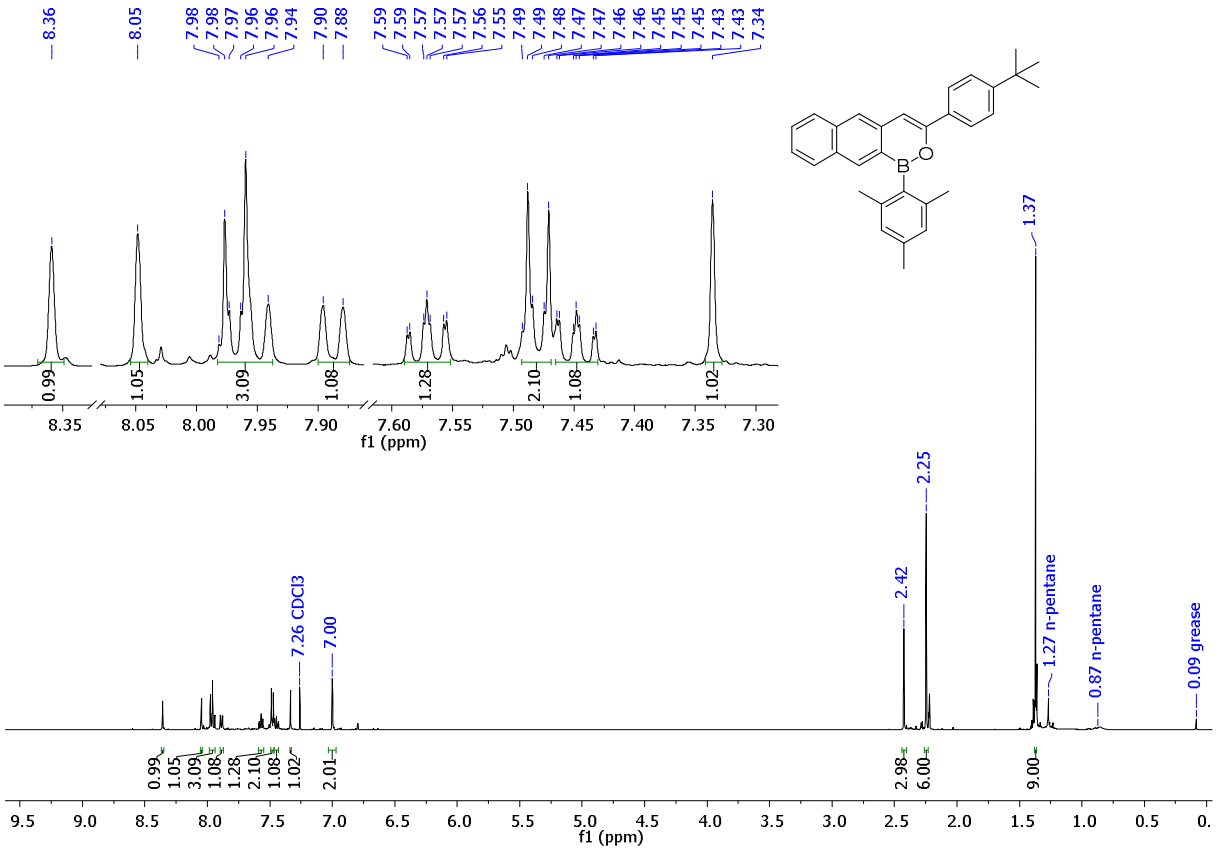

Figure S22: ^{1}H NMR spectrum of **5a** ($CDCl_3$, 500.2 MHz).

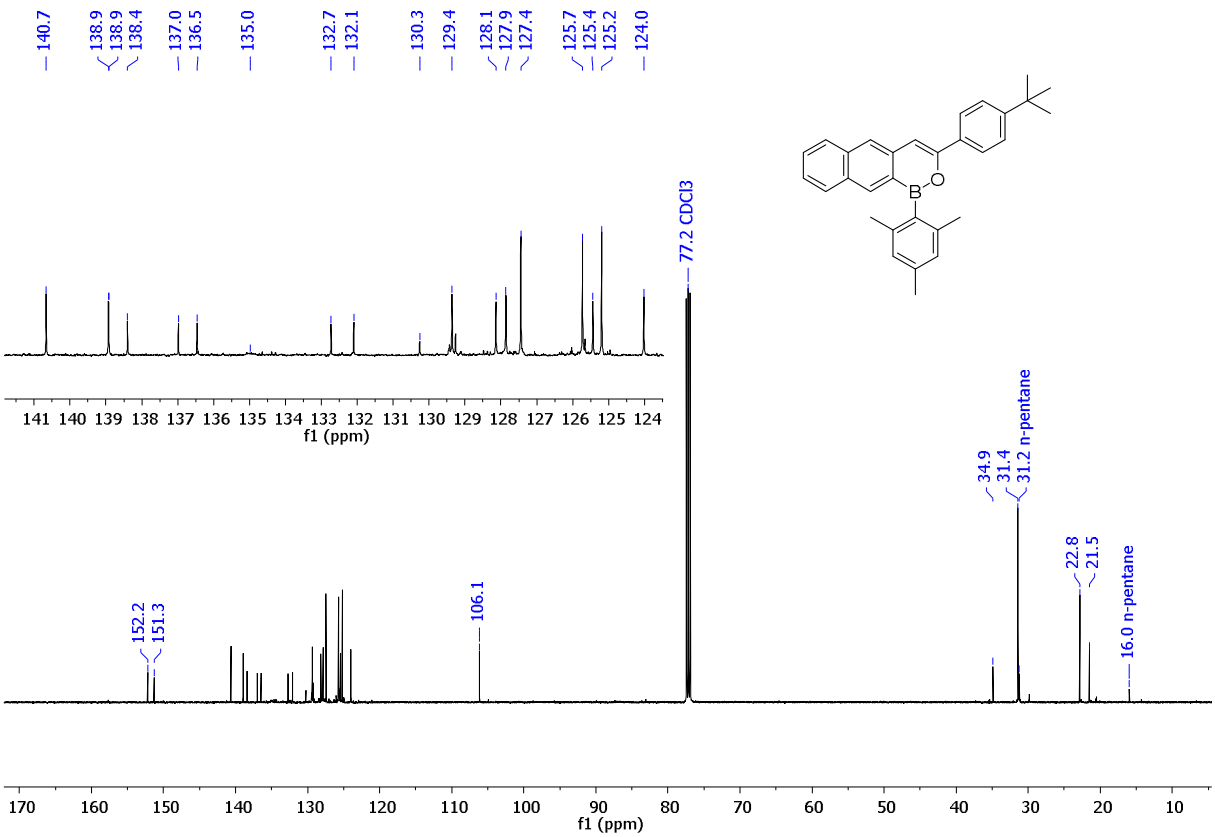

Figure S23: $^{13}C\{^{1}H\}$ NMR spectrum of **5a** ($CDCl_3$, 125.8 MHz)

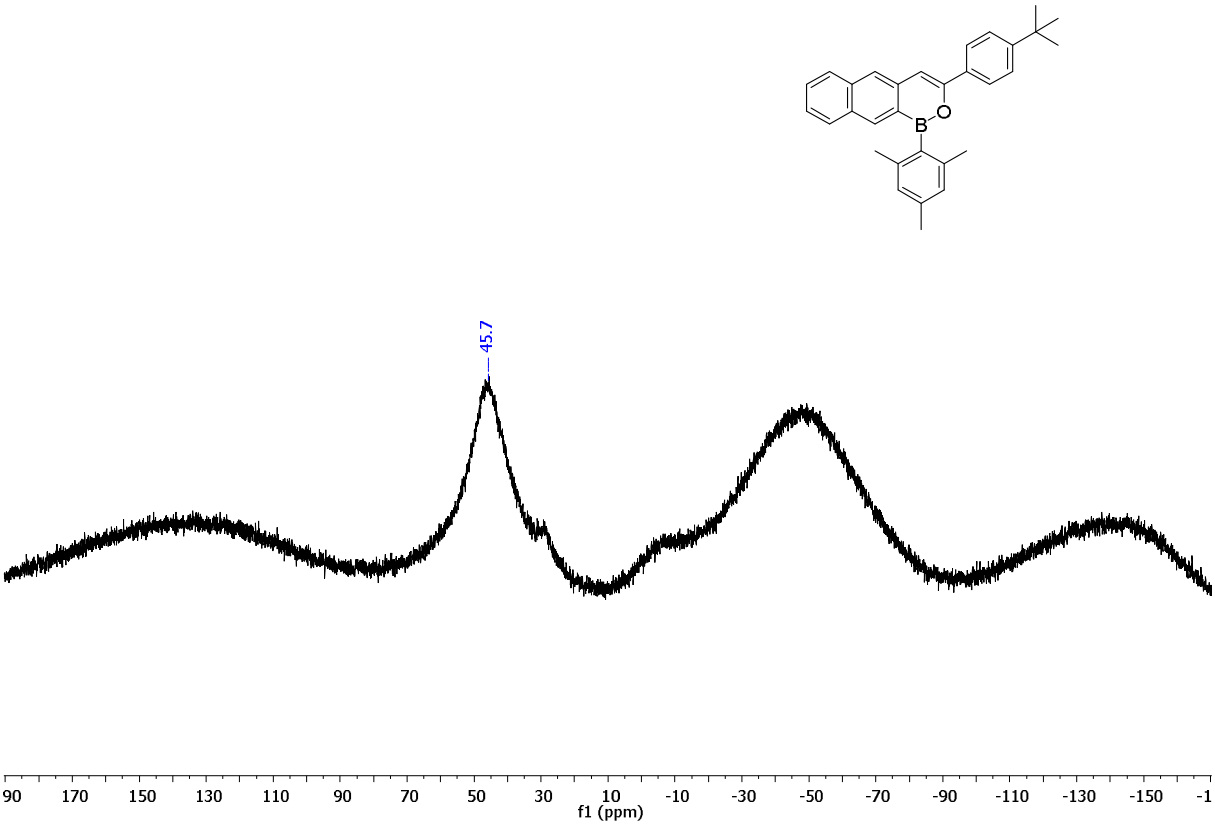

Figure S24: ^{11}B NMR spectrum of **5a** ($CDCl_3$, 96.3 MHz).

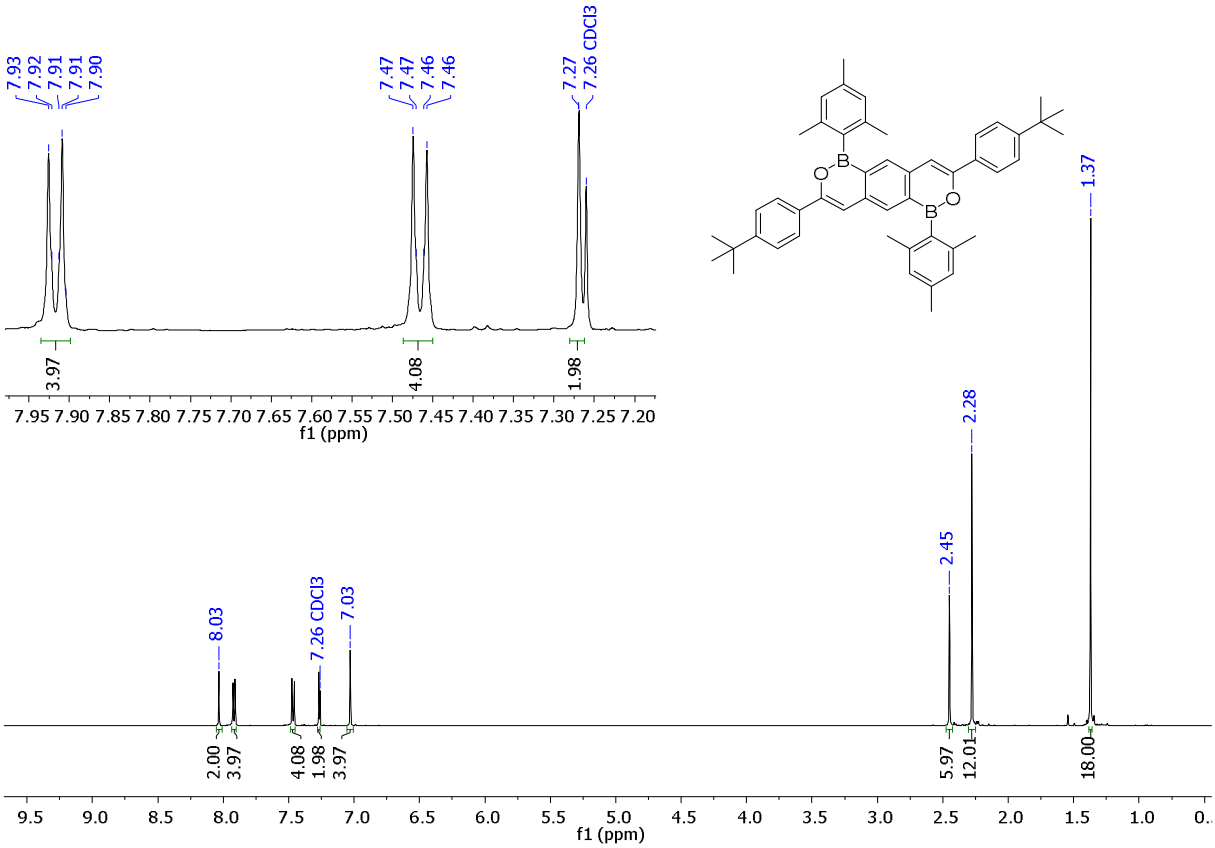

Figure S25: ^{1}H NMR spectrum of **6a** ($CDCl_3$, 500.2 MHz).

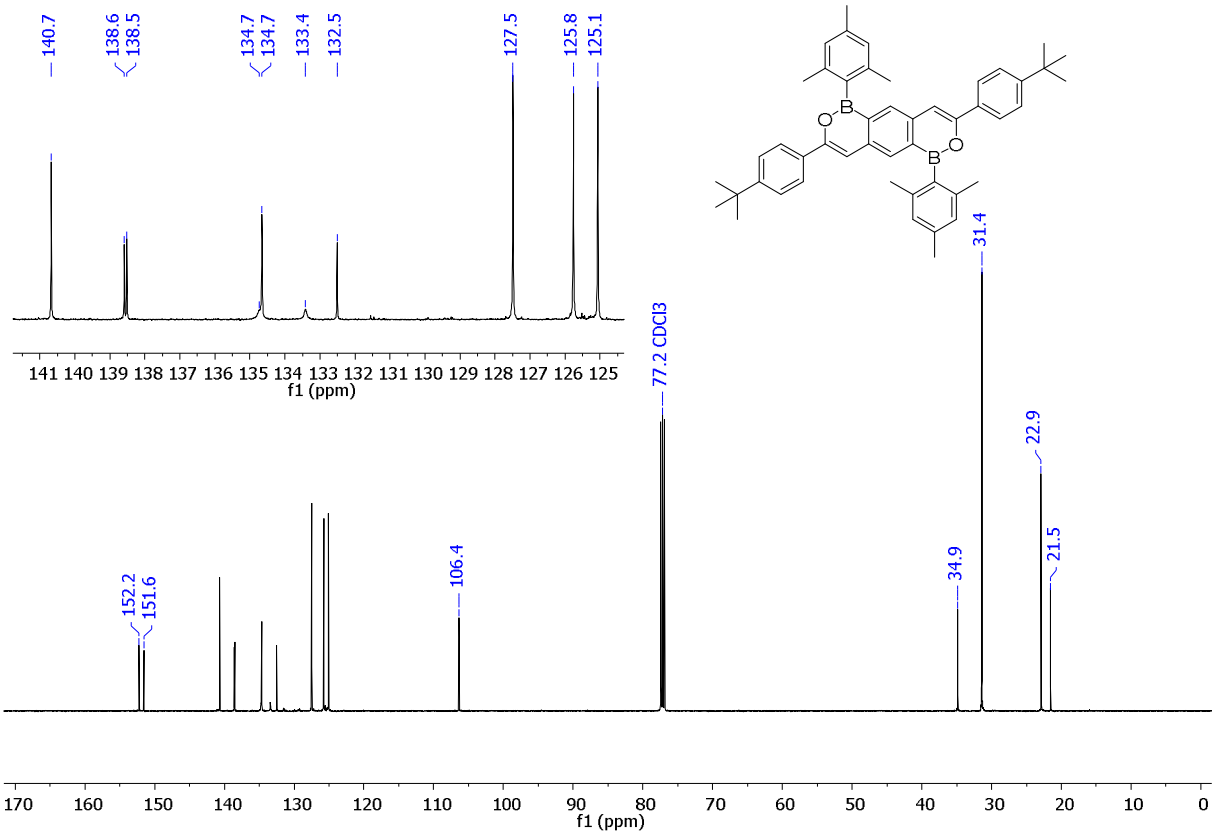

Figure S26: $^{13}C\{^{1}H\}$ NMR spectrum of **6a** ($CDCl_3$, 125.8 MHz).

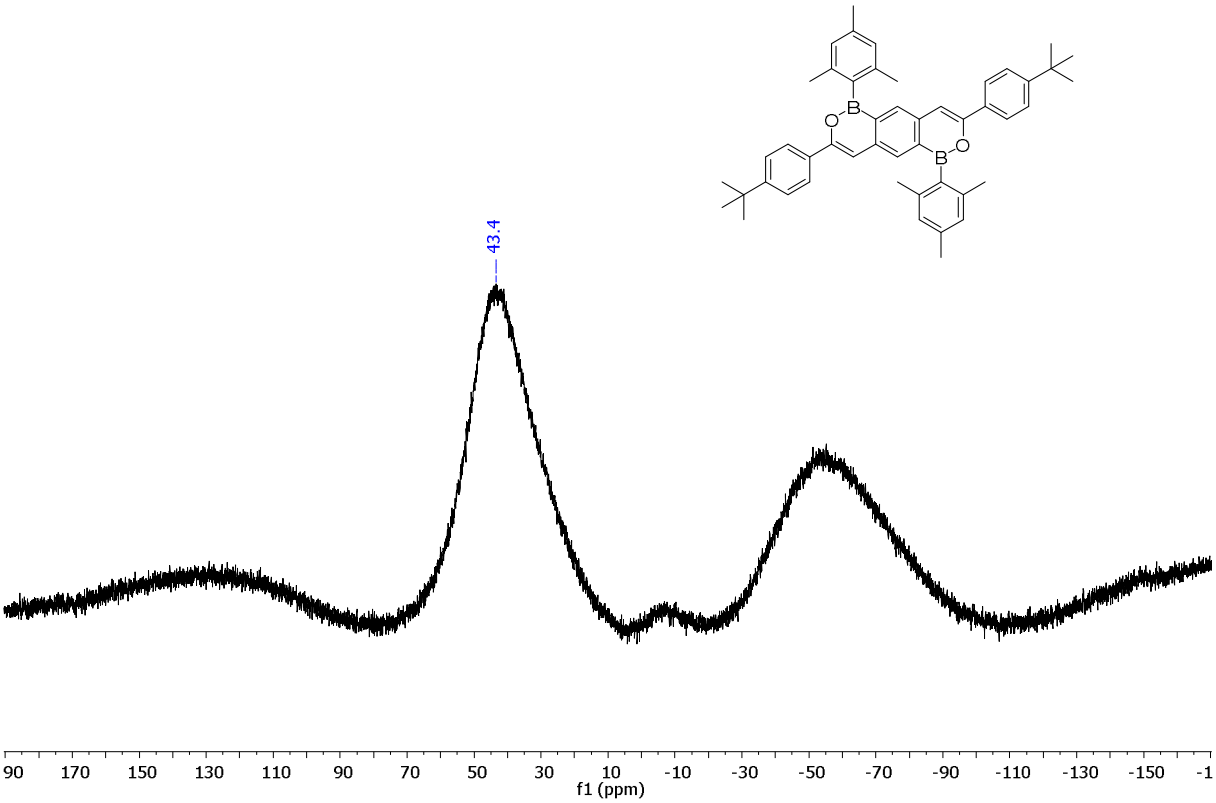

Figure S27: ^{11}B NMR spectrum of **6a** ($CDCl_3$, 96.3 MHz).

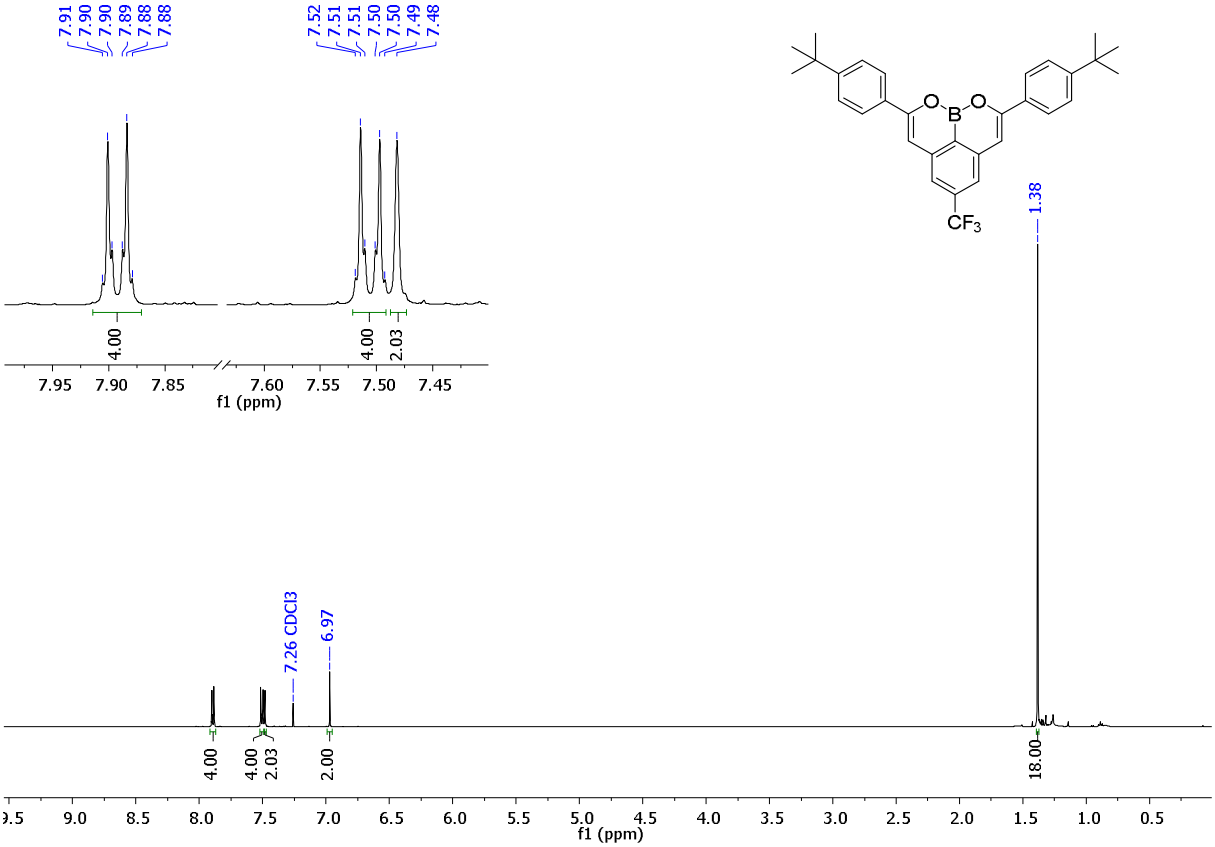

Figure S28: ^{1}H NMR spectrum of **8a** ($CDCl_3$, 500.2 MHz).

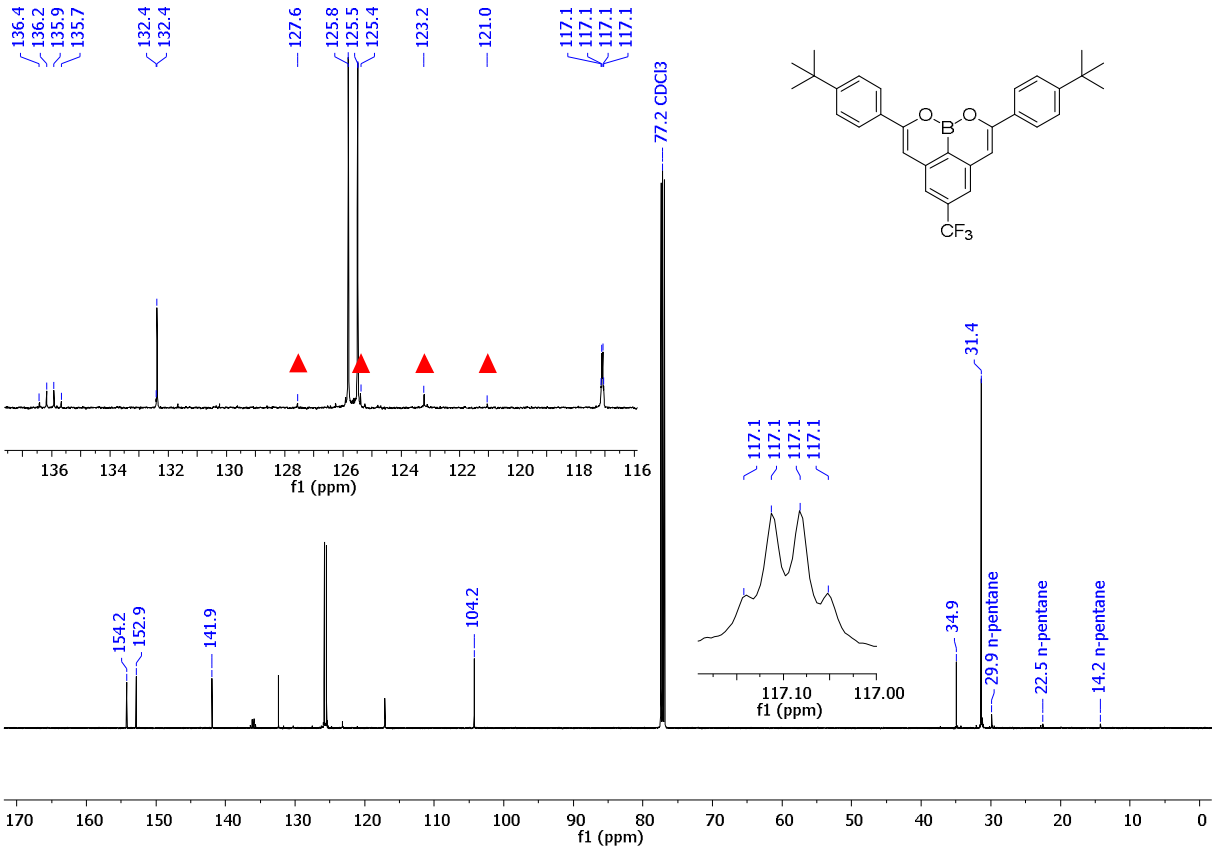

Figure S29: $^{13}C\{^{1}H\}$ NMR spectrum of **8a** ($CDCl_3$, 125.8 MHz; ▲: CF_3 resonance).

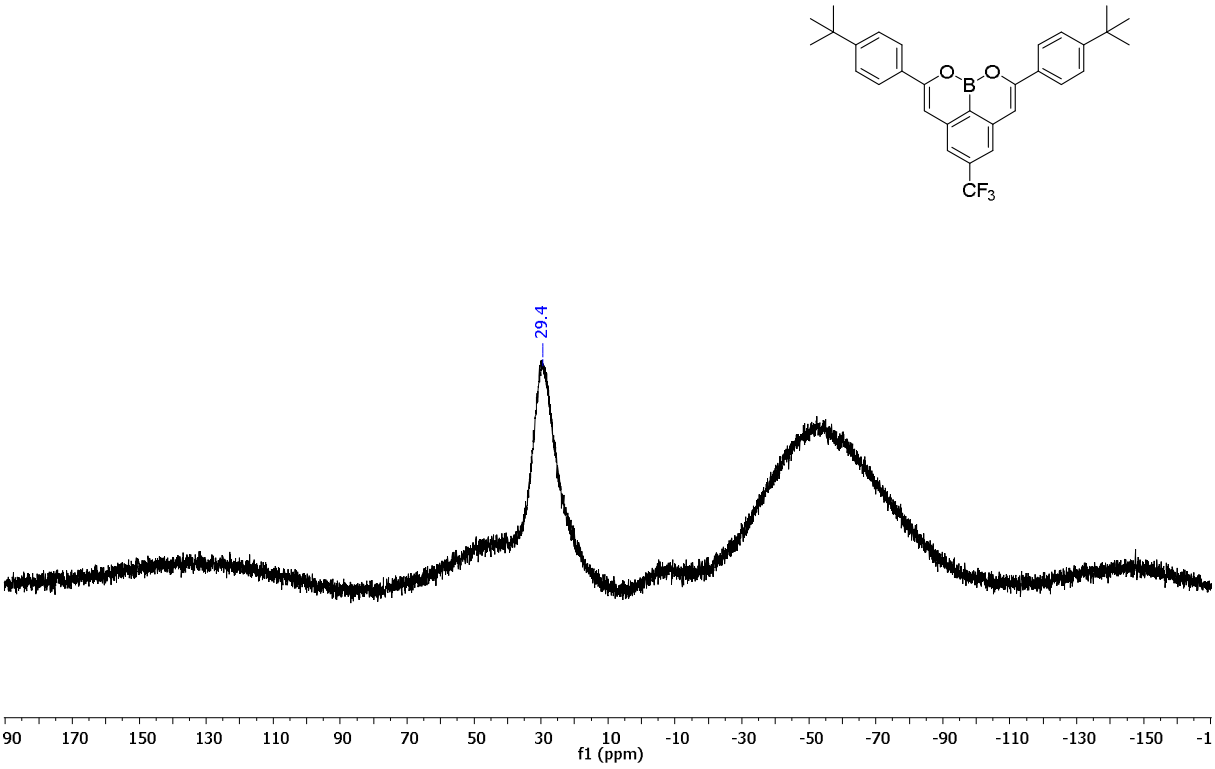

Figure S30: ^{11}B NMR spectrum of **8a** ($CDCl_3$, 96.3 MHz).

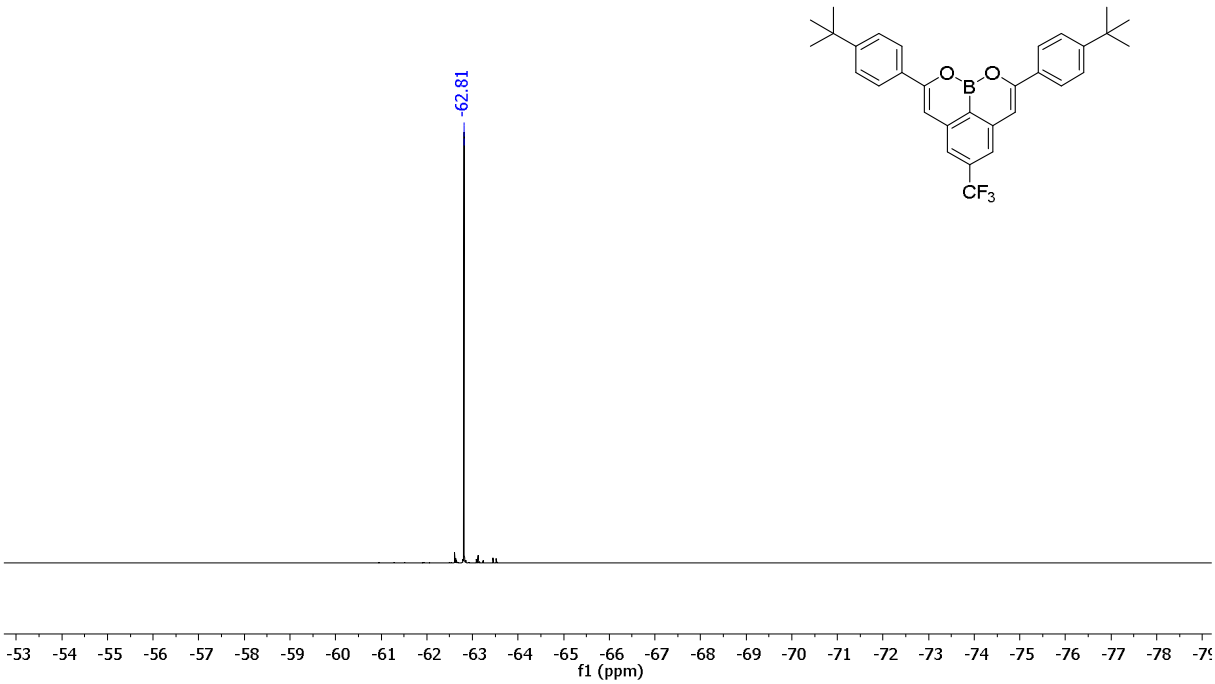

Figure S31: $^{19}F\{^{1}H\}$ NMR spectrum of **8a** ($CDCl_3$, 470.4 MHz).

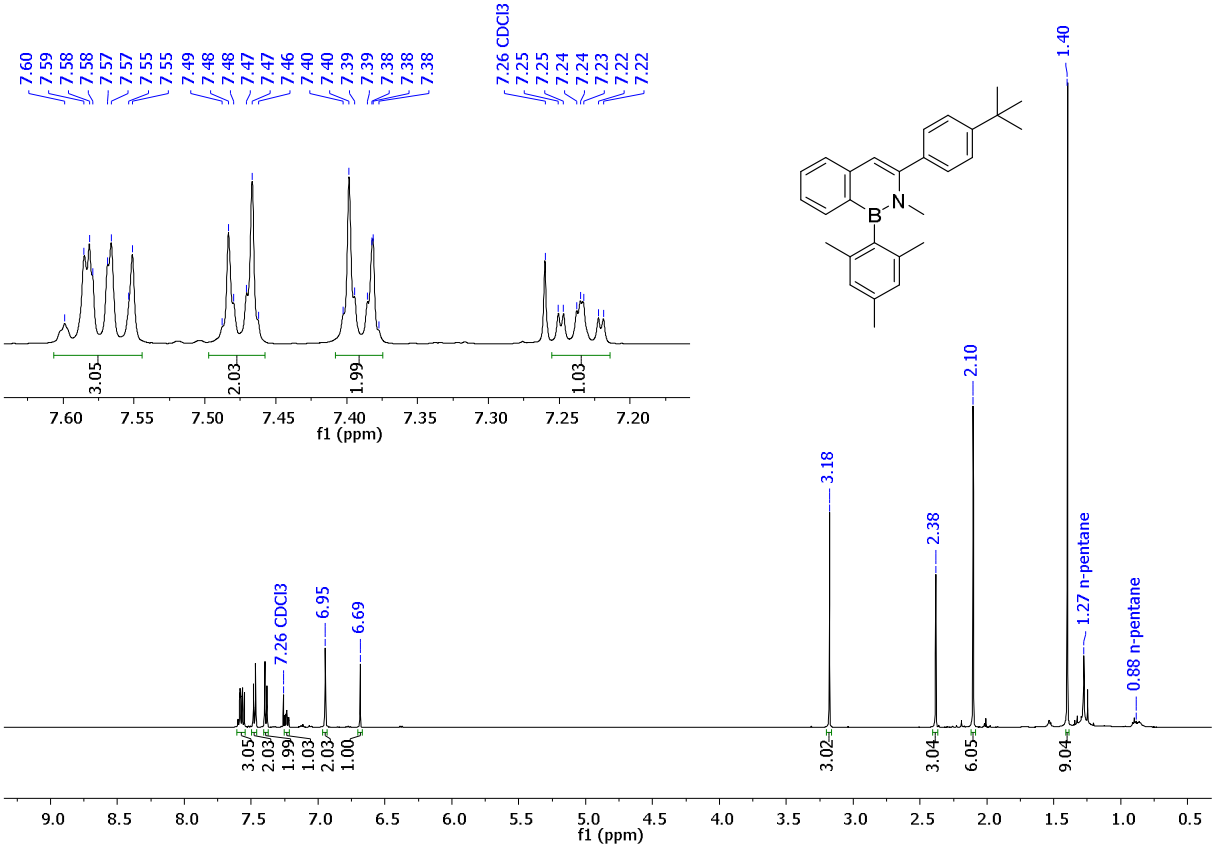

Figure S32: ^{1}H NMR spectrum of **4b** ($CDCl_3$, 500.2 MHz).

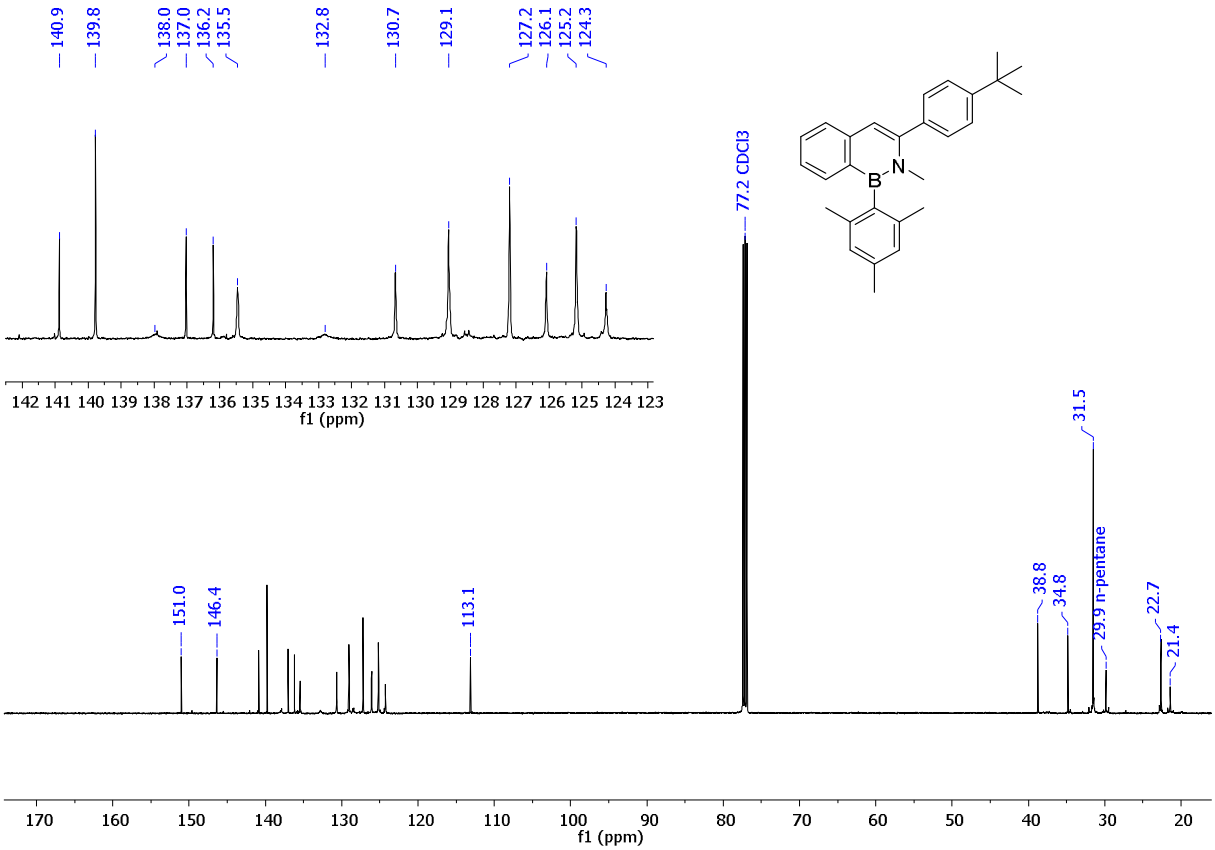

Figure S33: $^{13}C\{^{1}H\}$ NMR spectrum of **4b** ($CDCl_3$, 125.8 MHz).

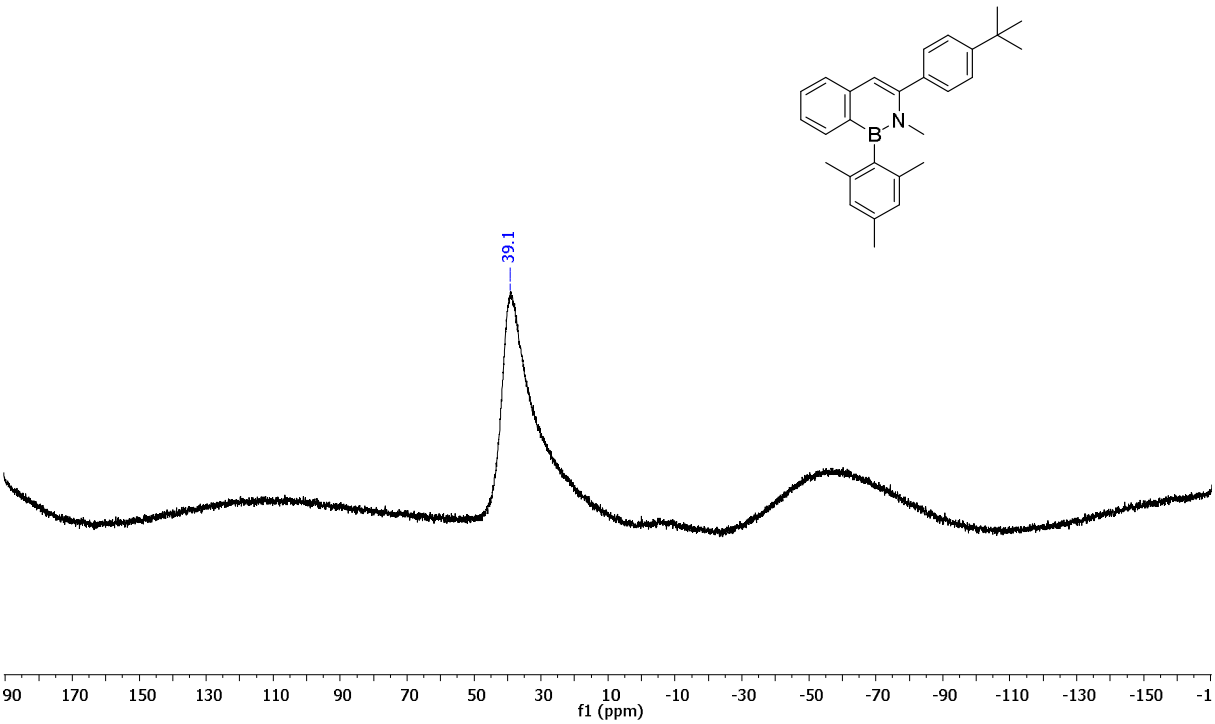

Figure S34: ^{11}B NMR spectrum of **4b** ($CDCl_3$, 96.3 MHz).

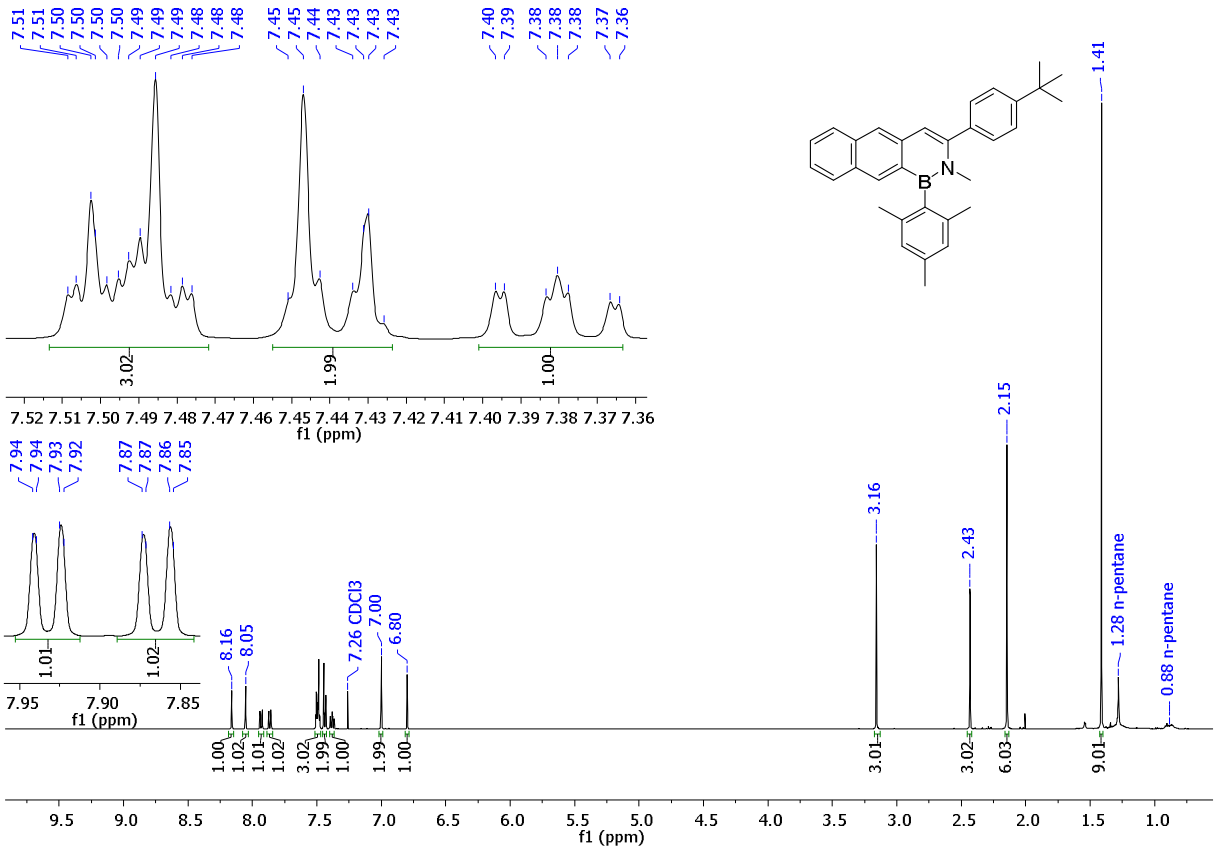

Figure S35: ^{1}H NMR spectrum of **5b** ($CDCl_3$, 500.2 MHz).

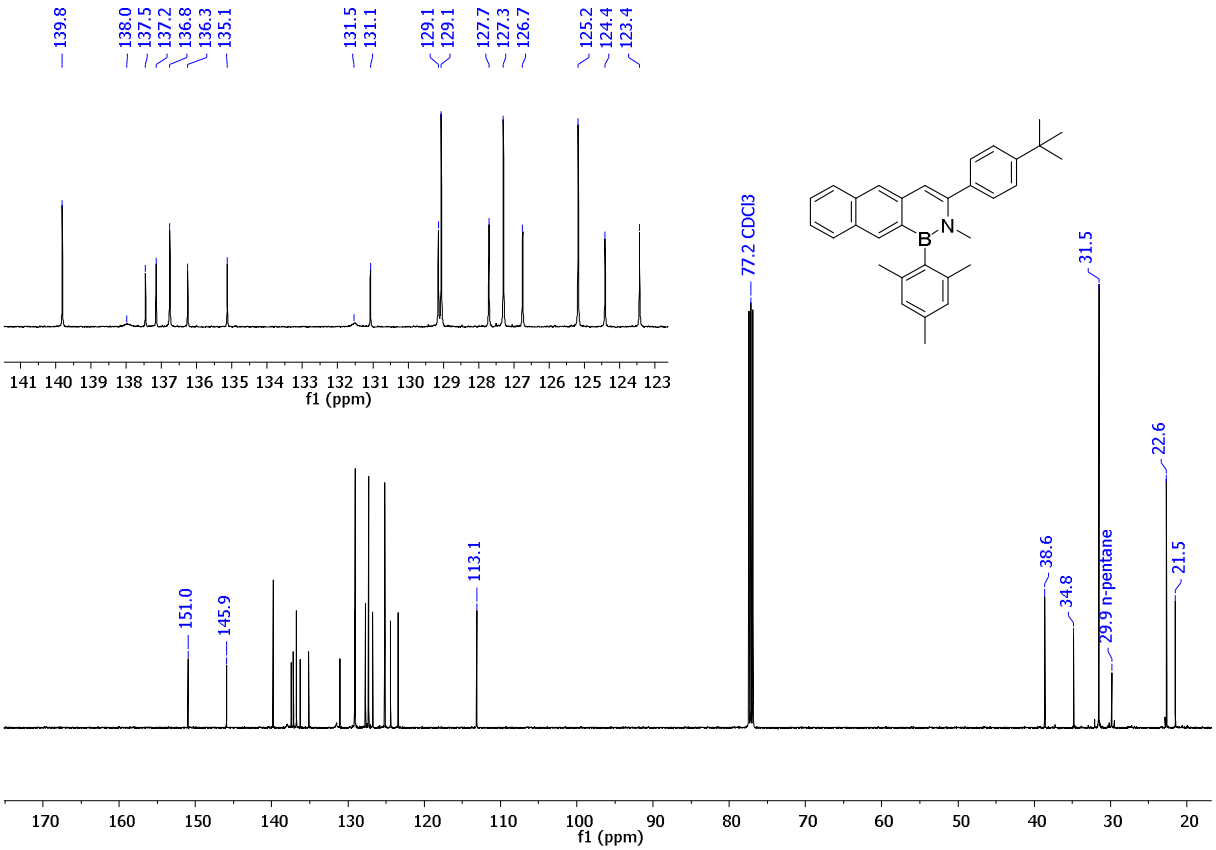

Figure S36: $^{13}C\{^{1}H\}$ NMR spectrum of **5b** ($CDCl_3$, 125.8 MHz).

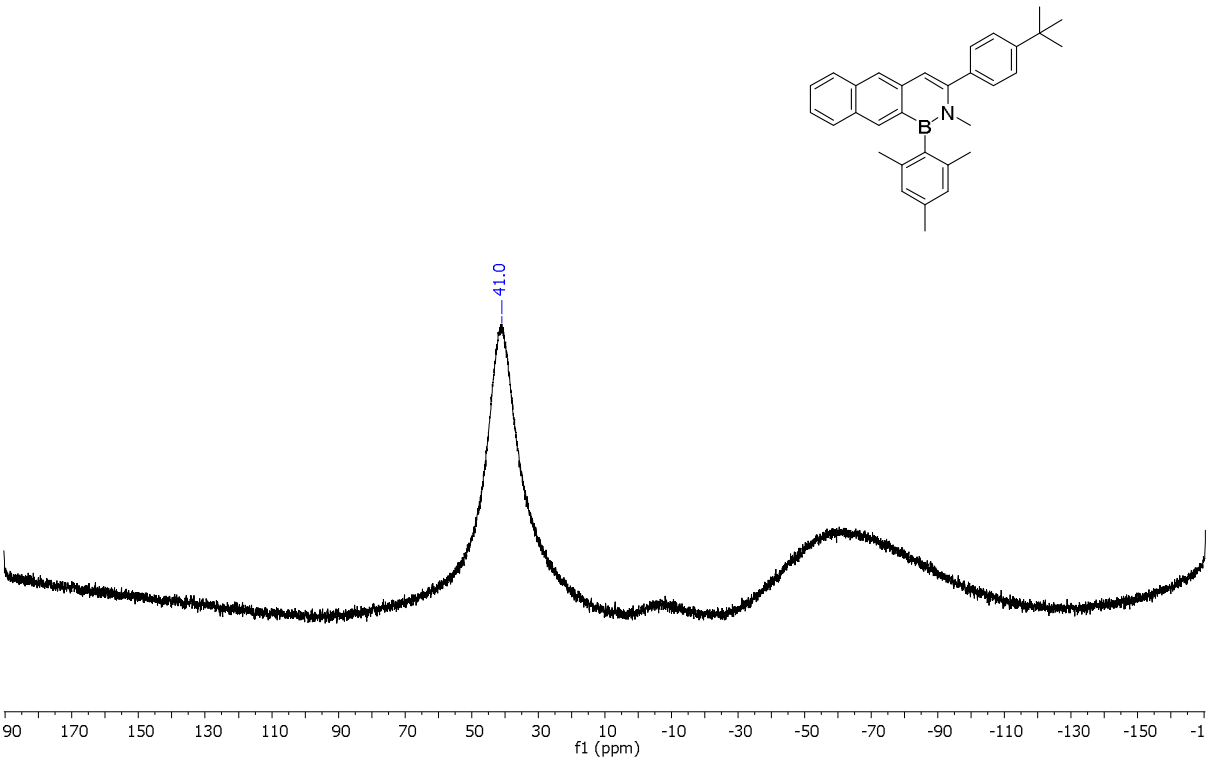

Figure S37: ^{11}B NMR spectrum of **5b** ($CDCl_3$, 96.3 MHz).

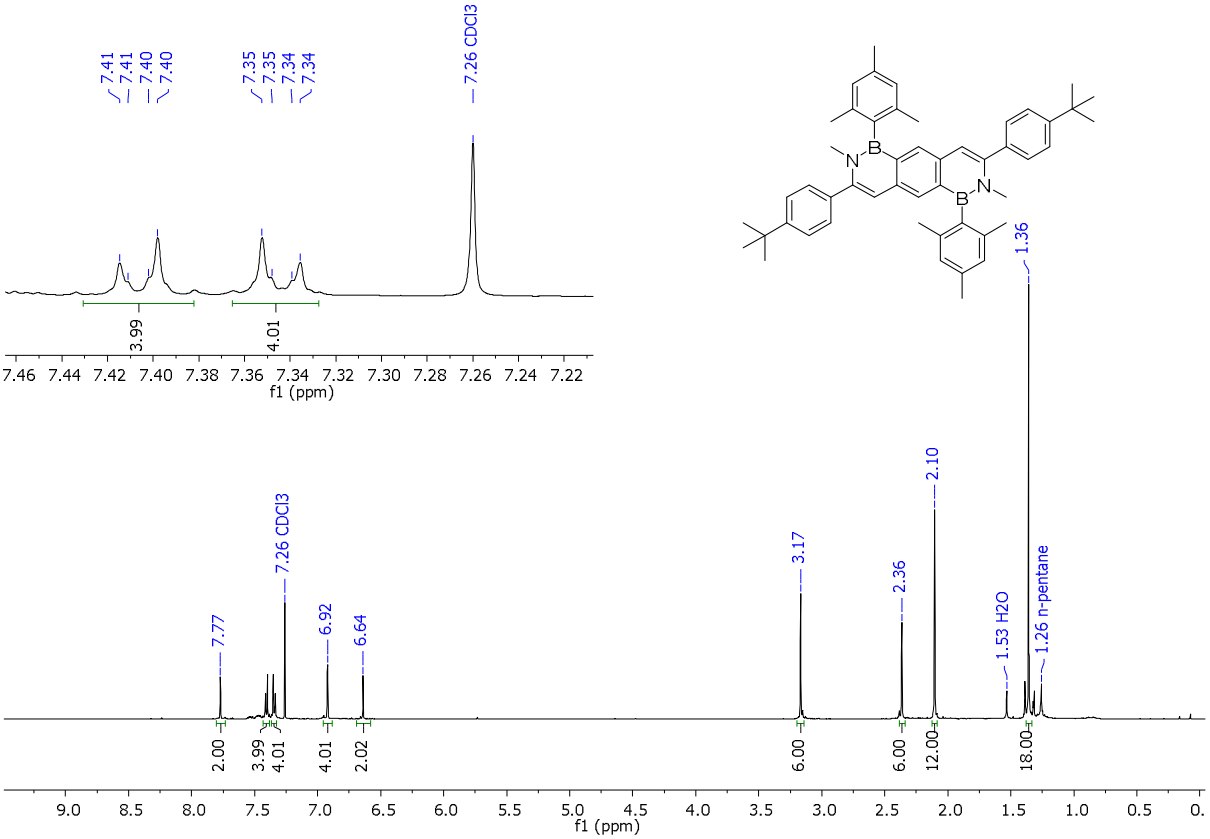

Figure S38: ^{1}H NMR spectrum of **6b** ($CDCl_3$, 500.2 MHz).

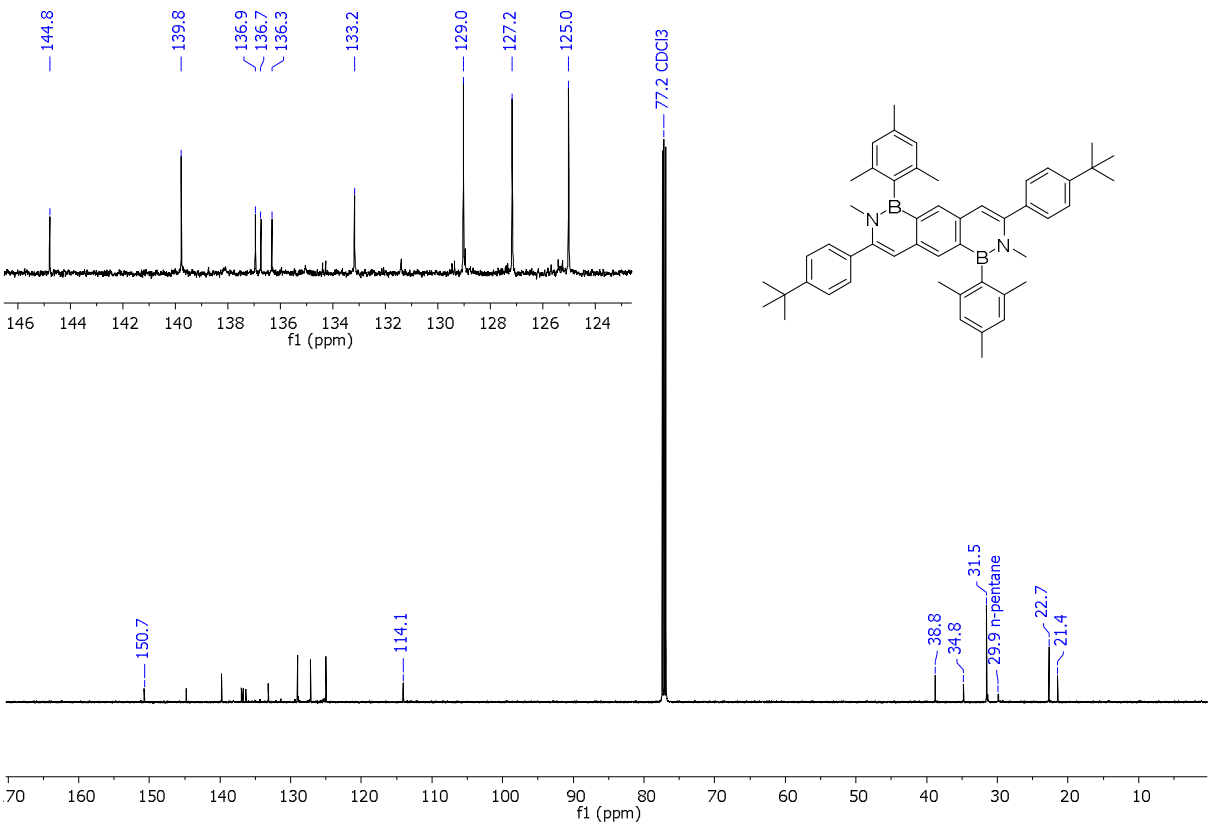

Figure S39: $^{13}C\{^{1}H\}$ NMR spectrum of **6b** ($CDCl_3$, 125.8 MHz).

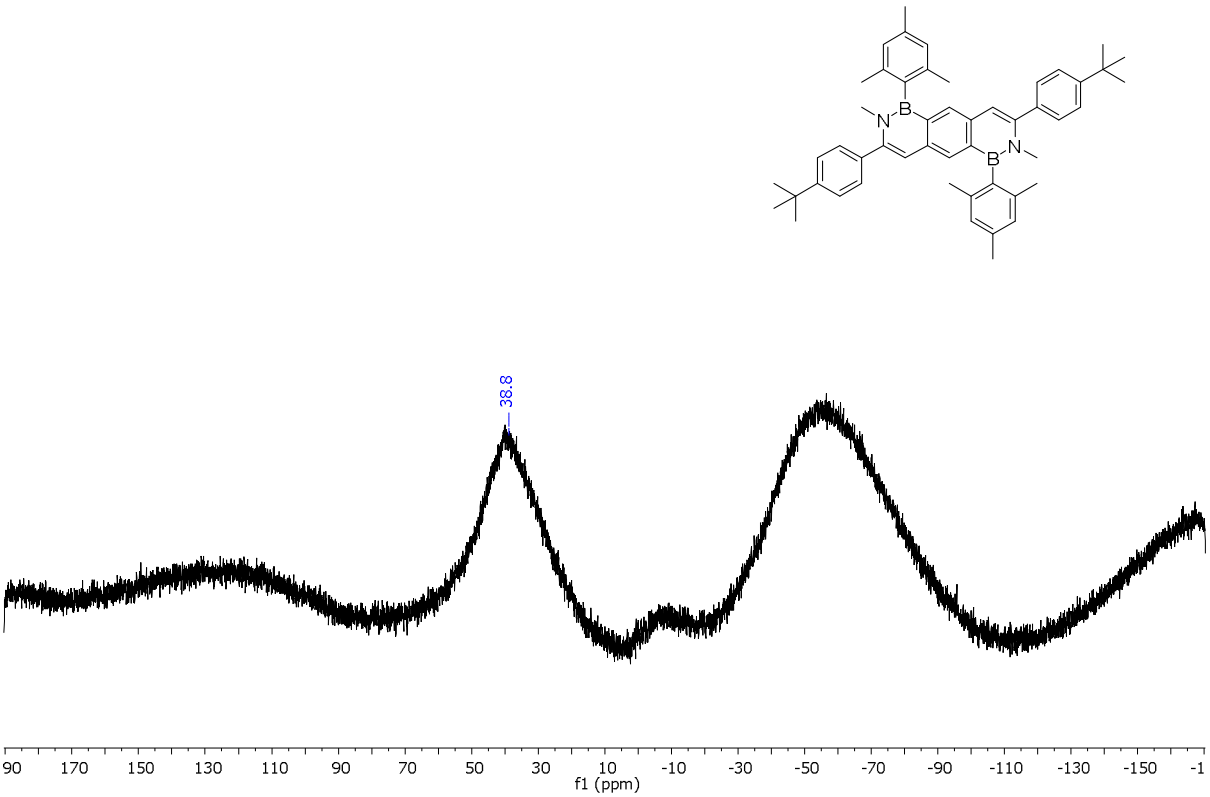

Figure S40: ^{11}B NMR spectrum of **6b** ($CDCl_3$, 96.3 MHz).

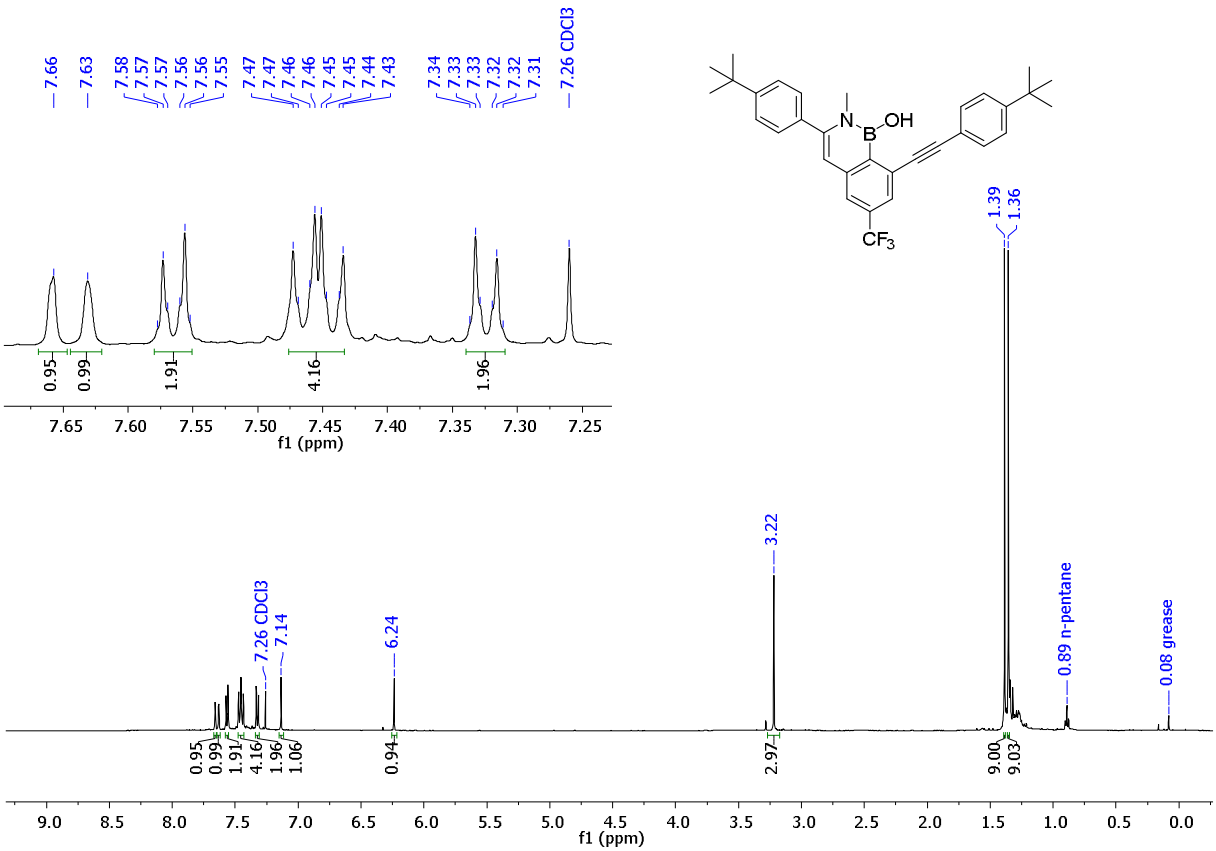

Figure S41: ^{1}H NMR spectrum of **8c** ($CDCl_3$, 500.2 MHz).

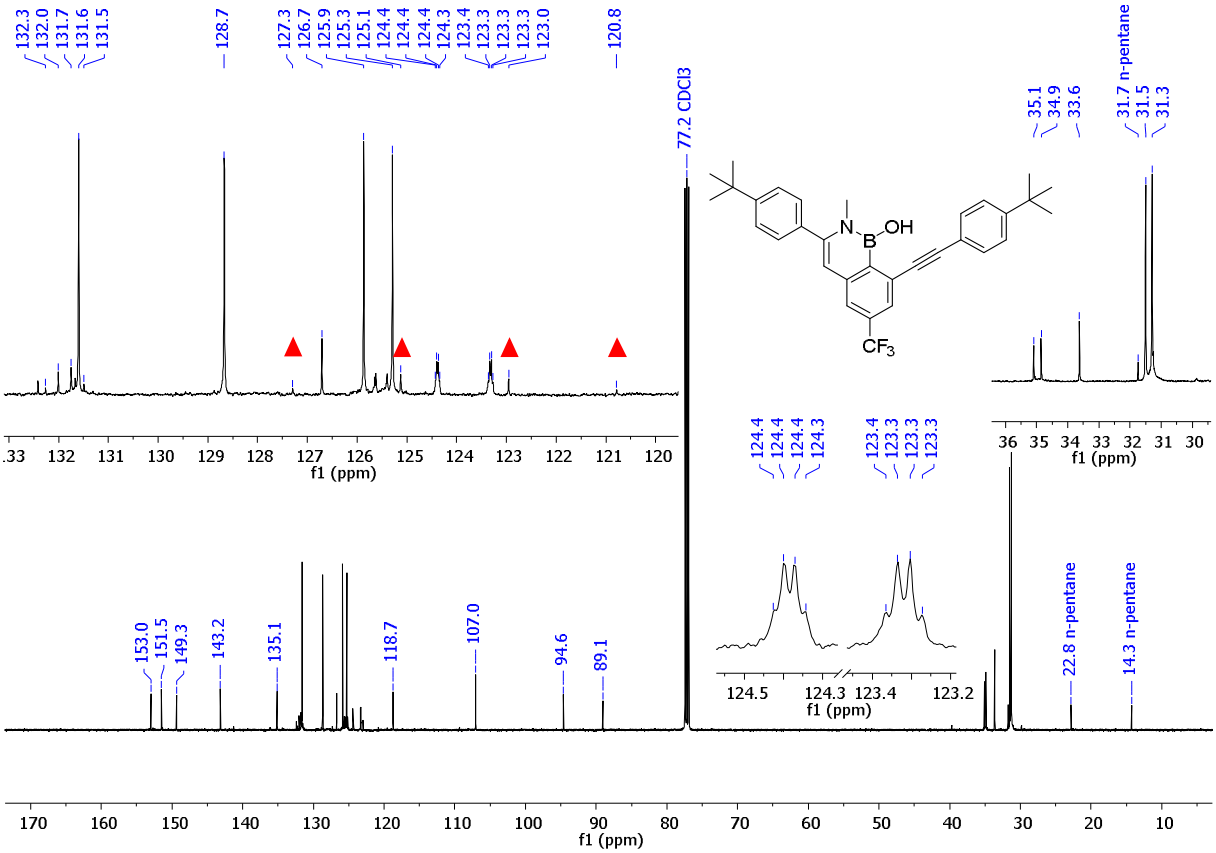

Figure S42: $^{13}C\{^{1}H\}$ NMR spectrum of **8c** ($CDCl_3$, 125.8 MHz; ▲: CF_3 resonance).

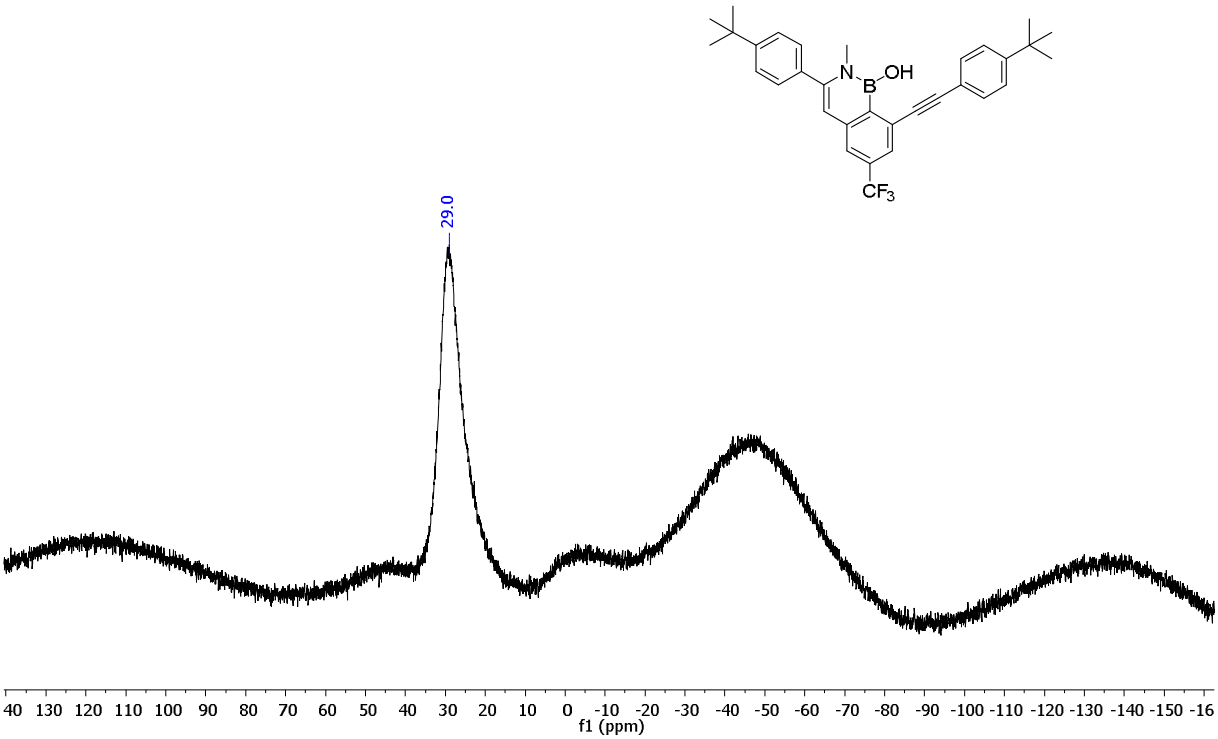

Figure S43: ^{11}B NMR spectrum of **8c** ($CDCl_3$, 96.3 MHz).

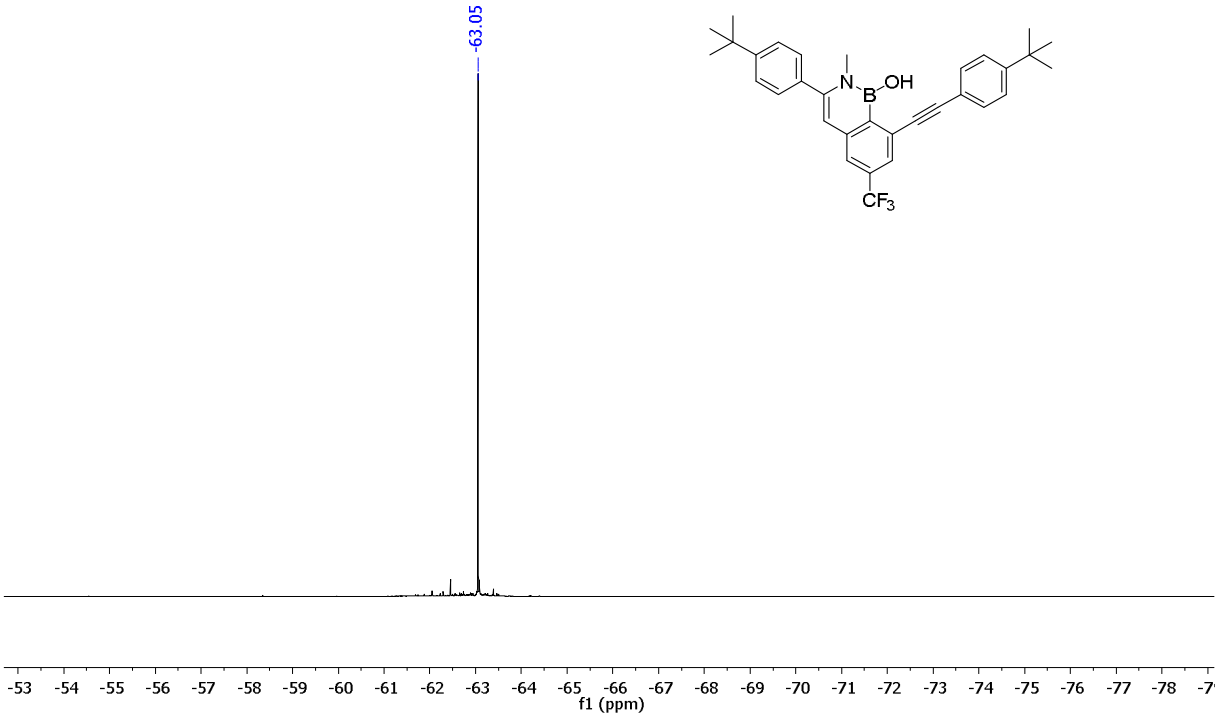

Figure S44: $^{19}F\{^1H\}$ NMR spectrum of **8c** ($CDCl_3$, 470.4 MHz).

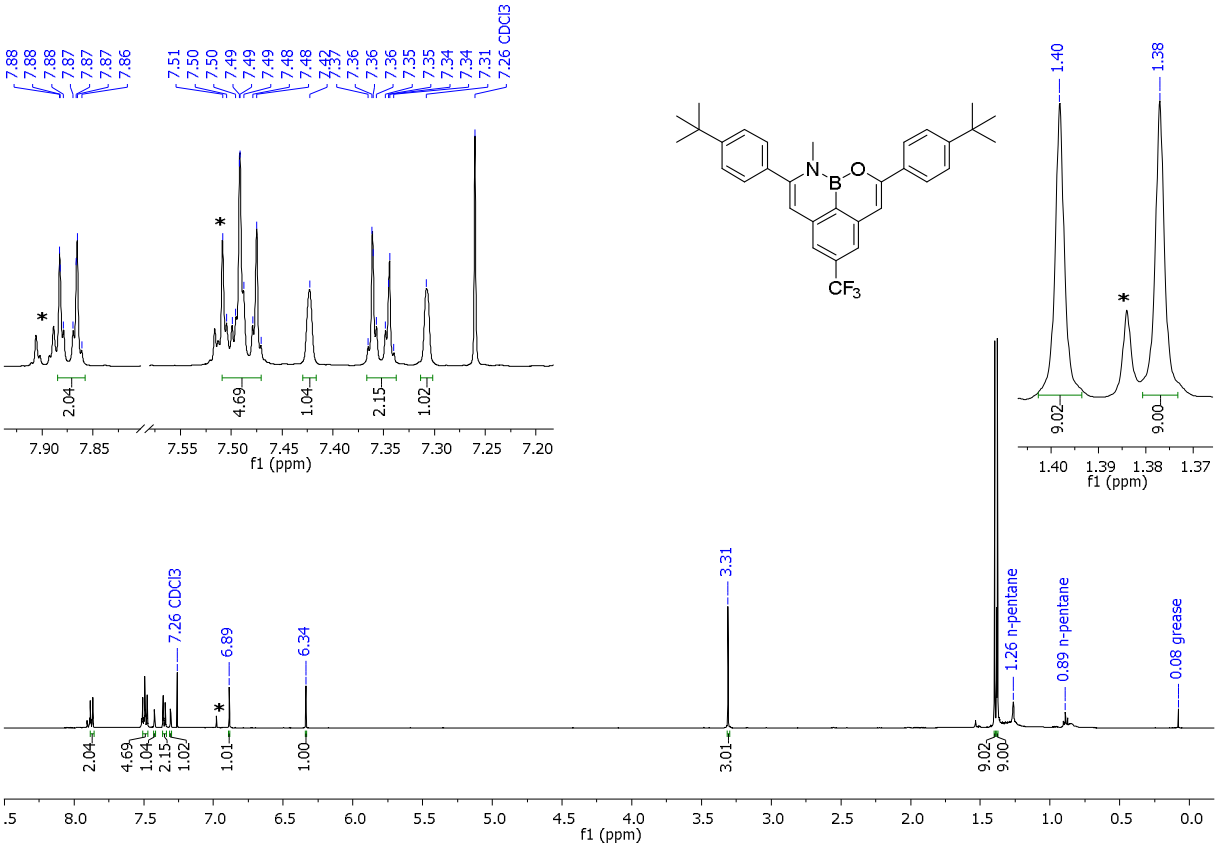

Figure S45: ^{1}H NMR spectrum of **8ab** ($CDCl_3$, 500.2 MHz; resonances of **8a** are marked with asterisks).

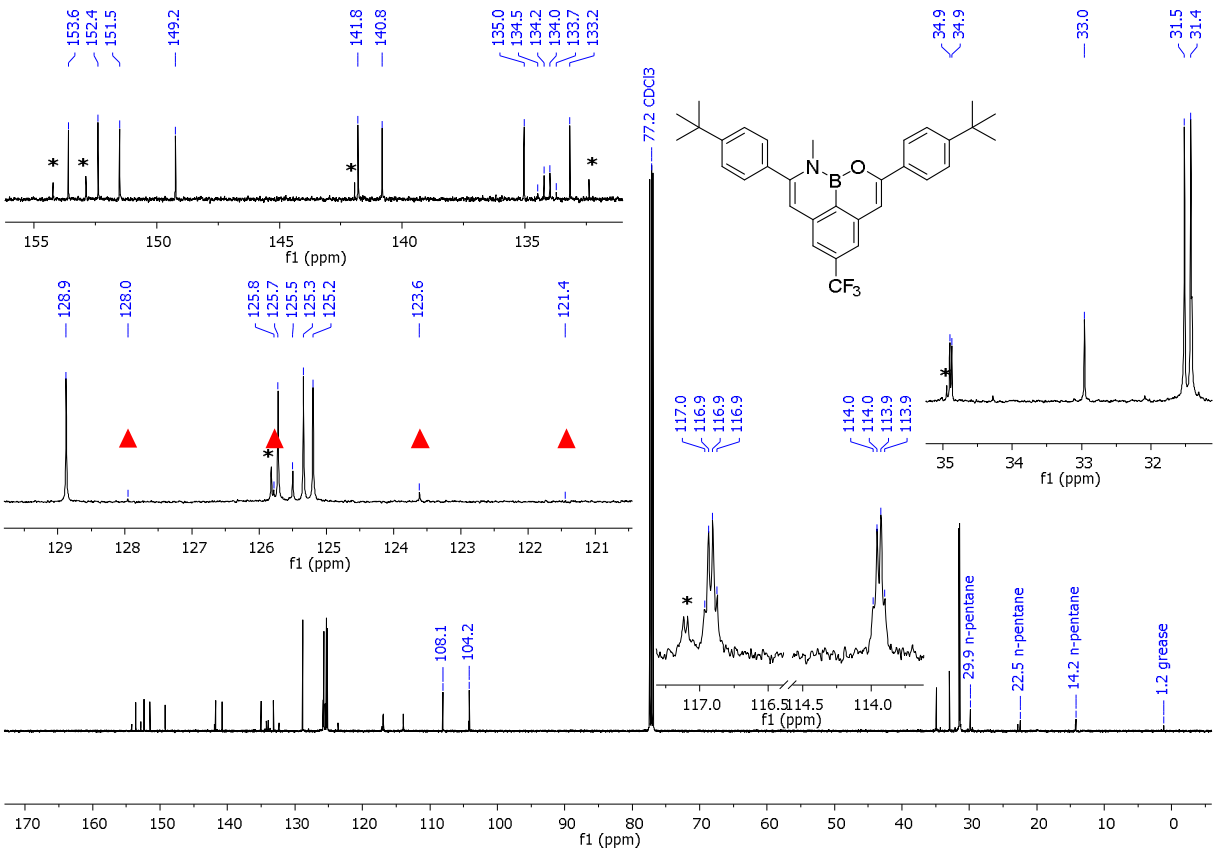

Figure S46: $^{13}C\{^{1}H\}$ NMR spectrum of **8ab** ($CDCl_3$, 125.8 MHz; ▲: CF_3 resonance; resonances of **8a** are marked with asterisks).

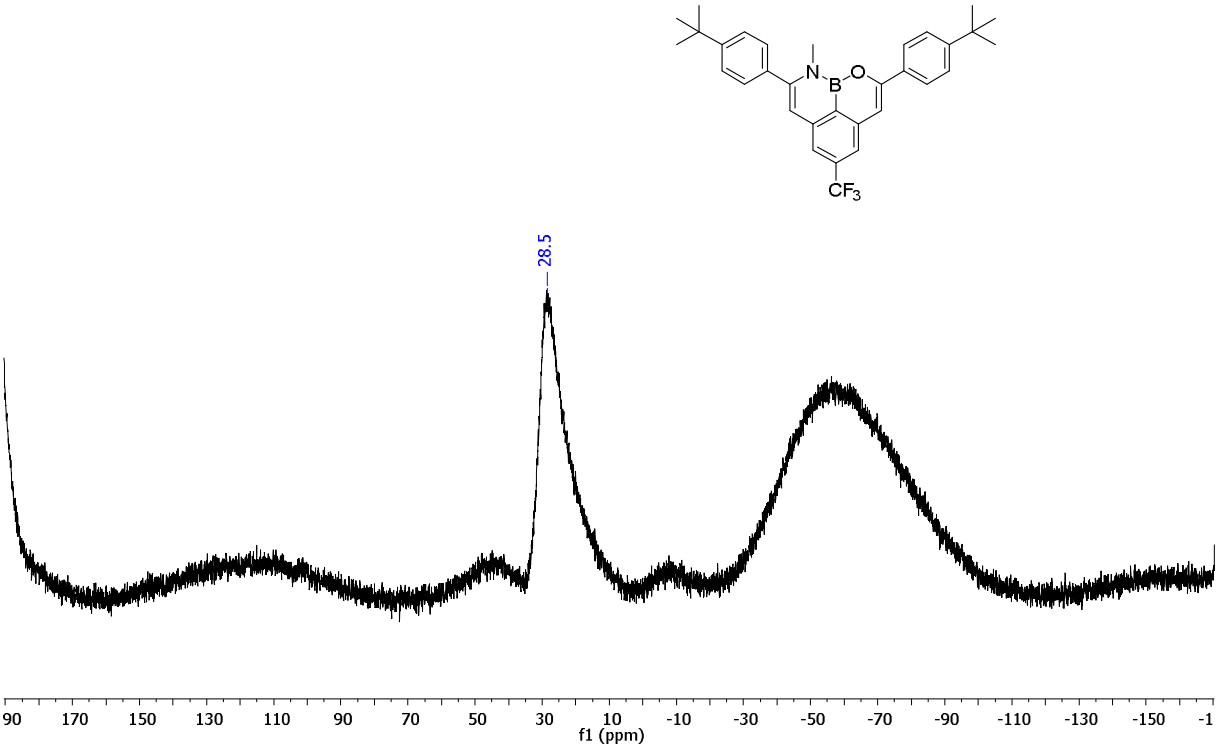

Figure S47: ^{11}B NMR spectrum of **8ab** ($CDCl_3$, 96.3 MHz).

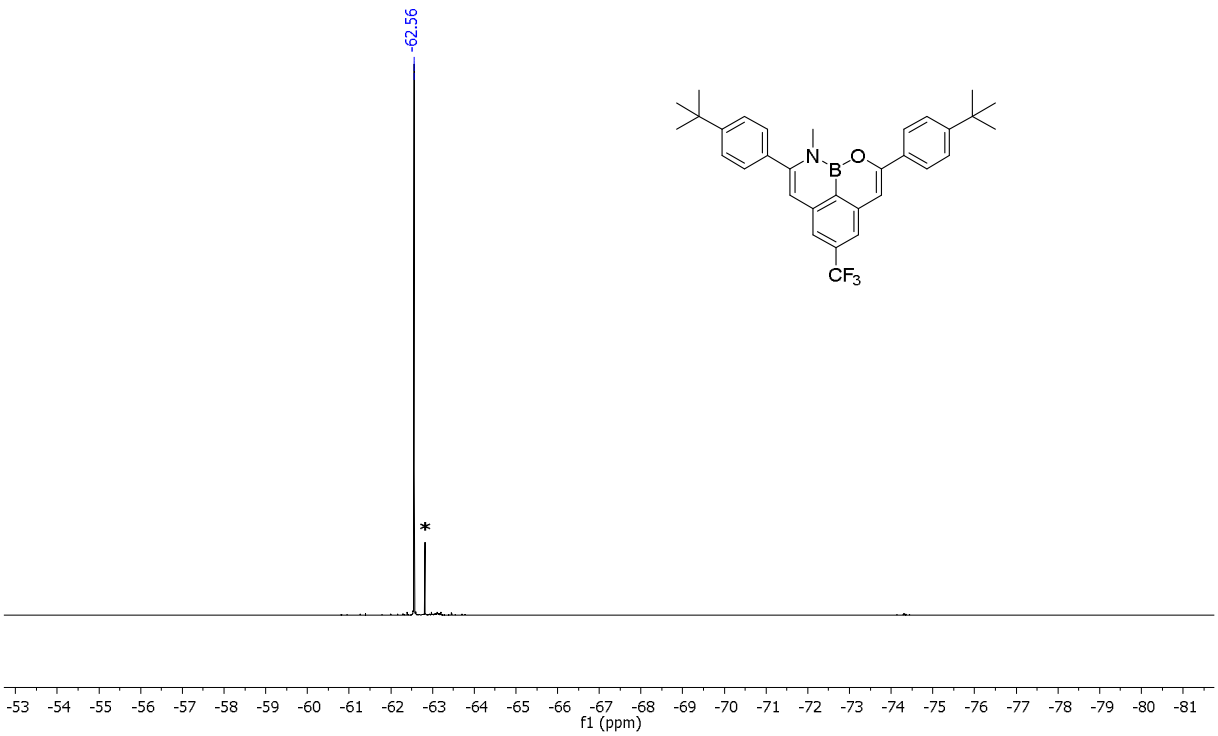

Figure S48: $^{19}F\{^1H\}$ NMR spectrum of **8ab** ($CDCl_3$, 470.4 MHz; the resonance of **8a** is marked with an asterisk).

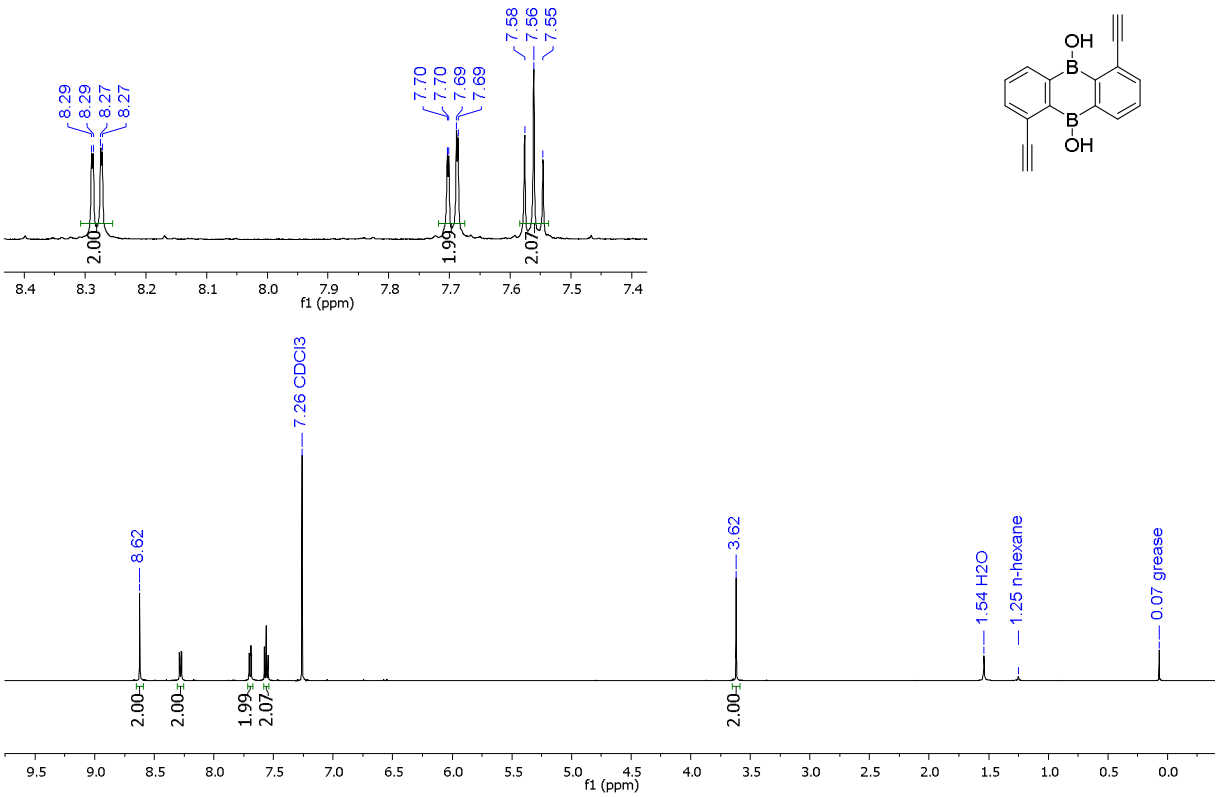

Figure S49: ^{1}H NMR spectrum of **26** ($CDCl_3$, 500.2 MHz).

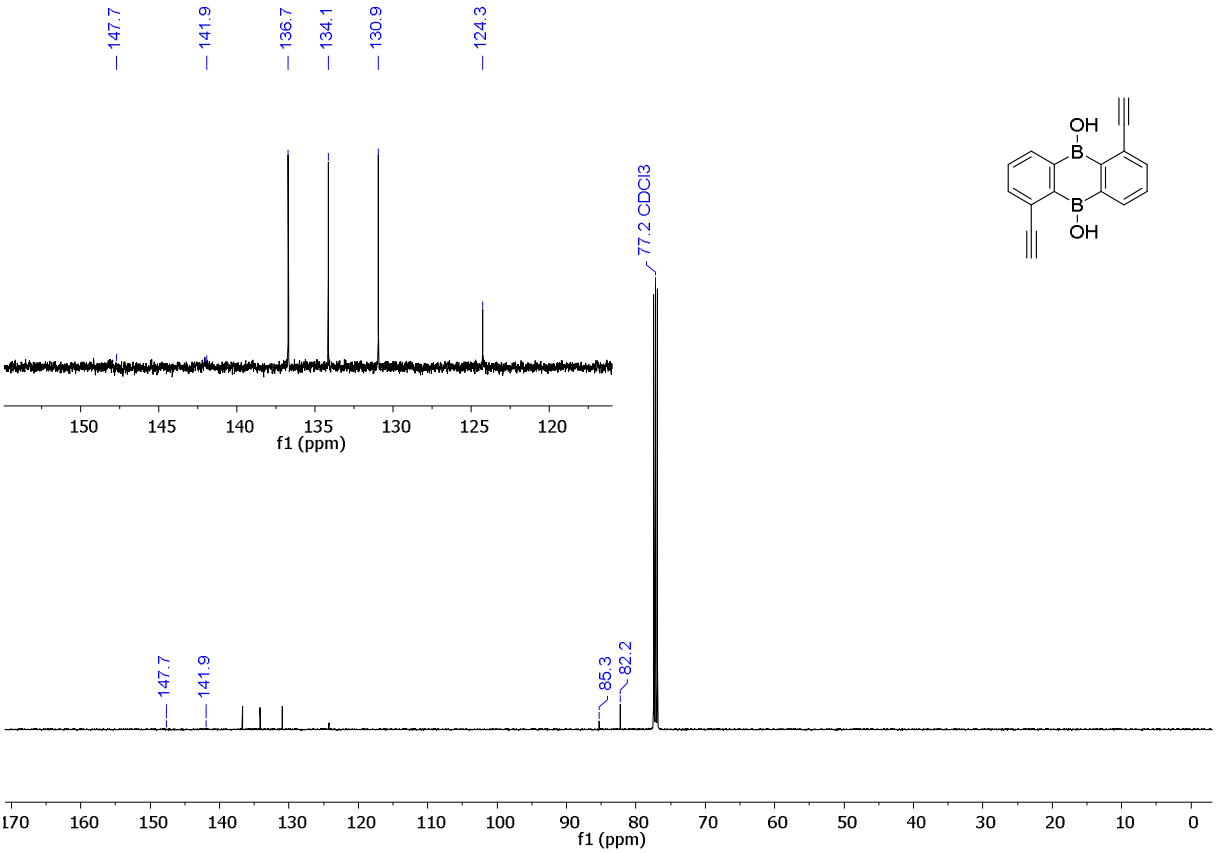

Figure S50: $^{13}C\{^{1}H\}$ NMR spectrum of **26** ($CDCl_3$, 125.8 MHz).

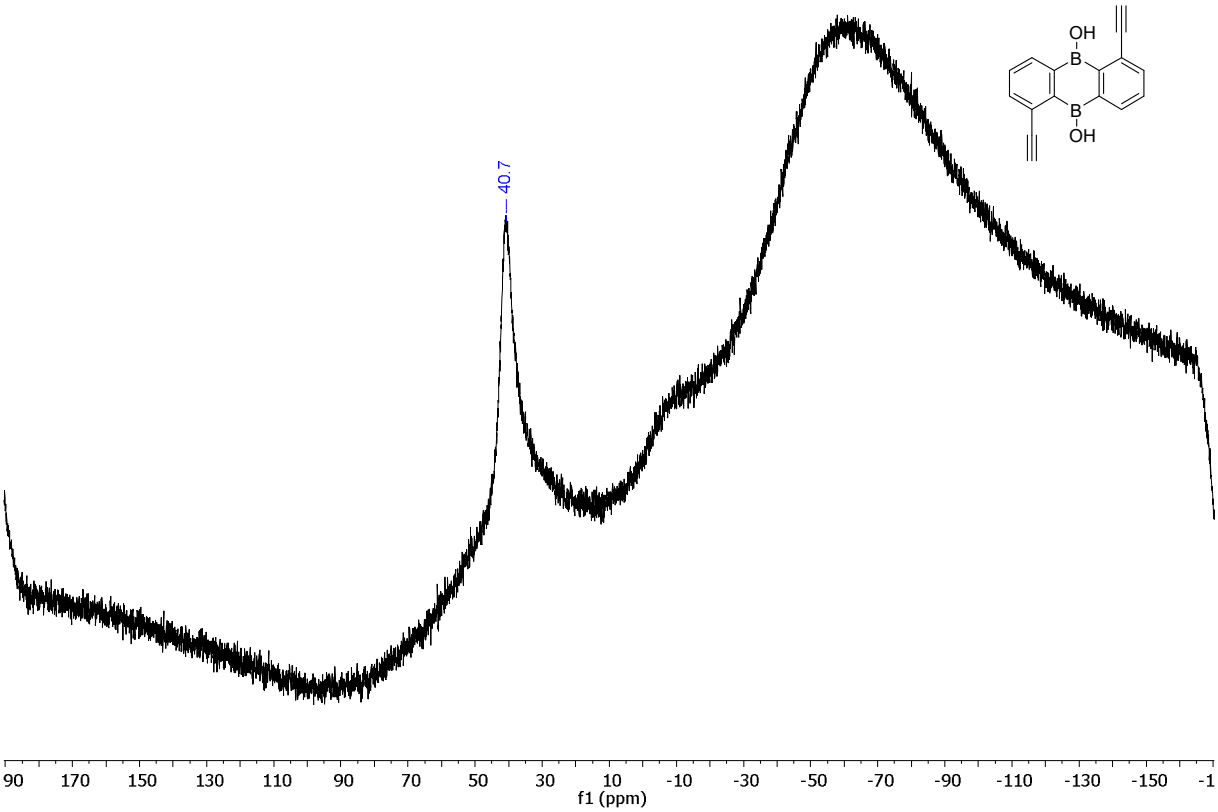

Figure S51: ^{11}B NMR spectrum of **26** ($CDCl_3$, 96.3 MHz).

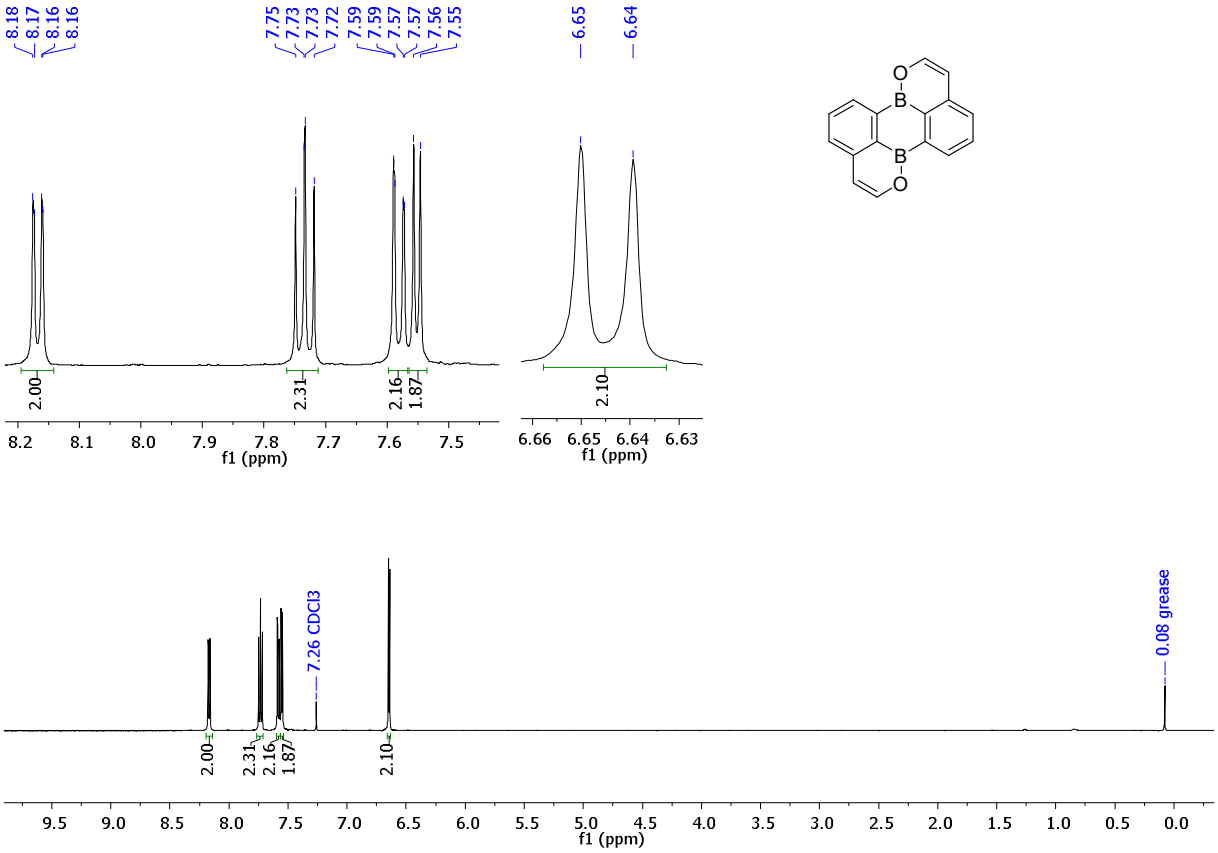

Figure S52: ^{1}H NMR spectrum of **9** ($CDCl_3$, 500.2 MHz).

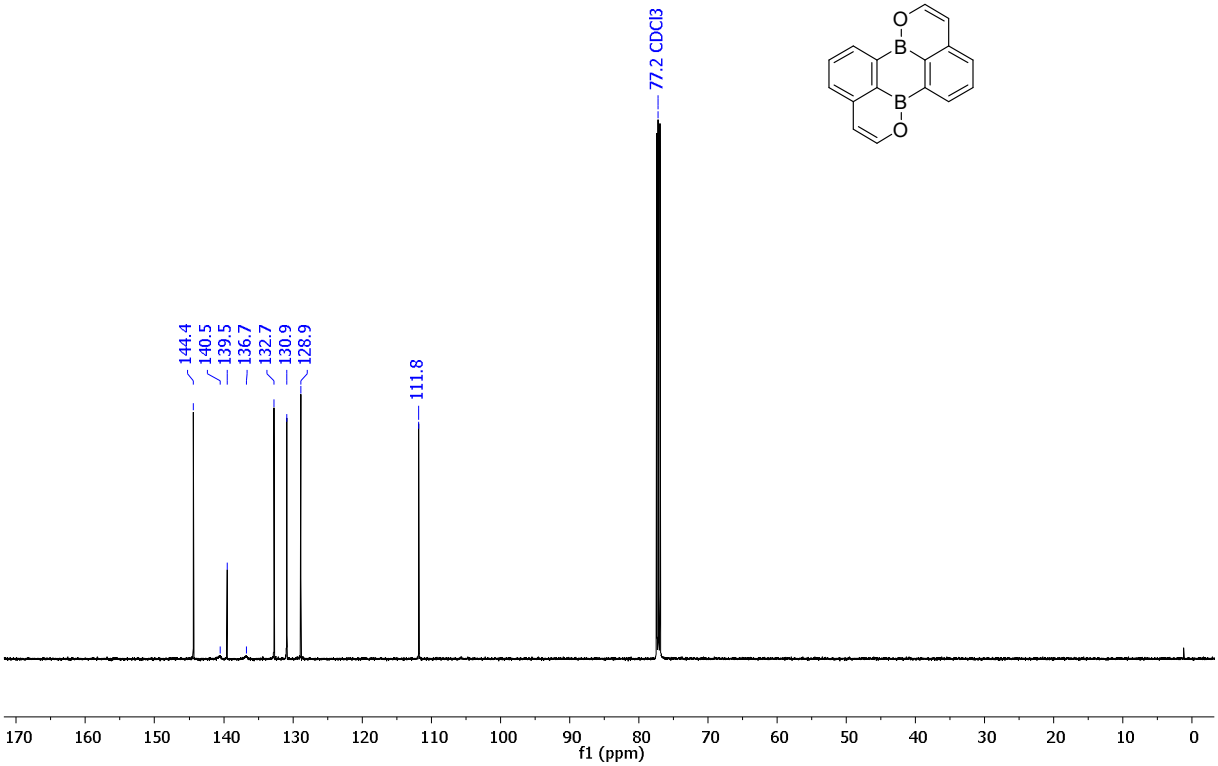

Figure S53: $^{13}C\{^{1}H\}$ NMR spectrum of **9** ($CDCl_3$, 125.8 MHz).

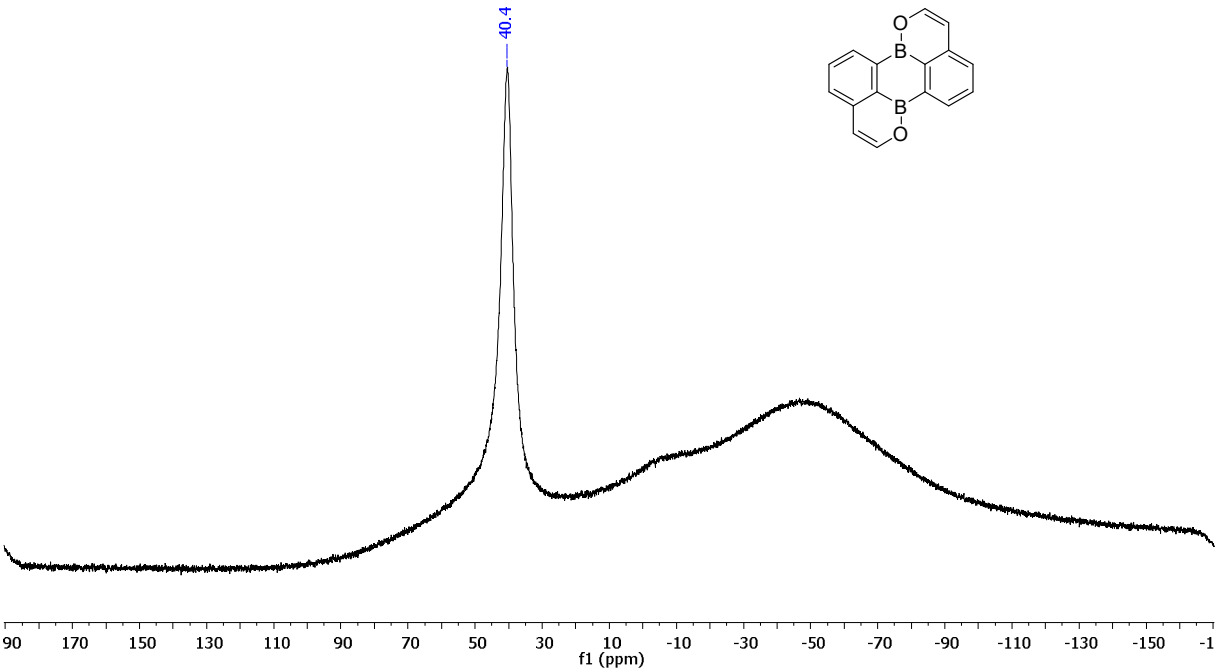

Figure S54: ^{11}B NMR spectrum of **9** ($CDCl_3$, 96.3 MHz).

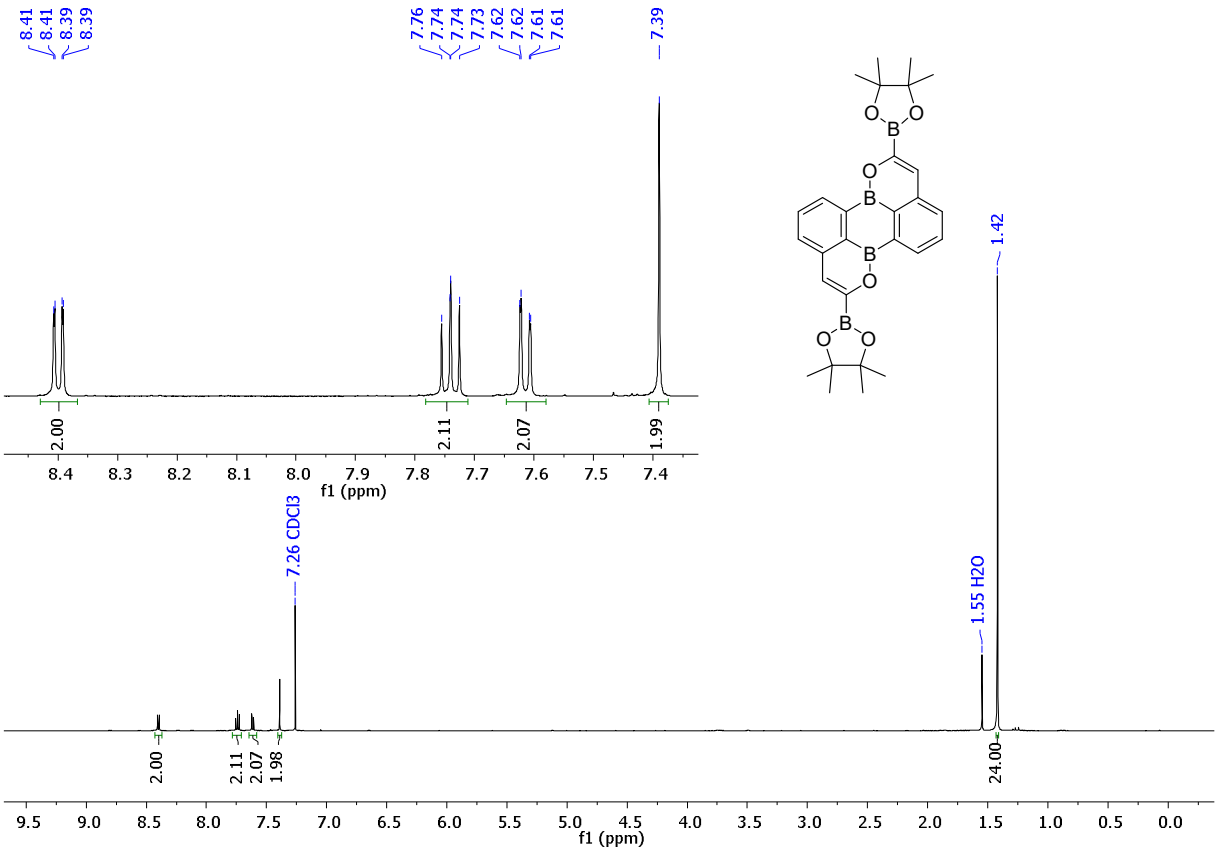

Figure S55: ^{1}H NMR spectrum of **10** ($CDCl_3$, 500.2 MHz).

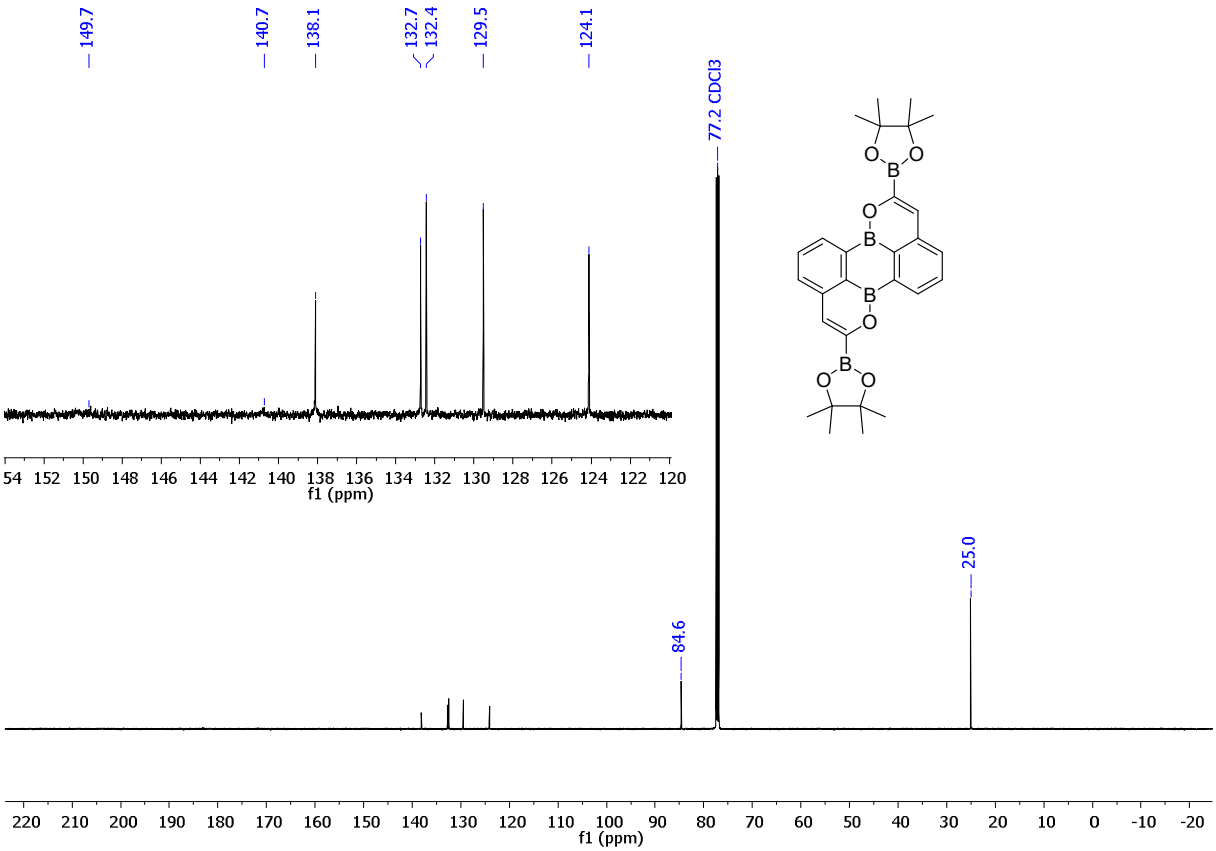

Figure S56: $^{13}C\{^{1}H\}$ NMR spectrum of **10** ($CDCl_3$, 125.8 MHz).

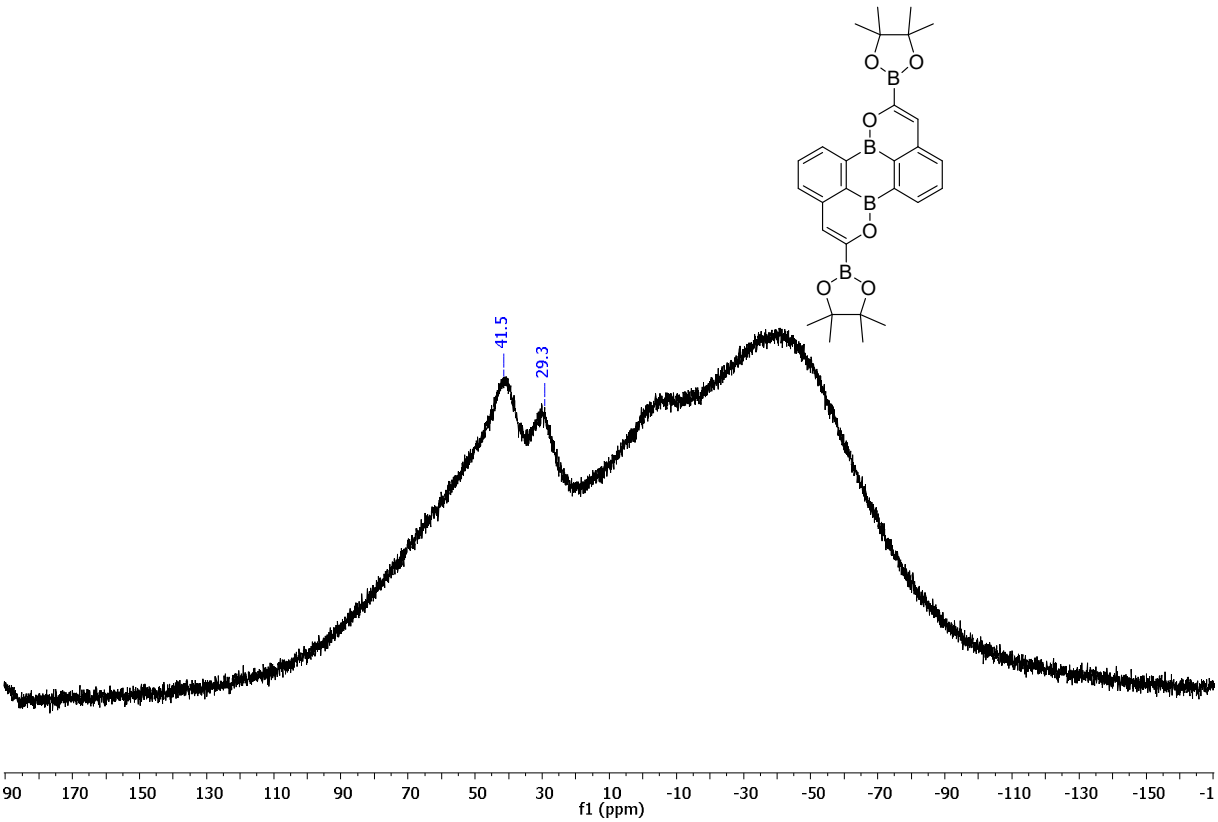

Figure S57: ^{11}B NMR spectrum of **10** ($CDCl_3$, 96.3 MHz).

4. Photophysical and electrochemical data

Table S1: Photophysical and electrochemical data of the compounds **4a,b–6a,b**, **8a–c**, **9**, and **10** . Optical measurements were performed in $CHCl_3$, and electrochemical measurements were performed in THF (room temperature, supporting electrolyte: $[n\text{Bu}_4\text{N}][PF_6]$ (0.1 M), scan rate 200 mV s^{-1}).

	λ_{abs} [nm] (ε [M^{-1} cm^{-1}])	λ_{onset} [nm][a]	λ_{ex} [nm]	λ_{em} [nm][b]	Φ_{PL} [%][c]	E_{HOMO}/E_{LUMO} [eV][d]	$E_{1/2}$ [V]	E_G^{opt} [eV][e]
4a	301 (21861) 312 (20685) 332 (12098) 348 (sh)	364	301	390	8 6[g]	–	–[f]	3.41
4b	293 (14001) 323 (sh) 332 (sh)	351	293	383	4 6[g]	-	–[f]	3.53
5a	290 (45925) 297 (45316) 328 (sh) 339 (34508) 351 (20644) 379 (sh) 395 (sh)	419	339	426 (sh) 445	20 31[g]	−5.18/−2.22	−2.58	2.96
5b	268 (44824) 326 (9621) 341 (12571) 379 (sh) 405 (sh)	422	341	428 (sh) 448 470 (sh)	32 51[g]	−4.94/−2.00	−2.80	2.94
6a	312 (sh) 326 (sh) 343 (sh) 360 (75215) 373 (56253) 404 (13108) 425 (8628)	447	360	452 475 507 (sh)	41 49[g]	–	–[f]	2.77
6b	347 (27027) 388 (sh)	422	347	426 446	16 52[g]	−4.74/−1.80	−3.00	2.94
8a	270 (13015) 314 (25351) 329 (sh) 366 (5963) 386 (4312)	399	314	397 419 443 468 510 (sh)	43 52[g]	–	–[f]	3.11
8ab	307 (30228) 315 (sh) 329 (27393) 374 (10481) 393 (sh)	412	332	398 (sh) 415 434 461 (sh) 491 (sh)	34 44[g]	-	–[f]	3.01
8c	294 (30871) 310 (29122) 350 (sh)	-	-	-	-	-	–[f]	-
9	355 (6631) 371 (11202) 389 (10413)	399	370	400 418 437	30 50[g] 47[h]	−5.62/−2.51	−2.29	3.11
10	350 (6217) 366 (11242) 383 (10850)	393	350	393 411 430	34 47[h]	−5.69/−2.53	−2.27	3.16

[a] Each onset wavelength (λ_{onset}) was determined by constructing a tangent on the point of inflection of the bathochromic slope of the most red-shifted absorption maximum. [b] Resolved vibrational fine structure. [c] Quantum yields were determined by using a calibrated integrating sphere. [d] $E_{HOMO} = E_{LUMO} - E_G^{opt}$, $E_{LUMO} = -4.8$ eV$-E_{1/2}^{Red1}$ ($FcH/FcH^+ = -4.8$ eV vs vacuum level). [e] Optical band gap $E_G^{opt} = 1240/\lambda_{onset}$. [f] Compound shows no reversible reduction. [g] Quantum yields measured in *c*-hexane. [h] Quantum yield measured in THF. sh = shoulder.

4.1. UV/Vis absorption and emission spectra

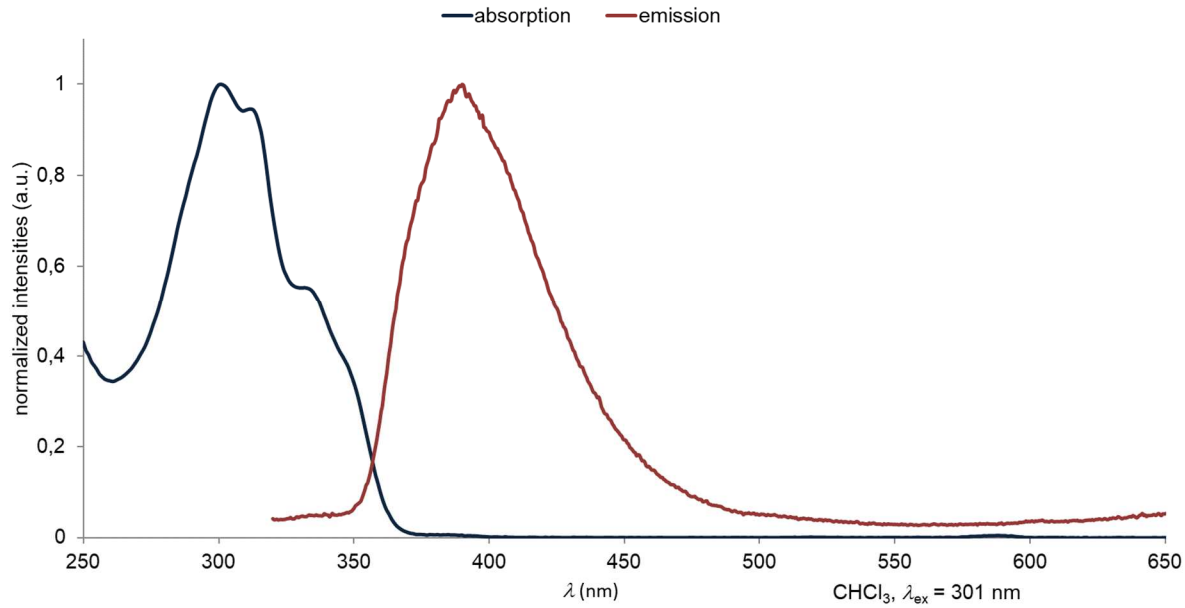

Figure S58: Normalized UV/Vis absorption and emission spectra of **4a**.

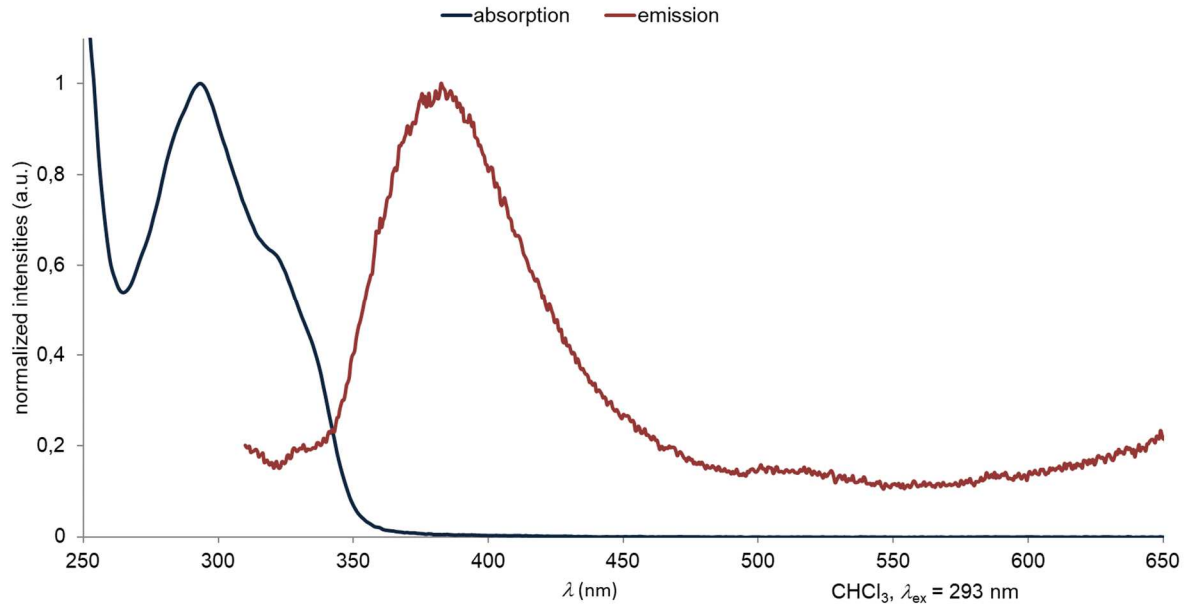

Figure S59: Normalized UV/Vis absorption and emission spectra of **4b**.

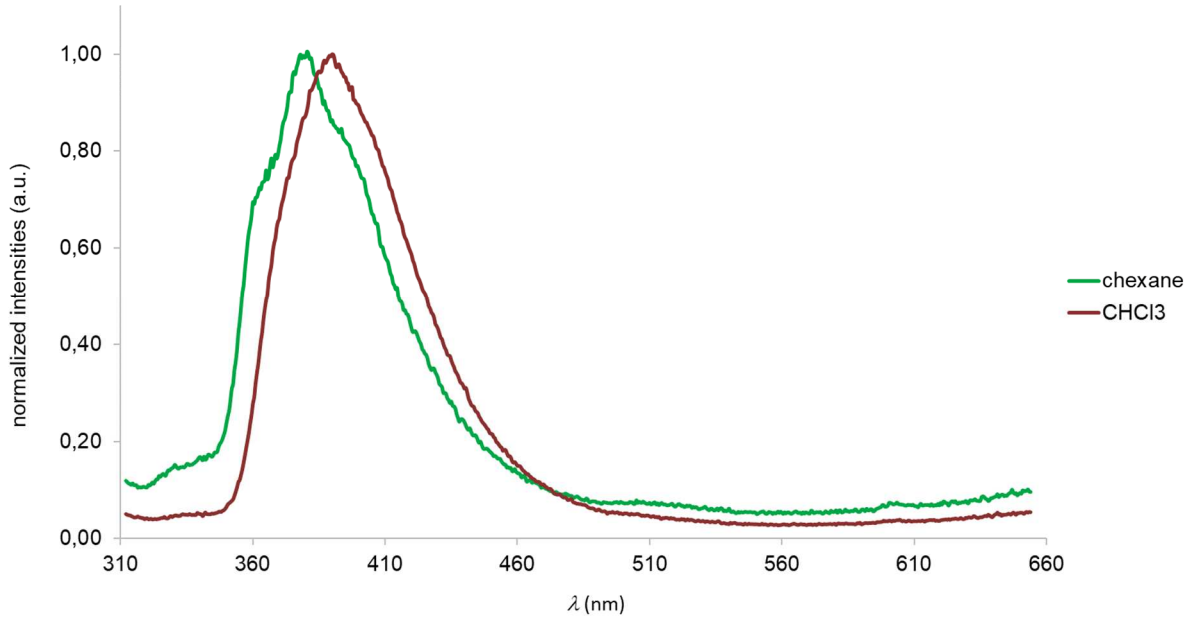

Figure S60: Normalized emission spectra of **4a** in $CHCl_3$ and *c*-hexane.

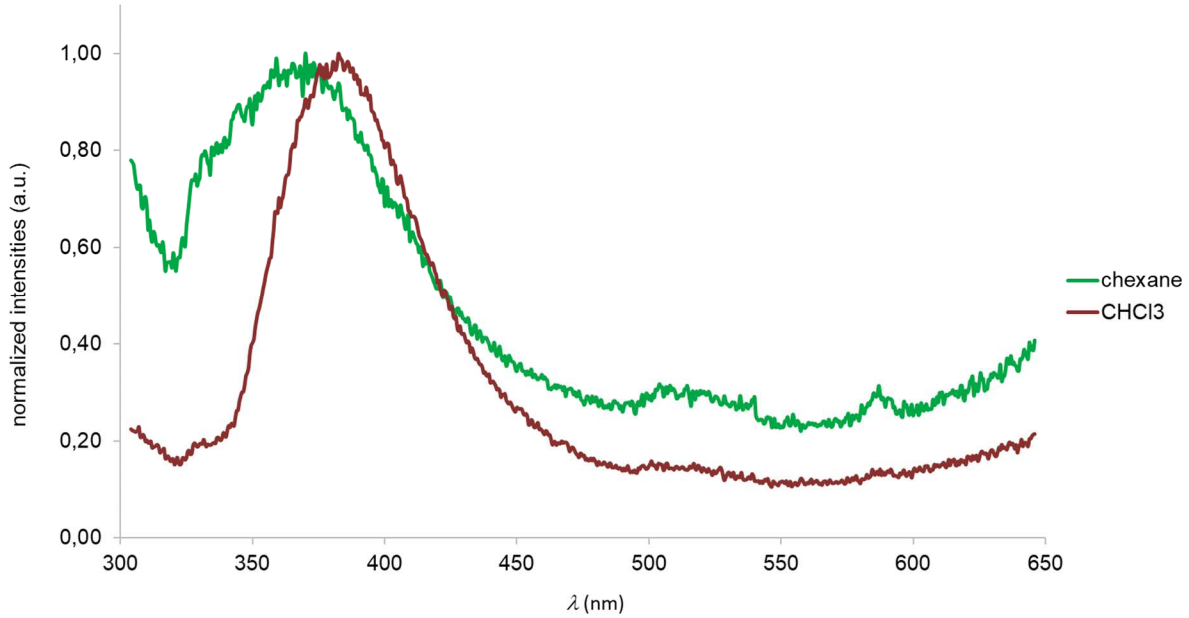

Figure S61: Normalized emission spectra of **4b** in $CHCl_3$ and *c*-hexane.

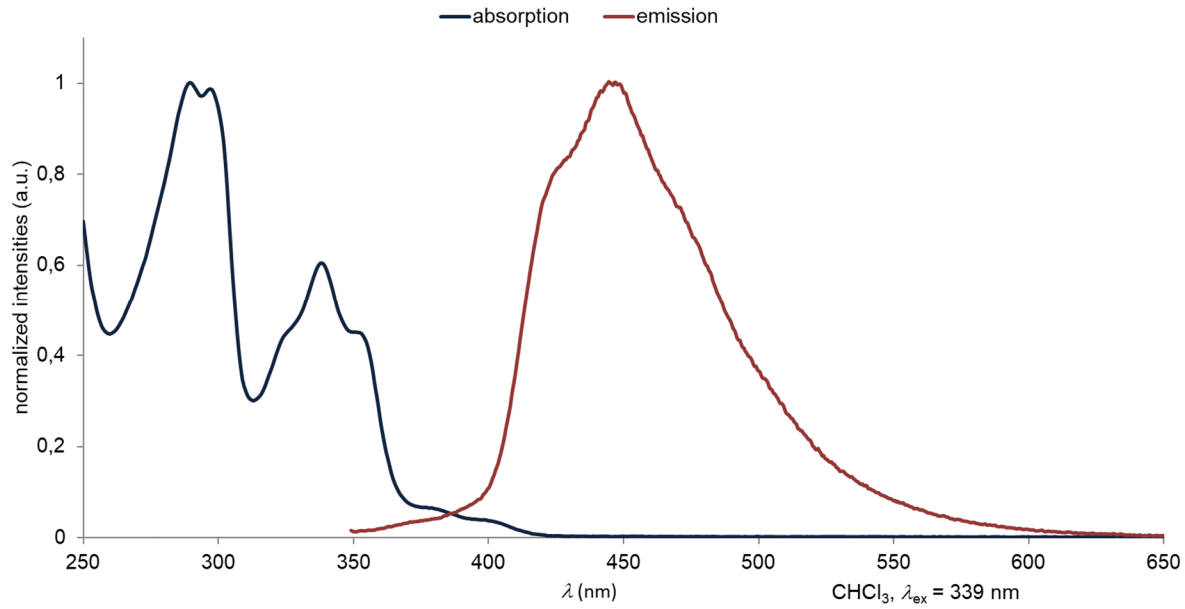

Figure S62: Normalized UV/Vis absorption and emission spectra of **5a**.

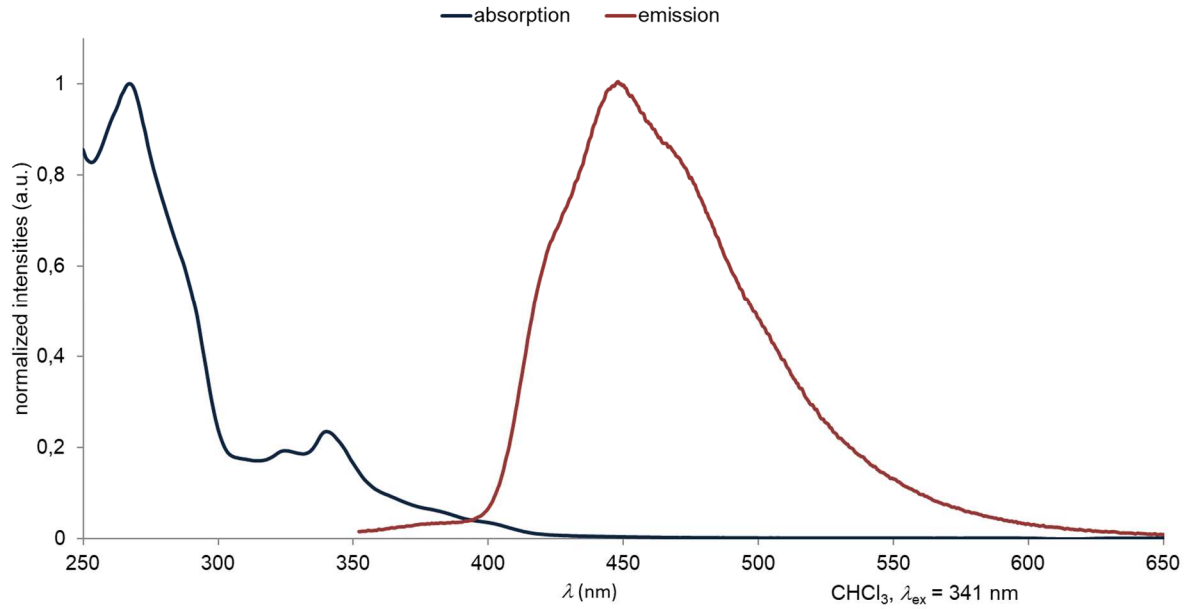

Figure S63: Normalized UV/Vis absorption and emission spectra of **5b**.

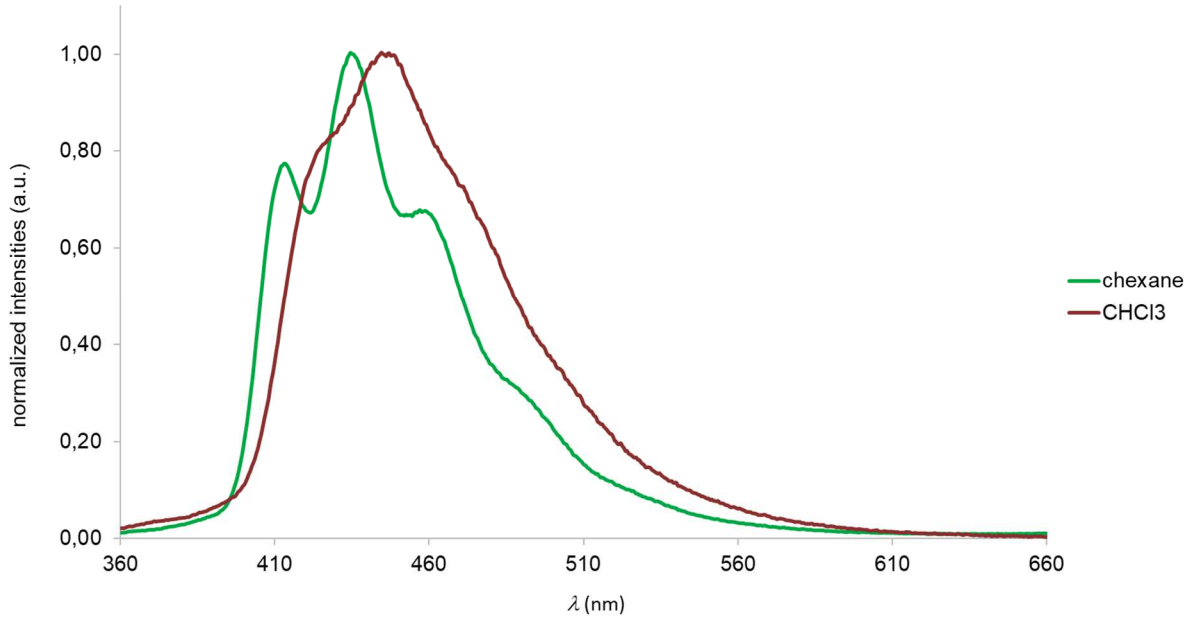

Figure S64: Normalized emission spectra of **5a** in $CHCl_3$ and *c*-hexane.

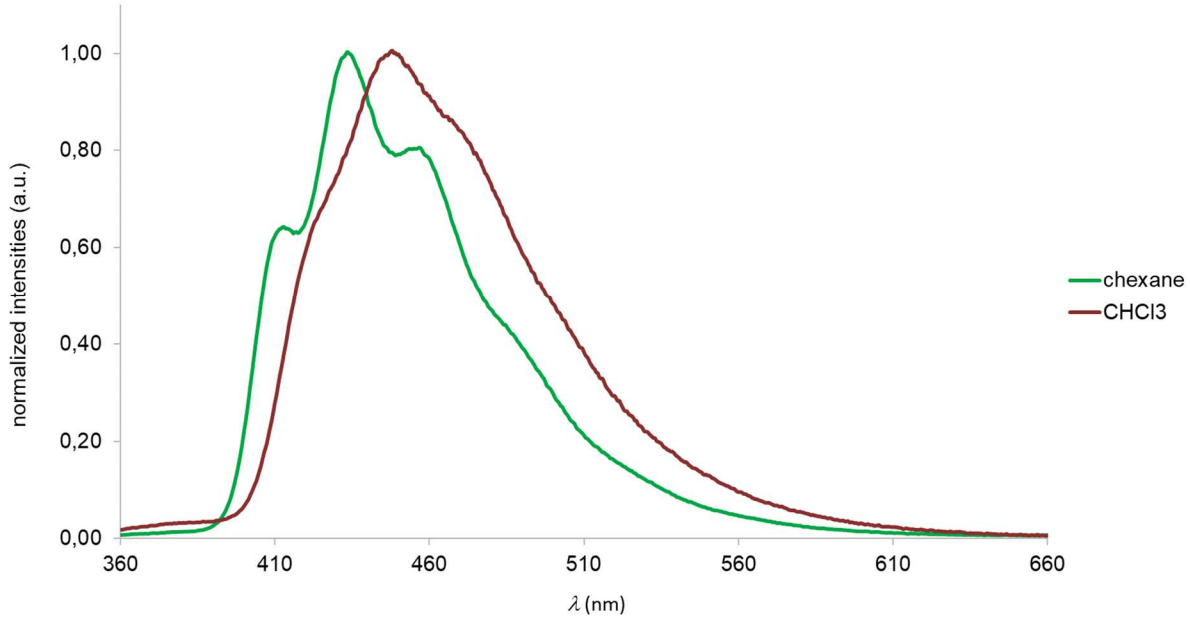

Figure S65: Normalized emission spectra of **5b** in $CHCl_3$ and *c*-hexane.

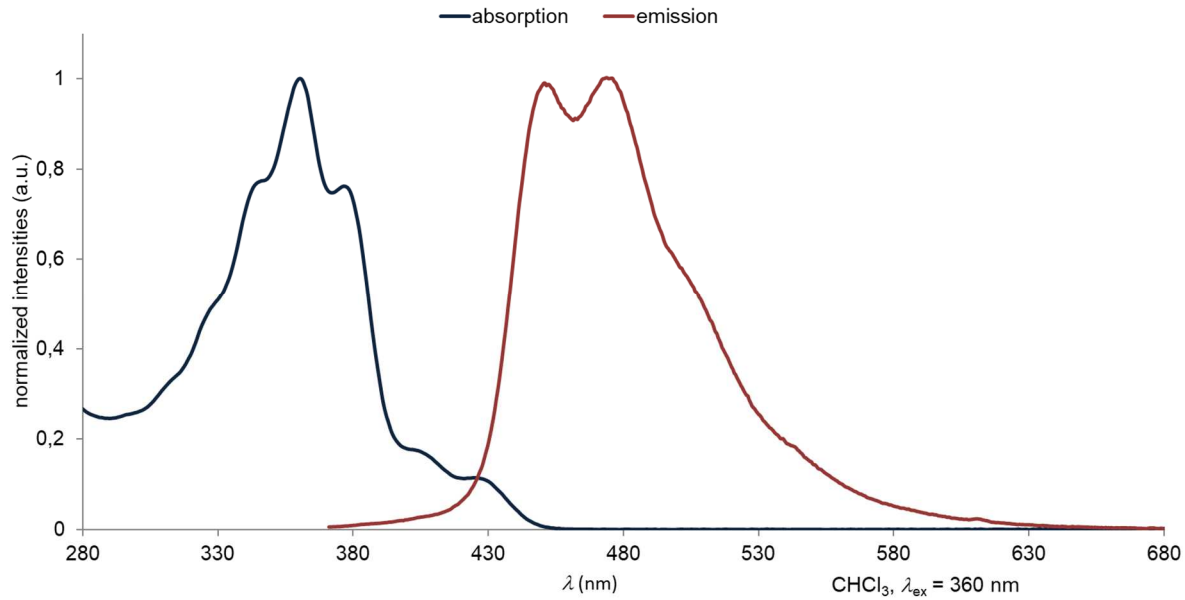

Figure S66: Normalized UV/Vis absorption and emission spectra of **6a**.

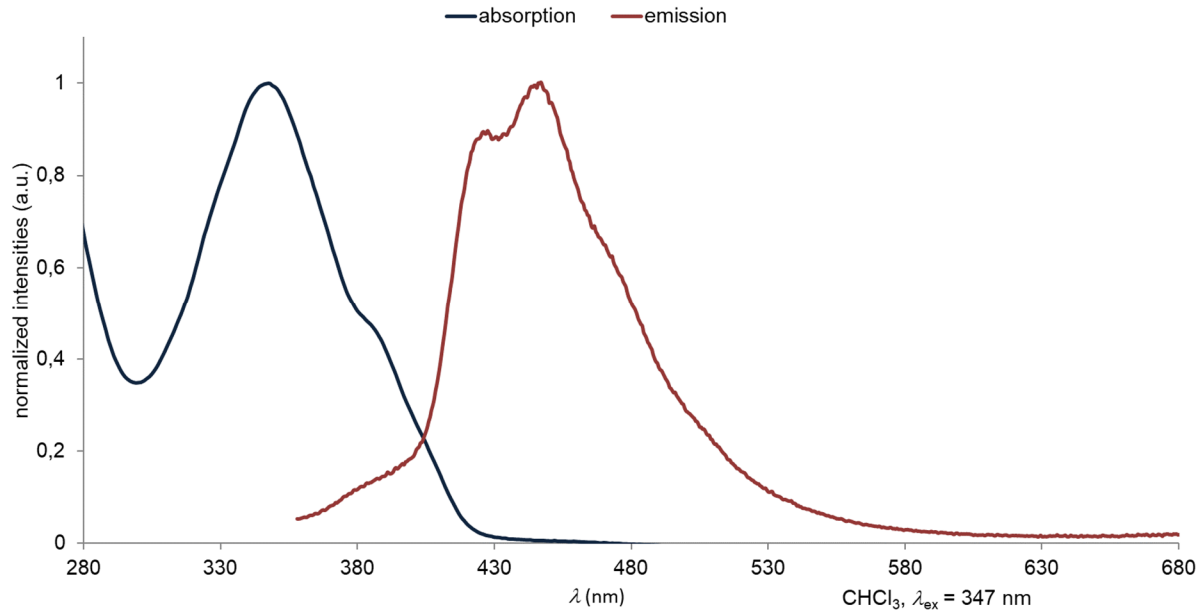

Figure S67: Normalized UV/Vis absorption and emission spectra of **6b**.

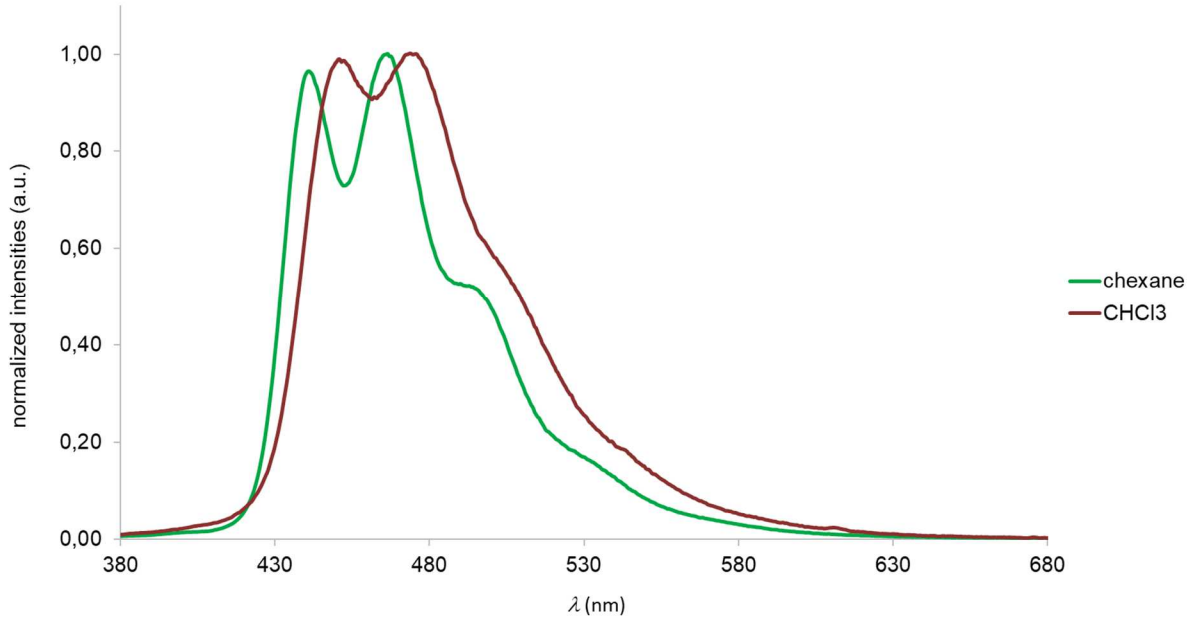

Figure S68: Normalized emission spectra of **6a** in $CHCl_3$ and *c*-hexane.

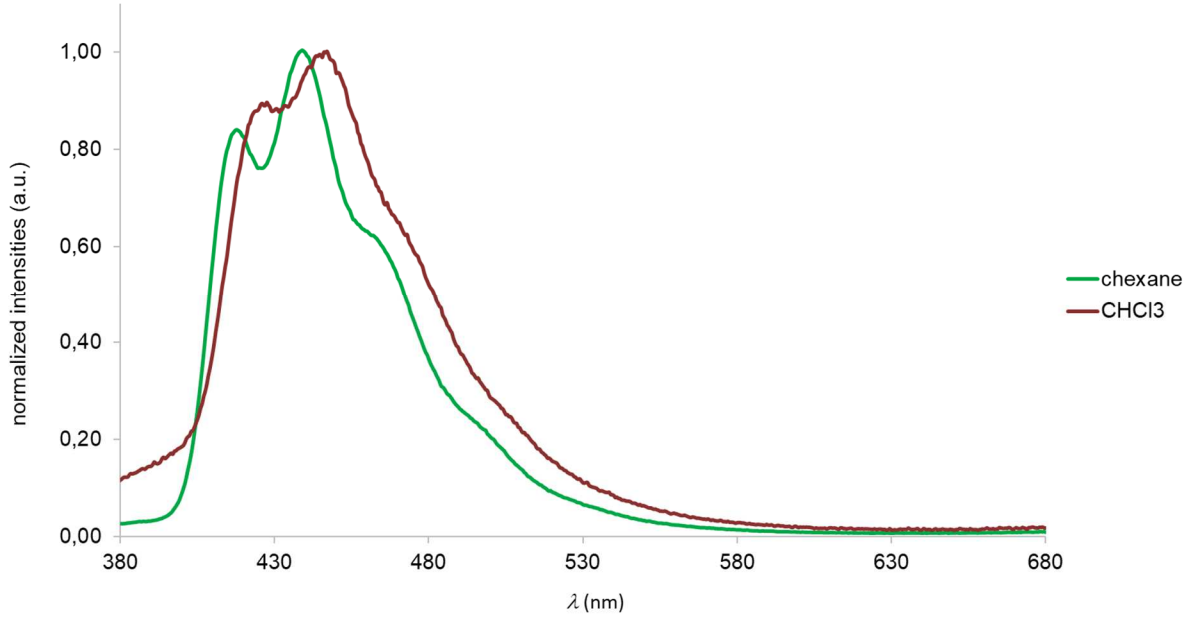

Figure S69: Normalized emission spectra of **6b** in $CHCl_3$ and *c*-hexane.

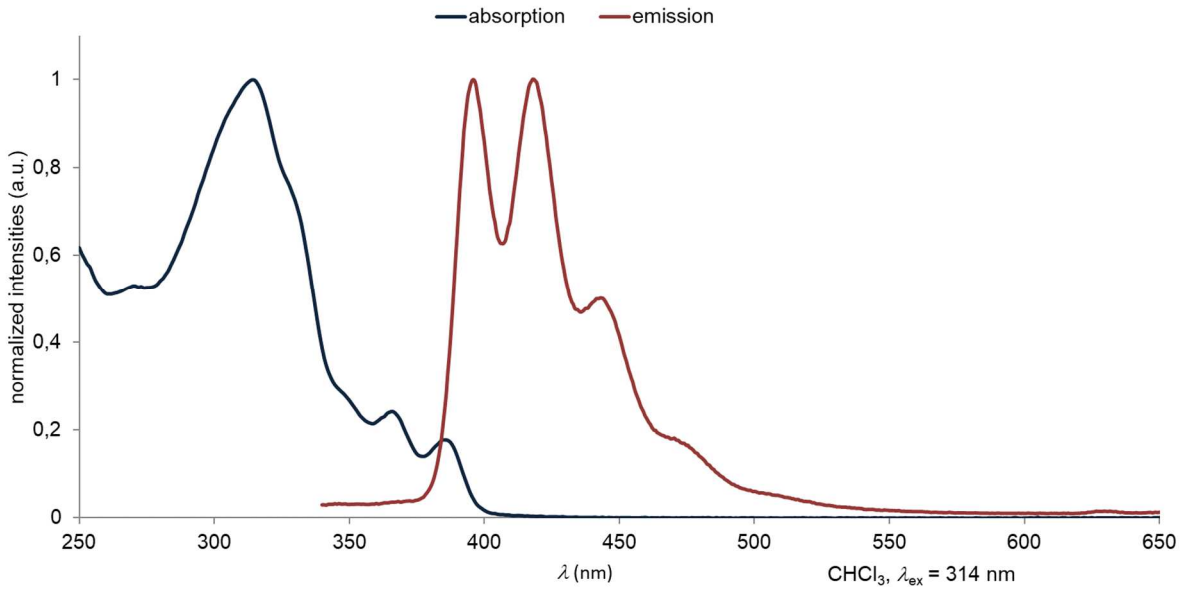

Figure S70: Normalized UV/Vis absorption and emission spectra of **8a**.

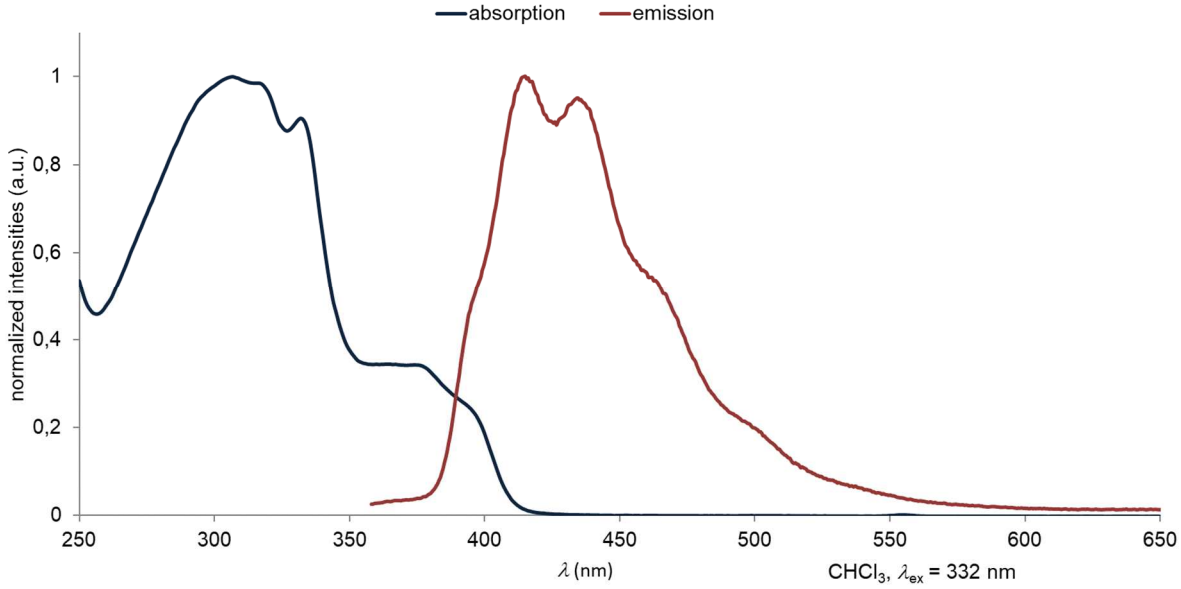

Figure S71: Normalized UV/Vis absorption and emission spectra of **8ab**.

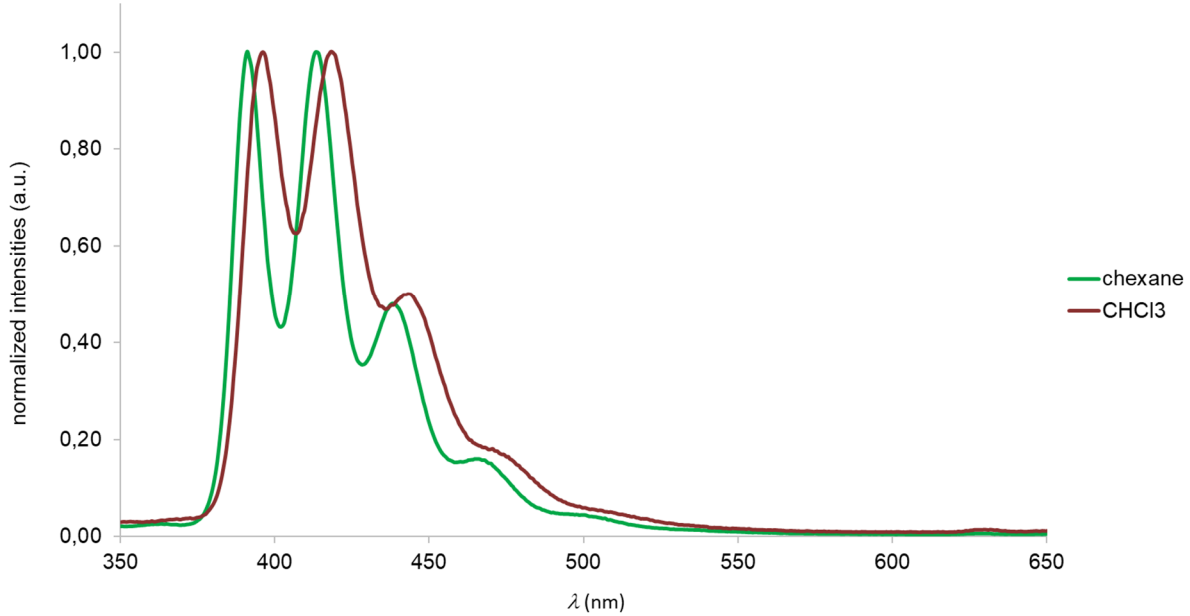

Figure S72: Normalized emission spectra of **8a** in $CHCl_3$ and *c*-hexane.

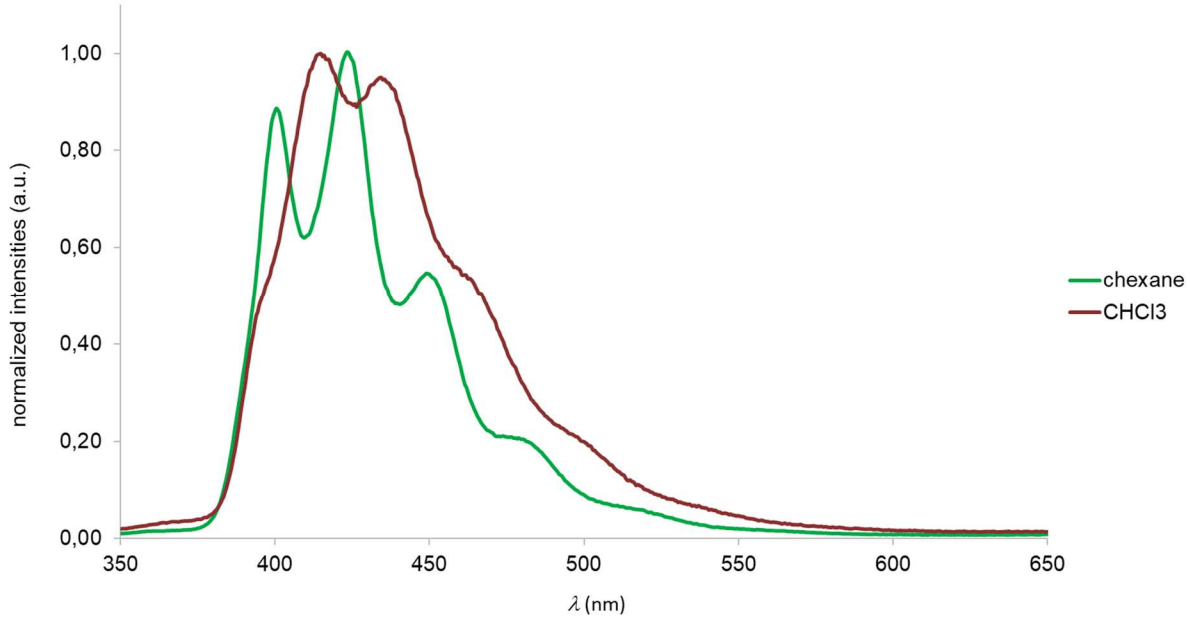

Figure S73: Normalized emission spectra of **8ab** in $CHCl_3$ and *c*-hexane.

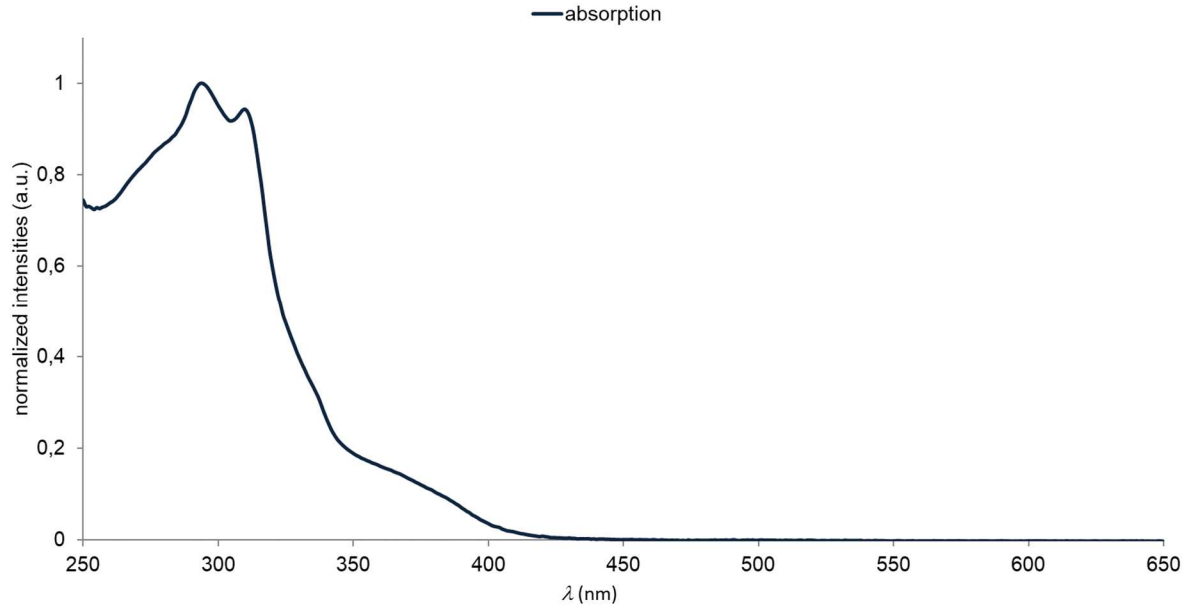

Figure S74: Normalized UV/Vis absorption spectra of **8c** in $CHCl_3$.

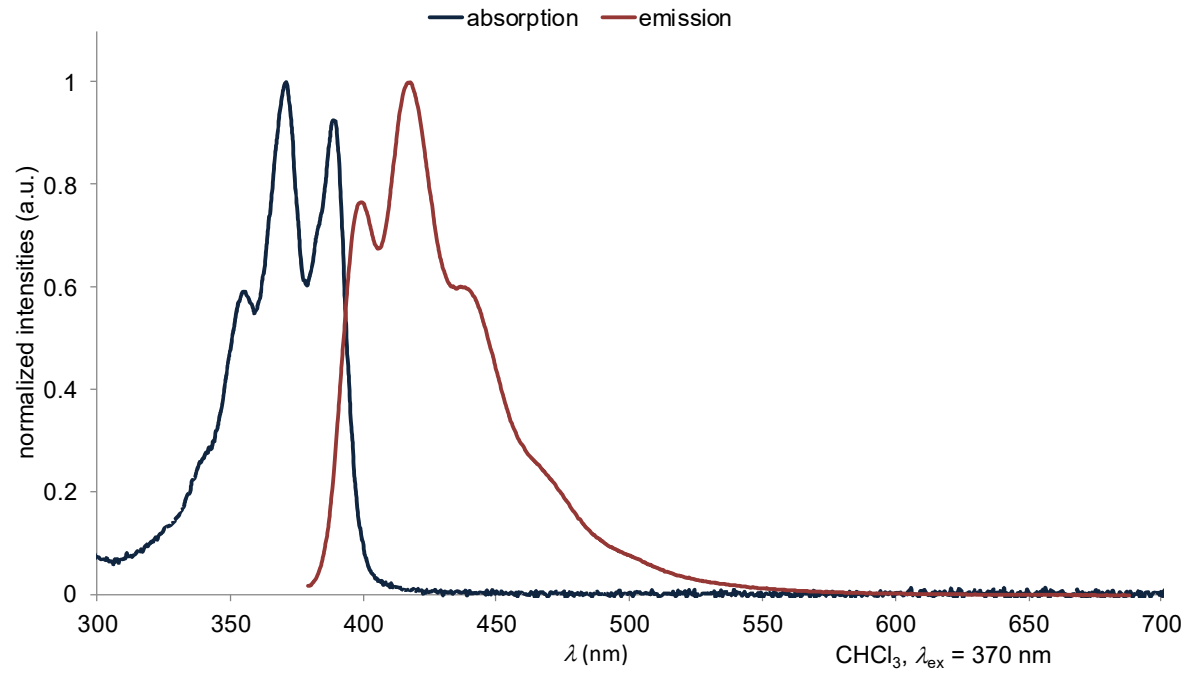

Figure S75: Normalized UV/Vis absorption and emission spectra of **9**.

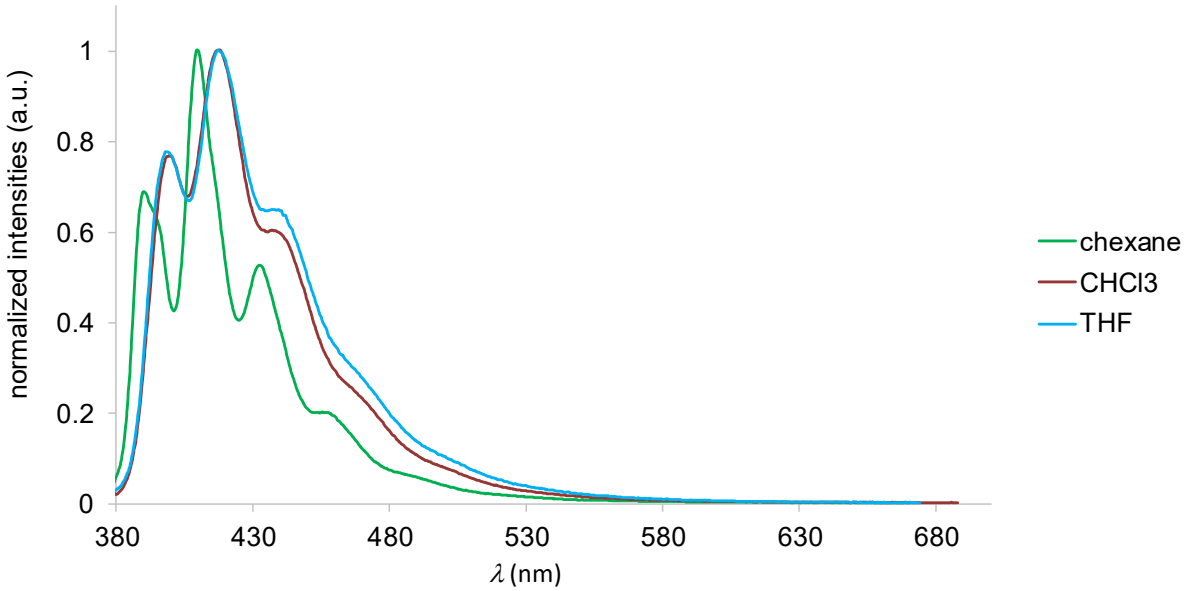

Figure S76: Normalized emission spectra of **9** in various solvents.

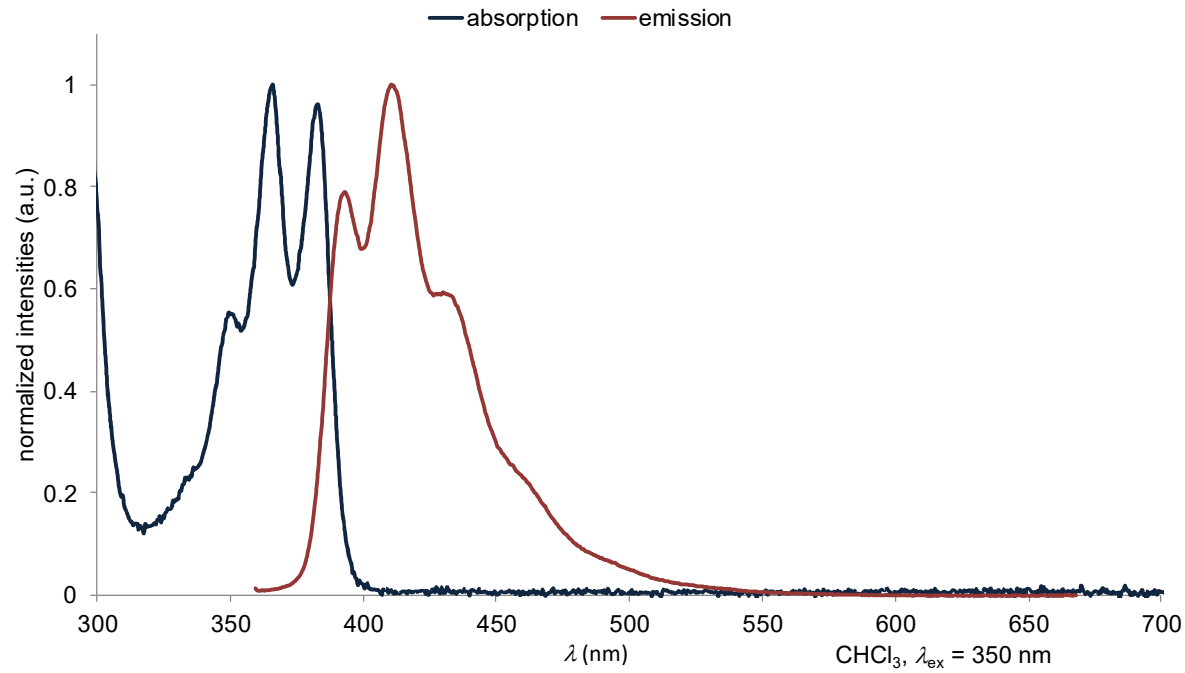

Figure S77: Normalized UV/Vis absorption and emission spectra of **10**.

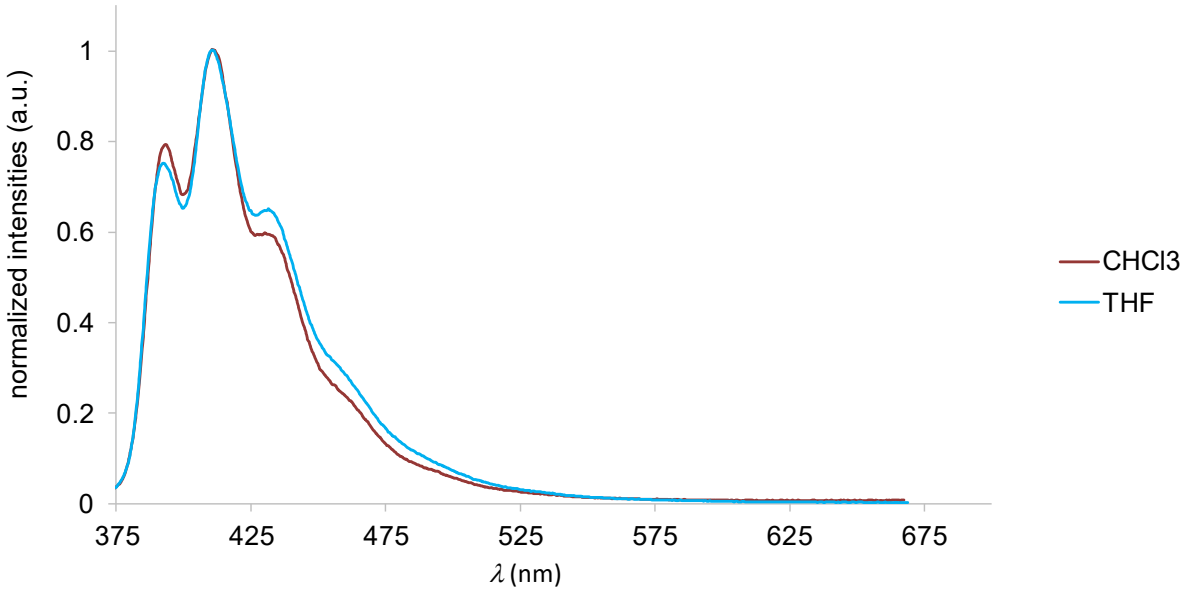

Figure S78: Normalized emission spectra of **10** in $CHCl_3$ and THF.

4.2. Plots of cyclic voltammograms

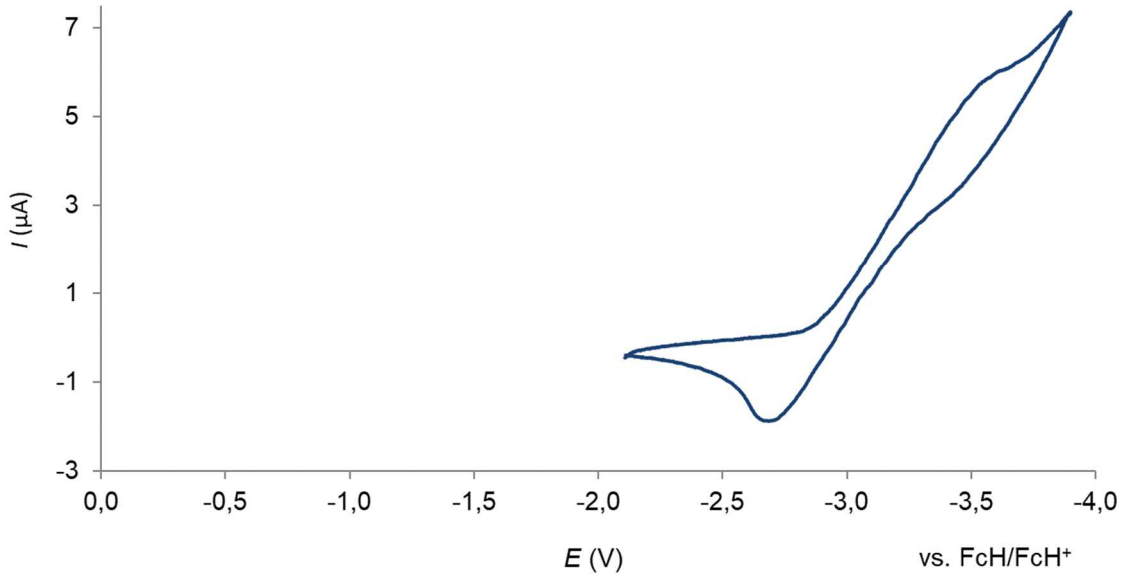

Figure S79: Cyclic voltammogram of **4a** in THF (cathodic scan; room temperature, supporting electrolyte: [*n*Bu$_4$N][PF$_6$] (0.1 M), scan rate 200 mV s^{-1}).

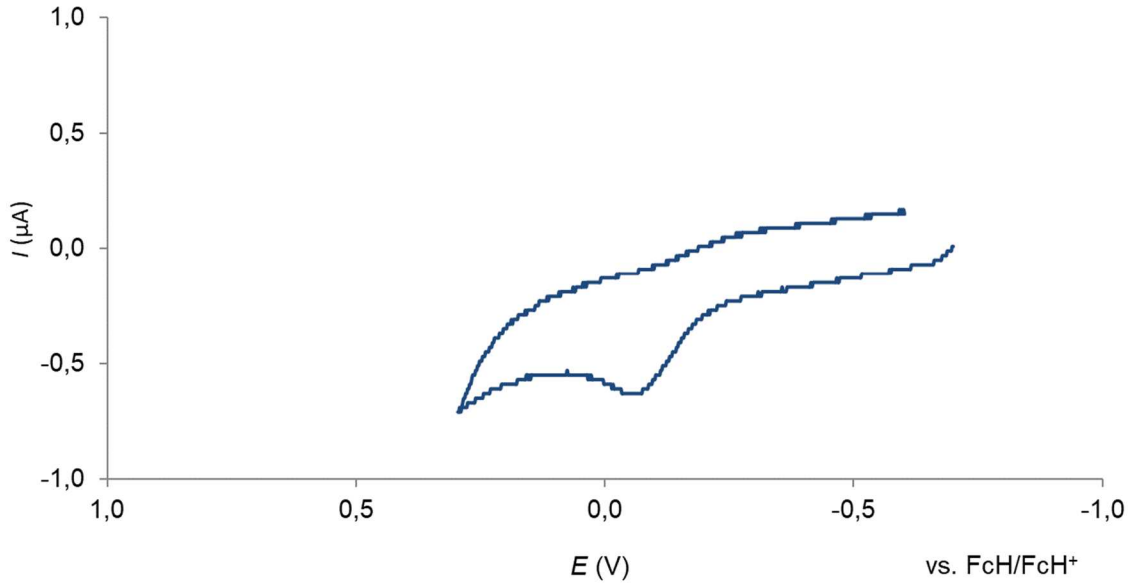

Figure S80: Cyclic voltammogram of **4a** in THF (anodic scan; room temperature, supporting electrolyte: [*n*Bu$_4$N][PF$_6$] (0.1 M), scan rate 200 mV s^{-1}).

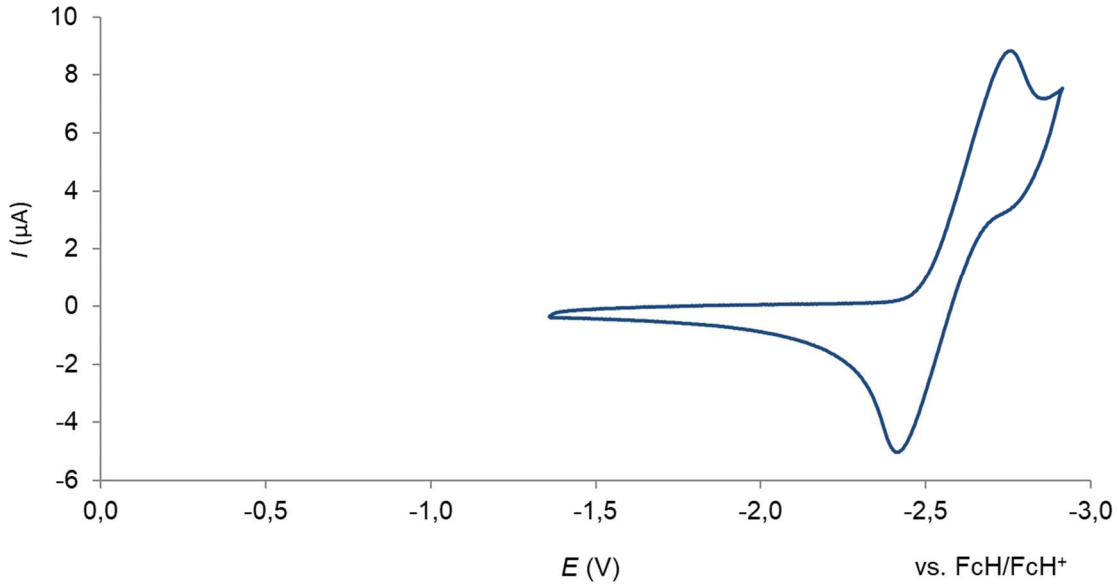

Figure S81: Cyclic voltammogram of **5a** in THF (cathodic scan; room temperature, supporting electrolyte: [*n*Bu$_4$N][PF$_6$] (0.1 M), scan rate 200 mV s^{-1}).

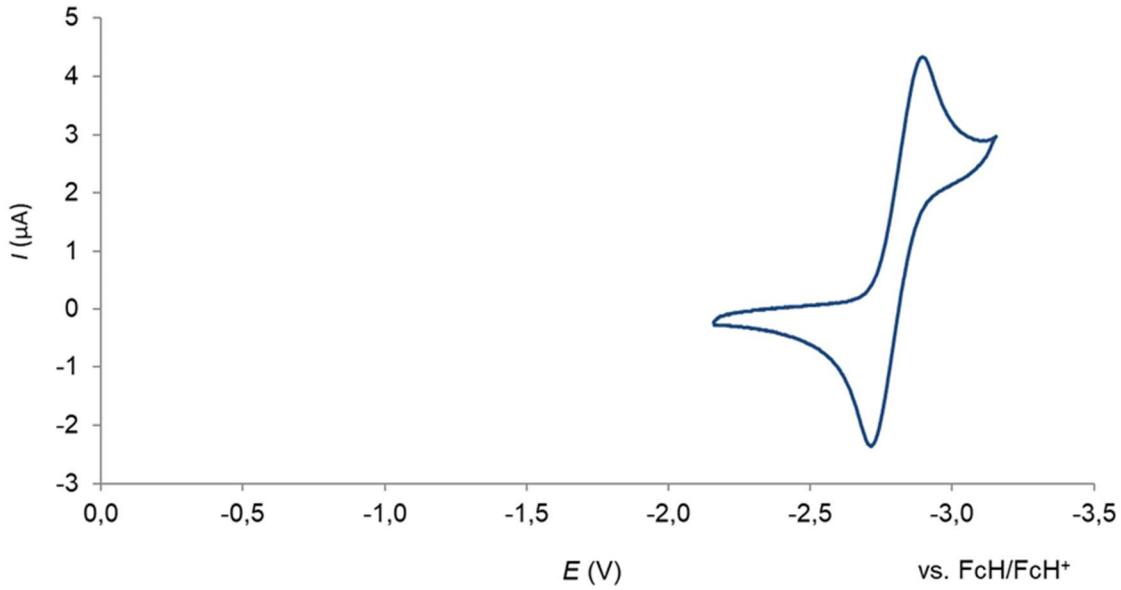

Figure S82: Cyclic voltammogram of **5b** in THF (cathodic scan; room temperature, supporting electrolyte: [*n*Bu$_4$N][PF$_6$] (0.1 M), scan rate 200 mV s^{-1}).

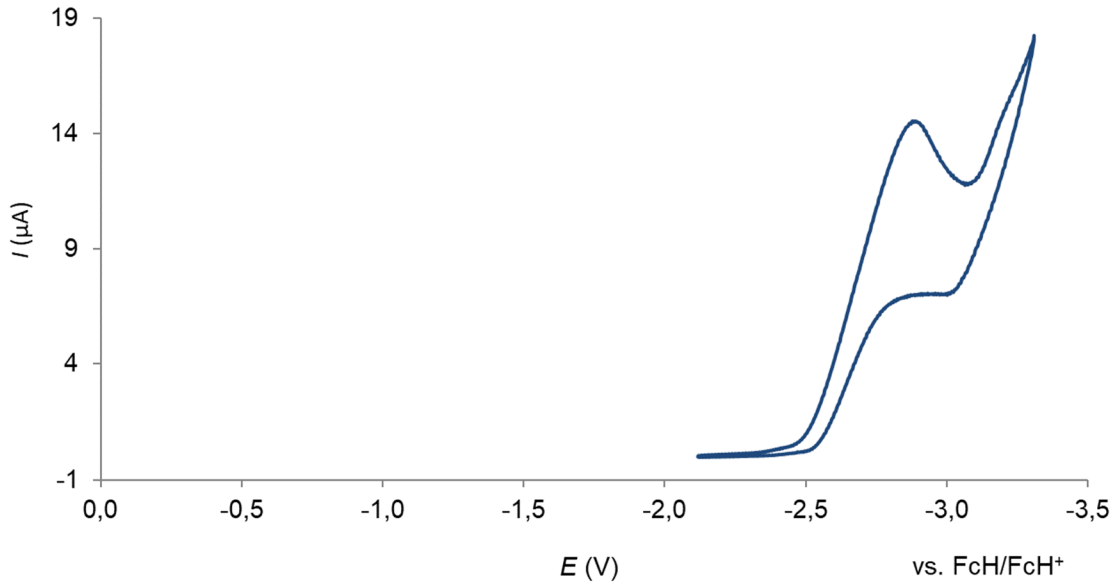

Figure S83: Cyclic voltammogram of **6a** in THF (cathodic scan; room temperature, supporting electrolyte: [*n*Bu$_4$N][PF$_6$] (0.1 M), scan rate 200 mV s^{-1}).

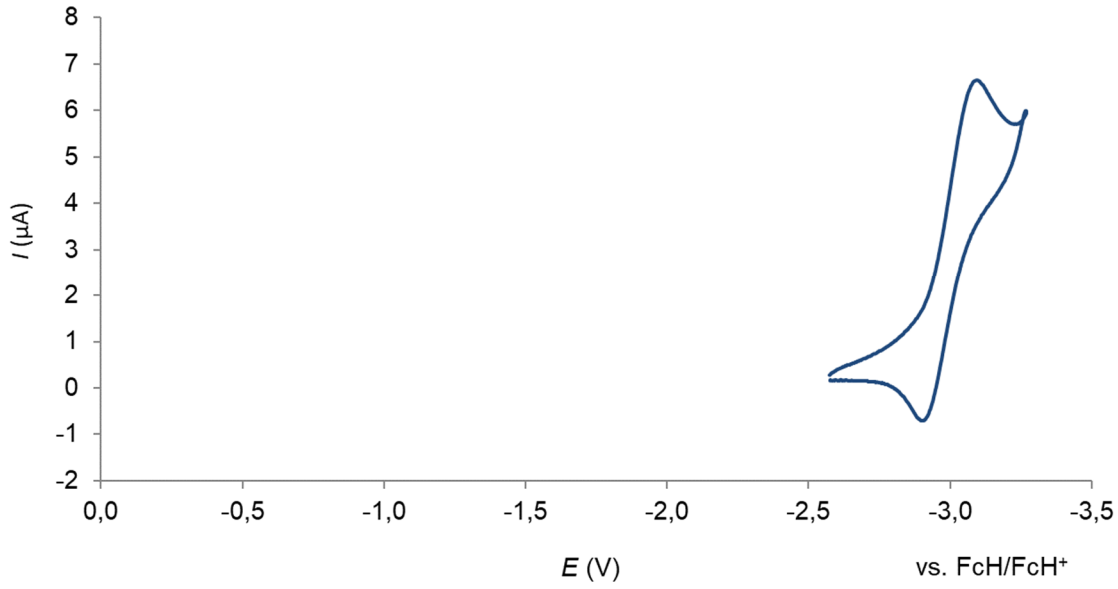

Figure S84: Cyclic voltammogram of **6b** in THF (cathodic scan; room temperature, supporting electrolyte: [*n*Bu$_4$N][PF$_6$] (0.1 M), scan rate 200 mV s^{-1}).

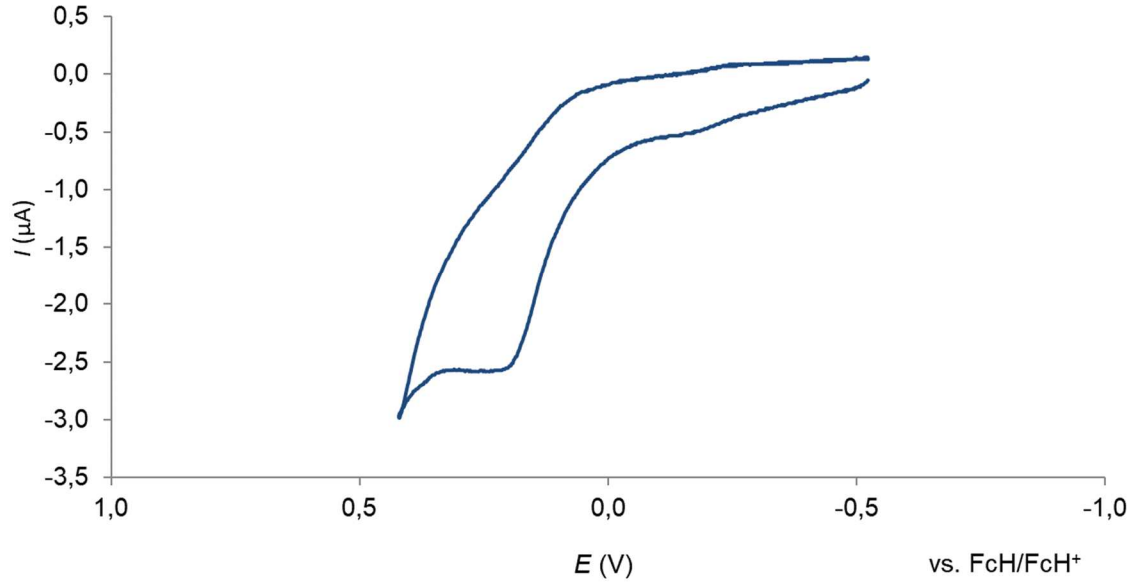

Figure S85: Cyclic voltammogram of **8a** in THF (anodic scan; room temperature, supporting electrolyte: [*n*Bu$_4$N][PF$_6$] (0.1 M), scan rate 200 mV s^{-1}).

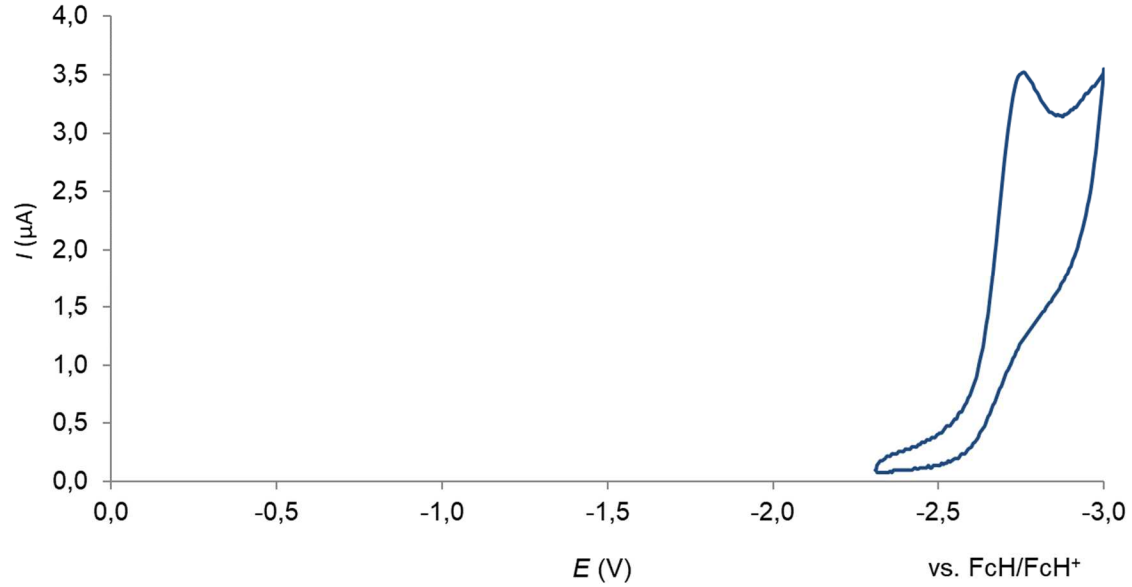

Figure S86: Cyclic voltammogram of **8ab** in THF (cathodic scan; room temperature, supporting electrolyte: [*n*Bu$_4$N][PF$_6$] (0.1 M), scan rate 200 mV s^{-1}).

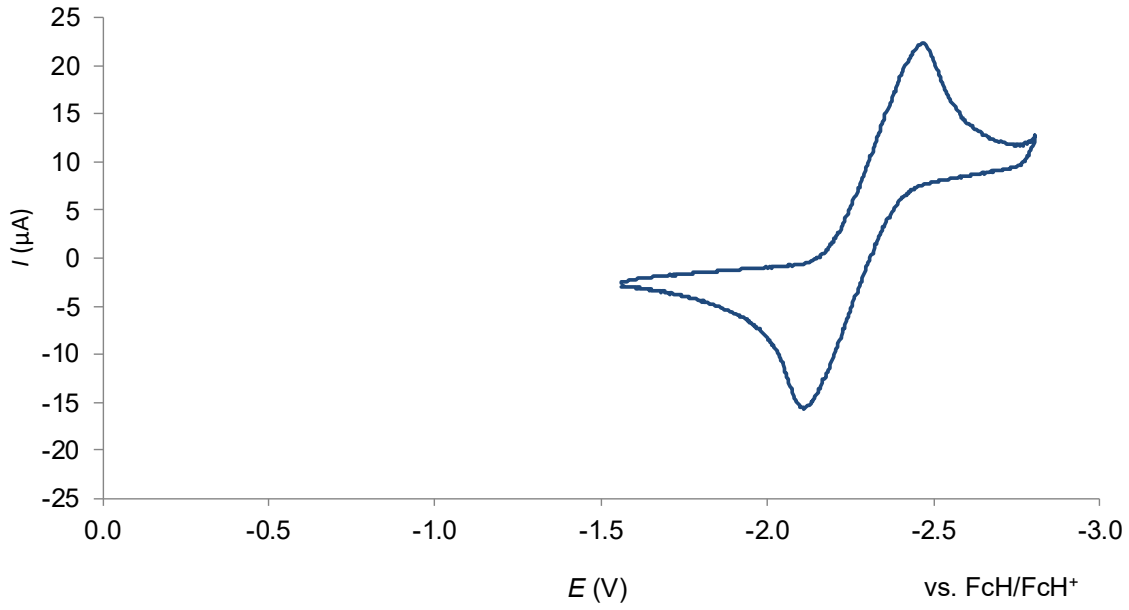

Figure S87: Cyclic voltammogram of **9** in THF (cathodic scan, room temperature, supporting electrolyte: [*n*Bu$_4$N][PF$_6$] (0.1 M), scan rate 200 mV s^{-1}).

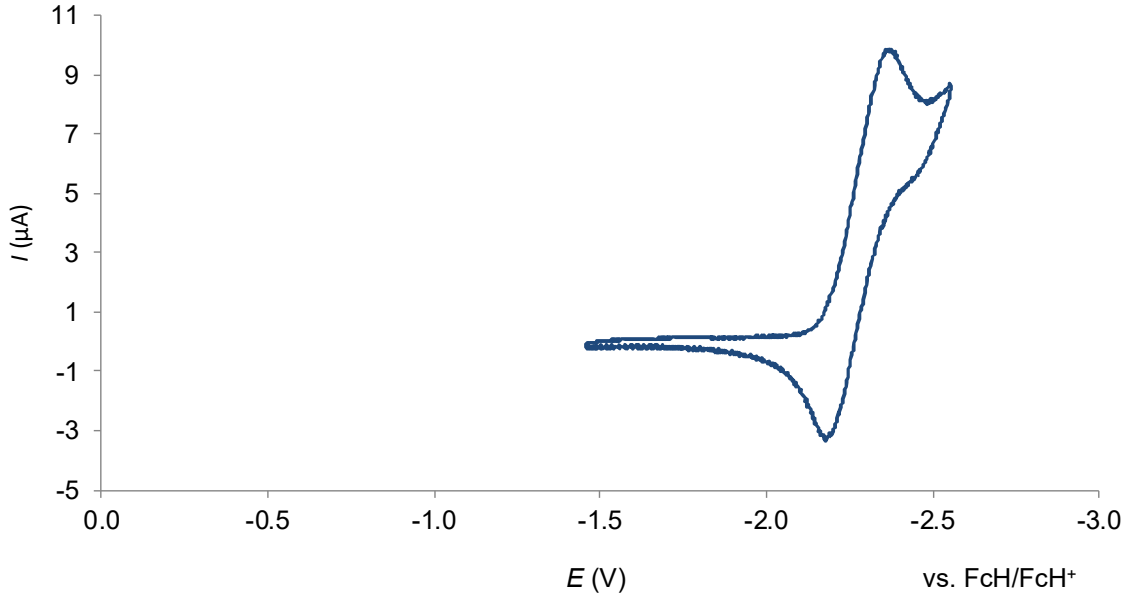

Figure S88: Cyclic voltammogram of **10** in THF (cathodic scan, room temperature, supporting electrolyte: [*n*Bu$_4$N][PF$_6$] (0.1 M), scan rate 200 mV s^{-1}).

5. X-ray crystal structure analyses

Data for all structures were collected on a STOE IPDS II two-circle diffractometer with a Genix Microfocus tube with mirror optics using MoK_α radiation (λ = 0.71073 Å) and were scaled using the frame-scaling procedure in the *X-AREA*[S11] program system. The structures were solved by direct methods using the program *SHELXS*[S12] and refined against F^2 with full-matrix least-squares techniques using the program *SHELXL-97*.[S12]

There are two molecules in the asymmetric unit of **1a** (CCDC 2058862). The H atoms bonded to O were freely refined. Due to the absence of anomalous scatters, the absolute structure could not be determined: Flack-x-parameter: −0.5(9).

There are two molecules and half a molecule of *n*-hexane (located on a centre of inversion) in the asymmetric unit of **2a** (CCDC 2058863). The H atoms bonded to O were freely refined.

In **3a**·acetone (CCDC 2058864), one t-butyl group is disordered over two sets of sites with a site occupation factor of 0.54(2) for the major occupied sites. Bond lengths and angles of the minor occupied sites were restrained to the values of the major occupied sites. The H atom bonded to O was freely refined. The molecule is located on a center of inversion and the acetone molecule is located on a two-fold rotation axis.

The compound **4a** (CCDC 2058865) requires no special comments.

In **4b** (CCDC 2058866), one t-butyl group is disordered over two sets of sites with a site occupation factor of 0.579(13) for the major occupied sites. The displacement parameters of all disordered atoms were restrained to an isotropic behavior. Due to the absence of anomalous scatterers, the absolute structure could not be determined: Flack-x-parameter: 1.7(9).

The crystal of **5b** (CCDC 2058867) was just weakly diffracting. As a result of that, R_{int} (0.143) and $R\sigma$ (0.120) are slightly increased.

In **6a** (CCDC 2058868), one t-butyl group is disordered over two sets of sites with a site occupation factor of 0.804(6) for the major occupied sites. The displacement parameters of the minor occupied sites were restrained to an isotropic behavior. The molecule is located on a center of inversion.

In **7a^{iPr}** (CCDC 2058869), one t-butyl group is disordered over two sets of sites with a site occupation factor of 0.766(6) for the major occupied sites. The displacement parameters of the minor occupied sites were restrained to an isotropic behaviour. The CF_3 group is disordered over three sets of sites with site occupation factors of 0.462(3), 0.273(3) and 0.265(3). The displacement parameters of of all F atoms were restrained to an isotropic behavior.

There are two molecules in the asymmetric unit of **8a** (CCDC 2058870). The contribution of the solvent was suppressed using the *SQUEEZE* routine in *PLATON*.[S13]

The crystal of **19** (CCDC 2058871) was twinned with a fractional contribution of 0.4597(16) for the minor domain. There are two molecules in the asymmetric unit.

In **24** (CCDC 2058872), one t-butyl group is disordered over two sets of sites with a site occupation factor of 0.920(10) for the major occupied sites. The minor occupied sites were refined with isotropic displacement parameters. Bond lengths and angles of the minor occupied sites were restrained to the values of the major occupied sites.

The completely planar (r.m.s. deviation for all non H atoms 0.007 Å) molecule **9** (CCDC 2068160) is located on a center of inversion. The crystal packing shows a herringbone pattern. The molecules form skew stacks with an interplanar distance of 3.39 Å. The offset between the centroids of two molecules is 3.21 Å.

10 (CCDC 2068161) is located on a two-fold rotation axis. The perylene moiety is completely planar (r.m.s. deviation for all non H atoms 0.014 Å). The molecules form planes perpendicular to the *c* axis with an interplanar distance of 3.36 Å. They are located in stacks with one molecule positioned directly over the other, but rotated about 90° along an axis perpendicular to the molecular plane.

CCDC files **1a**–**8a**, **19**, **24**, **9**, and **10** (2058862–2058872, 2068160, and 2068161) contain the supplementary crystallographic data for this paper and can be obtained free of charge from The Cambridge Crystallographic Data Centre via www.ccdc.cam.ac.uk/data_request/cif.

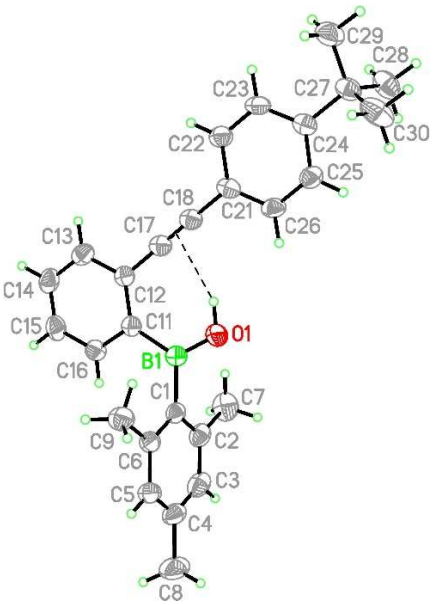

Figure S89 (CDCC 2058862): Molecular structure of **1a** in the solid state. Displacement ellipsoids are drawn at the 50% probability level. Selected bond lengths (Å), bond angles (°), and torsion angles (°): B(1)–O(1) = 1.349(5), B(1)–C(1) = 1.582(5), B(1)–C(11) = 1.578(5), C(17)–C(18) = 1.193(5); O(1)–B(1)–C(1) = 117.0(3), O(1)–B(1)–C(11) = 122.6(3), C(1)–B(1)–C(11) = 120.4(3), C(12)–C(17)–C(18) = 178.9(4), C(17)–C(18)–C(21) = 178.0(4); O(1)–B(1)–C(11)–C(12) = −9.0(5), B(1)–C(11)–C(12)–C(17) = 2.7(5).

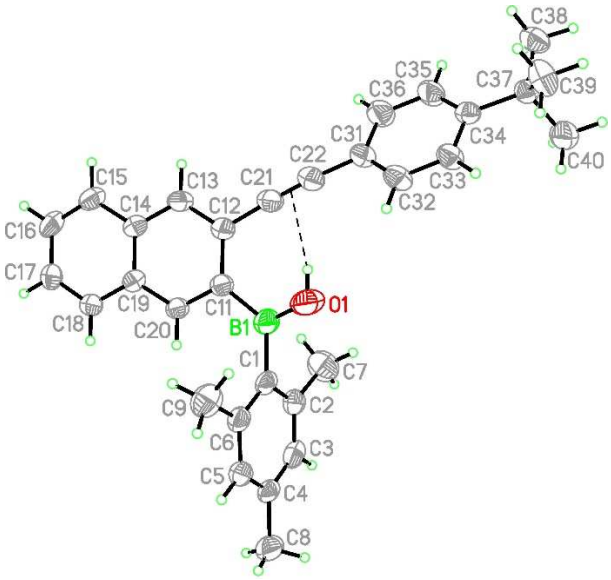

Figure S90 (CDCC 2058863): Molecular structure of **2a** in the solid state. Displacement ellipsoids are drawn at the 50% probability level. Selected bond lengths (Å), bond angles (°), and torsion angles (°): B(1)–O(1) = 1.351(5), B(1)–C(1) = 1.576(5), B(1)–C(11) = 1.574(5), C(21)–C(22) = 1.199(5); O(1)–B(1)–C(1) = 116.2(3), O(1)–B(1)–C(11) = 121.9(4), C(1)–B(1)–C(11) = 121.9(3), C(12)–C(21)–C(22) = 177.1(4), C(21)–C(22)–C(31) = 176.1(4); O(1)–B(1)–C(11)–C(12) = 12.0(6), B(1)–C(11)–C(12)–C(21) = 8.5(5).

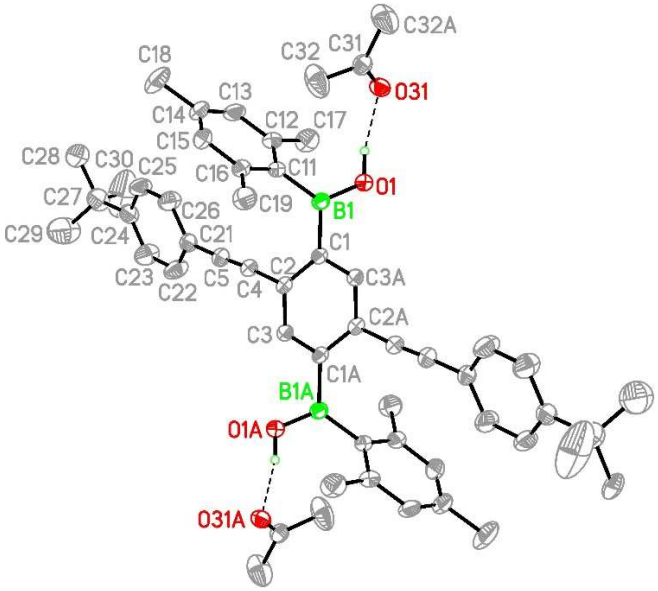

Figure S91 (CDCC 2058864): Molecular structure of **3a**·acetone in the solid state. Displacement ellipsoids are drawn at the 50% probability level, carbon bonded hydrogen atoms are omitted for clarity. Selected bond lengths (Å), bond angles (°), and torsion angles (°): B(1)–O(1) = 1.357(2), B(1)–C(1) = 1.582(2), B(1)–C(11) = 1.577(2), C(4)–C(5) = 1.198(2); O(1)–B(1)–C(1) = 114.2(1), O(1)–B(1)–C(11) = 121.1(1), C(1)–B(1)–C(11) = 124.6(1), C(2)–C(4)–C(5) = 174.7(2), C(4)–C(5)–C(21) = 177.5(2); O(1)–B(1)–C(1)–C(3A) = 26.1(2), O(1)–B(1)–C(1)–C(2) = −157.6(2), B(1)–C(1)–C(2)–C(4) = 7.6(3). Symmetry transformation used to generate equivalent atoms: –x+1, –y+1, –z+1.

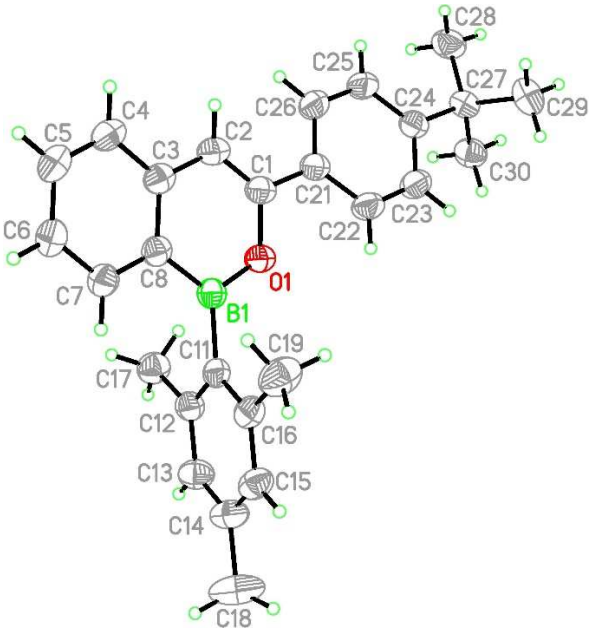

Figure S92 (CDCC 2058865): Molecular structure of **4a** in the solid state. Displacement ellipsoids are drawn at the 50% probability level. Selected bond lengths (Å), bond angles (°), torsion angles (°), and dihedral angles (°): B(1)–O(1) = 1.388(2), B(1)–C(8) = 1.533(2), B(1)–C(11) = 1.573(2), O(1)–C(1) = 1.380(2), C(1)–C(2) = 1.345(2), C(2)–C(3) = 1.439(2); B(1)–O(1)–C(1) = 122.7(1), O(1)–B(1)–C(8) = 117.5(1), C(1)–C(2)–C(3) = 122.7(1); C(1)–O(1)–B(1)–C(8) = −1.7(2), B(1)–O(1)–C(1)–C(2) = −0.4(2), C(1)–C(2)–C(3)–C(8) = −0.8(2), B(1)–C(8)–C(3)–C(2) = −1.3(2), O(1)–B(1)–C(8)–C(3) = 2.6(2); B(1)–O(1)–C(1)–C(2)–C(3)–C(8)//C(11)–C(12)–C(13)–C(14)–C(15)–C(16) = 83.1(1), C(1)–O(1)–B(1)–C(8)–C(3)–C(2)//C(21)–C(22)–C(23)–C(24)–C(25)–C(26) = 17.0(1).

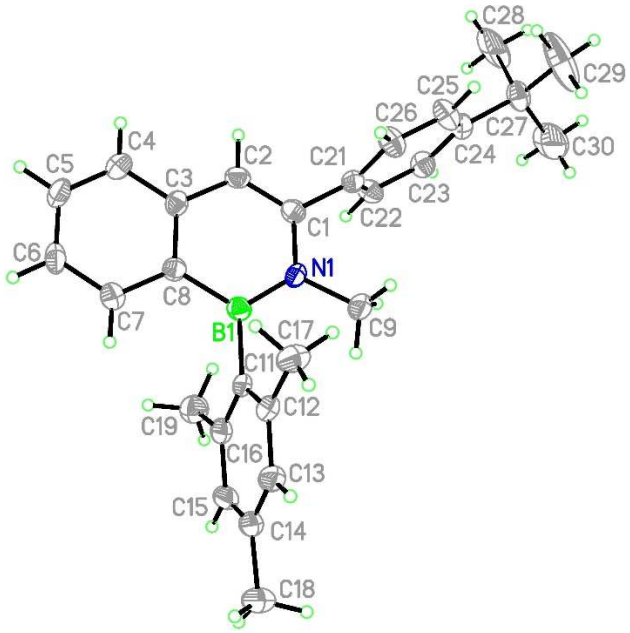

Figure S93 (CDCC 2058866): Molecular structure of **4b** in the solid state. Displacement ellipsoids are drawn at the 50% probability level. Selected bond lengths (Å), bond angles (°), torsion angles (°), and dihedral angles (°): B(1)–N(1) = 1.417(5), B(1)–C(8) = 1.545(6), B(1)–C(11) = 1.599(6), N(1)–C(1) = 1.403(5), N(1)–C(9) = 1.478(5), C(1)–C(2) = 1.356(6), C(2)–C(3) = 1.437(6); N(1)–B(1)–C(8) = 116.9(3), B(1)–N(1)–C(1) = 121.7(3), N(1)–C(1)–C(2) = 120.9(4), C(1)–C(2)–C(3) = 123.3(4), B(1)–C(8)–C(3) = 118.7(3); C(1)–B(1)–N(1)–C(8) = −1.6(6), B(1)–N(1)–C(1)–C(2) = 1.9(6), N(1)–C(1)–C(2)–C(3) = 0.3(6), C(1)–C(2)–C(3)–C(8) = −2.6(6), B(1)–C(8)–C(3)–C(2) = 2.7(6), N(1)–B(1)–C(8)–C(3) = −0.7(6); B(1)–N(1)–C(1)–C(2)–C(3)–C(8)//C(11)–C(12)–C(13)–C(14)–C(15)–C(16) = 78.0(1), C(1)–N(1)–B(1)–C(8)–B(3)–C(2)//C(21)–C(22)–C(23)–C(24)–C(25)–C(26) = 83.0(1).

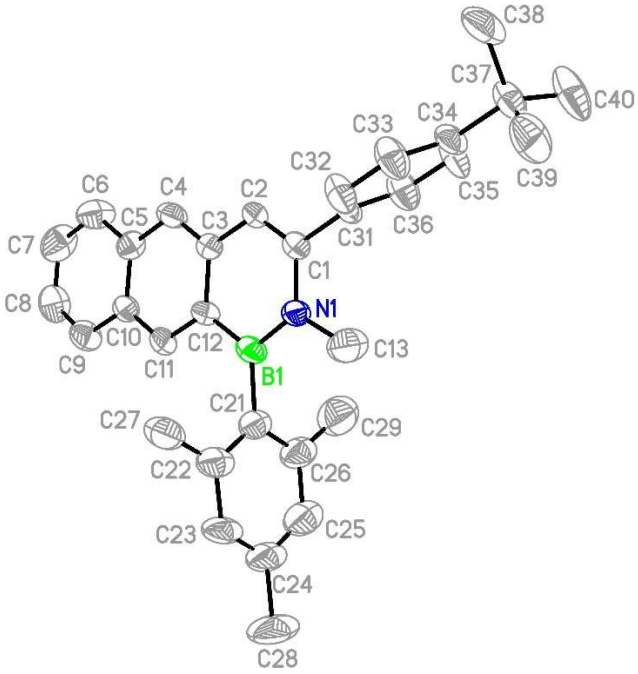

Figure S94 (CDCC 2058867): Molecular structure of **5b** in the solid state. Displacement ellipsoids are drawn at the 50% probability level, hydrogen atoms are omitted for clarity. Selected bond lengths (Å), bond angles (°), torsion angles (°), and dihedral angles (°): B(1)–N(1) = 1.435(7), B(1)–C(12) = 1.530(8), B(1)–C(21) = 1.582(8), N(1)–C(1) = 1.408(6), N(1)–C(13) = 1.471(7), C(1)–C(2) = 1.328(7), C(2)–C(3) = 1.447(7); N(1)–B(1)–C(12) = 116.5(5), B(1)–N(1)–C(1) = 121.6(4), N(1)–C(1)–C(2) = 121.5(4), C(1)–C(2)–C(3) = 123.6(5), B1(3)–C(12)–C(3) = 118.8(4); C(1)–N(1)–B(1)–C(11) = −0.2(9), B(1)–N(1)–C(1)–C(2) = −0.1(9), N(1)–C(1)–C(2)–C(3) = −1.0(9), C(1)–C(2)–C(3)–C(12) = 2.4(9), B(1)–C(12)–C(3)–C(2) = −2.6(8), N(1)–B(1)–C(12)–C(3) = 1.6(9); B(1)–N(1)–C(1)–C(2)–C(3)–C(12)//C(21)–C(22)–C(23)–C(24)–C(25)–C(26) = 85.3(2), C(1)–N(1)–B(1)–C(12)–C(3)–C(2)//C(31)–C(32)–C(33)–C(34)–C(35)–C(36) = 82.1(2).

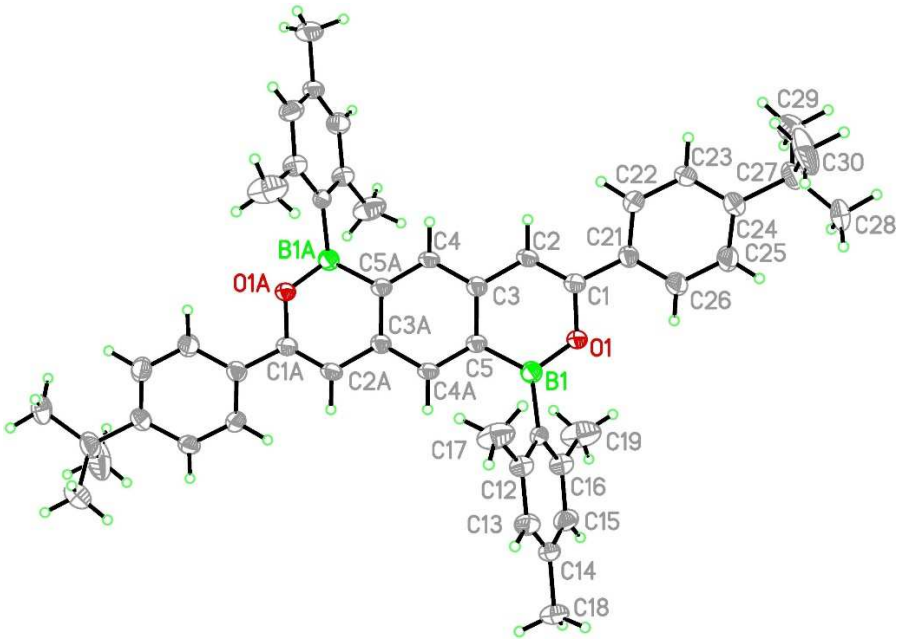

Figure S95 (CCDC 2058868): Molecular structure of **6a** in the solid state. Displacement ellipsoids are drawn at the 50% probability level. Selected bond lengths (Å), bond angles (°), torsion angles (°), and dihedral angles (°): B(1)–O(1) = 1.374(3), B(1)–C(5) = 1.549(3), B(1)–C(11) = 1.569(3), O(1)–C(1) = 1.381(2), C(1)–C(2) = 1.340(3), C(2)–C(3) = 1.441(3); O(1)–B(1)–C(5) = 117.33(18), B(1)–O(1)–C(1) = 122.89(16), C(1)–C(2)–C(3) = 122.77(19), C(2)–C(3)–C(5) = 118.45(18); C(1)–O(1)–B(1)–C(5) = 1.4(3), O(1)–B(1)–C(5)–C(3) = −0.1(3), B(1)–C(5)-C(3)–C(2) = −0.5(3), C(1)–C(2)–C(3)–C(5) = 0.0(3);); B(1)–O(1)–C(1)–C(2)–C(3)–C(5)//C(11)–C(12)–C(13)–C(14)–C(15)–C(16) = 75.7(1), C(1)–O(1)–B(1)–C(5)–C(3)–C(2)//C(21)–C(22)–C(23)–C(24)–C(25)–C(26) = 28.30(1).

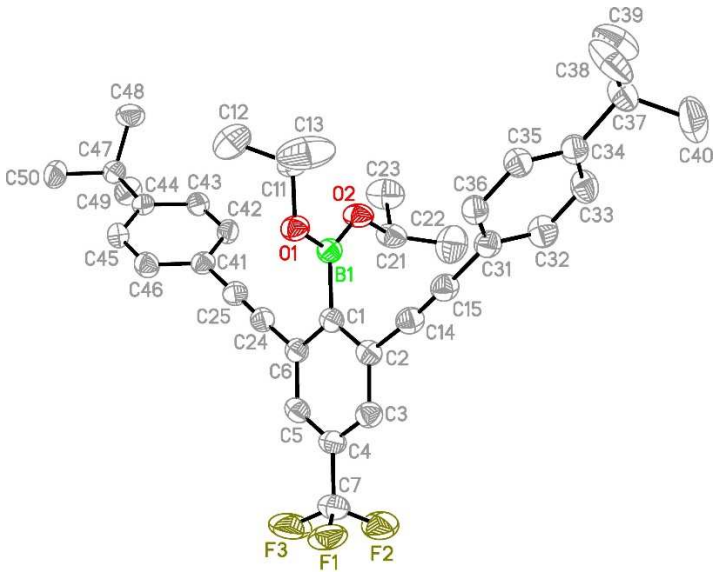

Figure S96 (CDCC 2058869): Molecular structure of **7a^{iPr}** in the solid state. Displacement ellipsoids are drawn at the 50% probability level, hydrogen atoms are omitted for clarity. Selected bond lengths (Å), bond angles (°), and torsion angles (°): B(1)–O(1) = 1.351(2), B(1)–O(2) = 1.352(2), B(1)–C(1) = 1.597(2), C(14)–C(15) = 1.197(2), C(24)–C(25) = 1.201(2); O(1)–B(1)–O(2) = 120.5(2), O(1)–B(1)–C(1) = 114.8(1), O(2)–B(1)–C(1) = 124.7(1), C(2)–C(14)–C(15) = 172.8(2), C(14)–C(15)–C(31) = 175.7(2), C(6)–C(24)–C(25) = 178.1(2), C(14)–C(15)–C(31) = 178.9(2); B(1)–C(1)–C(2)–C(14) = –6.2(2), B(1)–C(1)–C(6)–C(24) = 4.9(2).

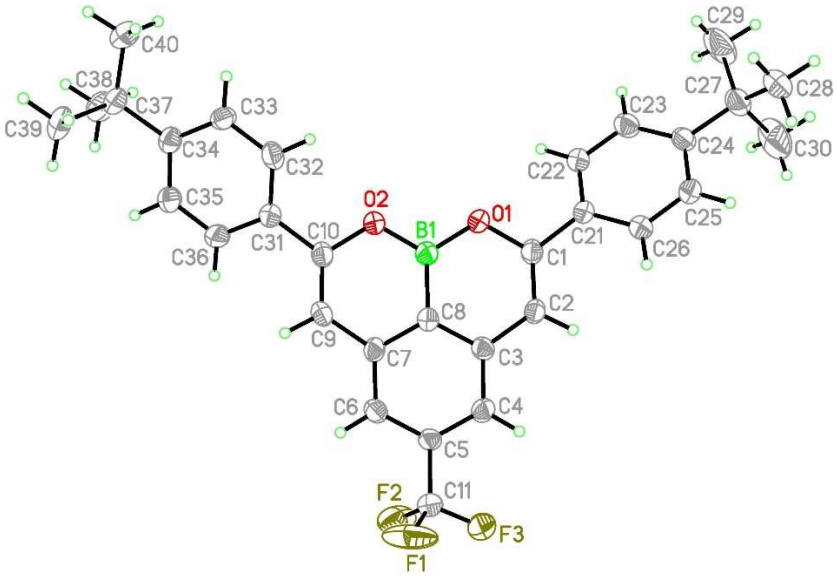

Figure S97 (CCDC 2058870): Molecular structure of **8a** in the solid state. Displacement ellipsoids are drawn at the 50% probability level. Selected bond lengths (Å), bond angles (°), and torsion angles (°): B(1)–O(1) = 1.381(5), B(1)–O(2) = 1.368(4), B(1)–C(8) = 1.495(5), O(1)–C(1) = 1.3841(4), O(2)–C(10) = 1.3841(4), C(1)–C(2) = 1.345(4), C(2)–C(3) = 1.444(5), C(7)–C(9) =1.445(5), C(9)–C(10) = 1.344(5); O(1)–B(1)–O(2) = 118.4(3), O(1)–B(1)–C(8) = 120.7(3), O(2)–B(1)–C(8) = 121.0(3), B(1)–O(1)–C(1) = 118.6(3), B(1)–O(2)–C(10) = 118.9(3), C(1)–C(2)–C(3) = 123.0(3), C(2)–C(3)–C(8) = 116.5(3), C(8)–C(7)–C(9) = 116.3(3), C(7)–C(9)–C(10) = 123.4(3); C(1)–O(1)–B(1)–C(8) = −0.7(5), C(8)–B(1)–O(2)–C(10) = −0.5(5), B(1)–C(8)–C(3)–C(2) =0.3(5), C(1)–C(2)–C(3)–C(8) = −0.9(5), B(1)–O(1)–C(1)–C(2) = 0.1(5), C(8)–C(7)–C(9)–C(10) = 1.2(5), B(1)–O(2)–C(10)–C(9) = 0.5(5); C(1)–O(1)–B(1)–C(8)–C(3)–C(2)//C(21)–C(22)–C(23)–C(24)–C(25)–C(26) = 33.6(1), C(10)–O(2)–B(1)–C(8)–C(7)–C(9)//C(31)–C(32)–C(33)–C(34)–C(35)–C(36) = 14.4(2).

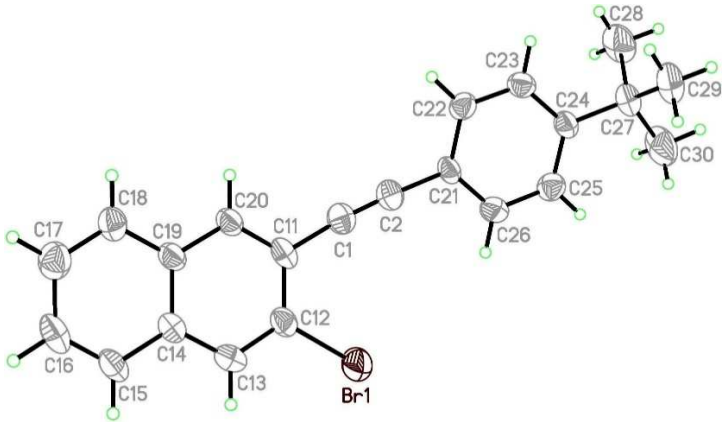

Figure S98 (CDCC 2058871): Molecular structure of **19** in the solid state. Displacement ellipsoids are drawn at the 50% probability level. Selected bond lengths (Å), bond angles (°), and torsion angles (°): Br(1)–C(12) = 1.883(9), C(1)–C(2) = 1.190(11); C(2)–C(1)–C(11) = 174.8(10), C(1)–C(2)–C(21) = 176.3(10); Br(1)–C(12)–C(11)–C(1) = −0.9(11).

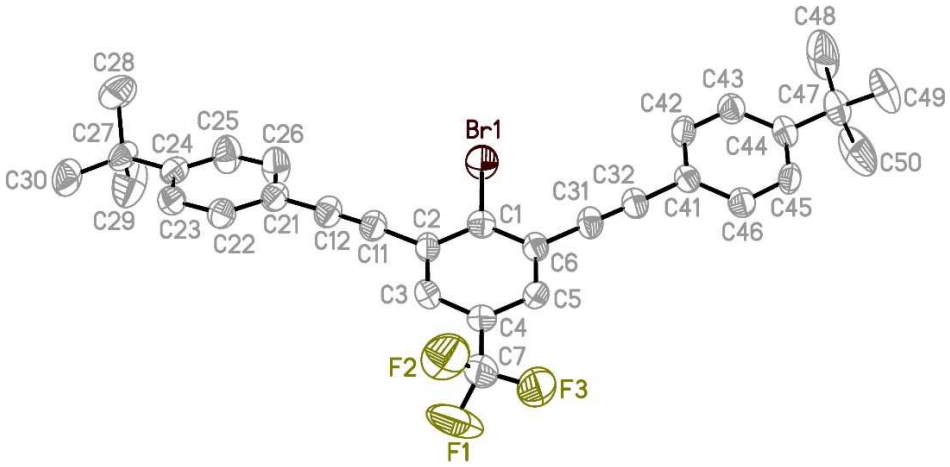

Figure S99 (CDCC 2058872): Molecular structure of **24** in the solid state. Displacement ellipsoids are drawn at the 50% probability level, hydrogen atoms are omitted for clarity. Selected bond lengths (Å), bond angles (°), and torsion angles (°): Br(1)–C(1) = 1.884(4), C(11)–C(12) = 1.188(5), C(31)–C(32) = 1.186(5); C(2)–C(11)–C(12) = 176.0(4), C(11)–C(12)–C(21) = 178.0(4), C(6)–C(31)–C(32) = 178.6(4), C(31)–C(32)–C(41) = 177.3(5); Br(1)–C(1)–C(2)–C(11) = 2.6(5), Br(1)–C(1)–C(6)–C(31) = 0.6(5).

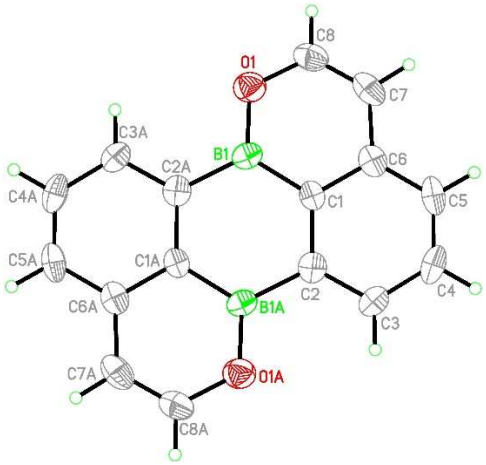

Figure S100 (CDCC 2068160): Molecular structure of **9** in the solid state. Displacement ellipsoids are drawn at the 50% probability level. Selected bond lengths (Å), bond angles (°), and torsion angles (°): B(1)–O(1) = 1.384(6), C(7)–C(8) = 1.331(7); O(1)–B(1)–C(1) = 119.4(5), O(1)–B(1)–C(2A) = 118.9(4), C(1)–B(1)–C(2A) = 121.7(4), C(6)–C(7)–C(8) = 121.7(5); O(1)–B(1)–C(1)–C(6) = 0.0(6), C(2)–C(1)–C(6)–C(7) = 179.5(5). Symmetry transformation used to generate equivalent atoms: −x+1, −y+2, −z+1.

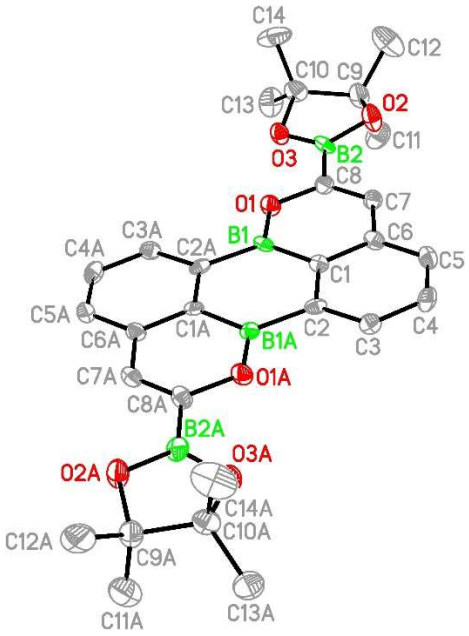

Figure S101 (CDCC 2068161): Molecular structure of **10** in the solid state. Displacement ellipsoids are drawn at the 50% probability level; hydrogen atoms are omitted for clarity. Selected bond lengths (Å), bond angles (°), and torsion angles (°): B(1)–O(1) = 1.380(7), B(2)–O(2) = 1.377(7), B(2)–O(3) = 1.372(8), B(2)–C(8) = 1.542(8), C(7)–C(8) = 1.341(8); O(1)–B(1)–C(1) = 119.4(5), O(1)–B(1)–C(2A) = 119.1(5), C(1)–B(1)–C(2A) = 121.5(5), C(6)–C(7)–C(8) = 123.7(5); O(1)–B(1)–C(1)–C(6) = −0.4(8), O(1)–C(8)–B(2)–O(2) = 173.9(6), O(1)–C(8)–B(2)–O(3) = −7.1(9), C(2)–C(1)–C(6)–C(7) = −179.9(5). Symmetry transformation used to generate equivalent atoms: −x+1/2, −y+3/2, z.

Table S2: Selected crystallographic data for **1a**–**3a**.

compound	**1a**	**2a**	**3a**·acetone
CCDC	2058862	2058863	2058864
formula	$C_{27}H_{29}BO$	$2(C_{31}H_{31}BO)\cdot 0.5(C_6H_{14})$	$C_{48}H_{52}B_2O_2\cdot C_3H_6O$
M_r	380.31	451.91	740.59
T (K)	173(2)	173(2)	173(2)
radiation, λ (Å)	0.71073	0.71073	0.71073
crystal system	Monoclinic	Triclinic	Monoclinic
space group	$P\,c$	$P\,-1$	$C\,2/c$
a [Å]	16.9020(7)	12.8766(8)	33.3265(16)
b [Å]	9.4331(5)	14.0599(9)	6.9745(2)
c [Å]	15.2863(7)	15.4098(10)	23.9282(12)
α [°]	90	96.874(5)	90
β [°]	113.082(6)	102.280(5)	125.567(3)
γ [°]	90	90.643(5)	90
V [Å^3]	2237.26(19)	2704.5(3)	4524.1(4)
Z	4	4	4
D_{calcd} (g cm^{-3})	1.129	1.110	1.087
μ (mm^{-1})	0.066	0.064	0.065
F(000)	816	970	1592
crystal size (mm^3)	0.190 x 0.170 x 0.140	0.140 x 0.120 x 0.030	0.280 x 0.220 x 0.090
Θ [°]	3.400 to 27.641	3.251 to 25.027	3.413 to 27.576
h	−21 to 22	−15 to 15	−43 to 42
k	−12 to 12	−16 to 16	−9 to 9
l	−19 to 19	−18 to 18	−31 to 31
reflections collected	23881	36720	35502
independent reflections	9440	9551	5184
R_{int}	0.0374	0.0526	0.0575
data/restraints/parameters	9440/2/537	9551/0/636	5184/66/290
R_1, wR_2 (I > 2σ(I))	0.0551, 0.1371	0.0862, 0.1754	0.0654, 0.1660
R_1, wR_2 (all data)	0.0653, 0.1435	0.1208, 0.1902	0.0793, 0.1751
Goodness-of-fit an F^2	1.105	1.149	1.048
largest diff. peak and hole (e Å^{-3})	0.270 and −0.177	0.361 and −0.396	0.278 and −0.244

Table S3: Selected crystallographic data for **4a**, **4b**, and **5b**.

compound	**4a**	**4b**	**5b**
CCDC	2058865	2058866	2058867
formula	$C_{27}H_{29}BO$	$C_{28}H_{32}BN$	$C_{32}H_{34}BN$
M_r	380.31	393.35	443.41
T (K)	173(2)	173(2)	173(2)
radiation, λ (Å)	0.71073	0.71073	0.71073
crystal system	Orthorhombic	Orthorhombic	Monoclinic
space group	*P bca*	$P\,2_12_12_1$	$P\,2_1/n$
a [Å]	23.7421(8)	9.3999(4)	14.4318(18)
b [Å]	21.8444(6)	11.8608(7)	9.4346(18)
c [Å]	8.6139(2)	20.7807(9)	19.482(2)
α [°]	90	90	90
β [°]	90	90	91.219(9)
γ [°]	90	90	90
V [Å^3]	4467.4(2)	2316.8(2)	2652.0(7)
Z	8	4	4
D_{calcd} (g cm^{-3})	1.131	1.128	1.111
μ (mm^{-1})	0.066	0.064	0.063
F(000)	1632	848	952
crystal size (mm^3)	0.290 x 0.280 x 0.270	0.230 x 0.140 x 0.090	0.150 x 0.030 x 0.030
Θ [°]	1.865 to 25.594	3.390 to 25.025	3.302 to 25.024
h	−28 to 28	−9 to 11	−17 to 17
k	−26 to 26	−14 to 14	−11 to 11
l	−10 to 10	−24 to 24	−23 to 23
reflections collected	39774	16025	15836
independent reflections	4130	4038	4667
R_{int}	0.0363	0.0464	0.1425
data/restraints/parameters	4130/0/266	4083/36/303	4667/0/311
R_1, wR_2 ($I > 2\sigma(I)$)	0.0451, 0.1163	0.0662, 0.1517	0.1032, 0.1848
R_1, wR_2 (all data)	0.0551, 0.1255	0.0718, 0.1551	0.2386, 0.2519
Goodness-of-fit an F^2	1.077	1.249	1.032
largest diff. peak and hole (e Å^{-3})	0.211 and −0.196	0.255 and −0.251	0.220 and −0.215

Table S4: Selected crystallographic data for **6a**, **7a^{iPr}**, and **8a**.

compound	**6a**	**7a^{iPr}**	**8a**
CCDC	2058868	2058869	2058870
formula	$C_{48}H_{52}B_2O_2$	$C_{37}H_{42}BF_3O_2$	$C_{31}H_{30}BF_3O_2$
M_r	682.51	586.51	502.36
T (K)	173(2)	173(2)	173(2)
radiation, λ (Å)	0.71073	0.71073	0.71073
crystal system	Triclinic	Monoclinic	Monoclinic
space group	$P\,{-}1$	$C\,2/c$	$C\,2/c$
a [Å]	8.5512(9)	32.1592(13)	35.674(2)
b [Å]	11.0326(10)	9.1287(2)	10.7160(5)
c [Å]	12.6835(12)	24.8768(10)	29.670(2)
α [°]	67.901(7)	90	90
β [°]	89.033(8)	112.858(3)	98.307(5)
γ [°]	67.825(7)	90	90
V [Å^3]	1015.70(18)	6729.6(4)	11223.3(11)
Z	1	8	16
D_{calcd} (g cm^{-3})	1.116	1.158	1.189
μ (mm^{-1})	0.065	0.081	0.086
F(000)	366	2496	4224
crystal size (mm^3)	0.260 x 0.160 x 0.080	0.240 x 0.210 x 0.160	0.330 × 0.240 × 0.100
Θ [°]	3.305 to 25.027	2.335 to 26.015	2.131 to 25.692
h	−10 to 10	−39 to 39	−43 to 43
k	−13 to 13	−11 to 11	−13 to 12
l	−15 to 15	−30 to 30	−35 to 35
reflections collected	14051	40358	22811
independent reflections	3576	6547	10274
R_{int}	0.0339	0.0395	0.0805
data/restraints/parameters	3576/18/266	6547/73/473	10274/0/667
R_1, wR_2 (I > 2σ(I))	0.0592, 0.1334	0.0527, 0.1239	0.0693, 0.1476
R_1, wR_2 (all data)	0.0808, 0.1425	0.0647, 0.1303	0.1687, 0.1857
Goodness-of-fit an F^2	1.153	1.105	1.001
largest diff. peak and hole (e Å^{-3})	0.193 and −0.187	0.212 and −0.216	0.254 and −0.262

Table S5: Selected crystallographic data for **19**, **24** and **9**.

compound	**19**	**24**	**9**
CCDC	2058871	2058872	2068160
formula	$C_{22}H_{19}Br$	$C_{31}H_{28}BrF_3$	$C_{16}H_{10}B_2O_2$
M_r	363.28	537.44	255.86
T (K)	173(2)	173(2)	173(2)
radiation, λ (Å)	0.71073	0.71073	0.71073
crystal system	Monoclinic	Orthorhombic	Monoclinic
space group	$P\,2_1/c$	$P\,bca$	$P\,2_1/n$
a [Å]	26.944(2)	19.2423(12)	7.9871(13)
b [Å]	6.2564(4)	10.9228(5)	4.6704(5)
c [Å]	22.5176(17)	26.3907(12)	16.324(3)
α [°]	90	90	90
β [°]	113.082(6)	90	101.395(12)
γ [°]	90	90	90
V [Å^3]	3492.0(5)	5546.8(5)	596.93(16)
Z	8	8	2
D_{calcd} (g cm^{-3})	1.382	1.287	1.423
μ (mm^{-1})	2.352	1.518	0.090
F(000)	1488	2208	264
crystal size (mm^3)	0.120 x 0.030 x 0.020	0.260 x 0.230 x 0.220	0.110 × 0.030 × 0.010
Θ [°]	1.809 to 25.026	2.279 to 25.401	4.176 to 25.016
h	−32 to 31	−23 to 17	−9 to 8
k	−7 to 7	−13 to 11	−5 to 5
l	−26 to 26	−30 to 31	−19 to 19
reflections collected	22631	20775	3067
independent reflections	22631	5072	1050
R_{int}	Not determined due to twinning	0.0510	0.0497
data/restraints/parameters	22631/0/416	5072/30/329	1050/0/91
R_1, wR_2 (I > 2σ(I))	0.0627, 0.1509	0.0605, 0.1241	0.1063, 0.1676
R_1, wR_2 (all data)	0.1299, 0.1923	0.0974, 0.1388	0.1371, 0.1783
Goodness-of-fit an F^2	0.984	1.062	1.342
largest diff. peak and hole (e Å^{-3})	1.261 and −0.945	0.553 and −0.386	0.226 and −0.196

Table S6: Selected crystallographic data for **10**.

compound	**10**
CCDC	2068161
formula	$C_{28}H_{32}B_4O_6$
M_r	507.77
T (K)	173(2)
radiation, λ (Å)	0.71073
crystal system	Tetragonal
space group	$P\,4_2/n$
a [Å]	19.5614(14)
b [Å]	19.5614(14)
c [Å]	6.7125(5)
α [°]	90
β [°]	90
γ [°]	90
V [Å^3]	2568.5(4)
Z	4
D_{calcd} (g cm^{-3})	1.313
μ (mm^{-1})	0.088
F(000)	1072
crystal size (mm^3)	0.110 × 0.030 × 0.030
Θ [°]	3.209 to 25.008
h	−22 to 23
k	−23 to 23
l	−7 to 7
reflections collected	12813
independent reflections	2266
R_{int}	0.1287
data/restraints/parameters	2266/0/172
R_1, wR_2 (I > 2σ(I))	0.1169, 0.1815
R_1, wR_2 (all data)	0.1878, 0.2140
Goodness-of-fit an F^2	1.265
largest diff. peak and hole (e Å^{-3})	0.332 and −0.313

6. Computational details and HOMO/LUMO analyses

Geometry optimizations and frequency calculations were carried out using the Gaussian 09 software package,[14] the B3LYP functional, and the 6-31G* basis set. The stationary points were characterized as minima (no imaginary frequencies in the vibrational analysis). The graphics were produced with Avogadro 1.1.1 and POV-Ray 3.7.0.

Table S7: Computed data of the compounds **4a,b**–**6a,b** and **8a**–**c** in comparison with selected experimental values (see Table 1).

	E_{HOMO}^{DFT} [eV]	E_{LUMO}^{DFT} [eV]	E'_{HOMO}^{DFT} [eV][a]	E'_{LUMO}^{DFT} [eV][b]	E_{LUMO}^{CV} [eV]	E_G^{DFT} [eV][c]	E'_G^{DFT} [eV][d]	E_G^{opt} [eV]
4a	−5.50	−1.27	−5.26	−2.03	-	4.23	3.23	3.41
4b	−5.34	−0.65	−5.15	−1.62	-	4.69	3.53	3.53
5a	−5.27	−1.59	−5.10	−2.23	−2.22	3.68	2.87	2.96
5b	−5.04	−1.27	−4.96	−2.03	−2.00	3.77	2.93	2.94
6a	−5.11	−1.65	−5.00	−2.27	-	3.46	2.73	2.77
6b	−4.78	−0.93	−4.78	−1.80	−1.80	3.85	2.98	2.94
8a	−5.45	−1.54	−5.22	−2.20	-	3.91	3.02	3.11
8ab	−5.12	−1.27	−5.01	−2.03	-	3.85	2.98	3.01
8c	−5.32	−1.59	−5.13	−2.23	-	3.73	2.90	-
5[e]	−5.11	−1.67	−5.01	−2.29	-	3.44	2.72	-
6[e]	−5.01	−1.71	−4.94	−2.31	-	3.30	2.63	-

[a] Scaled HOMO energies (E'_{HOMO}^{DFT}) were calculated from the scaled LUMO energies (E'_{LUMO}^{DFT}) and the computed HOMO-LUMO energy gaps ($E'_{HOMO}^{DFT} = E'_{LUMO}^{DFT} - E'_G^{DFT}$). [b] For better comparability with the E_{LUMO}^{CV} values, the computed LUMO energies (E_{LUMO}^{DFT}) have been scaled according to the following linear equation: $E'_{LUMO}^{DFT} = 0.65 \cdot E_{LUMO}^{DFT} - 1.20$. [c] Computed band gap $E_G^{DFT} = E_{LUMO}^{DFT} - E_{HOMO}^{DFT}$. [d] For better comparability with the E_G^{opt} values, the computed energy gaps (E_G^{DFT}) have been scaled according to the following linear equation: $E'_G^{DFT} = 0.65 \cdot E_G^{DFT} + 0.48$. [e] Carbonaceous model compounds of **5a,b** and **6a,b**.

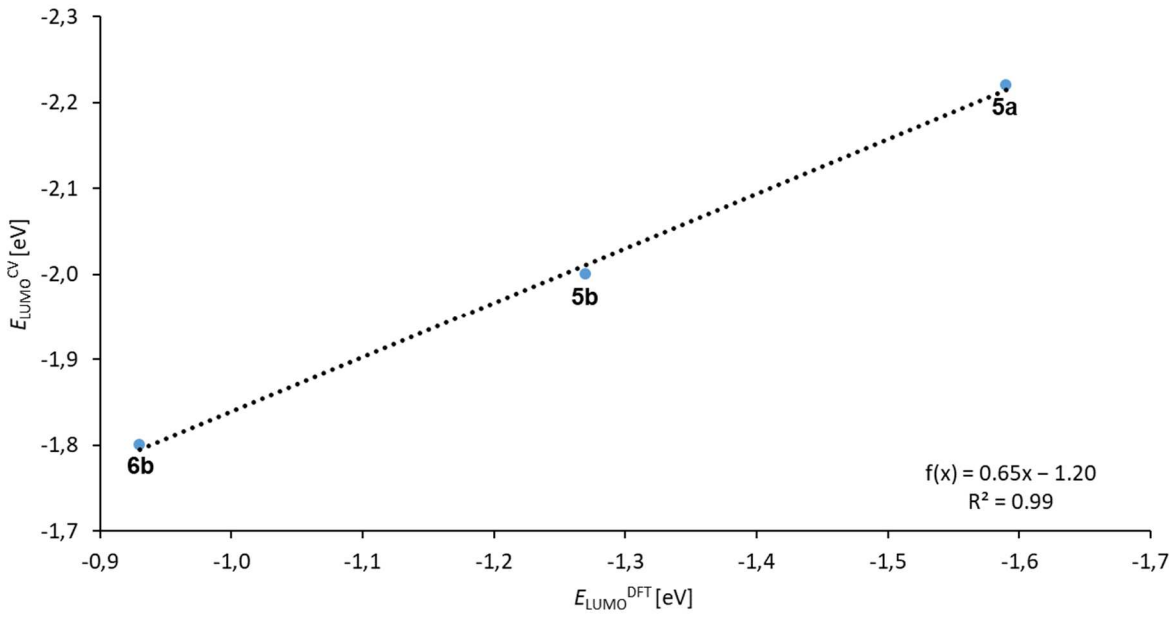

Figure S102: LUMO energies calculated from CV measurements plotted against the computed LUMO energies of **5a**, **5b**, and **6b**. The mathematical expression of the linear regression is given in the bottom right corner.

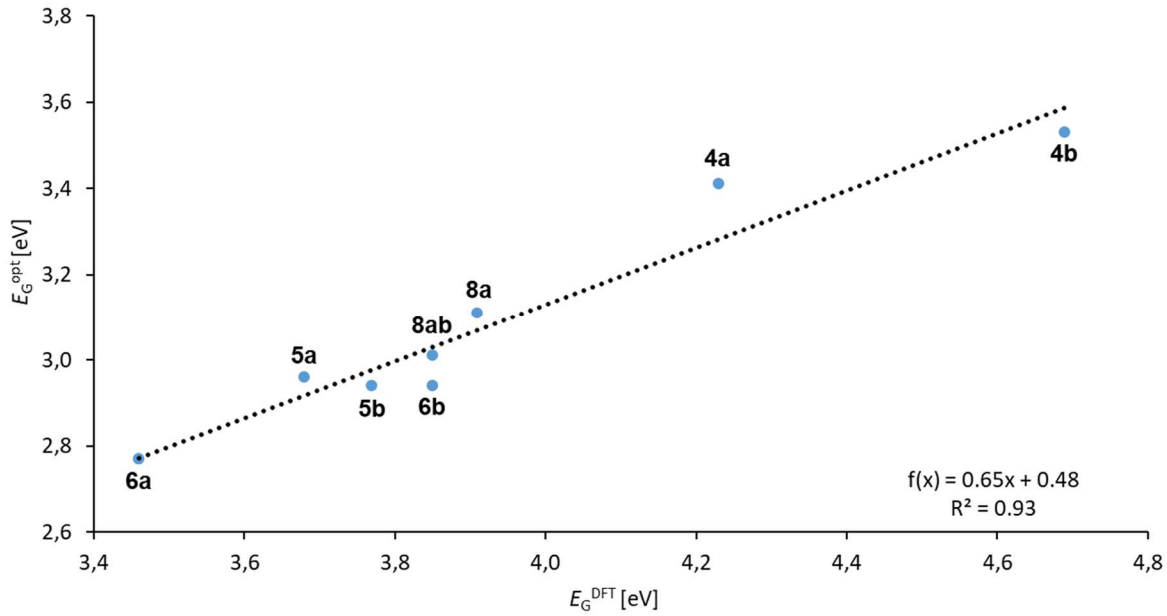

Figure S103: Spectroscopically determined HOMO-LUMO energy differences (E_G^{opt}) plotted against the computed energy gaps (E_G^{DFT}) of **4a,b–6a,b** and **8a**, **8ab**. The mathematical expression of the linear regression is given in the bottom right corner.

6.1. Computational details and HOMO/LUMO analyses for the compounds 4a,b–6a,b and 8a–c, calculated at the B3LYP/6-31G* level

4a (ΔE = 3.23 eV)	
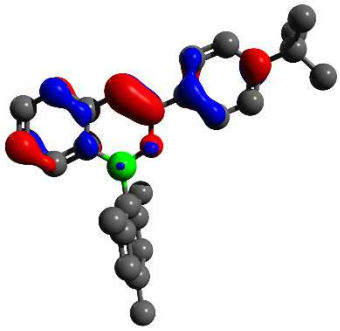	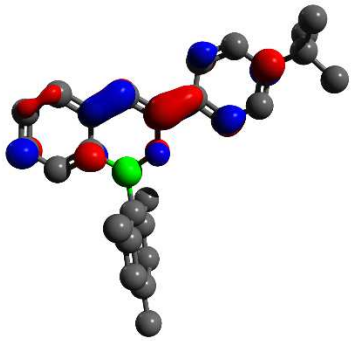
−5.26 eV	−2.03 eV
4b (ΔE = 3.53 eV)	
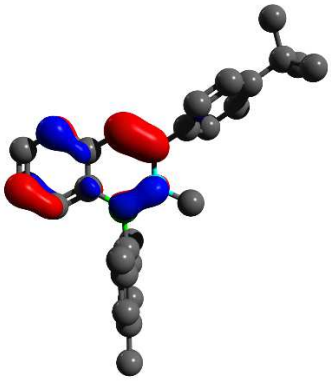	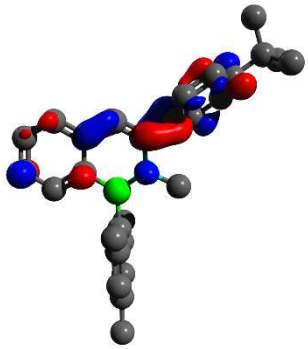
−5.15 eV	−1.62 eV
5a (ΔE = 2.87 eV)	
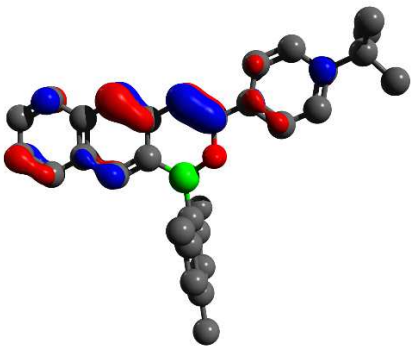	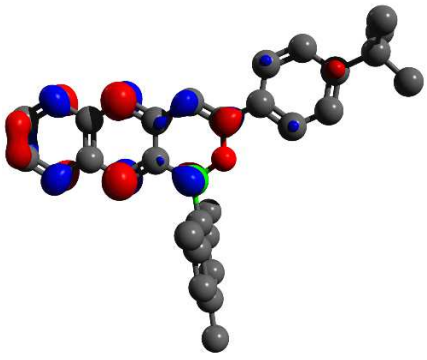
−5.10 eV	−2.23 eV

5b (ΔE = 2.93 eV)	
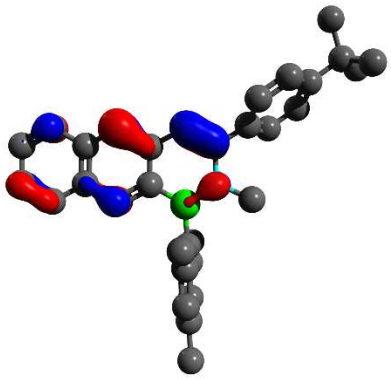	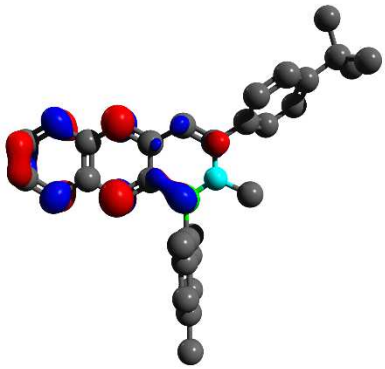
−4.96 eV	−2.03 eV
6a (ΔE = 2.73 eV)	
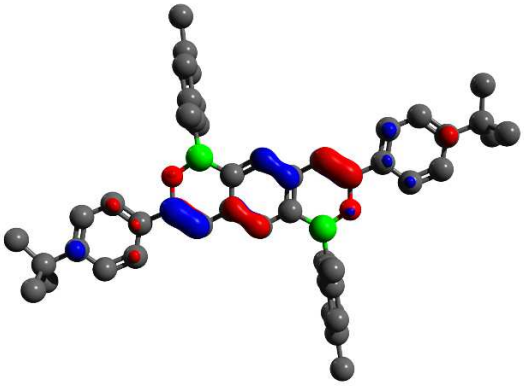	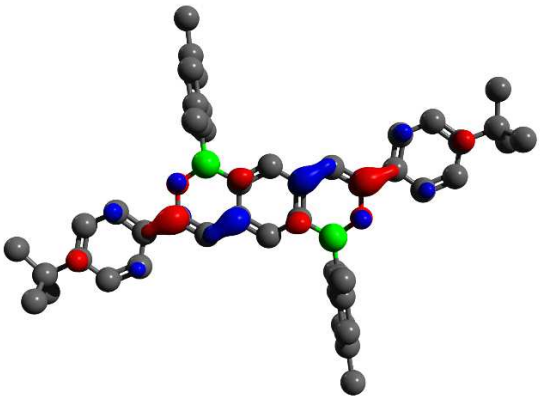
−5.00 eV	−2.27 eV
6b (ΔE = 2.98 eV)	
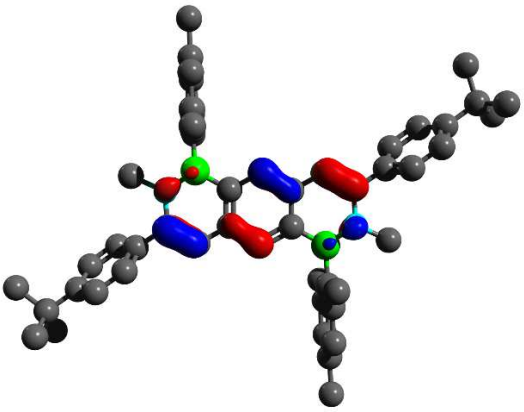	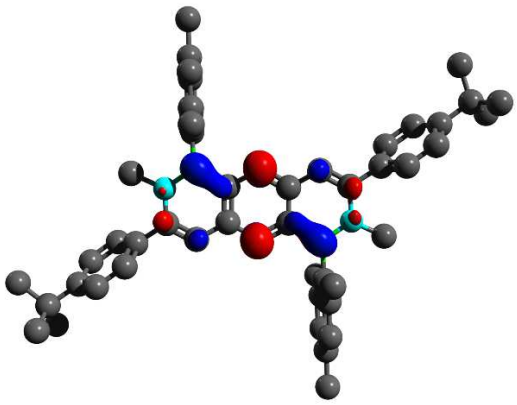
−4.78 eV	−1.80 eV

8a (ΔE = 3.02 eV)

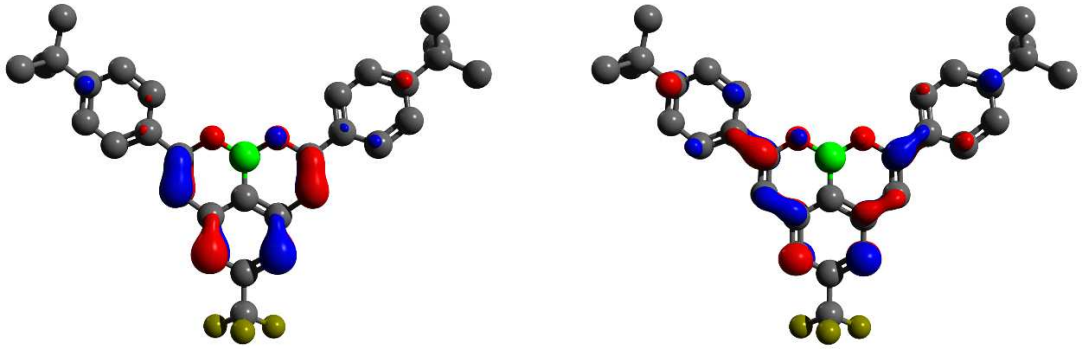

−5.22 eV −2.20 eV

8ab (ΔE = 2.98 eV)

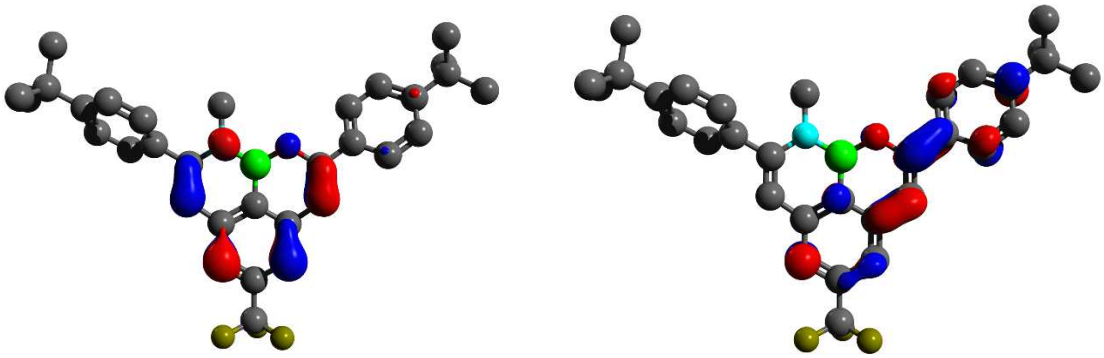

−5.01 eV −2.03 eV

8c (ΔE = 2.90 eV)

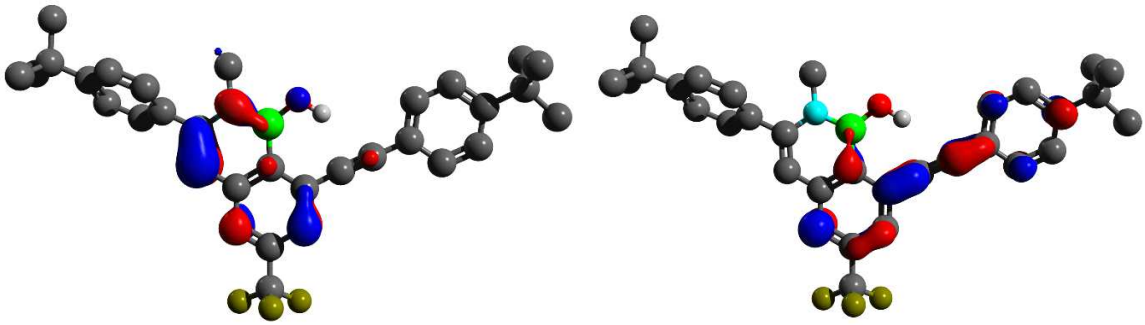

−5.13 eV −2.23 eV

Scheme S1: Isosurface plots (isovalue: 0.05 $a_0^{-3/2}$) and calculated orbital energy differences for the HOMOs (left) and LUMOs (right). Hydrogen atoms are omitted for clarity.

6.2. Computational details and HOMO/LUMO analyses for the compounds 5 and 6, calculated at the B3LYP/6-31G* level

5 (ΔE = 2.72 eV)	
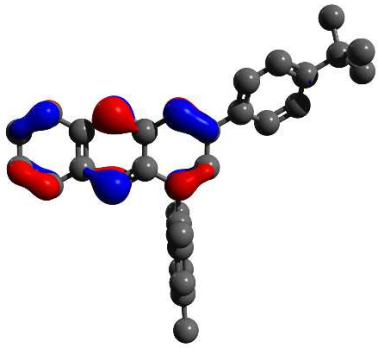	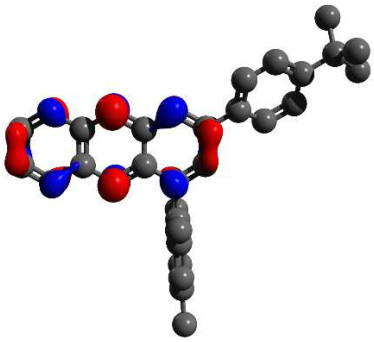
−5.01 eV	−2.29 eV
6 (ΔE = 2.63 eV)	
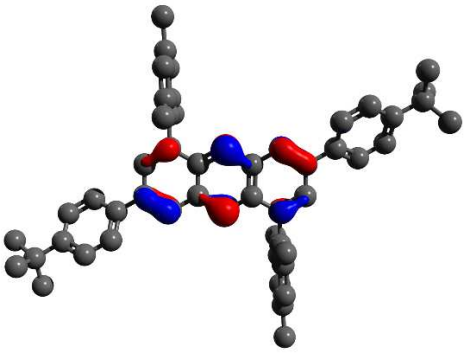	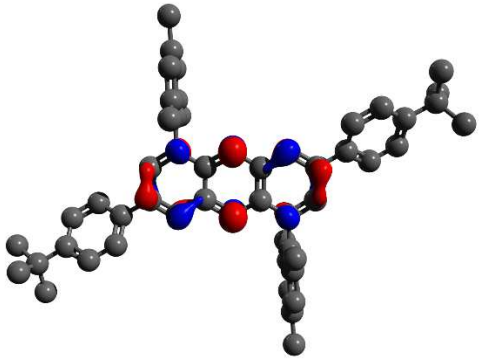
−4.94 eV	−2.31 eV

Scheme S2: Isosurface plots (isovalue: 0.05 $a_0^{-3/2}$) and calculated orbital energy differences for the HOMOs (left) and LUMOs (right). Hydrogen atoms are omitted for clarity.

6.3. Cartesian coordinates and total energies for 4a,b–6a,b, 8a–c, 5, and 6 calculated at the B3LYP/6-31G* level

4a

Total energy: –1146.5239842 Hartree

Atom coordinates:

1	6	0	-3.56602	2.30057	-0.06753
2	6	0	-2.21809	1.89010	-0.03684
3	6	0	-3.90806	3.64588	-0.09175
4	6	0	-1.19943	2.88487	-0.03929
5	6	0	-2.89487	4.62061	-0.08745
6	6	0	-1.55923	4.25020	-0.06246
7	1	0	-4.34462	1.54146	-0.07241
8	1	0	-0.78034	5.00948	-0.06174
9	5	0	-1.76730	0.42059	-0.00467
10	8	0	-0.39927	0.18356	0.00074
11	6	0	0.55085	1.16593	-0.01158
12	6	0	0.18203	2.47498	-0.01973
13	1	0	0.94768	3.24271	-0.00317
14	6	0	1.92944	0.64634	0.00088
15	6	0	-2.70125	-0.84855	0.00051
16	6	0	-2.92350	-1.56907	-1.19465
17	6	0	-3.33981	-1.28162	1.18342
18	6	0	-3.76828	-2.68284	-1.19104
19	6	0	-4.17672	-2.40245	1.15331
20	6	0	-4.40339	-3.11929	-0.02447
21	1	0	-3.93695	-3.22228	-2.12184
22	1	0	-4.66354	-2.72366	2.07288
23	6	0	-2.25556	-1.14329	-2.48655
24	1	0	-1.16431	-1.23482	-2.42305
25	1	0	-2.47436	-0.09552	-2.72966
26	1	0	-2.59263	-1.75563	-3.32911
27	6	0	-3.11151	-0.56020	2.49643
28	1	0	-3.31842	0.51331	2.41402
29	1	0	-2.07069	-0.65918	2.83166
30	1	0	-3.75089	-0.96426	3.28796
31	6	0	-5.28839	-4.34427	-0.03268
32	1	0	-5.80570	-4.45979	-0.99154
33	1	0	-6.04558	-4.29763	0.75744
34	1	0	-4.70395	-5.25989	0.13151
35	6	0	2.17159	-0.71600	0.22908
36	6	0	3.04467	1.47726	-0.21201
37	6	0	3.47076	-1.22245	0.25594
38	1	0	1.33188	-1.38229	0.38998
39	6	0	4.58676	-0.40079	0.05353
40	1	0	3.60023	-2.28317	0.44043
41	6	0	4.33400	0.96334	-0.18260
42	1	0	5.16369	1.64328	-0.35571
43	1	0	2.90823	2.53450	-0.41820
44	6	0	6.03309	-0.92391	0.07478
45	6	0	6.10373	-2.43884	0.34445
46	1	0	5.67142	-2.70068	1.31684
47	1	0	7.15011	-2.76408	0.35026
48	1	0	5.58302	-3.01561	-0.42828
49	6	0	6.82561	-0.19834	1.18852
50	1	0	6.38077	-0.38677	2.17227
51	1	0	6.84725	0.88550	1.03396
52	1	0	7.86334	-0.55306	1.21065
53	6	0	6.70177	-0.64604	-1.29306
54	1	0	7.73734	-1.00747	-1.29039
55	1	0	6.72320	0.42327	-1.52800
56	1	0	6.16573	-1.15525	-2.10202
57	1	0	-3.16096	5.67468	-0.10575
58	1	0	-4.95140	3.94868	-0.11455

4b

Total energy: –1165.9561748 Hartree

Atom coordinates:

1	6	0	-3.32014	2.42248	-0.13089
2	6	0	-2.02439	1.85985	-0.08107
3	6	0	-3.51275	3.79460	-0.17900
4	6	0	-0.90829	2.74294	-0.08006
5	6	0	-2.39979	4.65641	-0.17778
6	6	0	-1.11627	4.14111	-0.12913
7	1	0	-4.17904	1.75579	-0.13102
8	1	0	-0.25665	4.80805	-0.12973
9	5	0	-1.76881	0.34329	-0.01326
10	7	0	-0.39304	-0.08201	0.02894
11	6	0	0.65906	0.84420	-0.00305
12	6	0	0.41394	2.18640	-0.04095
13	1	0	1.26643	2.85801	-0.07262
14	6	0	2.07364	0.36442	-0.00462
15	6	0	-2.95269	-0.71189	0.02455
16	6	0	-3.46466	-1.26357	-1.17240
17	6	0	-3.54976	-1.09043	1.24873
18	6	0	-4.53128	-2.16734	-1.12868
19	6	0	-4.61461	-1.99839	1.25874
20	6	0	-5.12368	-2.54761	0.07902
21	1	0	-4.91027	-2.58408	-2.06078
22	1	0	-5.05895	-2.28184	2.21171
23	6	0	-2.86347	-0.88694	-2.51132
24	1	0	-1.81484	-1.20258	-2.58956
25	1	0	-2.87873	0.19860	-2.66760
26	1	0	-3.41017	-1.35230	-3.33800
27	6	0	-3.03983	-0.52805	2.56014
28	1	0	-2.00353	-0.83239	2.75790
29	1	0	-3.64938	-0.86941	3.40318
30	1	0	-3.05165	0.56850	2.55840
31	6	0	-6.29732	-3.49950	0.10466
32	1	0	-6.23848	-4.23209	-0.70800
33	1	0	-7.24933	-2.96377	-0.01199
34	1	0	-6.34884	-4.04786	1.05156
35	6	0	2.62296	-0.31829	-1.09744
36	6	0	2.91898	0.64825	1.07799
37	6	0	3.96166	-0.71158	-1.10266
38	1	0	2.00435	-0.52776	-1.96653
39	6	0	4.81106	-0.44068	-0.02025
40	1	0	4.34038	-1.23058	-1.97630
41	6	0	4.25405	0.25180	1.06753
42	1	0	4.87017	0.48957	1.93049
43	1	0	2.52007	1.18211	1.93627
44	6	0	6.29122	-0.86285	0.00980
45	6	0	6.71591	-1.60320	-1.27239
46	1	0	6.13981	-2.52334	-1.42254
47	1	0	7.77291	-1.88355	-1.20323
48	1	0	6.59873	-0.97609	-2.16349
49	6	0	6.53200	-1.80550	1.21308
50	1	0	5.92129	-2.71178	1.12984
51	1	0	6.28567	-1.32315	2.16476
52	1	0	7.58538	-2.10836	1.25552
53	6	0	7.18260	0.39325	0.15761
54	1	0	8.24123	0.10766	0.18686
55	1	0	6.96188	0.94544	1.07705
56	1	0	7.03842	1.07802	-0.68586
57	6	0	-0.04414	-1.50429	0.17963
58	1	0	-0.95636	-2.06633	0.37378

59	1	0	0.65107	-1.64606	1.01235
60	1	0	0.42673	-1.90472	-0.72347
61	1	0	-2.54966	5.73279	-0.21575
61	1	0	-4.51741	4.20755	-0.21814

5a

Total energy: –1300.1659375 Hartree

Atom coordinates:

1	6	0	3.34520	-0.74753	-0.00683
2	6	0	1.95668	-0.74135	-0.00178
3	6	0	4.09031	-1.94857	0.00018
4	6	0	1.25290	-1.99771	0.01057
5	6	0	3.38019	-3.19989	0.01410
6	6	0	1.96902	-3.19095	0.01952
7	1	0	3.88088	0.19986	-0.01642
8	1	0	1.43779	-4.14101	0.02974
9	6	0	5.51333	-1.96183	-0.00569
10	6	0	6.20786	-3.14800	0.00164
11	6	0	5.50790	-4.38379	0.01538
12	6	0	4.13372	-4.40933	0.02150
13	1	0	6.04211	-1.01154	-0.01628
14	5	0	1.10742	0.54544	-0.00594
15	8	0	-0.26886	0.39366	-0.00729
16	6	0	-0.90701	-0.82244	-0.00232
17	6	0	-0.19066	-1.97629	0.01400
18	1	0	-0.71559	-2.92482	0.03754
19	6	0	-2.37526	-0.70587	-0.00561
20	6	0	1.66082	2.02103	-0.00990
21	6	0	1.89795	2.69450	-1.22626
22	6	0	1.93740	2.68904	1.20471
23	6	0	2.40506	3.99925	-1.21306
24	6	0	2.44236	3.99135	1.18349
25	6	0	2.68491	4.66590	-0.01845
26	1	0	2.58487	4.50642	-2.15950
27	1	0	2.65177	4.49308	2.12722
28	6	0	1.59961	2.01994	-2.54978
29	1	0	0.53006	1.79731	-2.65354
30	1	0	2.13524	1.06717	-2.64784
31	1	0	1.88977	2.65272	-3.39469
32	6	0	1.67995	2.00517	2.53203
33	1	0	0.61453	1.77819	2.66579
34	1	0	1.99237	2.63371	3.37215
35	1	0	2.22080	1.05349	2.60819
36	6	0	3.23386	6.07411	-0.01588
37	1	0	3.36177	6.45534	-1.03409
38	1	0	4.20948	6.12360	0.48415
39	1	0	2.56684	6.76355	0.51700
40	6	0	-2.98864	0.54837	0.12855
41	6	0	-3.21578	-1.82653	-0.14204
42	6	0	-4.37771	0.67495	0.13632
43	1	0	-2.36897	1.43187	0.22878
44	6	0	-5.22065	-0.43597	0.00812
45	1	0	-4.79747	1.66887	0.24543
46	6	0	-4.59685	-1.68977	-0.13269
47	1	0	-5.20312	-2.58460	-0.24361
48	1	0	-2.79162	-2.81786	-0.26863
49	6	0	-6.75530	-0.33482	0.01200
50	6	0	-7.24532	1.11720	0.16763
51	1	0	-6.91000	1.56175	1.11147
52	1	0	-8.34094	1.13995	0.16317
53	1	0	-6.89849	1.75449	-0.65365
54	6	0	-7.32242	-1.16445	1.18887
55	1	0	-6.95168	-0.78746	2.14884
56	1	0	-7.04375	-2.22088	1.11497
57	1	0	-8.41791	-1.10874	1.20143
58	6	0	-7.31213	-0.89133	-1.32051
59	1	0	-8.40744	-0.83383	-1.32853
60	1	0	-7.03275	-1.93893	-1.47433
61	1	0	-6.93503	-0.31622	-2.17383
62	1	0	7.29432	-3.14648	-0.00307
63	1	0	6.06820	-5.31505	0.02107
64	1	0	3.59998	-5.35674	0.03204

5b

Total energy: –1319.5973473 Hartree

Atom coordinates:

1	6	0	3.17460	-1.08673	-0.06636
2	6	0	1.80504	-0.84029	-0.01555
3	6	0	3.70658	-2.39378	-0.08920
4	6	0	0.90808	-1.96506	0.01358
5	6	0	2.79933	-3.51084	-0.05821
6	6	0	1.41378	-3.26391	-0.00822
7	1	0	3.86461	-0.24556	-0.08886
8	1	0	0.72828	-4.10946	0.01191
9	6	0	5.10787	-2.64560	-0.14171
10	6	0	5.59452	-3.92999	-0.16237
11	6	0	4.69886	-5.03365	-0.13149
12	6	0	3.34157	-4.82996	-0.08097
13	1	0	5.78723	-1.79646	-0.16507
14	5	0	1.21073	0.58608	0.03228
15	7	0	-0.22114	0.69263	0.08279
16	6	0	-1.04161	-0.45235	0.06252
17	6	0	-0.50690	-1.70550	0.04714
18	1	0	-1.19083	-2.54829	0.02125
19	6	0	-2.52649	-0.30108	0.03719
20	6	0	2.12986	1.87784	0.04000
21	6	0	2.48554	2.51221	-1.17239
22	6	0	2.65380	2.39216	1.24813
23	6	0	3.33201	3.62572	-1.15914
24	6	0	3.49610	3.50935	1.22733
25	6	0	3.84548	4.14493	0.03275
26	1	0	3.59994	4.09772	-2.10330
27	1	0	3.89273	3.89014	2.16734
28	6	0	1.95692	1.99599	-2.49533
29	1	0	0.86736	2.11076	-2.56867
30	1	0	2.17243	0.92886	-2.62767
31	1	0	2.40125	2.53471	-3.33860
32	6	0	2.30910	1.74452	2.57386
33	1	0	1.23499	1.81227	2.79141
34	1	0	2.84296	2.22323	3.40121
35	1	0	2.56594	0.67848	2.57948
36	6	0	4.73239	5.36863	0.03099
37	1	0	5.33069	5.42978	-0.88476
38	1	0	5.41899	5.36795	0.88457
39	1	0	4.14017	6.29198	0.09237
40	6	0	-3.19331	0.27607	-1.05163
41	6	0	-3.30932	-0.80571	1.08618
42	6	0	-4.58573	0.35429	-1.08545
43	1	0	-2.62029	0.64811	-1.89706
44	6	0	-5.37517	-0.14074	-0.03756
45	1	0	-5.05221	0.80298	-1.95543
46	6	0	-4.69906	-0.72440	1.04649
47	1	0	-5.26461	-1.12524	1.88332
48	1	0	-2.81829	-1.26133	1.94172
49	6	0	-6.91286	-0.06970	-0.03937
50	6	0	-7.46746	0.59317	-1.31458
51	1	0	-7.11636	1.62556	-1.42433
52	1	0	-8.56200	0.62016	-1.26971
53	1	0	-7.18828	0.03836	-2.21757
54	6	0	-7.38929	0.75587	1.17959

55	1	0	-6.99717	1.77850	1.13759
56	1	0	-7.06277	0.31153	2.12571
57	1	0	-8.48455	0.81222	1.19800
58	6	0	-7.49542	-1.50031	0.05220
59	1	0	-8.59166	-1.46519	0.06007
60	1	0	-7.17229	-2.01477	0.96323
61	1	0	-7.18064	-2.10758	-0.80410
62	1	0	6.66552	-4.10927	-0.20228
63	1	0	5.09657	-6.04508	-0.14808
64	1	0	2.65734	-5.67510	-0.05769
65	6	0	-0.87880	1.99919	0.24519
66	1	0	-0.11659	2.74740	0.45813
67	1	0	-1.59570	1.97037	1.07108
68	1	0	-1.41857	2.30138	-0.65772

6a

Total energy: –2060.7976470 Hartree

Atom coordinates:

1	6	0	-0.24090	-1.39048	-0.00985
2	6	0	1.07987	-0.93422	-0.00951
3	6	0	-1.32702	-0.49796	-0.00597
4	6	0	1.33358	0.47370	-0.00606
5	6	0	-1.07332	0.90994	-0.00242
6	6	0	0.24753	1.36620	-0.00235
7	1	0	-0.42944	-2.46242	-0.01244
8	1	0	0.43608	2.43815	0.00047
9	6	0	-2.68928	-0.96463	-0.00506
10	6	0	-3.75200	-0.11605	0.00143
11	8	0	-3.54805	1.24003	0.00277
12	5	0	-2.30259	1.84367	0.00056
13	1	0	-2.86246	-2.03495	-0.01149
14	6	0	-5.17590	-0.49094	0.00461
15	6	0	-2.27629	3.41903	0.00144
16	5	0	2.30911	-1.86811	-0.01011
17	8	0	3.55460	-1.26468	-0.01122
18	6	0	3.75855	0.09134	-0.01065
19	6	0	2.69601	0.94020	-0.00511
20	1	0	2.86938	2.01045	0.00516
21	6	0	5.18208	0.46655	-0.00933
22	6	0	2.28209	-3.44345	-0.00936
23	6	0	-2.25418	4.13764	-1.21375
24	6	0	-2.26387	4.13631	1.21763
25	6	0	-2.21913	5.53556	-1.19557
26	6	0	-2.22849	5.53415	1.20131
27	6	0	-2.20905	6.25428	0.00330
28	1	0	-2.19878	6.07698	-2.14014
29	1	0	-2.21542	6.07450	2.14664
30	6	0	-2.29288	3.40221	2.54275
31	1	0	-1.45320	2.70168	2.63583
32	1	0	-3.21300	2.81495	2.65577
33	1	0	-2.23895	4.09842	3.38582
34	6	0	-2.27309	3.40525	-2.54003
35	1	0	-3.19298	2.81925	-2.66156
36	1	0	-1.43363	2.70374	-2.62708
37	1	0	-2.21149	4.10248	-3.38173
38	6	0	-2.20393	7.76557	0.00438
39	1	0	-1.70321	8.16614	-0.88381
40	1	0	-1.69599	8.16488	0.88907
41	1	0	-3.22620	8.16772	0.00898
42	6	0	-5.59885	-1.82929	0.04286
43	6	0	-6.17176	0.50143	-0.03101
44	6	0	-6.95178	-2.15860	0.04269
45	6	0	-7.95116	-1.17469	0.00579
46	6	0	-7.51968	0.16169	-0.03073
47	1	0	-5.87830	1.54426	-0.05934
48	1	0	-4.87141	-2.63446	0.07654
49	1	0	-7.22102	-3.20858	0.07388
50	1	0	-8.25168	0.96428	-0.05962
51	6	0	-9.45401	-1.50225	0.00404
52	6	0	-9.72451	-3.01786	0.05760
53	1	0	-9.30172	-3.53923	-0.80877
54	1	0	-10.80501	-3.20019	0.05650
55	1	0	-9.31431	-3.47388	0.96589
56	6	0	-10.12442	-0.84907	1.23656
57	1	0	-10.00100	0.23888	1.23947
58	1	0	-9.69517	-1.23619	2.16769
59	1	0	-11.20023	-1.06283	1.24276
60	6	0	-10.09948	-0.94199	-1.28616
60	1	0	-9.97432	0.14284	-1.36640
61	1	0	-11.17523	-1.15598	-1.29821
62	1	0	-9.65220	-1.39666	-2.17743
63	6	0	2.28005	-4.16213	-1.22474
64	6	0	2.25933	-4.16081	1.20658
65	6	0	2.25148	-5.56012	-1.20699
66	6	0	2.23138	-5.55887	1.18983
67	6	0	2.22306	-6.27880	-0.00834
68	1	0	2.25403	-6.10183	-2.15161
69	1	0	2.21816	-6.09958	2.13494
70	6	0	2.32173	-3.42950	-2.55033
71	1	0	3.24272	-2.84221	-2.65565
72	1	0	1.48274	-2.72924	-2.65167
73	1	0	2.27524	-4.12659	-3.39311
74	6	0	2.27901	-3.42705	2.53211
75	1	0	3.19906	-2.84123	2.65332
76	1	0	2.21674	-4.12333	3.37454
77	1	0	1.43977	-2.72514	2.61811
78	6	0	2.15911	-7.78878	-0.00804
79	1	0	2.65465	-8.21163	-0.88878
80	1	0	1.11981	-8.14466	-0.01907
81	1	0	2.63549	-8.21037	0.88379
82	6	0	6.17678	-0.51966	0.06636
83	6	0	5.60392	1.80751	-0.08135
84	6	0	7.52959	-0.18071	0.07578
85	1	0	5.88492	-1.56202	0.11981
86	6	0	7.95727	1.15108	0.00839
87	1	0	8.25492	-0.98432	0.13839
88	6	0	6.95290	2.13395	-0.07151
89	1	0	7.22785	3.18346	-0.13052
90	1	0	4.87555	2.60943	-0.15153
91	1	0	9.43971	1.56112	0.01707
92	6	0	10.38220	0.34625	0.11007
93	1	0	10.21771	-0.22752	1.02915
94	1	0	11.42368	0.68693	0.11522
95	1	0	10.26065	-0.33123	-0.74278
96	6	0	9.71291	2.47697	1.23426
97	1	0	9.49447	1.95629	2.17352
98	1	0	9.10274	3.38582	1.20671
99	1	0	10.76606	2.78337	1.25187
100	6	0	9.76903	2.32987	-1.28506
101	1	0	10.82135	2.63947	-1.28892
102	1	0	9.15626	3.23097	-1.39229
103	1	0	9.59620	1.70099	-2.16580

6b

Total energy: –2099.6615789 Hartree

Atom coordinates:

1	6	0	0.44756	-1.32745	-0.04260
2	6	0	-0.93114	-1.08790	-0.00202
3	6	0	1.38281	-0.27906	-0.05448
4	6	0	-1.38501	0.26852	0.02921

5	6	0	0.92895	1.07736	-0.02225
6	6	0	-0.44977	1.31691	0.01739
7	1	0	0.80521	-2.35526	-0.06350
8	1	0	-0.80746	2.34470	0.03808
9	6	0	2.79654	-0.53156	-0.08412
10	6	0	3.73574	0.45720	-0.08434
11	7	0	3.36022	1.81398	-0.08760
12	5	0	1.97935	2.21005	-0.05112
13	1	0	3.14198	-1.56082	-0.07260
14	6	0	5.18150	0.08610	-0.06721
15	6	0	1.56485	3.74127	-0.05520
16	5	0	-1.98152	-2.22049	0.03092
17	7	0	-3.36242	-1.82443	0.06818
18	6	0	-3.73804	-0.46770	0.06036
19	6	0	-2.79872	0.52098	0.05813
20	1	0	-3.14402	1.55029	0.04376
21	6	0	-5.18361	-0.09580	0.04089
22	6	0	-1.56743	-3.75181	0.03940
23	6	0	1.28229	4.41454	-1.26397
24	6	0	1.42052	4.45106	1.16057
25	6	0	0.88005	5.75609	-1.24239
26	6	0	1.01527	5.78833	1.14839
27	6	0	0.74080	6.46277	-0.04651
28	1	0	0.66689	6.25922	-2.18423
29	1	0	0.90822	6.31720	2.09462
30	6	0	1.69996	3.76927	2.48458
31	1	0	1.08496	2.86975	2.61022
32	1	0	1.49374	4.43690	3.32756
33	1	0	2.74723	3.44987	2.56402
34	6	0	1.41579	3.69998	-2.59337
35	1	0	0.81835	2.78078	-2.61713
36	1	0	2.45474	3.40735	-2.79511
37	1	0	1.08688	4.33626	-3.42151
38	6	0	0.30749	7.91079	-0.03570
39	1	0	0.08968	8.27015	-1.04664
40	1	0	1.08502	8.55972	0.38763
41	1	0	-0.59447	8.05585	0.57208
42	6	0	5.74542	-0.61839	-1.13661
43	6	0	6.00559	0.36258	1.03648
44	6	0	7.08304	-1.02163	-1.11264
45	6	0	7.91317	-0.74155	-0.02039
46	6	0	7.33593	-0.04182	1.05484
47	1	0	5.59247	0.87900	1.89915
48	1	0	5.12969	-0.85027	-2.00141
49	1	0	7.47114	-1.56160	-1.96931
50	1	0	7.93291	0.18602	1.93381
51	6	0	9.39119	-1.16665	0.04168
52	6	0	9.83859	-1.91713	-1.22688
53	1	0	9.26551	-2.83868	-1.37968
54	1	0	10.89439	-2.19628	-1.13702
55	1	0	9.73637	-1.29733	-2.12493
56	6	0	10.28170	0.08928	0.19670
57	1	0	10.04338	0.64955	1.10691
58	1	0	10.15562	0.76720	-0.65525
59	1	0	11.33919	-0.19731	0.24943
60	6	0	9.60837	-2.10064	1.25610
61	1	0	9.34786	-1.61050	2.19999
62	1	0	10.65991	-2.40658	1.31858
63	1	0	8.99584	-3.00525	1.16930
64	6	0	-1.43161	-4.46688	-1.17192
65	6	0	-1.27321	-4.41886	1.25123
66	6	0	-1.02450	-5.80557	-1.15514
67	6	0	-0.86967	-5.75805	1.23424
68	6	0	-0.74255	-6.47300	0.03959
69	1	0	-0.92160	-6.33911	-2.09887
70	1	0	-0.64430	-6.25442	2.17713
71	6	0	-1.71784	-3.79319	-2.49868
72	1	0	-1.10754	-2.89145	-2.63104
73	1	0	-2.76692	-3.47945	-2.57709
74	1	0	-1.51085	-4.46431	-3.33870
75	6	0	-1.39370	-3.69448	2.57650
76	1	0	-0.79209	-2.77779	2.58962
77	1	0	-1.06195	-4.32658	3.40670
78	1	0	-2.42993	-3.39570	2.78318
79	6	0	-0.33344	-7.92793	0.04443
80	1	0	0.11280	-8.22243	-0.91151
81	1	0	-1.19620	-8.58587	0.21706
82	1	0	0.39418	-8.13801	0.83647
83	6	0	-6.00879	-0.38005	-1.05530
84	6	0	-5.74541	0.62115	1.10793
85	6	0	-7.34352	0.02528	-1.07838
86	1	0	-5.59879	-0.90479	-1.91444
87	6	0	-7.91480	0.73384	-0.01170
88	1	0	-7.93596	-0.21355	-1.95465
89	6	0	-7.07849	1.02318	1.07904
90	1	0	-7.47098	1.57295	1.93013
91	1	0	-5.12735	0.85964	1.96922
92	6	0	-9.38380	1.19410	-0.00091
93	6	0	-10.13519	0.78749	-1.28277
94	1	0	-9.68700	1.23336	-2.17801
95	1	0	-11.17336	1.13371	-1.22667
96	1	0	-10.15704	-0.30019	-1.41592
97	6	0	-9.44058	2.73555	0.12244
98	1	0	-8.93713	3.21534	-0.72454
99	1	0	-8.95982	3.08930	1.04045
100	1	0	-10.48248	3.07823	0.13788
101	6	0	-10.11248	0.55742	1.20660
102	1	0	-11.15995	0.88185	1.23415
103	1	0	-9.65049	0.84174	2.15780
104	1	0	-10.09716	-0.53654	1.14140
105	6	0	-4.43329	-2.82545	0.19965
106	1	0	-3.97869	-3.79683	0.38833
107	1	0	-5.03971	-2.89574	-0.70871
108	1	0	-5.09978	-2.57144	1.02926
109	6	0	4.43187	2.81498	-0.21218
110	1	0	5.09859	2.56579	-1.04307
111	1	0	5.03786	2.87877	0.69701
112	1	0	3.97828	3.78803	-0.39469

8a

Total energy: −1674.350709 Hartree

Atom coordinates:

1	8	0	1.20242	-0.40147	0.01334
2	6	0	2.39130	0.28911	0.00985
3	5	0	0.00772	0.28713	0.02130
4	6	0	2.42964	1.65303	0.03403
5	6	0	0.00113	1.78887	0.02568
6	6	0	1.23488	2.46995	0.03312
7	8	0	-1.18059	-0.41199	0.02518
8	6	0	-2.37663	0.26593	0.02914
9	6	0	-2.42633	1.62989	0.02131
10	6	0	-1.23924	2.45762	0.02716
11	1	0	3.39596	2.14293	0.06809
12	1	0	-3.39564	2.11390	-0.00491
13	6	0	1.21783	3.87469	0.04538
14	6	0	-1.23616	3.86260	0.03479
15	6	0	-0.01260	4.54181	0.04331
16	1	0	-2.16561	4.42260	0.04230
17	1	0	2.14177	4.44371	0.06029
18	6	0	-0.01908	6.04911	-0.01624
19	9	0	-0.00243	6.49349	-1.29517

20	9	0	-1.11900	6.57625	0.56674
21	9	0	1.05873	6.58616	0.59818
22	6	0	-3.54378	-0.63382	0.02459
23	6	0	3.56767	-0.59810	-0.00440
24	6	0	3.43361	-1.96026	0.31572
25	6	0	4.84883	-0.13218	-0.33640
26	6	0	4.53828	-2.80370	0.31832
27	6	0	5.82703	-2.34395	-0.00161
28	6	0	5.94950	-0.98581	-0.33022
29	1	0	2.45457	-2.35226	0.56647
30	1	0	4.38675	-3.84789	0.57728
31	1	0	4.99421	0.90358	-0.62781
32	1	0	6.91569	-0.57453	-0.60029
33	6	0	7.01944	-3.31578	0.01179
34	6	0	7.18263	-3.90777	1.43236
35	1	0	7.38158	-3.11822	2.16593
36	1	0	8.02180	-4.61369	1.45604
37	1	0	6.28549	-4.44583	1.75574
38	6	0	6.76000	-4.46282	-0.99401
39	1	0	5.85392	-5.02616	-0.74765
40	1	0	7.60091	-5.16701	-0.99193
41	1	0	6.64496	-4.07348	-2.01194
42	6	0	8.34167	-2.62760	-0.37655
43	1	0	8.60087	-1.81937	0.31680
44	1	0	8.30359	-2.21152	-1.38975
45	1	0	9.15820	-3.35791	-0.35107
46	6	0	-4.84882	-0.16755	0.26771
47	6	0	-5.93333	-1.03344	0.23958
48	6	0	-5.78259	-2.40767	-0.02370
49	1	0	-5.02274	0.87864	0.49939
50	6	0	-3.38276	-2.00384	-0.22796
51	1	0	-6.92121	-0.62633	0.43621
52	6	0	-4.47894	-2.86564	-0.25216
53	1	0	-2.38904	-2.39578	-0.41128
54	1	0	-4.29747	-3.91500	-0.45641
55	6	0	-7.01439	-3.32799	-0.04629
56	6	0	-7.71761	-3.28147	1.33155
57	1	0	-7.04508	-3.62318	2.12650
58	1	0	-8.60117	-3.93138	1.33042
59	1	0	-8.04996	-2.26981	1.58707
60	6	0	-6.64540	-4.79296	-0.34804
61	1	0	-5.97429	-5.21005	0.41143
62	1	0	-6.16348	-4.89916	-1.32658
63	1	0	-7.55293	-5.40688	-0.35927
64	6	0	-7.99660	-2.84302	-1.13939
65	1	0	-8.33360	-1.81683	-0.95914
66	1	0	-8.88494	-3.48588	-1.16553
67	1	0	-7.52701	-2.87167	-2.12919

8ab

Total energy: –1693.7836859 Hartree

Atom coordinates:

1	7	0	1.06770	-0.62780	-0.05879
2	6	0	2.29391	0.05058	-0.04667
3	5	0	-0.14368	0.13845	-0.00931
4	6	0	2.36403	1.41973	-0.02661
5	6	0	-0.06009	1.64258	0.02482
6	6	0	1.20295	2.27133	0.00238
7	1	0	3.34975	1.87251	-0.00043
8	8	0	-1.39120	-0.48220	-0.01231
9	6	0	1.02663	-2.08647	-0.21776
10	1	0	0.00718	-2.37314	-0.47764
11	1	0	1.30646	-2.60883	0.70264
12	1	0	1.70325	-2.40892	-1.01381
13	6	0	-2.53671	0.27243	0.03994
14	6	0	-2.50070	1.63375	0.06181
15	6	0	-1.26323	2.38620	0.05463
16	1	0	-3.43990	2.17554	0.05919
17	6	0	-1.19167	3.78491	0.06912
18	6	0	1.25343	3.68025	0.01879
19	6	0	0.06520	4.40797	0.05059
20	1	0	-2.09438	4.38718	0.10065
21	1	0	2.20645	4.19880	0.01046
22	6	0	0.11865	5.91305	-0.00016
23	6	0	-3.76775	-0.53877	0.04414
24	6	0	3.56010	-0.73749	-0.03797
25	6	0	4.49616	-0.58669	-1.06699
26	6	0	3.88696	-1.60046	1.02106
27	6	0	5.09792	-2.28376	1.03682
28	1	0	3.19781	-1.71709	1.85329
29	6	0	6.04236	-2.14366	0.00372
30	6	0	5.71053	-1.27683	-1.04501
31	1	0	5.31247	-2.93334	1.88099
32	1	0	4.26861	0.07491	-1.89828
33	1	0	6.39950	-1.12691	-1.86887
34	6	0	7.36923	-2.92104	0.06224
35	6	0	8.14272	-2.52501	1.34268
36	1	0	9.08999	-3.07484	1.39938
37	1	0	7.57325	-2.74960	2.25059
38	1	0	8.37076	-1.45311	1.34742
39	6	0	8.27153	-2.63040	-1.15204
40	1	0	7.79302	-2.91818	-2.09506
41	1	0	9.20119	-3.20398	-1.06599
42	1	0	8.54283	-1.57045	-1.21476
43	6	0	7.07431	-4.43975	0.09182
44	1	0	8.01082	-5.00827	0.14374
45	1	0	6.53651	-4.75281	-0.81042
46	1	0	6.46589	-4.72048	0.95797
47	6	0	-3.75622	-1.86204	-0.42849
48	6	0	-4.98765	-0.02919	0.51316
49	6	0	-4.91923	-2.62329	-0.44955
50	1	0	-2.82733	-2.28810	-0.79102
51	6	0	-6.14880	-2.11565	0.00396
52	6	0	-6.14816	-0.79962	0.48833
53	1	0	-7.06257	-0.35720	0.86759
54	1	0	-5.03282	0.97361	0.92711
55	1	0	-4.86343	-3.63868	-0.83257
56	6	0	-7.41136	-2.99326	-0.04075
57	6	0	-7.18697	-4.26436	0.81258
58	1	0	-6.34177	-4.85755	0.44789
59	1	0	-8.07825	-4.90331	0.78665
60	1	0	-6.98594	-4.00372	1.85795
61	6	0	-7.69810	-3.40292	-1.50529
62	1	0	-6.86659	-3.96673	-1.94088
63	1	0	-7.86839	-2.52069	-2.13284
64	1	0	-8.59325	-4.03477	-1.55647
65	6	0	-8.65309	-2.26284	0.50509
66	1	0	-9.52461	-2.92458	0.44750
67	1	0	-8.88508	-1.36162	-0.07387
68	1	0	-8.52833	-1.97316	1.55471
69	9	0	-0.06582	6.37467	-1.26071
70	9	0	1.30531	6.40100	0.42565
71	9	0	-0.84509	6.47900	0.76299

8c

Total energy: –1693.7298025 Hartree

Atom coordinates:

1	6	0	-1.31698	1.80605	0.04877
2	6	0	-0.14650	1.00029	0.05113
3	6	0	-2.61244	1.18491	0.07049

4	6	0	-2.79253	-0.16944	0.10357
5	5	0	-0.34682	-0.53796	0.10913
6	7	0	-1.70525	-1.03524	0.14626
7	6	0	-1.21081	3.21539	0.01462
8	6	0	1.12049	1.65631	0.02013
9	6	0	1.20223	3.05328	-0.00988
10	6	0	0.03230	3.82357	-0.01333
11	1	0	-2.11206	3.82039	0.01581
12	1	0	2.17277	3.53588	-0.02581
13	6	0	-4.17971	-0.71683	0.07694
14	6	0	-5.08921	-0.38901	1.08818
15	6	0	-4.63924	-1.51568	-0.98295
16	6	0	-5.95399	-1.96693	-1.01681
17	6	0	-6.87348	-1.65033	-0.00019
18	6	0	-6.40747	-0.84961	1.04987
19	1	0	-4.75869	0.22777	1.91933
20	1	0	-7.07090	-0.57201	1.86127
21	1	0	-3.96723	-1.76459	-1.79977
22	1	0	-6.27076	-2.57309	-1.86098
23	6	0	-8.31871	-2.17352	-0.07919
24	6	0	-9.16698	-1.73634	1.13000
25	1	0	-8.75651	-2.11248	2.07413
26	1	0	-10.18299	-2.13426	1.03044
27	1	0	-9.24610	-0.64560	1.20096
28	6	0	-8.99199	-1.63048	-1.36238
29	1	0	-9.02532	-0.53511	-1.35444
30	1	0	-10.02125	-2.00176	-1.43873
31	1	0	-8.45816	-1.94164	-2.26640
32	6	0	-8.30624	-3.72032	-0.12357
33	1	0	-7.84219	-4.13484	0.77865
34	1	0	-7.75301	-4.10032	-0.98882
35	1	0	-9.33061	-4.10702	-0.18779
36	8	0	0.65563	-1.47535	0.15598
37	6	0	2.35006	0.92650	0.01961
38	6	0	3.42386	0.34927	0.01057
39	6	0	-1.92883	-2.47759	0.32473
40	1	0	-2.71096	-2.65577	1.06698
41	1	0	-0.99685	-2.92765	0.66378
42	1	0	-2.22557	-2.96383	-0.61073
43	6	0	4.67791	-0.32775	0.00108
44	6	0	4.74671	-1.72810	-0.14133
45	6	0	5.88223	0.38456	0.13468
46	6	0	5.97455	-2.37602	-0.14610
47	6	0	7.18672	-1.67430	-0.01109
48	6	0	7.10592	-0.28085	0.12787
49	1	0	3.82979	-2.30061	-0.24948
50	1	0	5.98597	-3.45643	-0.25737
51	1	0	8.00901	0.30931	0.23483
52	1	0	5.85182	1.46425	0.24541
53	6	0	8.52168	-2.43881	-0.01871
54	6	0	8.53701	-3.45605	1.14771
55	1	0	8.43583	-2.94762	2.11324
56	1	0	9.48203	-4.01266	1.15359
57	1	0	7.72320	-4.18418	1.06679
58	6	0	8.67381	-3.19547	-1.36019
59	1	0	7.86154	-3.91220	-1.52021
60	1	0	9.61803	-3.75317	-1.37635
61	1	0	8.67620	-2.49837	-2.20580
62	6	0	9.73392	-1.50282	0.14529
63	1	0	9.70115	-0.95470	1.09376
64	1	0	9.80062	-0.77374	-0.67027
65	1	0	10.65778	-2.09170	0.13678
66	1	0	-3.49190	1.81761	0.02007
67	6	0	0.14462	5.32183	-0.10943
68	9	0	-0.95591	5.94765	0.36247
69	9	0	0.30987	5.72747	-1.39081
70	9	0	1.20614	5.79047	0.58598
71	1	0	1.52663	-1.04507	0.16070

5

Total energy: −1276.8475802 Hartree

Atom coordinates:

1	6	0	-3.65879	-4.55286	0.07876
2	6	0	-5.02574	-4.64659	0.08204
3	6	0	-5.83093	-3.46984	0.06393
4	6	0	-5.24726	-2.23003	0.04315
5	6	0	-3.01027	-3.27867	0.05730
6	6	0	-3.82522	-2.08714	0.03907
7	1	0	-5.50580	-5.62139	0.09852
8	1	0	-6.91351	-3.56380	0.06673
9	1	0	-3.04246	-5.44885	0.09261
10	1	0	-5.85830	-1.33055	0.02940
11	6	0	-1.61679	-3.14470	0.05320
12	6	0	-0.99199	-1.89030	0.03058
13	6	0	-1.80756	-0.69684	0.01647
14	6	0	-3.20154	-0.83144	0.01934
15	1	0	-3.81882	0.06253	0.00672
16	1	0	-0.99889	-4.04054	0.06685
17	6	0	0.42846	-1.76509	0.02919
18	6	0	1.04672	-0.53489	0.01352
19	6	0	0.22373	0.63991	-0.00108
20	6	0	-1.14883	0.58766	-0.00161
21	1	0	1.02316	-2.67413	0.07043
22	1	0	0.70848	1.61151	-0.04067
23	6	0	-1.94440	1.85892	-0.03330
24	6	0	-2.32739	2.48372	1.17221
25	6	0	-2.30130	2.43894	-1.26876
26	6	0	-3.05176	3.67930	1.11958
27	6	0	-3.02636	3.63528	-1.27518
28	6	0	-3.40792	4.27536	-0.09311
29	1	0	-3.30078	4.07705	-2.23147
30	1	0	-3.34609	4.15575	2.05304
31	6	0	-1.91406	1.78851	-2.57858
32	1	0	-2.28557	0.75917	-2.64296
33	1	0	-0.82549	1.73748	-2.69849
34	1	0	-2.32034	2.34822	-3.42674
35	6	0	-1.96984	1.88112	2.51299
36	1	0	-0.88425	1.81086	2.64858
37	1	0	-2.36494	0.86366	2.61622
38	1	0	-2.37348	2.48457	3.33188
39	6	0	-4.16259	5.58430	-0.12509
40	1	0	-4.81135	5.69489	0.75055
41	1	0	-4.78651	5.66586	-1.02169
42	1	0	-3.47500	6.44094	-0.12942
43	6	0	2.52455	-0.40741	0.01377
44	6	0	3.33740	-1.31511	-0.68682
45	6	0	3.17015	0.62080	0.71498
46	6	0	4.72282	-1.19791	-0.67610
47	6	0	5.37548	-0.17153	0.02909
48	6	0	4.56098	0.73303	0.72312
49	1	0	2.87445	-2.10729	-1.26901
50	1	0	5.30563	-1.91985	-1.24186
51	1	0	5.00566	1.54274	1.29145
52	1	0	2.58129	1.33223	1.28767
53	6	0	6.91112	-0.07596	0.00928
54	6	0	7.43555	1.09325	0.86423
55	1	0	7.07073	2.06062	0.50065
56	1	0	8.53038	1.11787	0.82452
57	1	0	7.14525	0.99121	1.91612
58	6	0	7.39337	0.13683	-1.44576
59	1	0	6.98421	1.06418	-1.86265

60	1	0	7.08819	-0.68638	-2.10030
61	1	0	8.48791	0.20223	-1.48008
62	6	0	7.51886	-1.38685	0.56263
63	1	0	7.22058	-2.25789	-0.03013
64	1	0	7.19945	-1.56119	1.59642
65	1	0	8.61445	-1.33434	0.54902

6

Total energy: –2014.1648384 Hartree

Atom coordinates:

1	6	0	-1.98169	-2.06518	0.00867
2	6	0	-3.30531	-1.69672	0.00908
3	6	0	-3.73134	-0.32735	0.00144
4	6	0	-2.76685	0.65620	-0.00147
5	6	0	-0.96409	-1.04144	0.00354
6	6	0	-1.37671	0.34239	-0.00158
7	1	0	-4.06255	-2.47566	-0.01275
8	1	0	-3.05588	1.70378	0.02346
9	6	0	0.40530	-1.33249	0.00130
10	6	0	1.38132	-0.32426	-0.00128
11	6	0	0.96857	1.05955	0.00386
12	6	0	-0.40071	1.35061	0.00137
13	1	0	-0.72125	2.38873	0.00105
14	1	0	0.72582	-2.37063	0.00102
15	6	0	2.77164	-0.63781	0.00020
16	6	0	3.73590	0.34597	0.00551
17	6	0	3.30950	1.71529	0.01128
18	6	0	1.98594	2.08351	0.00927
19	1	0	3.06053	-1.68544	0.02571
20	1	0	4.06674	2.49419	-0.01012
21	6	0	1.61574	3.53706	0.00012
22	6	0	1.41442	4.22347	1.21667
23	6	0	1.47956	4.22455	-1.22374
24	6	0	1.08908	5.58319	1.18593
25	6	0	1.15344	5.58524	-1.20841
26	6	0	0.95801	6.28547	-0.01555
27	1	0	1.04852	6.10993	-2.15633
28	1	0	0.93339	6.10654	2.12774
29	6	0	1.67779	3.51503	-2.54508
30	1	0	1.01461	2.64730	-2.63953
31	1	0	2.70234	3.14032	-2.65364
32	1	0	1.47501	4.18864	-3.38345
33	6	0	1.54365	3.51174	2.54530
34	1	0	2.55221	3.10737	2.69075
35	1	0	0.85254	2.66366	2.61735
36	1	0	1.33005	4.19270	3.37496
37	6	0	0.63706	7.76222	-0.02084
38	1	0	-0.03829	8.02916	0.79961
39	1	0	0.16467	8.06657	-0.96083
40	1	0	1.54532	8.36835	0.09842
41	6	0	5.18226	0.01752	0.00774
42	6	0	5.68203	-1.09180	-0.69637
43	6	0	6.10894	0.79768	0.71371
44	6	0	7.03754	-1.40101	-0.68493
45	6	0	7.97039	-0.62340	0.02362
46	6	0	7.46820	0.48257	0.72192
47	1	0	5.00121	-1.70419	-1.28139
48	1	0	7.37458	-2.26440	-1.25254
49	1	0	8.13681	1.11673	1.29385
50	1	0	5.76351	1.65192	1.28973
51	6	0	9.46223	-1.00030	0.00525
52	6	0	10.32136	-0.03341	0.84175
53	1	0	10.26331	0.99412	0.46506
54	1	0	11.37212	-0.34162	0.79864
55	1	0	10.02170	-0.02939	1.89592
56	6	0	9.98303	-0.96954	-1.45159
57	1	0	9.87765	0.03177	-1.88456
58	1	0	9.43865	-1.66984	-2.09367
59	1	0	11.04467	-1.24395	-1.48344
60	6	0	9.64069	-2.42505	0.58192
61	1	0	9.08498	-3.17128	0.00447
62	1	0	9.28838	-2.47493	1.61854
63	1	0	10.69913	-2.71288	0.56789
64	6	0	-1.61178	-3.51881	0.00022
65	6	0	-1.40890	-4.20439	1.21697
66	6	0	-1.08392	-5.56422	1.18674
67	6	0	-0.95471	-6.26739	-0.01440
68	1	0	-0.92705	-6.08694	2.12870
69	6	0	-1.47744	-4.20722	-1.22335
70	6	0	-1.15162	-5.56796	-1.20750
71	1	0	-1.04809	-6.09334	-2.15519
72	6	0	-1.53610	-3.49166	2.54526
73	1	0	-0.84361	-2.64463	2.61633
74	1	0	-1.32298	-4.17245	3.37518
75	1	0	-2.54392	-3.08561	2.69112
76	6	0	-1.67728	-3.49862	-2.54495
77	1	0	-2.70232	-3.12517	-2.65315
78	1	0	-1.47425	-4.17247	-3.38307
79	1	0	-1.01516	-2.63018	-2.64026
80	6	0	-0.63423	-7.74424	-0.01918
81	1	0	-1.54298	-8.35008	0.09782
82	1	0	0.03912	-8.01154	0.80277
83	1	0	-0.15980	-8.04862	-0.95815
84	6	0	-5.17745	0.00222	-0.00425
85	6	0	-6.10998	-0.77756	0.70159
86	6	0	-5.67262	1.10525	-0.71425
87	6	0	-7.03182	1.41842	-0.71510
88	1	0	-4.98876	1.71511	-1.29841
89	6	0	-7.96514	0.64498	-0.01167
90	1	0	-7.35794	2.27847	-1.28960
91	6	0	-7.46429	-0.46069	0.69715
92	1	0	-8.14353	-1.08987	1.26632
93	1	0	-5.76735	-1.62935	1.28288
94	6	0	-9.47224	0.95537	0.00547
95	6	0	-10.25259	-0.25042	-0.57009
96	1	0	-9.95596	-0.45011	-1.60611
97	1	0	-11.33089	-0.04913	-0.55748
98	1	0	-10.07748	-1.16312	0.00897
99	6	0	-9.92859	1.21236	1.46158
100	1	0	-9.74357	0.34623	2.10549
101	1	0	-11.00385	1.42740	1.49225
102	1	0	-9.39770	2.06863	1.89297
103	6	0	-9.82449	2.19861	-0.83318
104	1	0	-9.32603	3.09934	-0.45704
105	1	0	-10.90480	2.37758	-0.79134
106	1	0	-9.55183	2.07104	-1.88699

7. References

S1 C. Li, S. K. Mellerup, X. Wang and S. Wang, *Organometallics*, 2018, **37**, 3360–3367.

S2 S. Kirschner, J. M. Mewes, M. Bolte, H. W. Lerner, A. Dreuw and M. Wagner, *Chem. Eur. J.*, 2017, **23**, 5104–5116.

S3 F. Cottet, E. Castagnetti and M. Schlosser, *Synthesis*, 2005, **5**, 798–803.

S4 S. H. Chanteau and J. M. Tour, *J. Org. Chem.*, 2003, **68**, 8750–8766.

S5 K. Suzuki, A. Kobayashi, S. Kaneko, K. Takehira, T. Yoshihara, H. Ishida, Y. Shiina, S. Oishi and S. Tobita, *Phys. Chem. Chem. Phys.*, 2009, **11**, 9850–9860.

S6 A. M. Brouwer, *Pure Appl. Chem.*, 2011, **83**, 2213–2228.

S7 T.-S. Ahn, R. O. Al-Kaysi, A. M. Müller, K. M. Wentz and C. J. Bardeen, *Rev. Sci. Instrum.*, 2007, **78**, 086105.

S8 Z. U. Levi and T. D. Tilley, *J. Am. Chem. Soc.*, 2009, **131**, 2796–2797.

S9 H. Arslan, F. J. Uribe-Romo, B. J. Smith and W. R. Dichtel, *Chem. Sci.*, 2013, **4**, 3973–3978.

S10 Stoe & Cie, *X-AREA*. *Diffractometer control program system*. Stoe & Cie, Darmstadt, Germany, 2002.

S11 G. M. Sheldrick, *Acta Crystallogr. A*, 2008, **64**, 112–122.

S12 A. L. Spek, *Acta Crystallogr. D*, 2009, **65**, 148–155.

S13 Gaussian 09, Revision D.01, M. J. Frisch, G. W. Trucks, H. B. Schlegel, G. E. Scuseria, M. A. Robb, J. R. Cheeseman, G. Scalmani, V. Barone, B. Mennucci, G. A. Petersson, H. Nakatsuji, M. Caricato, X. Li, H. P. Hratchian, A. F. Izmaylov, J. Bloino, G. Zheng, J. L. Sonnenberg, M. Hada, M. Ehara, K. Toyota, R. Fukuda, J. Hasegawa, M. Ishida, T. Nakajima, Y. Honda, O. Kitao, H. Nakai, T. Vreven, J. A. Montgomery, Jr., J. E. Peralta, F. Ogliaro, M. Bearpark, J. J. Heyd, E. Brothers, K. N. Kudin, V. N. Staroverov, T. Keith, R. Kobayashi, J. Normand, K. Raghavachari, A. Rendell, J. C. Burant, S. S. Iyengar, J. Tomasi, M. Cossi, N. Rega, J. M. Millam, M. Klene, J. E. Knox, J. B. Cross, V. Bakken, C. Adamo, J. Jaramillo, R. Gomperts, R. E. Stratmann, O. Yazyev, A. J. Austin, R. Cammi, C. Pomelli, J. W. Ochterski, R. L. Martin, K. Morokuma, V. G. Zakrzewski, G. A. Voth, P. Salvador, J. J. Dannenberg, S. Dapprich, A. D. Daniels, O. Farkas, J. B. Foresman, J. V. Ortiz, J. Cioslowski, and D. J. Fox, Gaussian, Inc., Wallingford, CT, USA, 2013.